Development of Novel Catalytic Process Based on Organometallic Research of Nickel(I)/NHC Complex

ニッケル１価/NHC 錯体の有機金属化学研究を基盤とした
新たな触媒反応経路の開拓

By
Takahiro Inatomi
2019

CONTENTS

1. Introduction

1-1. General Nickel Catalysis 2
1-2. Ligand Effect for Catalytic Reaction 7
1-3. N-Heterocyclic Carbene Chemistry 8
1-4. Odd Oxidation States of Nickel Species 11
1-5. This Thesis 15
1-6. References 16

2. Dimeric Ni(I)/NHC Species in Catalysis

2-1. Introduction 20
2-2. Synthesis and Characterizations 24
2-3. Catalysis and Reactivity 30
2-4. Summary 48
2-5. References 50

3. Monomeric Ni(I)/NHC species bearing Monodentate 2e Donor Ligand in catalysis

3-1. Introduction 54
3-2. Synthesis and Characterizations 56
3-3. Catalysis and Reactivity 66
3-4. Summary 68
3-5. References 69

4. Monomeric Ni(I)/NHC species bearing bidentate 4e Donor Ligand in catalysis

4-1. Introduction 73
4-2. Synthesis and Characterizations 76
4-3. Catalysis and Reactivity 79
4-4. Summary 90
4-5. References 91

5. Conclusion 94

6. Experimental 97

7. Acknowledgments 158

Chapter 1
Introduction

1-1. General Nickel Catalysis

In the field of chemistry, nickel is inexpensive and abundantly present on the earth compared to palladium and platinum, which are cognate elements, so it is attracting attention as a metal for catalyst in various organic transformations. On the other hand, in the field of catalytic chemistry, although it is regarded as a promising alternative metal for a precious metal catalyst such as palladium and rhodium, nickel is more preferable as a catalyst precursor or an organometallic complex.

Basic reactions of organometallic complexes can be described by combining seven elementary reactions. (Figure 1-1) It consists of 1) coordination and elimination of ligand, 2) oxidative addition and reductive elimination, 3) insertion and β-elimination, 4) oxidative cyclization and reductive cleavage, 5) metal exchange reaction, 6) metathesis reaction, 7) comproportionation and disproportionation, and the like. These elementary reactions have paired relationships, and it is possible to construct new organic substances and metal complexes through these elementary reactions. [Coordination and elimination] are to give / receive a non-bonding electron pair of a ligand composed of organic molecules to the metal center. This forms a "coordination bonding" between the metal and the ligand. [Oxidative addition and reductive elimination] are reactions that cleave bond of molecules by a metal center to form two metal-ligand bonds and generate new bonds via cleavage of two metal-ligand bonds. That is, the oxidation state of the metal is increased by the metal giving 2 electrons in the oxidative addition, and it is reduced in the case of receiving 2 electrons in the reductive elimination. [Insertion and β-elimination] are addtion of metal-ligand (hydrogen in most cases) bonds to unsaturated bonds of organic molecules and its reverse reaction. Coordination of the unsaturated bonds to the metal center is necessary in the insertion reaction. Unlike the above addition

and elimination reactions, this reaction does not cause a change in oxidation numbers. [Oxidative cyclization and reductive cleavage] occur with formation and decomposition of metallacycles with unsaturated bonds, where the oxidation number of the metal center increases and decreases like oxidative addition and reductive elimination. [Metal exchange reaction] is a reaction in which a metal complex and another metal species exchanges the respective ligands, and may be a reversible reaction in some cases. [Metathesis reaction] is a very special example, but the phenomenon occurs in which bonds are recombined between two or more kinds of olefin molecules. This reaction is a unique reaction form, and in 2005 Yves Chauvin, Richard R. Schrock, Robert H. Grubbs won the Nobel prize. [1] Finally, [comproportionation and disproportionation] is a chemical reaction which reacts two or more metal species of the same type with each other to give two or more different types of products. It is important that these reactions occur with change of the oxidation states of metal centers.

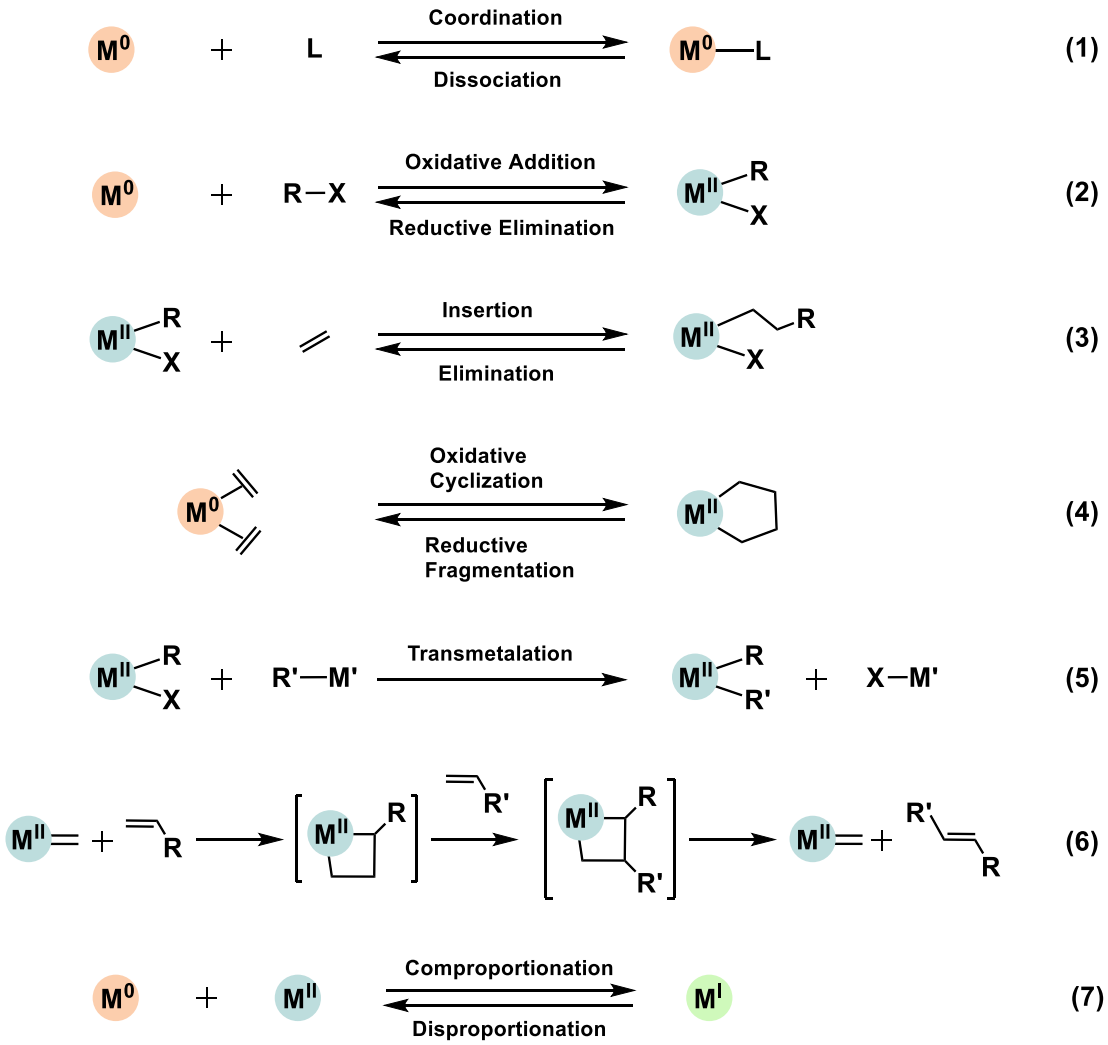

Figure 1-1. Prototypical examples of elementary organometallic reaction steps, highlighting changes in oxidation state.

In general, metal complexes of nickel can cleave various chemical bonds (i.e. C-H, C-C, C-O, C-N, etc.) due to the small atomic radius of nickel and abundance of electrons. [2] Therefore, in recent years, the chemistry of nickel catalysis has been actively developed in order to make a new choice other than those of 4d-transition metal catalysis. However, there are obvious problems when using nickel. Then, in the case of nickel and palladium, oxidation state of the catalytically active species in the catalyst cycle is generally zero. However, zero-valent nickel is unstable compared to the corresponding zero-valent palladium. In the catalyst cycle, the 0 valent nickel species tends to be activated,

compared with palladium. In other words, it can be said that the reactivity is high. (Figure 1-2) This is easy to understand in view of the electronic arrangement of both metallic elements. That is, the electron configuration in the ground state of nickel is Ar $3d^8$ $4s^2$, and there is unoccupied d orbit. On the other hand, the electronic configuration of palladium is Kr $4d^{10}$, which is closed shell in the ground state.

^{28}Ni Nickel 58.69	^{46}Pd Palladium 106.42
[Ar]$3d^8 4s^2$	[Kr]$4d^{10}$
-1, 0, +1, +2, +3, +4	0, +1, +2, +3, +4, +5, +6
Smaller atomic radius	Larger atomic radius
Less electronegative	More electronegative
Harder	Softer
Facile oxidative addition	Facile reductive elimination

Figure 1-2. Comparison of basic characteristics of nickel and palladium, including accessible oxidation states.

The general reaction mechanism of cross-coupling reaction via organic nickel species is shown below. (Fig. 1-3) 11 Normally, stable nickel divalent catalyst precursor is often used as the catalytic reaction mainly composed of nickel, but a 0-valent nickel source is often used. i) The nickel divalent catalyst precursor forms 0-valent nickel complex which is catalytically active by using suitable reducing agent. ii) Subsequently, oxidative addition reaction with electrophilic substrate occurs to form nickel divalent intermediate. iii) Subsequently, a metal exchange reaction with an organometallic reagent (that is, a transmetalation reaction) forms divalent organonickel intermediate . iv) Finally, a series of catalytic reactions is established by regenerating 0-valent nickel complex and releasing the corresponding product by the reductive elimination reaction of the divalent nickel complex. In such a catalyst cycle, there is obviously a rate limiting step. In the case of the Ni(0)-Ni(II) cycle, the reduction process from the divalent nickel complex to the zero valent complex requires the highest activation barrier. (In contrast, using palladium,

oxidative addition step oxidized from zero-valent palladium complex to divalent complex is the rate-determining step.)

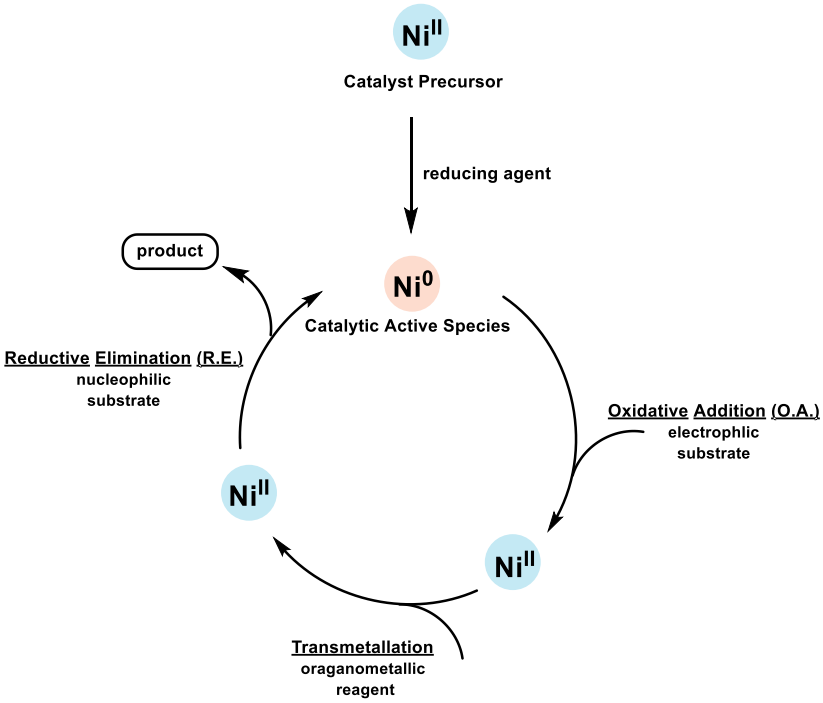

Figure 1-3. General reaction mechanism for nickel-catalyzed cross-coupling reactions.

1-2. Ligand Effect for Catalytic Reaction

[Ligand] is a generic term for compounds that play a role of giving/receiving electrons to/from a metal complex. Basically in this thesis, we mainly take the ligand as σ-electron donor from ligand to metal, so we omit describing the other coordination mode.

There are roughly two types of coordination form in metal complexes. One is L-type ligand, which donates two electrons to the empty d orbital of the metal center to form σ-bond. At this time, there occurs a phenomenon called "back-donation" of electrons from the occupied metal d orbit center to the unoccupied ligand π * orbital. (Figure 1-4) The other one is X type ligand corresponding to many anionic compounds. Needless to say, since it has a negative charge, an anionic compound performs a nucleophilic attack to the metal complex. Therefore, the oxidation state of the metal center increases by +1.

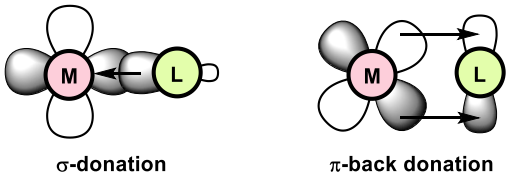

Figure 1-4. Binding in transition metal-ligand.

In the conventional catalytic reaction, the ligand is an important key factor affecting the reaction efficiency and selectivity of the product obtained by the catalytic reaction.[3] Usually the reactivity of the metal complex depends on the steric effect and electronic influence of ligand. For example in the catalytic cross-coupling reactions, the steric effect of the ligand means an increase in kinetic stability of the catalytically active species and promotion of a reductive elimination reaction by steric repulsion between ligands. On the other hand, regarding the electronic effect, it is assumed that the reactivity in oxidative addition process is improved by electron donation to the metal center. Recent studies have revealed that electron-donating ligands in some metal complex can improve the efficiency

of catalytic reactions as described above. In particular, phosphorus-based ligands are frequently used as representative ancillary ligands.[4-7] (Figure 1-5) Phosphine is an organic phosphorus compound, and trivalent and pentavalent tautomers exist.

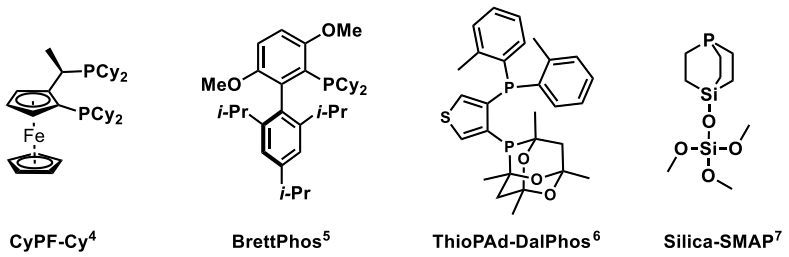

Figure 1-5. Optimized ligands in some catalytic reaction.

Alkyls and arylphosphines increase the electron density of metal center due to their strong σ-donating properties. It is also known that stable complex forms due to the strong back-donation from the metal d orbit to σ* orbit of P-R bond which hybridizes with phoshorus d orbit. In particular, tert-butyl phosphine ($PtBu_3$) is very bulky and the strongest donor among trialkylphosphines due to the three tert-butyl groups, so it is useful as an electron rich ligand. [8]

1-3. N-Heterocyclic Carbene Chemistry

Catalytic chemistry using phosphine as a ligand has continued developping even in recent. However, since alkyl or aryl C-H bond in the coordinating phosphine ligand can sometimes add to the adjacent active metal center, it can also cause poisoning of the catalyst in catalytic reaction.[9] Recently, an alternative ligand called N-heterocyclic carbene (NHC) has been reported and attracts attention. The NHC ligand is a stable triplet carbene species that can be easily synthesized and isolated. Several general synthetic methods exist. The best known synthetic method begins with the synthesis of diimine derivatives using glyoxal derivatives which are primary amines and dialdehydes. Diimine

and imidazolium compounds are relatively stable and can be synthesized in large quantities. Carbene can be formed from an imidazolium compound by a deprotonation reaction using a strong base. (Scheme 1-1, eq 1) Asymmetric imidazole carbenes, where different groups are substituted on the pair of imidazole nitrogens, have also been developed, and those can be synthesized by reacting a mono-substituted imidazole compound with a halogenated compound. (Scheme 1-1, eq 2) Furthermore, relatively stable carbene is also possible to be isolated by introducing bulky substituents onto the imidazole nitrogen.

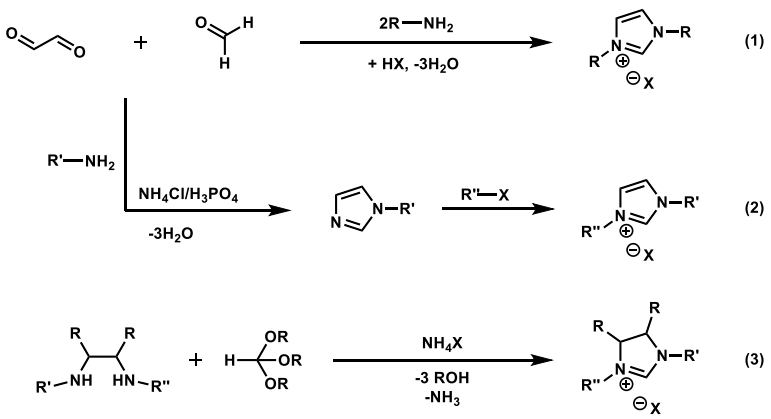

Scheme 1-1. Various approach to the synthesis of normal NHC.

In general, carbene has only 6 electrons around the carbon. So it is chemically unstable because it deviates from the octet rule and it always has high reactivity. However, if a nitrogen atom is present at the adjacent site of the carbene carbon, the empty orbital of the carbene and the unshared electron pair of nitrogen are conjugated. Because the induction effect caused by the electronegativity of nitrogen is added, the carbene is stabilized. In addition, this effect is strengthened by being conformationally fixed in a ring shape. Due to its specific nature, it stabilize many transition metal complexes, and moreover, various substituents have been introduced onto the imidazole nitrogens.[10-13] (Figure 1-6)

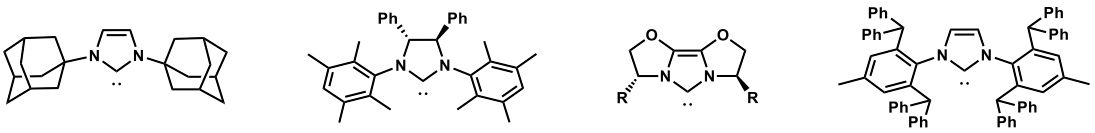

Figure 1-6. Examples of unique NHC ligands design

In 1992, Arduengo reported that it is possible to synthesize isolable carbenes without causing dimerization between carbenes by introducing bulky substituents at the wingtip groups on the imidazole nitrogen.[10] Grubbs, et al. showed that a bulky NHC ligand played effective role in ruthenium-catalyzed metathesis reaction to form unsaturated reaction site by kicking off the trans-located phosphine ligand in 1999. [14] (Figure 1-7)

Meanwhile, Herrman, et al. reported that adding NHC ligand to palladium catalyst precursor is effective for catalytic cross-coupling reaction.[15] In palladium complexes, Nolan, et al. synthesized several highly active NHC complexes of palladium(II) for cross-coupling reactions.[16] Although there are not many examples of nickel complexes, Matsubara, et al. reported similar reports in our laboratory.[17] These reports have one thing in common. Only one NHC molecule binds to a metal center. In these reports, a ligand located at the trans position of the NHC ligand is readily eliminated to form coordinatively unsaturated active site. Such reactivity can be derived from the bulkiness and σ-electron donating ability of the NHC ligand And moreover, it can stabilize kinetically unsaturated site of the metal center.

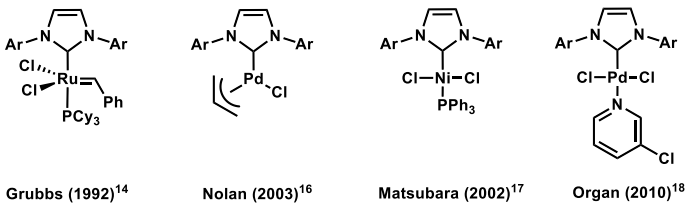

Figure 1-7. Active pre-catalyst bearing bulky NHC ligands

Since the NHC ligand can adjust its steric bulkiness, it is also used as a tool for stabilizing unstable chemical species. (Figure 1-8) Driess, et al. succeeded in isolating silyldiium dicationic compounds for the first time by using a bidentate NHC ligand.[19] In addition, Braunschweig, et al. succeeded in synthesizing diboryl diborene compounds linked by boron and determining the structure of the diborene compound having delocalized π electrons for the first time.[20]

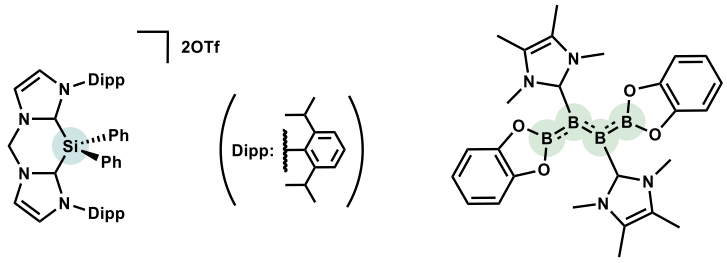

Figure 1-8. Examples of NHC-stabilized unstable silyldiium and diborene compounds.

1-4. Odd Oxidation States of Nickel Species

As to the type of oxidation state of nickel, as indicated by 1-1, the oxidation number of nickel from -1 to +4 has been known to date.[21] Among them, monovalent and trivalent, which are odd number oxidation states having unpaired electrons, have been rarely known compared with the studies of usual zero- and di-valent nickel. This is considered to be due to the problem of thermodynamic stability of monovalent or trivalent nickel species. Basically in the whole parts of this thesis, monovalent nickel species are mainly concerned.

In 1914, the first monovalent nickel complex was reported by Bellucci and Corelli,[22] and in 1970, as a result of X-ray crystal structure analysis, it was confirmed by Jarchow, Schulz and Nast et al.[23] It was an anionic, dinuclear monovalent nickel complex. Various monovalent nickel complexes have been synthesized and isolated since then. (Fig. 1-9)

[24-28] These monovalent nickel complexes are thermally stable by steric protection by their own ligand design using sterically bulky substituents. In particular, the first monovalent nickel complexes using NHC ligands are discovered accidentally by Caddick et al.[27] In this report, the reaction of $Ni(cod)_2$ with I^tBu (1,3-di-tertbutylimidazol-2-ylidene) eventually forms a monovalent nickel complex. However, it was found that the carbon - nitrogen bond of the imidazole ring was cleaved by leaving it for a long time. In the following year, 2005, Sigman et al. showed a method for dinuclear nickel (II) from the comproportionation reaction of nickel(0) and nickel(II) complexes in the presence of IPr (1,3 - bis (2,6 - diisopropylphenyl) imidazol-2-ylidene). However, there are few studies on reactivity of monovalent nickel complexes.[28]

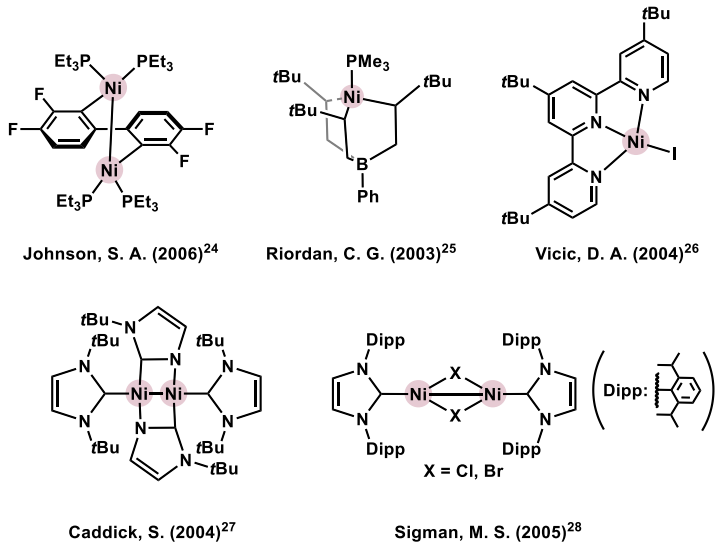

Figure 1-9. Various Ni(I) complexes bearing bulky ligands

Vicic, et al. reported that planar tetracoordinate monovalent nickel complexes are formed by treating an equivalent of terpyridine ligand with dimethylnickel(II) complex.[26] The reaction of methylnickel(I) complex with iodocyclohexane gave the product methylcyclohexane in a yield of 79%. In view of the fact that the product is given in moderate yield in the alkyl cross coupling reaction using the monovalent nickel complex

as a catalyst, it is suggested that the monovalent nickel complex is involved in the catalytic reaction. (Scheme 1-4) Vicic, et al. found that similar nickel complexes were formed from nickel(0) complex, alkyl halide, and terpyridine ligand, and found Negishi coupling using $Ni(cod)_2$ / terpyridie as a catalyst.[29] In the reaction mechanism involving the monovalent nickel complex, reaction of monovalent nickel complex with alkyl halide produces alkyl radicals along with the formation of cationic nickel(II) complex. Nickel(III) complex is formed by nucleophilic attack of radical species to cationic nickel(II) complex, and the original nickel(I) complex is regenerated by reductive elimination and organozinc reagent.[30] (Figure 1-10)

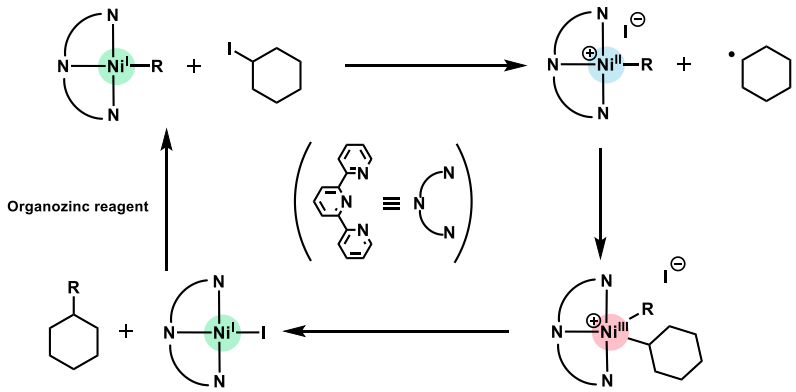

Figure 1-10. Proposed reaction mechanism for nickel-catalyzed Negishi cross-coupling by Vicic, et al.

The first catalytic reaction using nickel was reported by Kochi, et al. in 1979. Generation of monovalent nickel complex was suggested in this report. That is, when an aryl halide acts on a nickel(0) complex, electron transfer from a nickel(0) complex to an aryl halide occurs to form an ionic pair of cationic Ni(I) and anionic organic radical.[31] (Scheme 1-2) Kochi also showed that monovalent nickel complex acts as an active intermediate in the homo-coupling reaction of aryl halides using nickel catalyst. From these findings, it is suggested that by selecting an appropriate ligand, a catalytically active monovalent nickel complex can be formed in the activation of a usual aryl halides. In

these reactions, dramatic increase of the reaction rates in the coupling reactions are a characteristic feature. The reason for this is considered to be that metal complexes having active unpaired electrons are used, and that the reduction from an unstable trivalent radical species to a monovalent species can be accelerated.

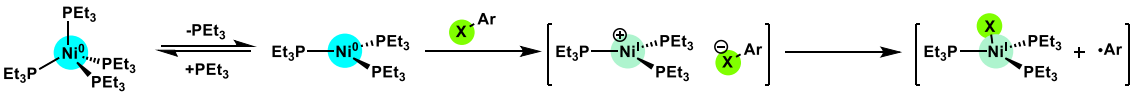

Scheme 1-2. Oxidative addition of aryl halides to [Ni(PEt3)4]: Kochi's mechanistic Proposal.

On the other hand, in our laboratory, it has become clear that monovalent nickel complex can be accidentally obtained by using nickel(0) complex with aryl halide using bulky NHC ligand IPr by Miyazaki. It also reports that the complex is isolated as a stable compound and has a certain catalytic activity against Kumada-Tamao-Corriu coupling.[32] (Scheme 1-3) Since the obtained monovalent nickel complex is a d^9 complex, it is a paramagnetic nature and is expected to be generally unstable. However, in fact, it was isolated and determined, and it became clear that it is a relatively stable monovalent complex. This complex reacts with heavy chloroform which is heavy solvent, radicals are drawn out of halogen, and quantitatively nickel(II) halogen complex is produced. It is also known that an equilibrium reaction in which one of the NHC ligand in bis-carbene monovalent nickel complex is eliminated in heavy benzene has been found to produce dinuclear nickel complex **1**. It is also known that bis-carbene monovalent nickel complex can be obtained by adding NHC ligand to dinuclear nickel complex. In 2011, Louie, et al. also successfully synthesized a similar monovalent nickel complex using a NHC ligand (1,3-bis (2,4,6-trimethylphenyl) imidazol-2-ylidene) Kumada, and Suzuki coupling reaction were achieved using this complex as catalyst.[33]

In the above study, two molecules of NHC ligand are bound to one nickel center. However, in 2001, Herrman, et al. reported that in the Kumada coupling of the aryl halide, the NHC ligand added to the nickel catalyst precursor has a larger difference in reaction rate when 1 equivalent is used for the NHC ligand .[34] From this report, and researches by Grubbs and Nolan, the following can be considered. That is, since such a monovalent nickel complex contains two bulky NHC ligands, it is highly likely to lead to a process with low activity. Therefore, in order to further improve the catalytic activity, it is expected that construction of a monovalent nickel complex having only one molecule of NHC ligand will lead to achieving high activity and highly efficient catalytic reaction.

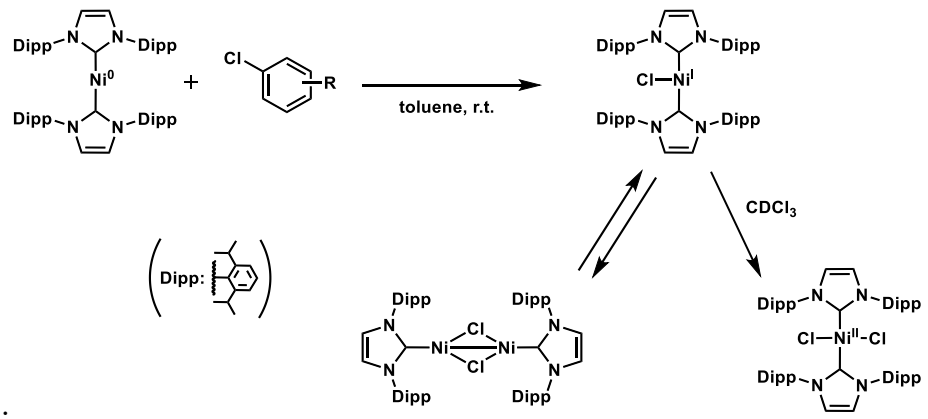

Scheme 1-3. Reactivity of bis-NHC-ligated Ni(I) complex

1-5. The Subjects and Contents of This Thesis

In this paper, we aimed to develop new catalytic reaction process via Ni (I) / NHC catalyst system and to obtain knowledge about its mechanism. Below is a brief summary of the content of each chapter.

[Chapter 2] proposes a novel catalytic process centered on novel aryl bridged Ni(I) dinuclear complex. We are also considering several experimental results that resulted in that background.

In [Chapter 3], we have developed various unprecedented monomeric Ni(I) complexes and discussed the structural features, spin state, etc. of them. In addition, Buchwald-Hartwig amination and Suzuki-Miyaura cross-coupling reaction, which are catalytic reactions using the obtained complexes, are carried out, and their catalytic activity is also considered.

In [Chapter 4], we developed a Ni(I) complex with a bidentate ligand bipyridyl ligand bound, focusing on its specific spin state, reactivity and ability as a catalyst . Especially by introducing bipyridyl ligand, handling became easier, so we investigated some reactivity by nickel monovalent species making use of it.

1-6. References

1. (a) Chauvin, Y. *Angew. Chem. Int. Ed*. **2006**, *45*, 3741-3747. (b) Grubbs, R. H. *Angew. Chem. Int. Ed.* **2006**, *45*, 3760-3765. (c) Schrock, R. R. *Angew. Chem. Int. Ed*. **2006**, *45*, 3748-3759.
2. [C-H bonds activation], recent reviews: (a) Philipp, Z.; Christian, L.; *J. Am. Chem. Soc.* **2017**, *139*, 4233-4242. (b) Yamaguchi, J.; Muto, K.; Itami, K. *Topics in Current Chemistry* **2016**, *374*, 1-33. (c) Bo, S.; Zhi-Chao, C.; Zhang-Jie, S. *Acc. Chem. Res.* **2015**, *48*, 886−896. (d) Castro, L. C.M.; Chatani, N. *Chem. Lett.* **2015**, *44*, 410-421. (e) Mickael, H.; Vincent, R.; Chetcuti, M. J. *ACS Catalysis* **2015**, *5*, 1283-1302. (f) Andrew C. M. *C-H Bond Activation in Organic Synthesis* **2015**, 113-144. (g) Xiao-hua, C.; Bing, X. *ARKIVOC* **2015**, 184-211. [C-O bonds activation], recent reviews: (a) Xin, L.; Xin, H. *J. Organomet. Chem.* **2018**, *864*, 68-80. (b) Lin, G; Magnus, R. *Acc. Chem. Res.* **2018**, *51*, 1185-1195. (c) Manoj, M.; Pankaj, B. *New J. Chem.,* **2017**, *41*, 13211-13214. (d) Tobisu, M.; Chatani, N. *Topics in Current Chemistry* **2016**, *374*, 1-28. (e) Tobisu, M.; Chatani, N. *Acc. Chem. Res.* **2015**, *48*, 1717-1726. (f) Bo, S.; Zhi-Chao, C.; Zhang-Jie, S. *Acc. Chem. Res.* **2015**, *48*, 886−896. (g) Lukas, J, G.; Kaethe, G.; Corneliu, S. *Angew. Chem. Int. Ed.* **2009**, *48*, 3569 – 3571. [C-C bonds activation], recent reviews: (a) Lin, G; Magnus, R. *Acc. Chem. Res.* **2018**, *51*, 1185-1195. (b) Manoj, M.; Pankaj, B. *New J. Chem.,* **2017**, *41*, 13211-13214. (c) Valentine, P. A. *ACS Catalysis* **2015**, *5*, 1964-1671. (d) Bo, S.; Zhi-Chao, C.; Zhang-Jie, S. *Acc. Chem. Res.* **2015**, *48*, 886−896. (e) Ogata, K.; Fukuzawa, S. *Yuki Gosei Kagaku Kyokaishi* **2012**, *70*, 2-10. (f) Nakao, Y. *Shokubai* **2008**, *50*, 705-709. [C-N bonds activation], for examples: (a) Hui, Y.; Bin, H.; Hanmin, H. *Chem. Eur.J.* **2018**, *24*, 7114–7117. (b) Hui, Y.; Bin, H.; Hanmin, H. *J. Org. Chem.* **2018**, *83*, 13922-13929. (c) Jennie, L.; Weiye, G.; Brian, P. B.; Joseph, W. T.; John W. T.; Michelle R. G.;

Mary, P. W. *Org. Lett.* **2018**, *20*, 3030-3033. (d) Hui, Y.; Bin, H.; Hanmin, H. *Org. Lett.* **2017**, *19,* 3520-3523. (e) Corey H. B.; Jennie, L.; Jianyu, X.; Jacob, J. P.; Mary, P. W. *J. Am. Chem. Soc.* **2017**, *139*, 5313-5316. (f) Shengyang, N.; Wenzhong, Z.; Haibo, M.; Jianlin, H.; Yi, P. *Org. Lett.* **2017**, *19*, 2536-2539. (g) Shicheng, S.; Michal, S. *Synthesis* **2017**, *49*, 3602-3608.

3. For examples, see: (a) Ligand Design in Metal Chemistry; Stradiotto, M.; Lundgren, R. J. Eds. Wiley-VCH: Weinheim, Germany, 2016. (b) Andy, A. T.; Klaus, S.; Ilia, K.; Zhaohong, L.; Peng, L.; Buchwald, S. L. *J. Am. Chem. Soc.* **2018**, *140*, 13976-13984. (c) Zhang, Y.; Lavigne, G.; Lugan, N.; Cesar, V. *Chem. Eur.J.* **2017**, *23,* 13792-13801. (d) Kim, J.; Cho, S. H. *ACS Catalysis* **2019**, *9*, 230-235. (e) Liu, W.; Sahoo, B.; Spannenberg, A.; Junge, K.; Beller, M. *Angew. Chem. Int. Ed.* **2018**, *57*, 11673-11677. (f) Naksomboon, K.; Valderas, C.; Gomez-Martinez, M.; Alvarez-Casao, Y.; Fernandez-Ibanez, M. A. *ACS Catalysis* **2017**, *7*, 6342-6346.
4. Bronco, S.; Consiglio, G.; Di Benedetto, S.; Fehr, M.; Spindler, F.; Togni, A. Helvetica Chimica Acta 1995, 78, 883-886.
5. Fors, B. P.; Watson, D. A.; Biscoe, M. R.; Buchwald, S. L. *J. Am. Chem. Soc.* **2008**, *130*, 13552-13554.
6. Clark, J. S. K.; McGuire, R. T.; Lavoie, C. M.; Ferguson, M. J.; Stradiotto, M. *Organometallics* **2019**, *38*, 167-175.
7. Kawamorita, S.; Hamasaka, G.; Ohmiya, H.; Hara, K.; Fukuoka, A.; Sawamura, M. *Org. Lett.* **2008**, *10*, 4697-4700.
8. Littke, A. F.; Fu, G. C. *Angew. Chem. Int. Ed.* **1999**, *38*, 2411-2413.
9. (a) Kar, G.; Priver, S. H..; Jones, L. A.; Guo, Si-Xuan; Torriero, A. A. J.; Bond, A. M.; Bennett, M. A.; Bhargava, S. K. *Dalton Trans.* **2015**, *44*, 3367-3377. (b) Estevan, F.; Garcia-Bernabe, A.; Lahuerta, P.; Sanau, M.; Ubeda, M. A.; Ramirez de Arellano, M. C. *Inorg. Chem.* **2000**, *39*, 5964-5969. (c) Estevan, F.; Garcia-Bernabe, A.; Lahuerta, P.; Sanau, M.; Ubeda, M. A.; Galan-Mascaros, J. R. *J. Organomet. Chem.* **2000**, *596*, 248-251. (d) Aarif, A. M.; Estevan, F.; Garcia-Bernabe, A.; Lahuerta, P.; Sanau, M.; Ubeda, M. A. *Inorg. Chem*. **1997**, *36*, 6472-6475.
10. Arduengo, A. J. III; Kline, M.; Calabrese, J. C.; Davidson, F. *J. Am. Chem. Soc.* **1991**, *113*, 9704-9705.
11. Jensen, D. R.; Sigman, M. S. *Org. Lett*. **2003**, *5*, 63-65.
12. Glorius, F.; Altenhoff, G.; Goddard, R.; Lehmann, C. *Chem. Commun*. **2002**, *22*, 2704-2705.
13. Berthon-Gelloz, G.; Siegler, M. A.; Spek, A. L.; Tinant, B.; Reek, J. N. H.; Marko, I. E. *Dalton Trans.* **2010**, *39*, 1444-1446.
14. Ulman, M.; Grubbs, R. H. *J. Org. Chem.* **1999**, *64*, 7202-7207.
15. Weskamp, T.; Bohm, V. P. W.; Herrmann, W. A. *J. Organomet. Chem.* **1999**, *585*, 348-352.
16. Viciu, M. S.; Germaneau, R. F.; Nolan, S. P. *Org. Lett*. **2002**, *4*, 4053-4056.
17. Matsubara, K.; Ueno, K.; Shibata, Y. *Organometallics* **2006**, *25*, 3422-3427.

18. Organ, M. G.; Abdel-Hadi, M.; Avola, S.; Hadei, N.; Nasielski, J.; O'Brien, C. J.; Valente, C. *Chem. Eur.J.* **2007**, *13,* 150-157.
19. Hermannsdorfer, A.; Stephan, D. W.; Driess, M. *Chem. Commun.,* **2018**, *54*, 13523—13526
20. Hermann, A.; Cid, J.; Mattock, J. D.; Dewhurst, R. D.; Krummenacher, I.; Vargas, A.; Ingleson, M. J.; Braunschweig, H. *Angew. Chem. Int. Ed*. **2018**, *57*, 10091 –10095.
21. Lin, C.-Y.; Power, P. P. *Chem. Soc. Rev.*, **2017**,*46*, 5347-5399.
22. Bellucci, I.; Corelli, R. *Z. Anorg. Allg. Chem.*, **1914**, *86*, 88‑104.
23. (a) Jarchow, O.; Schulz, H.; Nast, R. *Angew. Chem., Int. Ed. Engl.*, **1970**, *9*, 71. (b) Jarchow, O. *Z. Kristallogr.*, **1972**, *136*, 122‑134.
24. Keen, A. L.; Johnson, S. A. *J. Am. Chem. Soc.* **2006**, *128*, 1806-1807.
25. Schebler, P. J.; Mandimutsira, B. S.; Riordan, C. G.; Liable-Sands, L. M.; Incarvito, C. D.; Rheingold, A. L. *J. Am. Chem. Soc.* **2001**, *123*, 331-332.
26. Anderson, T. J.; Jones, G. D.; Vicic, D. A. *J. Am. Chem. Soc.* **2004**, *126*, 8100-8101.
27. Caddick, S.; Cloke, F. G. N.; Hitchcock, P. B.; Lewis, A. K. de K. *Angew. Chem. Int. Ed.* **2004**, *43*, 5824-5827.
28. Dible, B. R.; Sigman, M. S.; Arif, A. M. *Inorg. Chem*. **2005**, *44*, 3774-3776.
29. Jones, G. D.; McFarland, C.; Anderson, T. J.; Vicic, D. A. *Chem. Commun*. **2005**, *33*, 4211-4213.
30. Jones, G. D.; Martin, J. L.; McFarland, C.; Allen, O. R.; Hall, R. E.; Haley, A. D.; Brandon, R. J.; Kanovalova, T.; Desrochers, P. J.; Pulay, P.; Vicic, D. A. *J. Am. Chem. Soc.* **2006**, *128*, 13175-13183.
31. Tsou, T. T.; Kochi, J. K. *J. Am. Chem. Soc.* **1979**, *101*, 6319-6332.
32. Miyazaki, S.; Koga, Y.; Matsumoto, T.; Matsubara, K. *Chem. Commun.* **2010**, *46*, 1932.
33. Zhang, K.; Conda-Sheridan, M.; Cooke, S. R.; Louie, J. *Organometallics* **2011**, *30*, 2546-2552.
34. Bohm, V. P. W.; Gstottmayr, C. W. K.; Weskamp, T.; Herrmann, W. A. *Angew. Chem. Int. Ed.* **2001**, *40*, 3387-3389.

Chapter 2
Dimeric Ni(I)/NHC species in catalysis

2-1. Introduction

Considerable progress has been made during the course of the last three decades toward the development of organotransition-metal-catalyzed cross-coupling reactions of aryl halides, using various metal catalysts or catalyst precursors with ligands and/or cocatalysts. These methods have been successfully applied to the synthesis of a large number of organic products for electronic devices, liquid crystals, and medicinal chemistry.[1] The Kumada–Tamao–Corriu cross-coupling reaction of an aryl or alkyl halide with a Grignard reagent in the presence of a Ni, Pd, Co, or Fe catalyst is one of the most useful reactions for the formation of aryl–aryl or alkyl–aryl bonds under mild conditions.[1]

A general catalytic system using a mixture of $Ni(cod)_2$ and a bulky N-heterocyclic carbene (NHC) ligand, such as IPr or IMes, is widely employed in various cross-coupling reactions including the Kumada–Tamao–Corriu cross-coupling reactions.[2] Despite the wide variety of substrates and applications that have been developed for coupling reactions involving Grignard reagents, very little is currently known about the mechanisms of these reactions. The classical catalytic cycle proposed for these transformations is shown in Scheme 2-1(1).[3] In contrast, the results of several studies involving Ni and Pd catalysts have provided evidence that radical pathways, including single-electron-transfer processes, are involved in the cross-coupling reactions.[4] We have developed a well-defined Ni(I) compound bearing a bulky NHC, $NiCl(IPr)_2$ (where IPr is 1,3-bis(2,6-diisopropylphenyl)imidazol-2-ylidene), which was active in the Kumada coupling reaction of aryl halides.[5] The active Ni(I) species could be generated in situ in the cross-coupling reactions reported above, because this Ni(I) complex, $NiCl(IPr)_2$, can be formed from a mixture of $Ni(cod)_2$, IPr, and an aryl halide.[5] Several other well-defined Ni(I) complexes have also been reported to act in a range of other catalytic cycles.[6]

Scheme 2-1(2) shows a proposed catalytic cycle between Ni(I) and Ni(III) species. It is noteworthy, however, that there have been no studies in the literature providing clear evidence of how these reactions proceed, including, for example, reports pertaining to the structures of possible intermediates. This lack of information prompted us to investigate the mechanism of the Kumada coupling reaction using Ni(I) species to develop a deeper mechanistic understanding of the reaction. The work in this study is based on the hypothesis that a dinuclear Ni(I) species would be more plausible as an intermediate in these reactions than a mononuclear Ni(I) species (Scheme 2-1(3),(4)). This hypothesis was formed on the basis that the unpaired electrons on the nickel centers could readily form metal–metal bonds in the presence of an appropriately bulky ligand, which could stabilize the formation of coordinatively unsaturated dinuclear compounds that would be capable of performing as highly active and efficient cooperative catalysts.

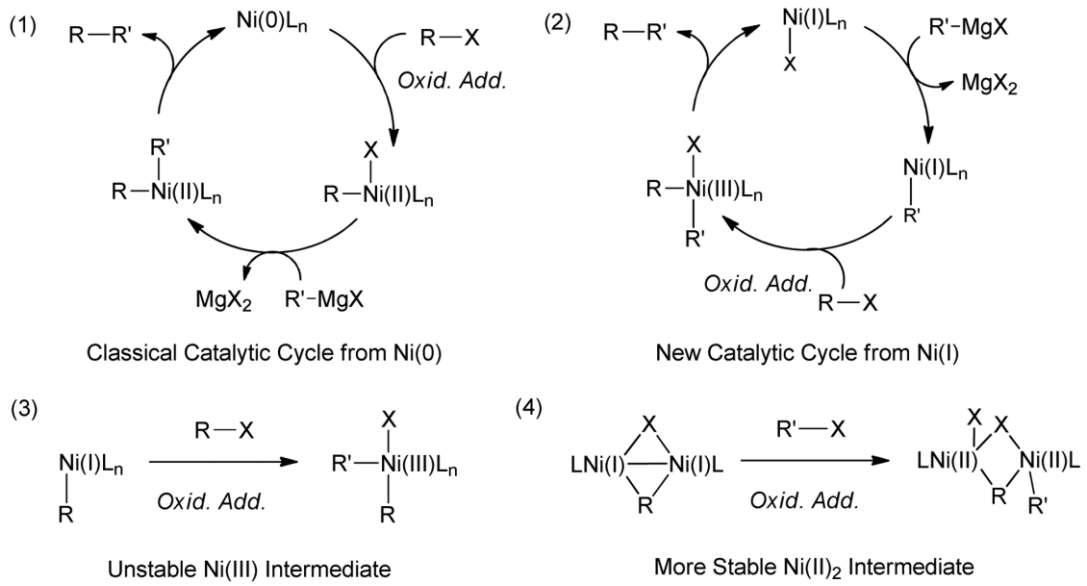

Scheme 2-1. (1) Classical Catalytic Cycle between Ni(0) and Ni(II), (2) Proposed Cycle between Ni(I) and Ni(III), (3) Oxidation States in the Oxidative Addition to a Monomeric Ni(I) Center, and (4) Oxidation States of the Dimeric Ni Centers

Dinuclear complexes containing two linked metal atoms have attracted considerable attention as potential catalysts for a variety of organic transformations, because synergistic and cooperative effects by the multinuclei centers in catalysis can activate inert and/or specific bonds much more efficiently than the corresponding mononuclear catalysts.[7-9] However, there are very few examples in the literature of dinuclear catalysts that have been designed and applied to cross-coupling reactions. A dinuclear nickel catalyst using a multidentate ligand was used to catalyze the Negishi cross-coupling reaction of an aryl chloride, where it performed much more effectively than a mononickel catalyst system.[10] In palladium chemistry, dinuclear Pd(I) complexes have been reported to catalyze the Buchwald–Hartwig amination of aryl halides, even at room temperature.[11a] Schoenebeck et al. also recently studied catalytic cross-coupling reactions of aryl halides and the mechanism using dinuclear Pd(I) complexes.[11b-d]

With regard to the dinuclear Ni(I) complexes discussed in this report, the oxidation states of the nickel atoms could be regarded as the most important feature of their catalytic cycle. Oxidative addition to a mononuclear Ni(I) complex would lead to a formal change in oxidation state of the nickel atom from +1 to +3 (Scheme 2-1(3)).[3] In contrast, oxidative addition to a dinuclear Ni(I) complex would lead to a change in the formal oxidation states of both nickel atoms from +1 to +2. Therefore, we hypothesized that the two stable nickel(II) centers are generated favorably in this diNi(I) catalyst system (Scheme 2-1(4)). NHC ligands are some of the most versatile and useful candidates for the construction of active catalysts, because they are strongly electron donating (i.e., two electrons) and can also generate strong trans effects.[12] Bulky NHC ligands, such as IPr and IMes (where IMes is 1,3-bis(2,4,6-trimethylphenyl)imidazol-2-ylidene), have been used to good effect in various catalytic cross-coupling reactions, providing high levels of efficiency and

chemoselectivity. Among the many Ni(I) complexes reported to date bearing a range of phosphorus and other ligands,[13] several recent reports have revealed that bulky NHC ligands can also kinetically stabilize Ni(I) species and that the resulting systems can be used to catalyze various reactions, including Kumada–Tamao–Corriu coupling,[4,6b,6c]Suzuki coupling,[6a] Buchwald–Hartwig amination,[6b] and hydrodehalogenation reactions.[6d] It is noteworthy that mononuclear Ni(I) NHC complexes were used in all of these examples. On the other hand, the synthesis and stoichiometric reactions of a variety of dinuclear Ni(I) IPr complexes having a Ni–Ni single bond have been reported.[14] Taken together, these results provide a strong indication that the efficiency of catalytic reactions using these ligands would differ considerably from those using smaller ligands, most probably because of differences in the mechanisms of these reactions resulting from differences in the oxidation states of the metal centers.

Herrmann et al. reported that the catalytic activity of an in situ generated active nickel species in the Kumada–Tamao–Corriu cross-coupling of aryl fluoride was strongly dependent upon the amount of IPr added to the system.[15] The addition of 1 equiv of NHC to a nickel precursor provided a nickel species bearing one NHC ligand that was much more active than the corresponding nickel species bearing two NHC ligands generated by the addition of 2 equiv of NHC. As noted above, $NiCl(IPr)_2$ can act as an active catalyst but has two molecules of IPr.[4] Therefore, it remains unclear how a nickel catalyst bearing only one IPr ligand was more active in the cross-coupling reactions. The results of our most recent study showed that the complex formed from mixed IPr/PPh_3 and Ni(I) exhibited higher activity in the Kumada coupling reaction of aryl halides than $NiCl(IPr)_2$.[6b] Here, we found that the oxidative addition of aryl chloride to an in situ generated nickel(0) complex bearing an IPr ligand gave a coordinatively unsaturated

dinuclear Ni(I) complex, which exhibited catalytic performance higher than that of the monomeric Ni(I) catalyst $NiCl(IPr)_2$. We wish to report the isolation and structural elucidation of these dinickel complexes, as well as an evaluation of their catalytic performance. The results of mechanistic studies, including stoichiometric reactions, kinetic experiments, and DFT calculations, will also be discussed.

2-2. Synthesis and Characterizations

2-2-1. Synthesis and Structures of the Dinickel(I) Aryl Complexes.

The dinuclear Ni(I) oxidative addition products $[Ni(IPr)]_2(\mu\text{-}Cl)(\mu\text{-}\eta^2\text{-}C_6H_4R)$ (**1a**, R = 4-CH_3; **1b**, R = 4-OCH_3) were successfully prepared by addition of *p*-chlorotoluene and *p*-chloroanisole to a solution of $Ni(cod)_2$ and IPr (1 equiv with respect to nickel) in THF at room temperature (Scheme 2-2). Instead of forming the expected mononickel(II) adducts via the oxidative addition of the aryl halides to a Ni(0) center, these two oxidative addition reactions rather unexpectedly afforded **1a**,**b** in a selective manner. The isolated yields of **1a**,**b** following their purification upon recrystallization were 44 and 29%, respectively. Trace amounts of the dinuclear μ-chloride $[Ni(IPr)]_2(\mu\text{-}Cl)_2$ (**2**)[16] and 4,4′-dimethylbiphenyl or 4,4′-dimethoxybiphenyl were detected in the crude ^{1}H NMR spectra. Addition of only IPr to a solution of $Ni(cod)_2$ in THF gave a dark green solution, which most likely contained an $(IPr)Ni^0$ THF complex rather than a $(NHC)Ni^0$ dimer (reddish brown).[17] The solution became dark reddish brown following the addition of *p*-chlorotoluene, indicating formation of the compound **1a**. In the absence of IPr, $Ni(cod)_2$ did not react with *p*-chlorotoluene under these conditions. Furthermore, the use of other nonpolar solvents, including *n*-hexane and benzene-d_6, resulted in the formation of

numerous byproducts, and the addition of 2 equiv of IPr to $Ni(cod)_2$ followed by *p*-chlorotoluene resulted in the formation of the mononuclear Ni(I) product $NiCl(IPr)_2$ (**4**).[4]

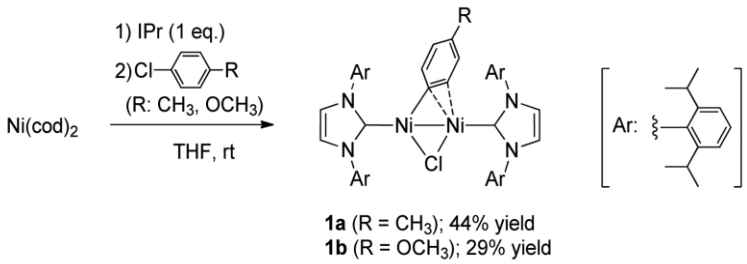

Scheme 2-2. Synthesis of Dinickel(I) Oxidative Addition Products 1a,b

Addition of 1 equiv of a Grignard reagent and aryl halide independently to compound **1a** in THF at room temperature afforded diNi(I) complexes, representing interesting transformations. The reaction of **1a** with *p*-tolylmagnesium chloride for 18 h led to a transmetalation reaction at the bridging chloride ligand, which yielded the corresponding biaryl complex $[Ni(IPr)]_2(\sigma{:}\eta^2\text{-}C_6H_4CH_3)_2$ (**3a**) (Scheme 2-3(1)). The yield of **3a** as dark green crystals following its purification upon recrystallization from THF at −30 °C was 43%.

On the other hand, the reaction of **1a** with 4-chlorotoluene afforded the dinickel μ-chloride **2** (Scheme 2-3(2)). A similar outcome was also observed for the reaction of **1a** with several other aryl halides, including *p*-chloroanisole and chlorobenzene. The formation of **2** from the reactions of **1a** with a range of aryl halides suggested that the oxidative addition of the aryl chlorides to **1a** and the subsequent reductive elimination of the biaryl products were occurring at the unsaturated dinickel centers. Detailed experimental results and discussion are given below. Interestingly, the reverse reaction from **2** to **1a** was demonstrated by the reaction of **2** with 1.0 equiv of *p*-tolylmagnesium chloride (Scheme 2-3 (2)). A crude ^{1}H NMR spectrum of the reaction showed that **1a** was

being formed as the major species, together with only small amounts of **3a** and **2**. It is noteworthy that the dinuclear framework in **1a** remained intact even after the stoichiometric reactions.

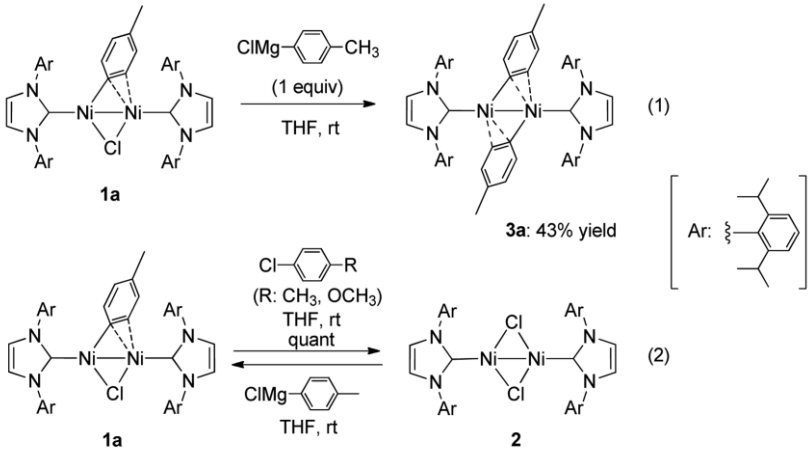

Scheme 2-3. Reactions of 1a (1) with Tolylmagnesium Chloride and (2) with 4-Chlorotoluene and 4-Chloroanisole and the Reverse Reaction

The ^{1}H NMR spectra of **1a**,**b** showed characteristic diamagnetic high-field signals at δ 6.07 (4H in **1a**) or δ 6.17 and 6.72 (2H + 2H in **1b**), which were attributed to the aryl protons of the bridging tolyl or anisyl group. These signals indicated the occurrence of a shielding effect derived from the aryl rings of the IPr ligands, where the bridging aryl protons were located in close proximity to the aryl rings of IPr. The integrated ratio of the signals assigned as the methyl protons of the σ-tolyl or anisyl moiety and the isopropyl methine protons of the carbene ligand was 3:8, which indicated that the ratio of the σ-aryl moiety and the carbene ligand was 2:1. This observation suggested formation of an oxidative addition product bearing two NHC ligands in a manner similar to that reported by Radius et al.[18,19] for a series of nickel biscarbene complexes. However, the actual structures of **1a**,**b**, which were determined by X-ray crystallography using single crystals derived from hexane solutions, revealed, rather unexpectedly, that compounds **1a**,**b** were coordinatively unsaturated 30e dinickel adducts. The oxidation state of each nickel atom

was found to be +1, and therefore in contrast to that of the divalent mononickel analogues generated as a result of the oxidative addition of aryl halides to Ni(0) complexes.[20] The distance between the two nickel centers in **1a** was found to be 2.3954(5) Å (Figure 2-1), which suggested the existence of a single bond.[14] One of the C═C bonds in the σ-aryl moiety was coordinated to one of the two metal centers in the η^2 mode, and the ring structure was close to that of a cyclohexatriene, in that the C3–C4 and C5–C6 bond lengths were 1.382(5) and 1.375(4) Å, shorter than the C2–C3, C4–C5, and C6–C1 bond lengths, which were 1.417(4), 1.406(4), and 1.431(4) Å, respectively. The C1–C2 bond length was elongated to 1.423(4) Å because it was π-coordinated to the nickel atom. However, solution-phase NMR analyses of compound **1a** suggested that the protons and carbons belonging to this aryl moiety, as well as those of the IPr ligand, were symmetrical.[21] The links between the two nickel atoms and the carbene carbon atoms were slightly bent, as shown by the Ni2–Ni1–C8(carbene) and Ni1–Ni2–C35(carbene) bond angles, which were 158.50(8) and 167.98(8)°, respectively. The generation of a space-filling model of **1a** from the crystal structure data revealed that the phenyl rings and the methyl groups of the two IPr ligands formed a pocket over the two nickel atoms and tightly surrounded the σ-tolyl moiety (Figure 2-2). The bending of the Ni–Ni–C(carbene) bond angles could therefore be explained in terms of the steric hindrance between the IPr and the tolyl groups. Depending on the leaning direction of the σ-aryl moiety in the fluxional motion in solution, the geometry of each nickel center could change slightly, which would result in a change in the Ni–Ni–C(carbene) bond angle. The crystal structure of **1b** was also determined and was found to be quite similar to that of **1a** (see the S.I.).

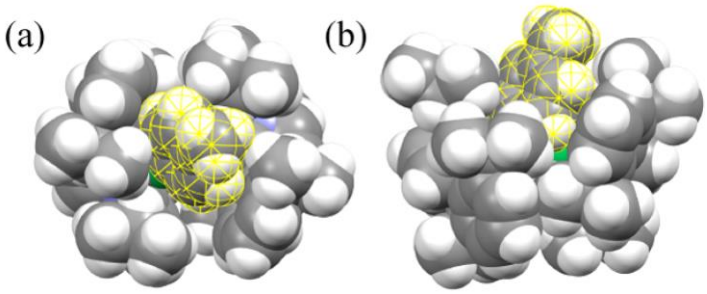

Figure 2-2. Space-filling models of 1a generated from the crystallographic data (yellow mesh, σ-tolyl group; gray, carbon; white, hydrogen; green, nickel): (a) top view; (b) side view.

A single-crystal X-ray diffraction study of **3a** was also conducted and revealed successful incorporation of the bridging 4-tolyl group instead of chlorine. The structural features of **3a** were also found to be similar to those of **1a**, as shown in Figure 2-1b. The Ni–Ni distance was determined to be 2.4067(8) Å (Table 2-1), which indicated the presence of a bonding interaction between the two nickel atoms, and one of the C═C bonds of each σ-aryl group was coordinated to a nickel center, being similar to that observed in **1a**. Other bimetallic coordination effects for μ-σ-aryl groups have been reported in gold complexes.[22] Johnson et al. reported coordination in diNi(I) complexes similar to that in complexes **1** and **3**.[23]

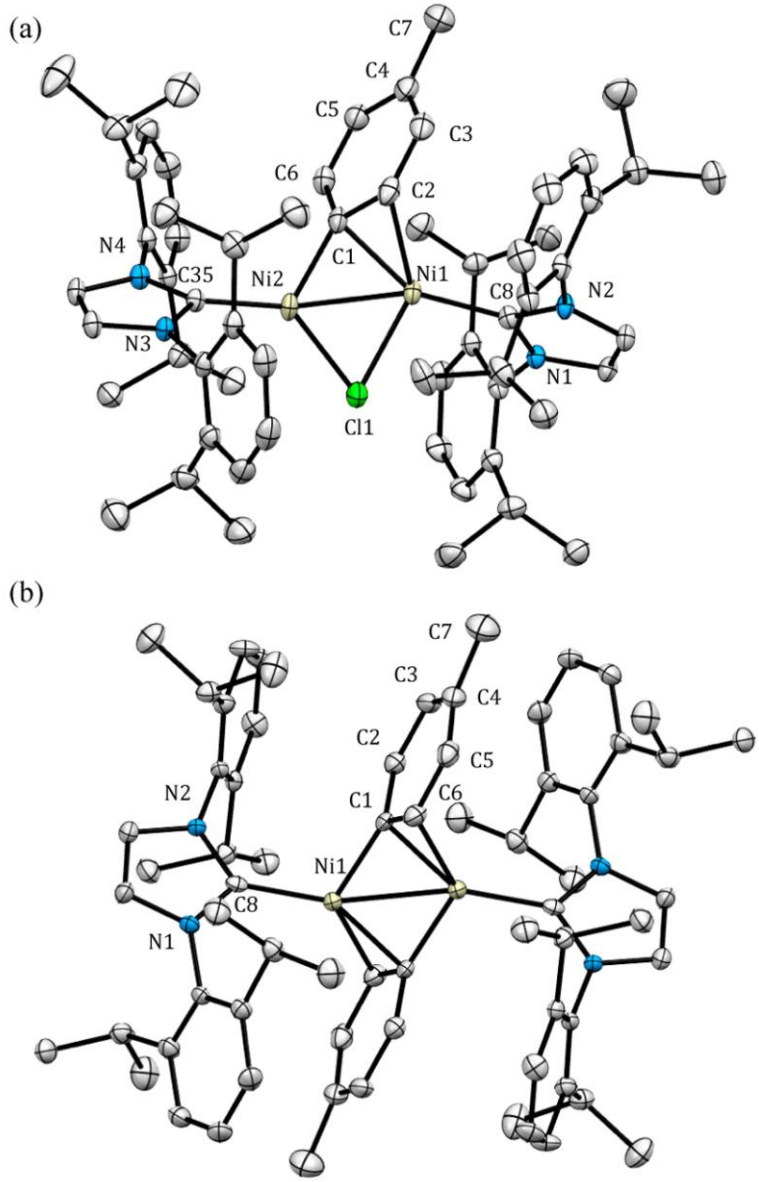

Figure 2-1. ORTEP drawings of (a) 1a and (b) 3a (thermal ellipsoids at the 50% probability level). All of the hydrogen atoms have been omitted for clarity. Half of the 3a molecule has been shown by a symmetric operation.

Table 2-1. Representative Bond Distances (Å) and Angles (deg) of 1a and 3a

1a		3a	
Bond Distances (Å)			
Ni1−Ni2	2.3954(5)	Ni1−Ni1′	2.4067(8)
Ni1−C1	1.983(3)	Ni1−C1	1.936(3)
Ni2−C1	1.914(3)	Ni1−C6	2.376(3)
Ni1−C2	2.210(3)	Ni1−C8	1.894(3)
Ni1−C8	1.910(3)	C1−C2	1.432(4)
Ni2−C35	1.855(3)	C2−C3	1.390(4)
C1−C2	1.423(4)	C3−C4	1.395(5)
C2−C3	1.417(4)	C4−C5	1.381(5)
C3−C4	1.382(5)	C5−C6	1.415(5)
C4−C5	1.406(4)	C6−C1	1.404(4)
C5−C6	1.375(4)		
C6−C1	1.431(4)		
Bond Angles (deg)			
Ni2−Ni1−C8	158.50(8)	Ni1′−Ni1−C8	160.12(9)
Ni1−Ni2−C35	167.98(8)	Ni1−C1−Ni1′	76.3(1)
Ni1−Cl1−Ni2	65.29(2)		
Ni1−C1−Ni2	75.8(1)		

2-3. Catalysis and Reactivity

2-3-1. Catalytic Application of 1a for the Kumada Coupling

Compound **1** was found to catalyze the Kumada cross-coupling reaction of weakly active aryl halides. Compounds **1a** and **4** exhibited clear differences in their catalytic activity, as shown in Table 2-2. For example, the coupling of 4-chloroanisole with phenylmagnesium chloride in the presence of **1a** for 18 h at ambient temperature gave 4-methoxybiphenyl in 85% yield (Table 2-2, entry 1). In contrast, the use of compound **4** as a catalyst resulted in a much lower yield of the cross-coupling product of 33% (Table 2-2, entry 3). Compound **1a** also exhibited moderate activity toward the inactive substrate 4-fluoroanisole and gave a 42% yield of the corresponding biaryl product following purification by silica gel column chromatography (Table 2-2, entry 2). It is noteworthy

that the Kumada coupling of anisole derivatives can also yield unwanted byproducts as a result of the elimination of the methoxy group.[24] Free IPr (5 equiv relative to **4**) was added to the reaction mixture to avoid the formation of the diNi(I) complex **2** in solution as a result of the slow equilibrium reaction between **4** and **2**. Furthermore, the rapid Kumada coupling of aryl chlorides in the presence of **2** was briefly discussed in our previous report.[6b]

Table 2-2. Kumada Cross-Coupling of Aryl Halides Mediated by Ni(I) Complexes

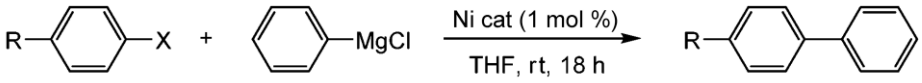

entry	cat.	R	X	additive	yield (%)[a]
1	1a	OMe	Cl		85
2	1a	OMe	F		42
3	4	OMe	Cl	IPr (5 mol %)	33
4	4	OMe	Br	IPr (5 mol %)	93
5	4	Ph	Br	IPr (5 mol %)	89

The above profiles of the Kumada coupling reactions are in good agreement with those in the literature using nickel precatalysts and the imidazolium salt IPr/HCl.[15] In our preliminary study, stoichiometric reaction of *p*-tolylmagnesium chloride in THF with the monomeric Ni(I) complex **4** gave not the transmetalated Ni(I) complex [$(IPr)_2NiPh$] or the diNi(I) complex **1a** but the reduced Ni(0) compound [$(IPr)_2Ni$] (Scheme 2-4). It can be noted that the added amount of IPr strongly affects the catalytic processes in the Kumada cross-coupling reactions.

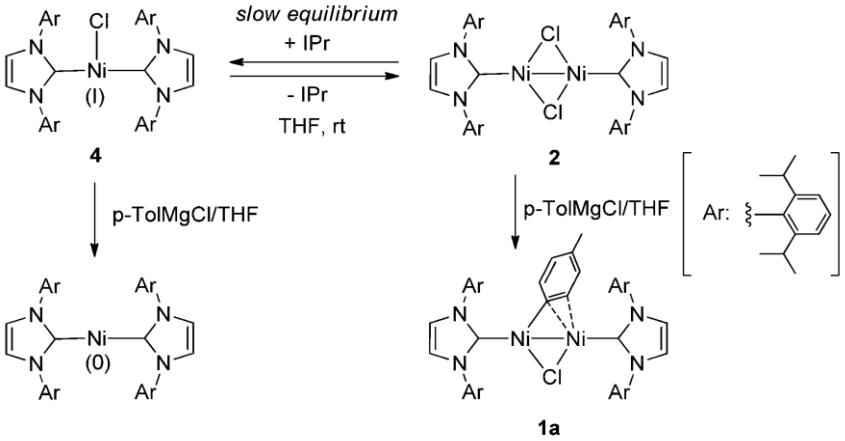

Scheme 2-4. Preliminary Stoichiometric Reactions of 2 and 4vwith Phenylmagnesium Chloride

2-3-2. Possible Dinickel Cycles in the Kumada Coupling Reaction.

The results presented above on the reactivity of the diNi(I) species suggested the possibility of two catalytic cycles in the Kumada cross-coupling of aryl halides involving the dinickel species **1**–**3**, as shown in Scheme 2-5. One of these cycles would involve the reaction of compounds **1** and **2**. Briefly, the oxidative addition of an aryl halide to **1** would result in the formation of a metastable dinickel(II) species, which would smoothly eliminate the corresponding biaryl product to give **2**. Compound **1** would then be regenerated via a transmetalation reaction with arylmagnesium chloride. A similar process involving **3** as an intermediate could also be possible. In this case, the reaction of a Grignard reagent with **1** instead of an aryl halide would result in the formation of complex **3** via a transmetalation process. The reductive elimination of biaryls in the presence of an aryl halide would then form **1** as the oxidative addition product (Scheme 2-5).

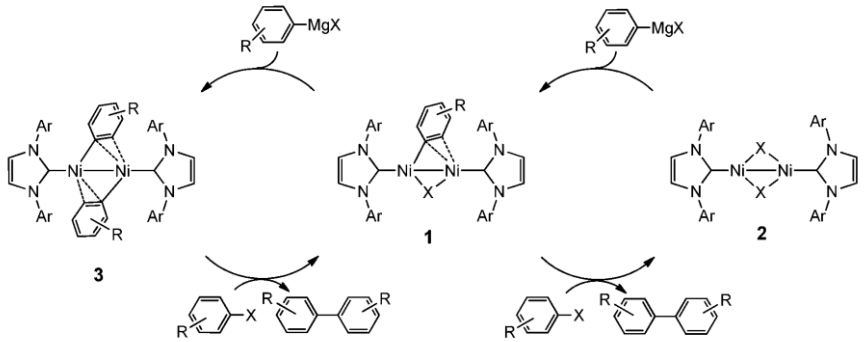

Scheme 2-5. Two Possible Reaction Mechanisms in the Kumada Coupling of Aryl Halides

Several experiments were conducted to verify the possibility of the proposed cycles. The first of these experiments involved the reaction of **3a** with 2 equiv of chlorobenzene in THF at room temperature for 21 h. Notably, the major product of this reaction was not compound **1** but **2** (Scheme 2-6). It is possible that compound **1** is generated from **3** and the subsequent reaction of **1** with chlorobenzene readily occurs to yield **2** in this reaction. In addition, only 4,4′-dimethylbiphenyl and biphenyl were observed as the organic products, and no 4-methylbiphenyl was detected by GC-MS (Scheme 2-6). We could not detect **1c** in this reaction even when a smaller amount of chlorobenzene was added to **3**. Given that compound **3** was found to be stable in the absence of chlorobenzene, the reductive elimination of 4,4′-dimethylbiphenyl would most likely occur in a concerted manner involving the coordination and oxidative addition of chlorobenzene.[25] Given that no 4-methylbiphenyl was formed as a cross-coupling product from the *p*-tolyl group in **3** and chlorobenzene, it is likely that any other routes responsible for the separation to monomeric *p*-tolylNi(I) species from **3** would be negligible during the oxidative addition of chlorobenzene. The reductive elimination of two σ-aryl groups from dinickel centers has also been reported in the literature.[23]

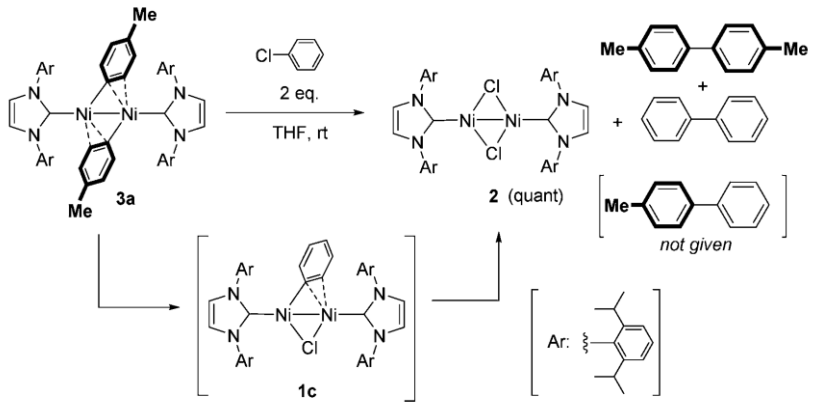

Scheme 2-6. Stoichiometric Reaction of 3a with Chlorobenzene

2-3-3. Product Distribution of Biaryls in the Stoichiometric Reactions.

Complex **1a** was treated with 1 equiv of 4-chloroanisole in THF for 6 h at room temperature to determine where the bridging σ-aryl group from **1a** ended up in the cross-coupling and/or homocoupling products. It is noteworthy that all of the possible coupling products, including 4,4′-dimethylbiphenyl, 4-methyl-4′-methoxybiphenyl, and 4′4-dimethoxybiphenyl, were unexpectedly detected by GC-MS analysis in this reaction (Scheme 2-7). The product ratio of these three compounds was 13:37:50. In the catalytic process as given in Table 2-2, no homocoupling products from aryl halides were detected, showing that the stoichiometric reaction products using **1a** are not consistent with those in the catalytic reactions.

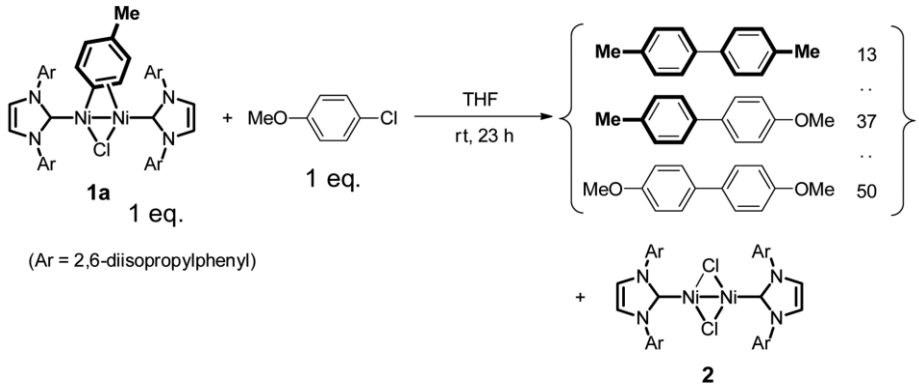

Scheme 2-7. Stoichiometric Reaction of 1a with p-Chloroanisole

Phenylmagnesium chloride was also added to a reaction mixture consisting of **1a** and a stoichiometric amount of 4-chloro- or 4-bromoanisole. After 18 h at room temperature, all of the starting aryl halides had been consumed, and the yields of the extracted biaryl products were determined by GC-MS analysis. All six of the possible biaryl products were detected in this reaction (Scheme 2-8). Surprisingly, the 4-methoxybiphenyl cross-coupling product was formed in the highest yield (71%) from 4-haloanisole, despite only 1 equiv of 4-haloanisole being added to **1a**. Most notably, the yield of 4-methyl-4′-methoxybiphenyl was much higher than that of 4-methylbiphenyl (e.g., 27 vs 2% from 4-bromoanisole and 9 vs 2% from 4-chloroanisole, respectively) (Figure 2-3). The former of these two products could also be obtained by the oxidative addition of haloanisole to **1a** (Scheme 2-7), whereas the latter of the two products could be derived from the reaction of **1a** with phenylmagnesium chloride via the formation of bis(σ-aryl)dinickel complex **3** (Scheme 2-6), according to the above stoichiometric reactions. This result therefore confirmed that the oxidative addition process from **1a** to **2** was preferred over the transmetalation process from **1a** to **3**. This result was especially interesting because 4-chloroanisole is usually less active toward the oxidative addition of carbon–chlorine bonds. Reports pertaining to the occurrence of competition between oxidative addition and transmetalation reactions in catalytic cycles are scarce, and the findings presented in the current report therefore represent an important development in our understanding of the reactivity of Ni(I) complexes. Although no supporting results were generated during the course of this study to explain why the rate of the transmetalation reaction was much slower than that of the oxidative addition, it is envisaged that the electron-rich Ni(I) center would disfavor interaction with the electron-rich aromatic carbon of the Grignard reagent.

It is also possible that a facile electron transfer process could have occurred from the electron-rich nickel to the aryl halide acceptor.[26]

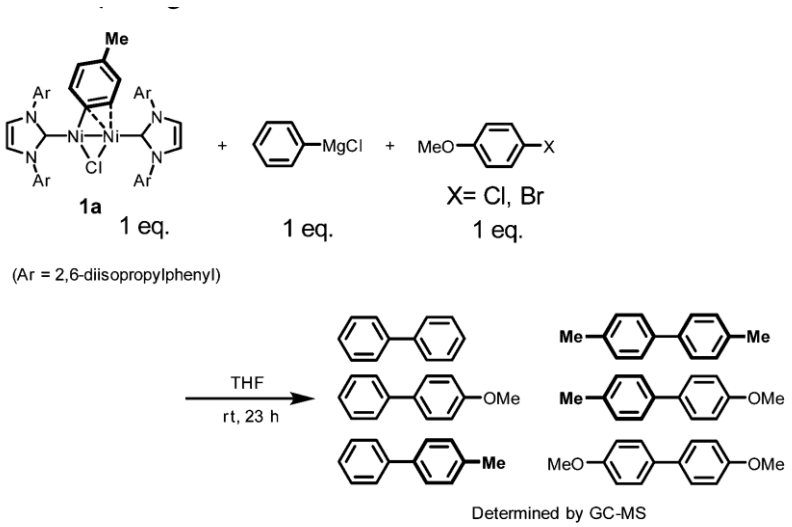

Scheme 2-8. Stoichiometric Reaction of 1a with p-Haloanisole and Phenylmagnesium Chloride

The product ratios of 4-methyl-4′-methoxybiphenyl and 4-methylbiphenyl were low at 9 and 2%, respectively, in Figure 2-3, when 4-chloroanisole was used as the substrate. In contrast, the product ratio of 4-methoxybiphenyl generated from 4-chloroanisole was high at 71%. Furthermore, ^{1}H NMR analysis of the crude reaction mixtures showed that the majority of the compound **1a** remained intact after the reactions with 4-chloroanisole, as shown in Figure 2-4a, whereas compound **1a** was converted almost exclusively to the bromide analogue of compound **2**, $[Ni(IPr)]_2(\mu\text{-}Br)_2$ (**2′**),[13i] when 4-bromoanisole was added to the reaction mixture (Figure 2-4b). The remarkable contrast in these results indicated that **1a** was in no way involved in the formation of the catalytic product 4-methoxybiphenyl from 4-chloroanisole. It was therefore envisaged that a significant amount of some highly active nickel species was being formed during the course of both

of these reactions and that this unknown active species was responsible for the formation of the catalytic product 4-methoxybiphenyl.

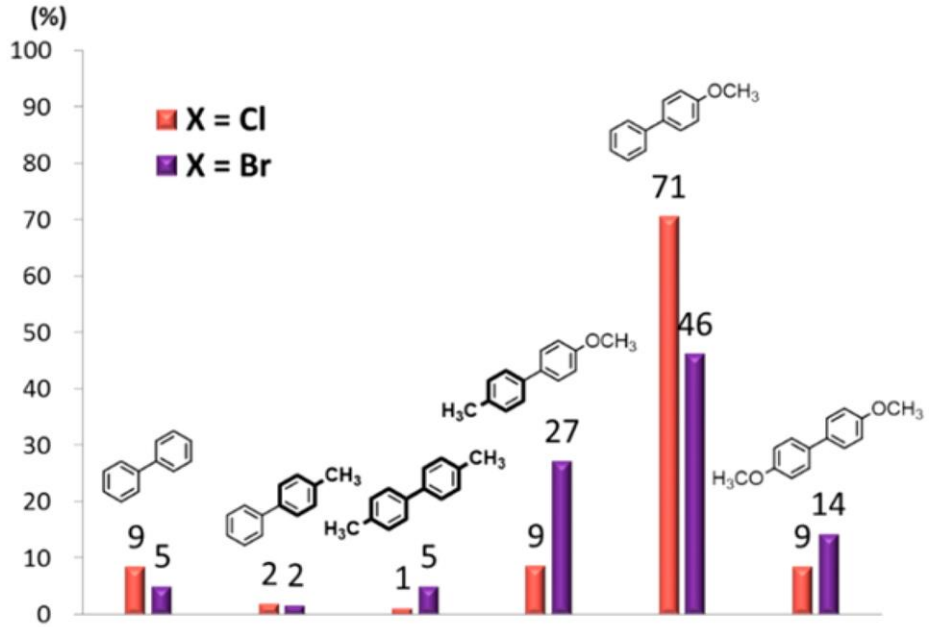

Figure 2-3. Product distribution of the biaryl derivatives in the stoichiometric reactions of 1a with MeO(C6H4)X (X = Cl, Br) and PhMgCl.

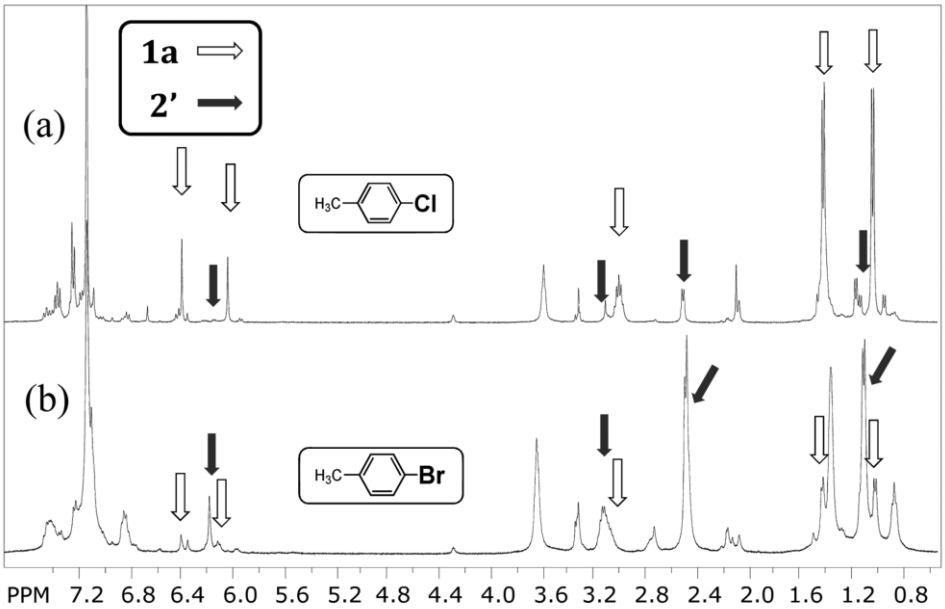

Figure 2-4. 1H NMR spectra (400 MHz, in C6D6, room temperature) of the stoichiometric reaction mixtures using (a) 4-chloroanisole and (b) 4-bromoanisole.

2-3-4. Kinetics and Theoretical Studies in the Oxidative Addition of 4-Chlorotoluene to Dinickel(I) Species 1a

The results of a detailed investigation of the processes involved in the oxidative addition of aryl halides to the diNi(I) systems, such as **1a** and **2**, could provide significant understanding of how organometallic reactions can proceed on such unsaturated dinuclear systems. It is noteworthy that oxidative addition reactions to monovalent dinickel species are uncommon in comparison with normal zerovalent nickel species. Several different pathways could be proposed to account for formation of **2** and the biaryl products formed during this multistep reaction. For example, a mononickel(III) oxidative adduct could be formed, according to a pathway similar to that proposed in the monomeric Ni(I) system.[6] Alternatively, the addition of an aryl halide species to Ni(I)–Ni(I) could lead to the formation of the dinickel Ni(II)–Ni(II) system (Scheme 2-1(4)). It was envisaged that the kinetic parameters of the transformation could be estimated by the monitoring of a low-temperature reaction by NMR spectroscopy. Because the reaction proceeds slowly, even at low temperature, it was quite difficult to quench the reaction. After several attempts, the pseudo-first-order reaction rates of **1a** were determined experimentally using a large excess (30 equiv) of 4-chlorotoluene, which could be readily removed under reduced pressure to stop the reaction, at temperatures of −81, −70, −55, and −43 °C. The ^{1}H NMR spectra of the reaction mixture contained an independent signal at δ_H 6.06, which was assigned as the bridging aryl protons in **1a**. This signal rapidly diminished as the reaction proceeded, which indicated that the reaction could be regarded as an irreversible process involving the oxidative addition of 4-chlorotoluene to **1a**, followed by the reductive elimination of 4,4′-dimethylbiphenyl to form **2**. The observed rate constant was defined

as k_{obs} (Scheme 2-9). The concentration of **1a** (C_{1a}) and the time could therefore be plotted according to eq 1.

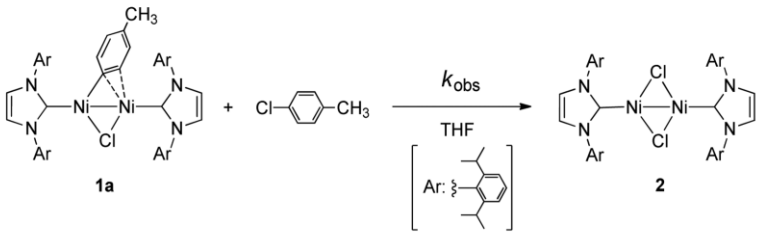

$$\ln C_{1a} = -k_{obs}t + \ln C_{1a}^{0} \quad (k_{obs} = kC_{4\text{-chlorotoluene}}) \qquad (1)$$

Scheme 2-9. Kinetic Parameter kobs in the Stoichiometric Reaction of 1a

Four different k_{obs} values were determined depending on the reaction temperatures to give the corresponding Arrhenius plot (Figure 2-5). The resulting $\Delta H^{\ddagger}$, $\Delta S^{\ddagger}$, and $\Delta G_{298}^{\ddagger}$ values were +2.40 ± 0.12 kcal mol^{-1} (+10.1 ± 0.5 kJ mol^{-1}), −56.52 ± 0.52 cal K^{-1} mol^{-1} (−237.4 ± 2.2 J K^{-1} mol^{-1}), and +19.3 ± 0.3 kcal mol^{-1} (+80.9 ± 1.1 kJ mol^{-1}), respectively.

The most striking feature of this reaction was its large negative activation entropy, which was over −50 cal K^{-1} mol^{-1}. The Gibbs free activation energy $\Delta G^{\ddagger}$ was therefore largely dependent on the activation entropy, which suggested that the rate-determining step was more likely to be the coordination of the aryl halide to the nickel species rather than the oxidative addition, reductive elimination, or the reaction responsible for the separation to a monomeric species from the dimeric species (if possible). These results were therefore consistent with the presence of the two bulky NHC ligands around the dinickel centers, which could hinder the approach of an aryl halide molecule, as indicated in Figure 2-2. However, this suggestion is dependent on the dinickel framework being maintained during the reaction.

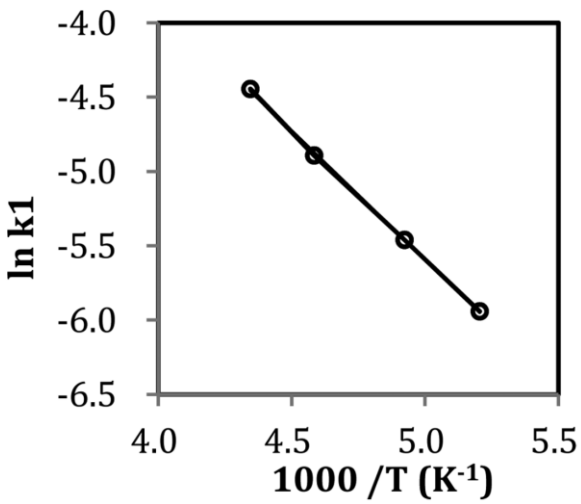

Figure 2-5. Arrhenius plot of the low-temperature reaction of 1a with 4-chlorotoluene.

The large negative activation entropy observed for this reaction prompted us to conduct a theoretical investigation of the reaction mechanism using density functional theory (DFT). DFT/PBE0 calculations (free energies in kcal mol^{-1}) based on the use of the complex $[Ni(IMe)]_2(\mu\text{-}Cl)(\mu{:}\eta^1,\eta^2\text{-}C_6H_5)$ (**A**) (with the simpler model ligand 1,3-bis(methyl)imidazol-2-ylidene (IMe), instead of IPr) and chlorobenzene (ClBz) as a model substrate provided a conceivable pathway for the reaction (Figures 2-6 and 7). When a more bulky 1,3-bis(phenyl)imidazol-2-ylidene (IPh) was employed in the DFT calculations, many processes involving subtle rotation movement of the phenyl rings in IPh should be taken into account. However, the overall sequence of the reaction steps using IMe was similar to that with IPh. Therefore, the steric effect of these NHC ligands may not affect the overall sequence so much even when the bulkier NHC ligand is employed for the Ni(I) complexes. Similar dinuclear processes have also been calculated by Schoenebeck et al.[11b-d]

In the initial step, chlorobenzene was added to complex **A** to form intermediate **B**, where the aromatic ring was coordinated to the complex in a η^2 fashion via the carbon

atoms at C2 and C3. The location of the transition state **TS$_{AB}$** revealed a moderate activation barrier of 15.5 kcal mol^{-1} (64.8 kJ mol^{-1}). The chlorobenzene group subsequently underwent a ring slippage rearrangement to form **C**, where the aromatic ring was still η^2 coordinated to the complex, but now via the carbon atoms at C1 and C2. During the course of this process, the Ni–Ni bond distance increased from 2.35 Å in **A** to 2.62 Å in **C**, with the concomitant activation of the C–Cl bond. Furthermore, the C–Cl bond distance increased from 1.75 Å in both the free chlorobenzene and **B** to 1.82 Å in **C**. This process was found to be slightly endergonic by 4.7 kcal mol^{-1} (19.7 kJ mol^{-1}) with respect to the initial reactants. During the following oxidative addition step, the C–Cl bond was cleaved and a new Ni–Cl bond was formed to give intermediate **D**, which no longer possessed a Ni–Ni bond (3.30 Å). Furthermore, both of the arene rings in **D** were coordinated to nickel in a σ fashion through a single C atom. The formation of **D** from **C** was found to strongly exergonic, releasing 44.9 kcal mol^{-1} (187.9 kJ mol^{-1}). The Ni–Cl bond started to form during this step, going from 3.12 Å in **C** to 2.76 Å in **TS$_{CD}$** and ultimately reaching 2.25 Å in **D**. This step was accompanied by the concomitant cleavage of the C–Cl bond, with the C···Cl distance increasing from 1.82 Å in **C** to 2.35 Å in **TS$_{CD}$** and finally becoming 3.00 Å in **D**.

In the following step, one of the two η^1-bound aryl ligands was brought into a bridging position (μ-η^1,η^2-C_6H_5) to give intermediate **E** via **TS$_{DE}$**. The bridging aryl moiety in intermediate **E** was η^2-coordinated to a Ni center containing a σ-coordinated aryl ring. This process required free activation energy of 26.2 kcal mol^{-1} (109.6 kJ mol^{-1}) from **D** and was endergonic by 23.9 kcal mol^{-1} (100.0 kJ mol^{-1}), but the free energy of the transition state **TS$_{DE}$** was still 14.0 kcal mol^{-1} (58.8 kJ mol^{-1}) lower than that of **A** + ClBz. The Ni–Ni distance was reduced to 2.84 Å following this step. During the following two

steps (i.e., **E** → **F** and then **F** → **G**), there was a reorientation of the μ-η^1,η^2-C_6H_5-bound aryl ligand, which brought the aryl moieties together to enable the formation of the C–C bond of the biphenyl product (note that the C–C bond distance in **E** was 3.13 Å). In **F**, the C–C bond distance was reduced to 2.73 Å, and the aryl ligand was coordinated in a μ-η^1 fashion. However, in **G**, the aryl unit was once again bound to the Ni in a μ-η^1,η^2 mode but was now also η^2 coordinated to the other Ni center bearing no σ-aryl ring. Finally, the formation of the C–C bond of the biphenyl product occurred via **TS$_{GH}$** ($d_{C–C}$ = 1.96 Å) to give complex **H** ($d_{C–C}$ = 1.48 Å), where the newly formed biphenyl (Ph-Ph) molecule was coordinated in a μ-η^2,η^2 fashion. This process was determined to be facile, with a free energy barrier of only 14.1 kcal/mol using IMe as the model spectator ligand. In the final step the Ph-Ph ligand was released to give the complex $[Ni(IMe)]_2(\mu\text{-}Cl)_2$ (**I**) in an exergonic reaction (ΔG = −21.9 kcal mol^{-1} (−91.6 kJ mol^{-1})). The overall reaction from **A** to **I** was found to be exergonic by −52.3 kcal mol^{-1} (−218.8 kJ mol^{-1}).

Remarkably, the relative Gibbs free energy of the most stable intermediate **D**, −40.2 kcal mol^{-1} (−168.2 kJ mol^{-1}), was still 12 kcal mol^{-1} (50.2 kJ mol^{-1}) higher than that of the final products, $[Ni(IMe)]_2(\mu\text{-}Cl)_2$ (**I**) and the biaryl compound. The result suggested that the compound **D** is the metastable intermediate over the oxidative addition and reductive elimination processes. The structure of **D** revealed that the terminal σ-aryl moiety located at the position adjacent to that of the carbene ligand could cause steric repulsion between the carbene and the σ-aryl moiety. Given that there was no bonding interaction between the nickel atoms in **D**, the equilibrium for the cleavage of the Ni–Cl bond by disproportionation could ultimately lead to the formation of the mixed biaryl products (Scheme 2-10).

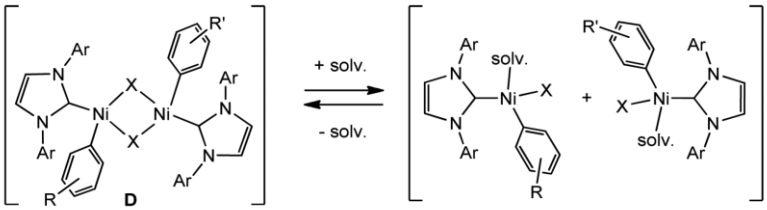

Scheme 2-10. Possible Disproportionation Equilibrium.

The initial coordination of the chlorobenzene substrate to the nickel atom had the largest activation barrier of all of the steps in the process, and its activation entropy was estimated to be −70 J K^{-1} mol^{-1}. The theoretical pathway in Figure 2-6 could be consistent with the real pathway, because the rate-limiting process would be the coordination of the aryl halide also in calculations. As indicated by the kinetics, the more sterically hindered IPr ligand would most likely require considerable negative activation entropy. Furthermore, the coordination of the aryl halide would most probably require activation energy higher than that calculated using IMe. In any case, the most important feature of this calculation is that the whole process is conducted on dinickel centers, which supports our hypothesis that this catalytic cycle involves both [Ni(I)–Ni(I)] and [Ni(II)–Ni(II)] species.

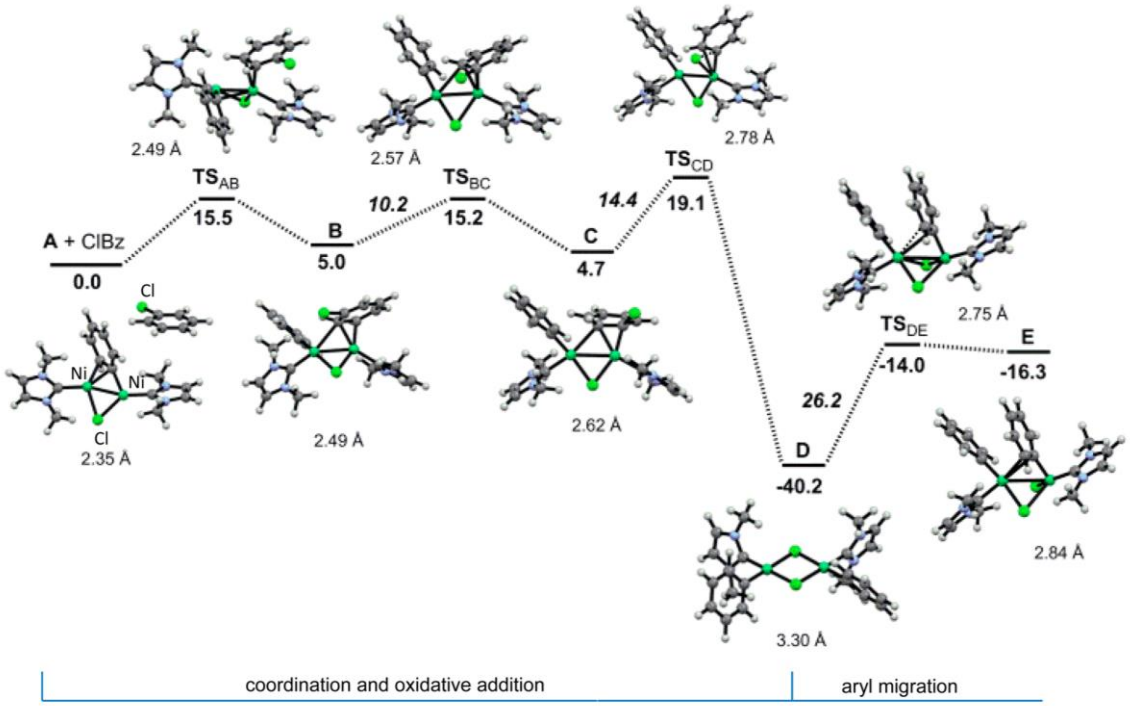

Figure 2-6. Reaction profile of the computed relative Gibbs free energies (kcal mol−1) for the reaction of [Ni(IMe)]2(μ-Cl)(μ:η1,η2-C6H5) (A) with chlorobenzene (ClBz) to give intermediate E (Ni−Ni bond distances in Å).

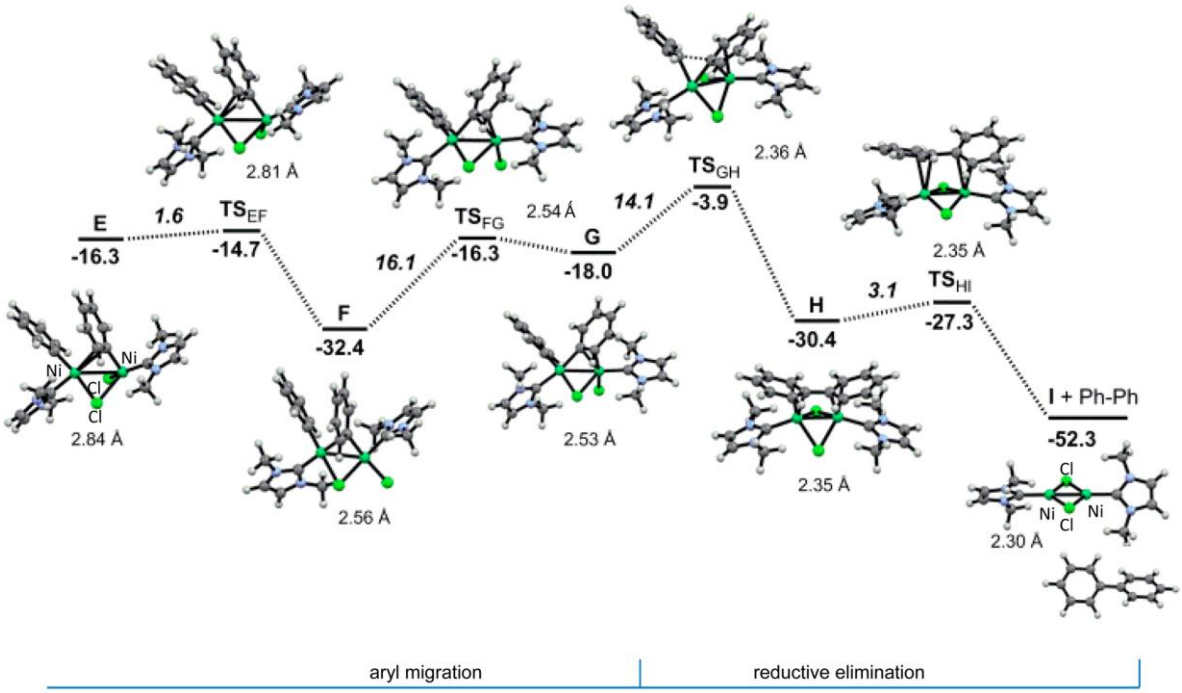

Figure 2-7. Figure 7. Reaction profile of the computed relative Gibbs free energies (kcal mol−1) for the reaction of intermediate E to give the final products [Ni(IMe)]2(μ-Cl)2 (I) and biphenyl (Ni−Ni bond distances in Å).

2-3-5. Alternative Catalytic Cycle Involving 2

In the stoichiometric reaction of **1a** with both 4-chlorotoluene and phenylmagnesium chloride, the consumption of **1a** was much slower than that of 4-chlorotoluene, which was consumed to form the product in catalysis (Figure 2-4). Furthermore, the distribution of the mixed biaryl products in the stoichiometric reaction of **1a** or **3** was completely different from that observed after the catalytic Kumada cross-coupling reaction, yielding only one cross-coupling product, where the stoichiometric reactions afforded all of the possible biaryl products as a result of a disproportionation reaction (Scheme 2-10). These experiments revealed that the catalytic cycles proposed above between **1a** and **2** and between **1a** and **3** are not involved in the real catalytic cycle. On the other hand, these results strongly support the following alternative pathway as shown in Scheme 2-11.

Oxidative addition of aryl halide to complex **2** would lead to the formation of a dinickel(II) adduct (**X**), and subsequent transmetalation with a Grignard reagent would give a nickel(II) diaryl species (**D**), which would undergo a facile reductive elimination reaction to give the biaryl product with the concomitant regeneration of complex **2**. This alternative cycle was believed to be much more likely than any of the other cycles for the following reasons. In comparison with complex **1a**, complex **2** seems to be sterically less hindered, and the reactions with aryl halide on **2** to give the intermediate **X** may not require such a large negative entropy, which was observed in the kinetic study of **1a** with 4-chlorotoluene. Therefore, this process would occur with greater ease than the corresponding reaction onto the more hindered compound **1a**. These reactions including oxidative addition and reductive elimination with the complex **2** in Scheme 2-11 are regarded as the processes similar to the calculated ones, which are shown in Figure 2-6. Additionally, a theoretical study of the process from **2** to **X** was also conducted using DFT

calculations with the 3-21G basis set for C, H, and N, 6-31G* for Cl, and CEP/LanL2DZ for Ni. The results of this study led to the proposal of a similar dinickel activation pathway, including the coordination and oxidative addition of chlorobenzene to diNi(I) dichloride (see the S.I.). The initiation process from the mixture of $Ni(cod)_2$, IPr, and aryl halide easily affords **1** and then **2** (Scheme 2-11), as the result of the reaction of **1** with aryl halide, indicating that this alternative cycle is also readily accessible from the general in situ catalyst system using nickel precursor and IPr.

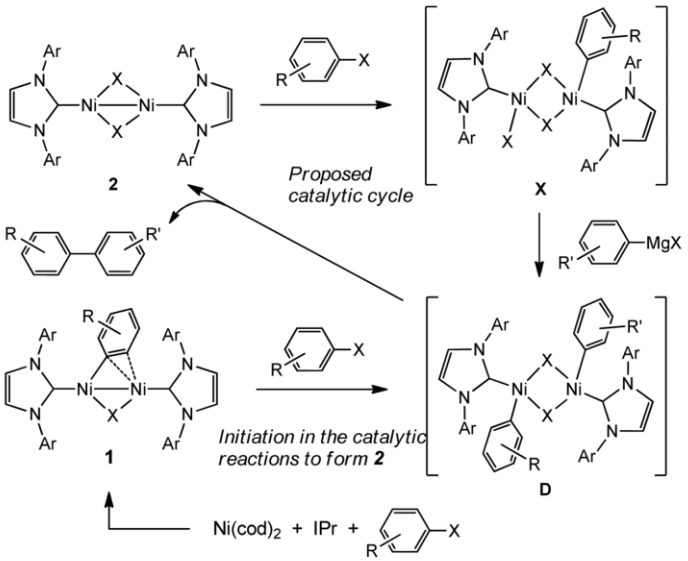

Scheme 2-11. Alternative Possible Catalytic Cycle Mediated by 2 and the Initiation Process Involving the Catalysis Reaction of 1 with Aryl Halide

Although we cannot determine the intermediary compound **X** from the reaction of **2** with aryl halides, we obtained a oxidative addition product from the stoichiometric reaction of **2** with 3,5-dichloropyridine at room temperature (Scheme 2-12). A single crystal suitable for X-ray crystallography was obtained following the concentration of a reaction mixture of **2** with 3,5-dichloropyridine. The divalent tetranickel complex **5** was successfully determined by X-ray diffraction analysis (see the S.I.). That is, oxidative

addition of aryl chloride on **2** can occur, suggesting the possibility of formation of the intermediate **X** in the catalytic cycle from **2** and aryl halide.

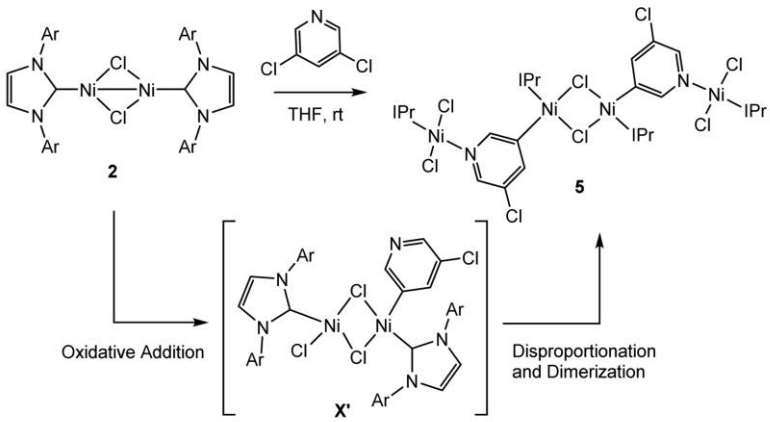

Scheme 2-12. Oxidative Addition Product 5 from 2 and 3,5-Dichloropyridine and Proposed Intermediate X′in the Reaction

The most important point found in these mechanistic studies is that the oxidation and reduction processes in these diNi(I) complexes are most likely distinct from the corresponding mononuclear Ni(I) and Ni(III) redox processes. Ni(III) complexes are generally synthesized by electrochemical oxidation or the oxidation of Ni(II) complexes with dioxygen.[27] In contrast, the oxidation states of the two Ni(I) centers increased from +1 to +2 in the current study during the oxidative addition of the aryl halide (Scheme 2-1). The bridging halogen ligand could play an important role in maintaining the proximal positions of both the nickel centers. Furthermore, the bulky NHC ligand IPr kinetically stabilized the dinuclear Ni(I) framework in a way that cannot be obtained for the smaller IMes ligand. Dinuclear systems of this type are consistent with the large negative entropy ($\Delta S^{\ddagger} = -56.52 \pm 0.52$ cal K^{-1} mol^{-1}) observed in the reaction of the similar diNi(I) system **1a** with aryl halide followed by the reductive elimination of the corresponding biaryl product.

2-4. Summary

Intermediary monovalent dinickel complexes have been found using a nickel(0) catalyst precursor and a bulky N-heterocyclic carbene ligand in the Kumada–Tamao–Corriu cross-coupling reaction of aryl halides. The compounds were obtained by oxidative addition of aryl halides to a Ni(0) precursor and were coordinatively unsaturated (30e), dinuclear μ-σ-aryl-μ-chloro Ni(I) species, which could react with both aryl halides and Grignard reagents. Further reaction with aryl halides yielded the C(Ar)–C(Ar) bond coupled biaryl products together with a (μ-chloro)Ni(I) dimer, whereas transmetalation with a Grignard reagent afforded bis(μ-σ-aryl)diNi(I) complexes.

Both of these dinuclear complexes had the same diNi(I) framework as the complex **2** and can be regarded as at least the analogues of the real active species in the catalytic cycle. Therefore, stoichiometric reactions of these complexes concerning the catalytic reaction were investigated. Experiments showing faster oxidative addition in comparison to transmetalation on the diNi(I) complexes indicated the possible reaction order of these complexes in the presence of both aryl halide and Grignard reagent. Kinetics for the oxidative addition of an aryl halide and the subsequent reductive elimination of a biaryl product showed large negative entropy, which suggested that the coordination of the aryl halide could be the rate-determining step as a consequence of the steric hindrance derived from the two bulky NHC ligands.

Although the semistable dinickel(II) intermediate, which would be formed by the reaction of the dinuclear μ-σ-aryl μ-chloro Ni(I) species with aryl halide, cannot be uncovered in this study, theoretical studies strongly suggested that coordination and oxidative addition of aryl halide onto the unsaturated Ni(I) species led to formation of the nickel(II) intermediate, retaining its dinuclear framework. It was of interest that the Gibbs

energy of the divalent intermediate was still higher than that of the final (μ-chloro)Ni(I) dimer, making it possible to smoothly restart the catalysis. However, this cycle was negligible in the real catalytic system, as concluded from the experimental results.

On the other hand, the above results were very helpful in understanding the most possible catalytic cycle via the formation of the diNi(I) μ-chloride complex **2** as the key compound in the catalytic process. It would allow for the faster oxidative addition of an aryl halide to form the divalent dinickel species, in comparison with the reaction with the starting dinuclear μ-σ-aryl μ-chloro Ni(I) complex **1**, because of possessing the less-hindered nickel centers in **2**, which would be immediately regenerated by transmetalation of the divalent dinickel species with a Grignard reagent and subsequent reductive elimination to give the cross-coupling products, enabling a fast catalytic process. It was quite interesting that the dinuclear system in oxidative addition of aryl halide and reductive elimination of biaryl works efficiently in the cross-coupling reaction. The DFT calculations for the mechanism revealed that oxidative addition occurs on one of the unsaturated nickel centers and then one of the terminal aryl groups migrates to the bridging position to couple with the aryl group on the other nickel. Moreover, the biaryl just after the C–C bond formation coordinates to both nickel centers. Such cooperative processes make the catalytic cross-coupling occur smoothly without a large energy barrier, led by the dinuclear system. We are conducting studies to apply the catalyst system to other cross-coupling reactions, these being generally challenging processes for nickel catalysts.

2-5. References

1. Cross-coupling reactions, recent reviews: (a) Metal-Catalyzed Cross-Coupling Reactions, 2nd ed.; De Meijere, A., Francois, D., Eds.; Wiley-VCH: Weinheim, Germany, 2004. (b) Han, F.-S. Chem. Soc. Rev. 2013, 42, 5270−5298. (c) Suzuki, A. Angew. Chem., Int. Ed. 2011, 50, 6723−6737. (d) Phapale, V. B.; Cárdenas, D. J. Chem. Soc. Rev. 2009, 38, 1598−1607. (e) Jana, R.; Pathak, T. P.; Sigman, M. S. Chem. Rev. 2011, 111, 1417−1492. (f) Frisch, A. C.; Beller, M. Angew. Chem., Int. Ed. 2005, 44, 674−688. (g) Corbet, J.-P.; Mignani, G. Chem. Rev. 2006, 106, 2651−2710. (h) Nicolaou, K. C.; Bulger, P. G.; Sarlah, D. Angew. Chem., Int. Ed. 2005, 44, 4442−4489.
2. For example, see: (a) Böhm, V. P. W.; Gstöttmayr, C. W. K.; Weskamp, T.; Herrmann, W. A. Angew. Chem., Int. Ed. 2001, 40, 3387−3389. (b) Tekavec, T. N.; Zuo, G.; Simon, K.; Louie, J. J. Org. Chem. 2006, 71, 5834−5836. (c) Kuhl, S.; Schneider, R.; Fort, Y. Adv. Synth. Catal. 2003, 345, 341−344. (d) Kim, C.-B.; Jo, H.; Ahn, B.-K.; Kim, C. K.; Park, K. J. Org. Chem. 2009, 74, 9566−9569. (e) Lohre, C.; Dröge, T.; Wang, C.; Glorius, F. Chem. - Eur. J. 2011, 17, 6052−6055. (f) Ritleng, V.; Henrion, M.; Chetcuti, M. J. ACS Catal. 2016, 6, 890−906.
3. Kumada coupling catalytic cycle: Herrmann, W. A. In Applied Homogeneous Catalysis with Organometallic Compounds; Cornils, B., Herrmann, W. A., Eds.; Wiley-VCH: Weinheim, Germany, 2002; Chapter 3, pp 824−825.
4. Radical catalysis: (a) Manolikakes, G.; Knochel, P. Angew. Chem., Int. Ed. 2009, 48, 205−209. (b) Ford, L.; Jahn, U. Angew. Chem., Int. Ed. 2009, 48, 6386−6389. (c) Gao, C.-Y.; Cao, X.; Yang, L.-M. Org. Biomol. Chem. 2009, 7, 3922−3925. (d) Jones, G. D.; McFarland, C.; Anderson, T. J.; Vicic, D. A. Chem. Commun. 2005, 4211−4213. (e) Jones, G. D.; Martin, J. L.; McFarland, C.; Allen, O. R.; Hall, R. E.; Haley, A. D.; Brandon, R. J.; Konovalova, T.; Desrochers, P. J.; Pulay, P.; Vicic, D. A. J. Am. Chem. Soc. 2006, 128, 13175−13183. (f) Ren, P.; Vechorkin, O.; von Allmen, K.; Scopelliti, R.; Hu, X. J. Am. Chem. Soc. 2011, 133, 7084−7095. (g) Breitenfeld, J.; Ruiz, J.; Wodrich, M. D.; Hu, X. J. Am. Chem. Soc. 2013, 135, 12004−12012.
5. Miyazaki, S.; Koga, Y.; Matsumoto, T.; Matsubara, K. Chem. Commun. 2010, 46, 1932−1934.
6. (a) Zhang, K.; Conda-Sheridan, M.; Cooke, S. R.; Louie, J. Organometallics 2011, 30, 2546−2552. (b) Nagao, S.; Matsumoto, T.; Koga, Y.; Matsubara, K. Chem. Lett. 2011, 40, 1036−1038. (c) Page, M. J.; Lu, W. Y.; Poulten, R. C.; Carter, E.; Algarra, A. G.; Kariuki, B. M.; Macgregor, S. A.; Mahon, M. F.; Cavell, K. J.; Murphy, D. M.; Whittlesey, M. K. Chem. - Eur. J. 2013, 19, 2158−2167. (d) Davies, C. J. E.; Page, M. J.; Ellul, C. E.; Mahon, M. F.; Whittlesey, M. K. Chem. Commun. 2010, 46, 5151−5153.
7. (a) Cariou, R.; Graham, T. W.; Dahcheh, F.; Stephan, D. W. Dalton Trans. 2011, 40, 5419−5422. (b) Fischer, R.; Langer, J.; Malassa, A.; Walther, D.; Görls, H.; Vaughan, G. Chem. Commun. 2006, 2510−2512. (c) Ohno, K.; Arima, K.; Tanaka, S.; Yamagata,

T.; Tsurugi, H.; Mashima, K. Organometallics 2009, 28, 3256−3263. (d) Rodriguez, B. A.; Delferro, M.; Marks, T. J. Organometallics 2008, 27, 2166−2168. (e) Velian, A.; Lin, S.; Miller, A. J. M.; Day, M. W.; Agapie, T. J. Am. Chem. Soc. 2010, 132, 6296−6297. (f) Hruszkewycz, D. P.; Wu, J.; Hazari, N.; Incarvito, C. D. J. Am. Chem. Soc. 2011, 133, 3280−3283. (g) Xue, F.; Zhao, J.; Hor, T. S. A. Dalton Trans. 2013, 42, 5150−5158. (h) Kalvet, I.; Bonney, K. J.; Schoenebeck, F. J. Org. Chem. 2014, 79, 12041−12046.

8. Reviews, for example: (a) van der Vlugt, J. I. Eur. J. Inorg. Chem. 2012, 2012, 363−375. (b) Dyson, P. J. Coord. Chem. Rev. 2004, 248, 2443−2458. (c) Nagashima, H. Monatsh. Chem. 2000, 131, 1225−1239. (d) Süss-Fink, G.; Therrien, B.; Vieille-Petit, L.; Tschan, M.; Romakh, V. B.; Ward, T. R.; Dadras, M.; Laurenczy, G. J. Organomet. Chem. 2004, 689, 1362−1369. (e) Metal Clusters in Chemistry; Braunstein, P., Rosé, J., Eds.; Wiley-VCH: Weinheim, Germany, 1999.
9. Takao, T.; Suzuki, H. Coord. Chem. Rev. 2012, 256, 695−708 and references cited therein..
10. Xi, Z.; Zhou, Y.; Chen, W. J. Org. Chem. 2008, 73, 8497−8501.
11. (a) Stambuli, J. P.; Kuwano, R.; Hartwig, J. F. Angew. Chem., Int. Ed. 2002, 41, 4746−4748. (b) Bonney, K. J.; Schoenebeck, F. Chem. Soc. Rev. 2014, 43, 6609−6638. (c) Proutiere, F.; Lyngvi, E.; Aufiero, M.; Sanhueza, I. A.; Schoenebeck, F. Organometallics 2014, 33, 6879−6884. (d) Yin, G.; Kalvet, I.; Schoenebeck, F. Angew. Chem., Int. Ed. 2015, 54, 6809−6813.
12. Recent reviews: (a) Valente, C.; Çalimsiz, S.; Hoi, K. H.; Mallik, D.; Sayah, M.; Organ, M. G. Angew. Chem., Int. Ed. 2012, 51, 3314− 3332. (b) Díez-González, S.; Marion, N.; Nolan, S. P. Chem. Rev. 2009, 109, 3612−3676. (c) Clavier, H.; Nolan, S. P. Chem. Commun. 2010, 46, 841−861. (d) Corberán, R.; Mas-Marzá, E.; Peris, E. Eur. J. Inorg. Chem. 2009, 2009, 1700−1716. (e) Schuster, O.; Yang, L.; Raubenheimer, H. G.; Albrecht, M. Chem. Rev. 2009, 109, 3445−3478. (f) Hahn, F. E.; Jahnke, M. C. Angew. Chem., Int. Ed. 2008, 47, 3122−3172
13. Ni(I) complexes: (a) Kitiachvili, K. D.; Mindiola, D. J.; Hillhouse, G. L. J. Am. Chem. Soc. 2004, 126, 10554−10555. (b) Melenkivitz, R.; Mindiola, D. J.; Hillhouse, G. L. J. Am. Chem. Soc. 2002, 124, 3846−3847. (c) Holland, P. L.; Cundari, T. R.; Perez, L. L.; Eckert, N. A.; Lachicotte, R. J. J. Am. Chem. Soc. 2002, 124, 14416−14424. (d) Eckert, N. A.; Dinescu, A.; Cundari, T. R.; Holland, P. L. Inorg. Chem. 2005, 44, 7702−7704. (e) Fujita, K.; Rheingold, A. L.; Riordan, C. G. Dalton Trans. 2003, 2004−2008. (f) Eaborn, C.; Hill, M. S.; Hitchcock, P. B.; Smith, J. D. Chem. Commun. 2000, 691− 692. (g) Ito, M.; Matsumoto, T.; Tatsumi, K. Inorg. Chem. 2009, 48, 2215−2223. (h) Marlier, E. E.; Tereniak, S. J.; Ding, K.; Mulliken, J. E.; Lu, C. C. Inorg. Chem. 2011, 50, 9290−9299. (i) Laskowski, C. A.; Bungum, D. J.; Baldwin, S. M.; Ciello, S. A. D.; Iluc, V. M.; Hillhouse, G. L. J. Am. Chem. Soc. 2013, 135, 18272−18275.
14. Laskowski, C. A.; Hillhouse, G. L. Organometallics 2009, 28, 6114−6120.

15. Böhm, V. P. W.; Weskamp, T.; Gstöttmayr, C. W. K.; Herrmann, W. A. Angew. Chem., Int. Ed. 2000, 39, 1602−1604.
16. Dible, B. R.; Sigman, M. S.; Arif, A. M. Inorg. Chem. 2005, 44, 3774−3776.
17. (a) Lee, C. H.; Laitar, D. S.; Müller, P.; Sadighi, J. P. J. Am. Chem. Soc. 2007, 129, 13802−13803. (b) Hoshimoto, Y.; Hayashi, Y.; Suzuki, H.; Ohashi, M.; Ogoshi, S. Organometallics 2014, 33, 1276-1282.
18. (a) Schaub, T.; Backes, M.; Radius, U. J. Am. Chem. Soc. 2006, 128, 15964−15965. (b) Zell, T.; Fischer, P.; Schmidt, D.; Radius, U. Organometallics 2012, 31, 5065−5073. (c) Radius, U.; Bickelhaupt, F. M. Coord. Chem. Rev. 2009, 253, 678−686.
19. Because complex 3a was detected as the minor product generated in the formation of 3b in solution, cogenerated 3c cannot be identified.
20. (a) McGuinness, D. S.; Cavell, K. J. Organometallics 1999, 18, 1596−1605. (b) Schaub, T.; Fischer, P.; Meins, T.; Radius, U. Eur. J. Inorg. Chem. 2011, 2011, 3122−3126.
21. These results suggested that the aryl moiety is undergoing a fast flip-flop motion between the two metal atoms in solution at room temperature. However, we do not have any evidence supporting the solution structure containing the η2-C□C interaction to the nickel center.
22. (a) Heckler, J. E.; Zeller, M.; Hunter, A. D.; Gray, T. G. Angew. Chem., Int. Ed. 2012, 51, 5924−5928. (b) Osawa, M.; Hoshino, M.; Hashizume, D. Dalton Trans. 2008, 2248−2252.
23. (a) Beck, R.; Johnson, S. A. Chem. Commun. 2011, 47, 9233− 9235. (b) Keen, A. L.; Doster, M.; Johnson, S. A. J. Am. Chem. Soc. 2007, 129, 810−819.
24. Yu, D.-G.; Li, B.-J.; Shi, Z.-J. Acc. Chem. Res. 2010, 43, 1486−1495.
25. Morrell, D. G.; Kochi, J. K. J. Am. Chem. Soc. 1975, 97, 7262−7270.
26. Tsou, T. T.; Kochi, J. K. J. Am. Chem. Soc. 1979, 101, 6319−6332.
27. (a) Iluc, V. M.; Miller, A. J. M.; Anderson, J. S.; Monreal, M. J.; Mehn, M. P.; Hillhouse, G. L. J. Am. Chem. Soc. 2011, 133, 13055−13063. (b) Gennari, M.; Orio, M.; Pécaut, J.; Bothe, E.; Neese, F.; Collomb, M.-N.; Duboc, C. Inorg. Chem. 2011, 50, 3707−3716. (c) Green, B. J.; Tesfai, T. M.; Xie, Y.; Margerum, D. W. Inorg. Chem. 2004, 43, 1463−1471. (d) Lee, C.-M.; Chuang, Y.-L.; Chiang, C.-Y.; Lee, G.-H.; Liaw, W.-F. Inorg. Chem. 2006, 45, 10895−10904. (e) Lee, C.-M.; Chiou, T.-W.; Chen, H.-H.; Chiang, C.-Y.; Kuo, T.-S.; Liaw, W.-F. Inorg. Chem. 2007, 46, 8913−8923.

Chapter 3
Monomeric Ni(I)/NHC species bearing Monodentate 2e Donor Ligand in catalysis

3-1. Introduction

Organonickel-catalyzed organic transformations have been widely studied in recent decades, and many useful reactions have been discovered.[1] A general feature of nickel-mediated reactions is oxidation of a zerovalent species to a nickel(II) species, which is then reduced to complete the catalytic cycle. However, zerovalent nickel species, unlike zerovalent palladium species, are generally unstable; therefore the development of efficient methods for reduction to nickel(0) is important in developing efficient catalytic processes.[2] On the other hand, Ni(I) species have recently been reported in useful cross-coupling reactions,[3] and well-defined Ni(I) complexes have been shown to mediate cross-coupling reactions of aryl and alkyl halides;[4] for example, Vicic et al. reported that a terpyridine-stabilized Ni(I) complex catalyzed the Negishi coupling of alkyl halides.[5] These Ni(I)-catalyzed processes have advantages over the usual nickel(0) catalysts for the following reasons: (1) reduction to Ni(I) species is easier than reduction to nickel(0) in catalytic cycles; (2) the unpaired electron weakens the nickel–ligand bonding interactions, resulting in easier elimination of ligand and/or the product in catalysis than the diamagnetic nickel species.[4] Therefore, the development of Ni(I)-catalyzed organic reactions and new catalytic systems is important in both organic and organometallic chemistry.

Examples of catalysts starting from well-defined Ni(I) precursors have rarely been reported,[4] although many examples of Ni(I) complexes are known.[6] This is because Ni(I) compounds are frequently thermally unstable and disproportionate to form nickel(0) and nickel(II) compounds. They are also extremely unstable in air and generally form oxidized compounds. Bulky N-heterocyclic carbene (NHC) ligands thermally stabilize Ni(I) species in catalysis.[4] Among such Ni(I) complexes, Ni(I) chloride bearing two IPr

ligands, i.e., $Ni(IPr)_2Cl$, where IPr is 1,3-bis(2,6-diisopropylphenyl)imidazol-2-ylidene, is in equilibrium with dinuclear Ni(I) chloride, $[Ni(IPr)]_2(\mu\text{-}Cl)_2$ (**1**), with elimination of one IPr ligand.[4a] This prompted us to add PPh_3 as a two-electron-donor ligand to **1**, prepared by another method,[7] resulting in efficient generation of a three-coordinate Y-shaped monomeric Ni(I) complex, $Ni(IPr)Cl(PPh_3)$ (**2a**).[8] Complex **2a** was more air-stable than **1**, and it catalyzed Kumada–Tamao–Corriu coupling and Buchwald–Hartwig aminations of aryl bromides more efficiently than did **1** and $Ni(IPr)_2Cl$.[8] PPh_3 is easily eliminated from **2a** to form an unsaturated and highly active, monomeric two-coordinate species, Ni(IPr)Cl, or the dimeric Ni(I) complex **1** because of the strong *trans* effect of the NHC ligand,[9] and the stable resting state, with recoordination of PPh_3, stabilizes the catalytic system. Excess PPh_3 did not deactivate the process and did not compete with the substrates for coordination to nickel. Our preliminary results showed that $Ni(IPr)_2Cl$ reduction with a Grignard reagent readily forms a zerovalent complex $Ni(IPr)_2$, without elimination of IPr, whereas **2a** eliminates phosphine in conjunction with the Grignard reagent to form a dimeric Ni(I) transmetalation product.[8] The introduction of other donor ligands, including other phosphines and pyridine derivatives, to **2** could be used to control the activity and stability of the Ni(I) complex **2**.

A large variety of bulky NHC ligands have been designed and built for use in catalysts.[10] We focused on the structural differences between IPr and 1,3-bis(mesityl)imidazol-2-ylidene (IMes); the different steric effects around the metal centers result in clear differences between their reactivities and stabilities. Ni(I) species bearing an IPr or IMes ligand differ significantly; for example, preparation of an IMes analogue of the dimeric Ni(I) compound **1** is impossible. This indicates that the monomeric IMes analogue of **2** and the IPr complex **2** cannot be synthesized using the

same method. However, several Ni(I) NHC complexes have been prepared from $Ni(cod)_2$ and NiX_2L_2 (X = halogen, L = 1,2-dimethoxyethane or triphenylphosphine) in the presence of an NHC.[7,11]

In this study, we prepared a series of Ni(I) complexes bearing IPr and IMes and various two-electron-donor ligands. These compounds were characterized using spectroscopy, superconducting quantum interference device (SQUID) measurements, and X-ray crystallography. The catalytic activities of the monomeric Ni(I) complexes in the Suzuki coupling and Buchwald–Hartwig amination of aryl bromides were compared.

3-2. Synthesis and Characterizations

3-2-1. Preparation of Monomeric Ni(I) NHC Complexes

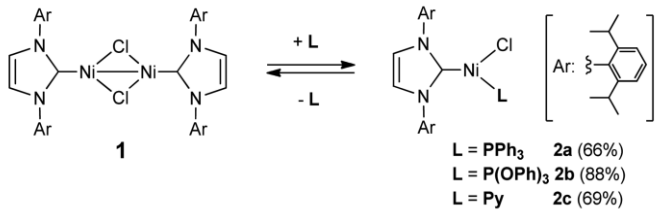

Scheme 3-1. Preparation of Mononickel(I) IPr Complexes

The IPr complexes **2** were synthesized from dimeric complex **1** and two-electron-donor ligands (Scheme 3-1). The $P(OPh)_3$ analogue Ni(IPr)Cl($P(OPh)_3$) (**2b**) was readily isolated in 88% yield as red-orange crystals. Addition of pyridine to a solution of **1** afforded Ni(IPr)Cl(pyridine) (**2c**), in which only one molecule of pyridine was coordinated to nickel, in 69% yield upon recrystallization.

Bisphosphines also reacted with **1**. However, the addition of 1,2-bis(diphenylphosphino)ethane (dppe) or 1,3-bis(diphenylphosphino)propane (dppp) gave not the expected Ni(I) complex **2** but mixtures containing zerovalent nickel complexes $Ni(dppe)_2$ (**5a**)[12] or $Ni(dppp)_2$ (**5b**).[13] Divalent complex $Ni(IPr)_2Cl_2$ (**6**) was also detected

as the product in the crude reaction mixture (see the SI). Zerovalent complexes **5a** and **5b** were isolated as crystals in 24% and 32% yield, respectively, although **6** could not be isolated. It should be noted that when 1,4-bis(diphenylphosphino)butane (dppb), in which the methylene chain is one carbon longer than dppp, was used as the ligand, the diNi(I) dppb complex $[Ni(IPr)Cl]_2(dppb)$ (**2d**) was successfully obtained in 74% yield upon recrystallization (Scheme 2).

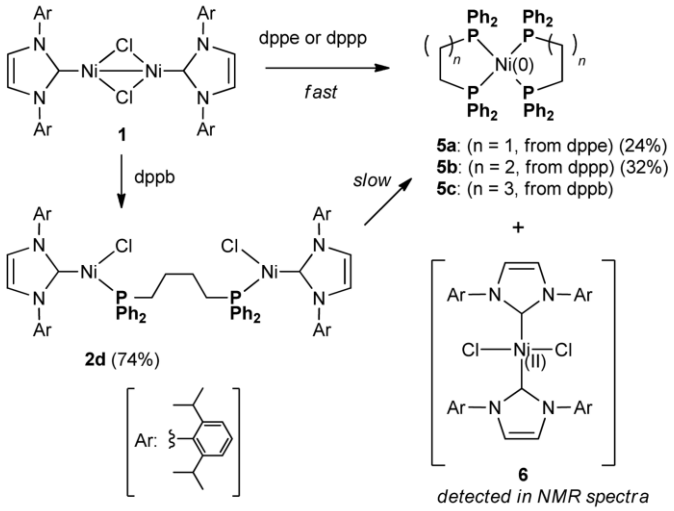

Scheme 3-2. Reaction of 1 with Bisphosphines

However, the complex **2d** rearranged slowly in the benzene-d_6 solution in a day to form a mixture of the zerovalent complex $Ni(dppb)_2$[14] (**5c**), suggesting that disproportionation occurred via formation of the diNi(I) intermediate **2** even in the reactions with dppe and dppp. Aggregation of the paramagnetic Ni(I) centers as a result of the short methylene linkages in dppe and dppp may enable facile electron transfer from one of the Ni(I) atoms to the other, generating nickel(0) and nickel(II) species, whereas the longer chain in dppb makes electron transfer slower. If electron transfer from Ni(I) to Ni(I) occurred through the bonding interaction, the dimeric Ni(I) complex **1** would easily heterolytically split into nickel(0) and nickel(II) species; however, this never occurs. Through-space electron transfer between the two Ni(I) centers closely linked by the bidentate ligands may be

necessary in the disproportionation. This is a rare and significant example of the electron transfer rate being controlled by the distance between two Ni(I) centers (Ni–P–$(CH_2)_3$–P–Ni and Ni–P–$(CH_2)_4$–P–Ni).[15] Complex **2d** was not used as a catalyst in the following catalytic studies, because the complex **5c** can be formed in situ under the catalytic conditions.

As noted above, the smaller IMes ligand did not provide the analogue of the dimeric Ni(I) IPr complex **1**, because the bulky ligand, i.e., IPr, is probably desirable to stabilize the coordinatively unsaturated dimer complex kinetically. The corresponding monomeric IMes analogues of **2** were therefore synthesized using Whittlesey's method.[11] $Ni(cod)_2$, $NiX_2(PPh_3)_2$ (X = Cl and Br), and IMes/HCl were mixed in the presence of $KN(SiMe_3)_2$ as a base, resulting in in situ generation of the free carbene, at room temperature. The reaction efficiently afforded the expected $Ni(IMes)X(PPh_3)$ (**3a**: X = Cl; **3b**: X = Br) in 84% and 49% yields by recrystallization (Scheme 3).

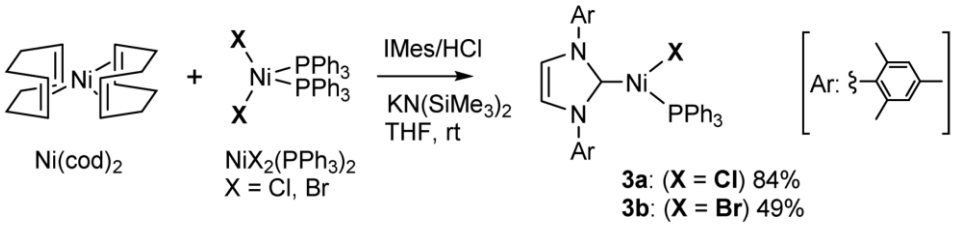

Scheme 3-3. Preparation of Mononickel(I) IMes Complexes.

These IMes analogues **3** were very unstable in air, but the bromide complex **3b** was more stable than the chloride counterpart **3a**.

Broad paramagnetic signals were observed in the ^{1}H NMR spectra of the monomeric Ni(I) compounds **2b**–**d**, **3a**, and **3b** at around δ 1–14, similar to those for **2a** (see the SI). As previously reported, an unpaired electron is delocalized only on the nickel d-orbital, providing sharp solvent signals in the ^{1}H NMR spectra.[4a] DFT calculations also supported

these results, as described below.

When crystals of **2a** and **2b** were dissolved in benzene-d_6, the dimeric compound **1** was generated in situ with liberation of the free ligand and was detected in the ^{1}H NMR spectrum. Addition of extra portions (2–5 equiv) of the ligand to the solutions resulted in the disappearance of **1**, indicating that there is equilibrium in solution between the monomeric and dimeric Ni(I) complexes in the presence of the donor ligands. The relative ratios of **1**:**2a**–**c** in equilibrium depended on the ligand: pyridine (**2c**) > PPh_3 (**2a**) > $P(OPh)_3$ (**2b**).[16] This trend is related to the π-acceptor abilities of these ligands, as expected. In contrast to the IPr complexes **2**, the diamagnetic dimeric complexes $[Ni(IMes)]_2(\mu\text{-}X)_2$ were not observed when crystals of **3a** and **3b** were dissolved in benzene-d_6. When 5 equiv of pyridine was added to a solution of **2c**, the ^{1}H NMR spectrum showed no sharp signals assignable to free pyridine, suggesting fast equilibrium between coordination and elimination of pyridine molecules. Although we have no direct information on the solution structure, we assume that elimination of pyridine gives a 13-electron linear structure without coordination of pyridine or formation of a tetracoordinate 17-electron complex, $Ni(IPr)Cl(pyridine)_2$, with tetrahedral geometry around the Ni(I) center.

The spin states of the series of monomeric Ni(I) complexes were investigated based on SQUID measurements of **2b**–**d**. It was previously reported that **2a** has $S = 1/2$ ($\chi_{mol}T$ = 0.44 cm^3 K mol^{-1} at −263 °C, where χ_{mol} is molar magnetic susceptibility) and a three-coordinate Y-shaped 15-electron structure.[8] The spin quantum numbers of the other complexes were also 1/2 [$\chi_{mol}T$ = 0.35 (**2b**), 0.52 (**2c**), 0.34 (**2d**, per nickel atom) at −253 °C] (see the SI). Any magnetic interaction between Ni(I) centers in the dinuclear complex **2d** was not observed, even at −268 °C, because the distance between the two

nickel atoms, which was estimated from the crystal structure (shown below), was too long (ca. 8.30 Å) for them to interact with each other. The theoretical value of $\chi_{mol}T$ is 0.375 cm^3 K mol^{-1} when $S = 1/2$; therefore that of **2c** is slightly higher than the theoretical value and also of those of the other complexes (Figure 3-1a). The ESR spectrum of **2c** in toluene at −263 °C showed three-axial anisotropy [g_{xx} = 2.042, g_{yy} = 2.235, g_{zz} = 2.452] (Figure 3-1b). The $\chi_{mol}T$ calculated from these g values is 0.47, which is almost in agreement with that from the SQUID results.

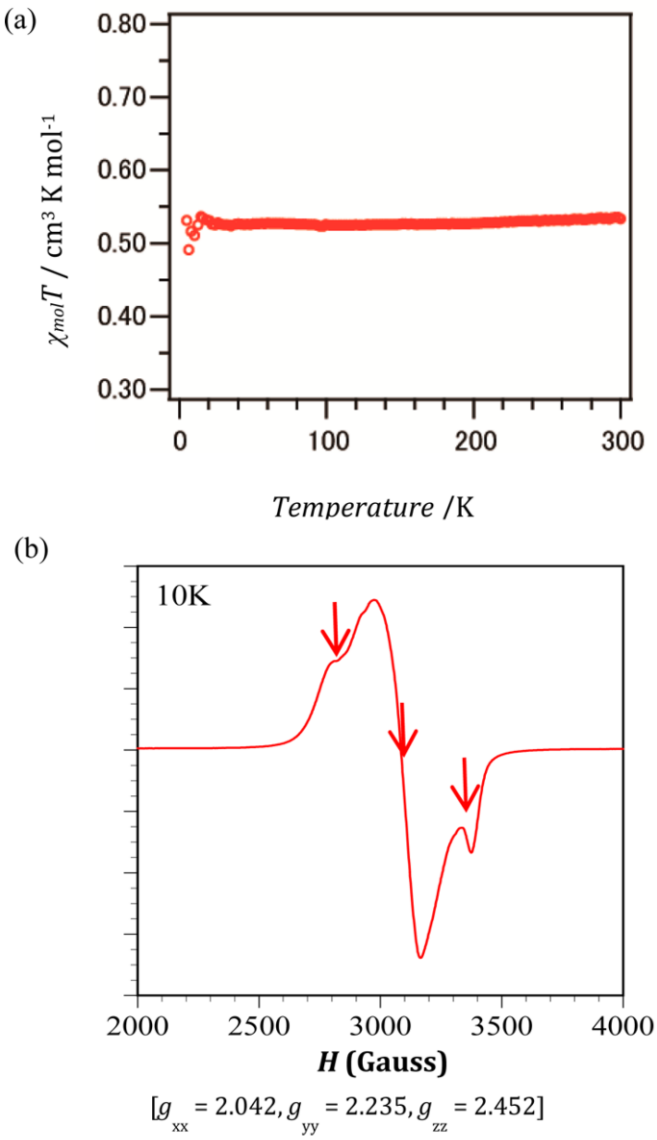

Figure 3-1. (a) χmolT versus temperature plots of 2c and (b) frozen solution ESR

spectrum of 2c at 10 K (−263 °C) in dilute toluene.

Figure 2 shows the crystal structures of **2b**, **2c**, **2d**, **3a**, and **3b**. Representative bond lengths and angles around the nickel atom, including those for **2a**, are listed in Table 3-1. The sum of the angles around the nickel atom was almost 360° in each complex, indicating planar three-coordinate geometries. The Ni–C(carbene) and Ni–Cl distances and the angles around the nickel atom did not differ between **2** and **3**, indicating that the differences between the shapes and sizes of the NHC ligands did not affect the structures around the nickel atom. On the basis of the π-acceptor ability of the phosphorus ligand, the P–Ni bond distance in **2b** was 0.1 Å shorter than that in **2a**. The Cl–Ni–C(carbene) angle in **2c**, which contains pyridine, is 142.1(1)°, which is much larger than those for the other phosphine complexes, i.e., 131–134°. The Ni–N(pyridine) bond distance was 2.200(3) Å, which is significantly longer than the usual nickel–nitrogen σ-bond distances, i.e., ca. 2.0 Å.[17] Delocalization of the unpaired electron in the Ni–N(pyridine) σ*-orbital was negligible (2.5%) (calculated below); therefore this elongation must be ascribed to other reasons. This weak interaction may stretch the Cl–Ni–C(carbene) hinge.

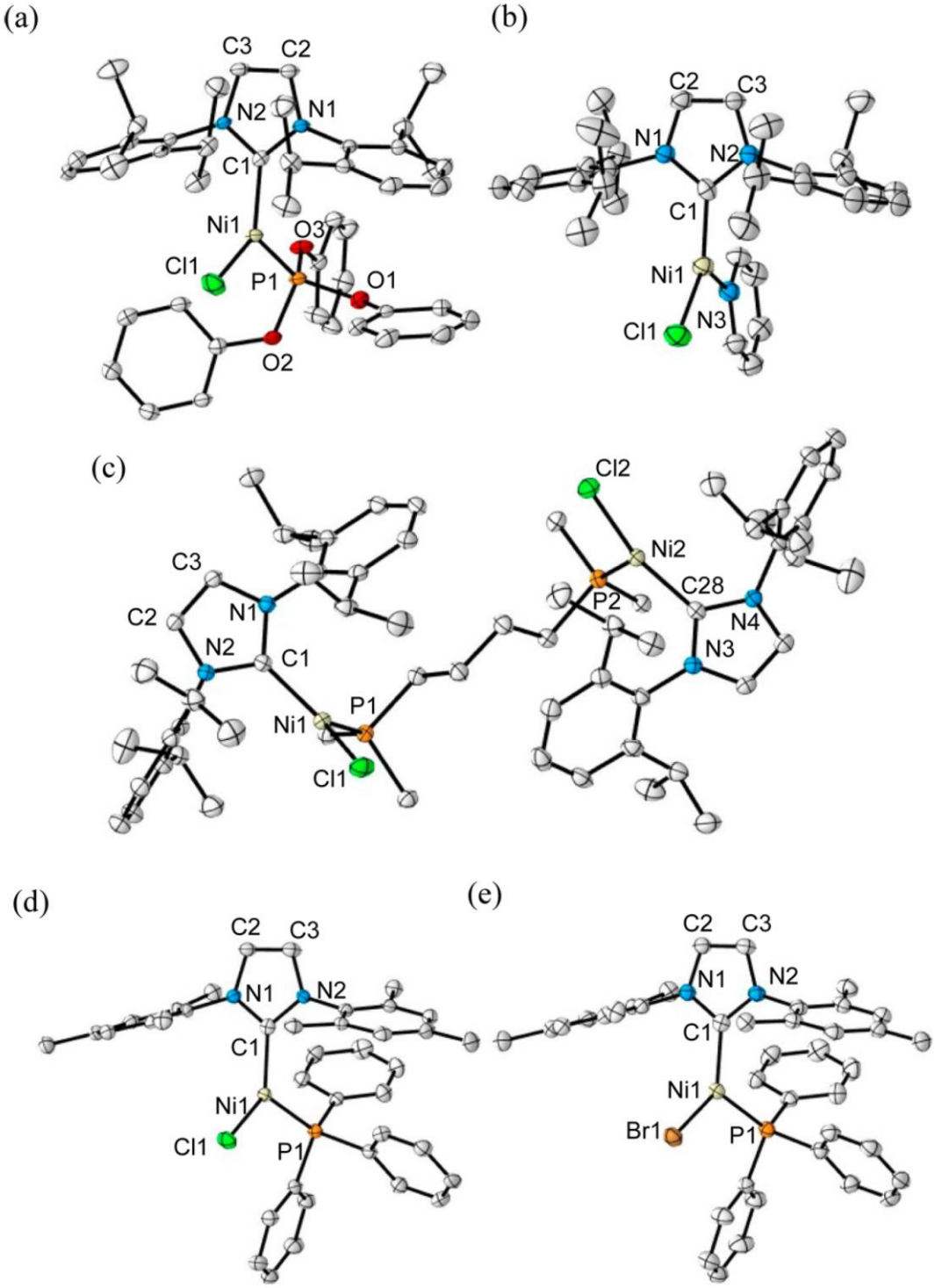

Figure 3-2. ORTEP drawings of nickel(I) complexes: (a) 2b, (b) 2c, (c) 2d, (d) 3a, and (e) 3b (50% probability thermal ellipsoids). All hydrogen atoms are omitted. Three THF molecules and four phenyl rings on dppb in 2d and two THF molecules in 3a and 3b are also omitted for clarity.

3-2-2. Theoretical Studies

The distribution of the single-electron-occupied molecular orbital (SOMO) was investigated by performing single-point DFT calculations at the fixed geometries given by the crystallographic coordinates of **2a**–**c** and **3a** with the B3LYP functional and 6-31G(d,p) basis set (Figure 3-3). In complex **2a**, the unpaired electron is localized mainly on the nickel d-orbital (51.4%) and the chlorine–nickel π*-orbital (11.9%). It also forms a phosphorus–nickel σ*-bond (12.4%).[4c] The distribution in **2b** was similar to that in **2a**: nickel d-orbital (47.8%), Ni–Cl π*-orbital (13.8%), and Ni–P σ-orbital (12.3%). In contrast, in **2c**, the unpaired electron is located mainly on nickel (80.7%), and the values for the Ni–Cl and Ni–N bonds are 4.5% and 2.5%, respectively. Generally, the nonbonding orbital energy of pyridine is lower than that of phosphorus; therefore the energy gap between nickel and nitrogen is larger than that between nickel and phosphorus, weakening the nickel–pyridine interactions, including donation and π-back-donation, compared with those in the Ni–P bond. There were no conspicuous differences between the IPr complex **2a** and the corresponding IMes analogue **3a**, suggesting that different substituents on the NHC ligands do not affect the electronic structures of these complexes.

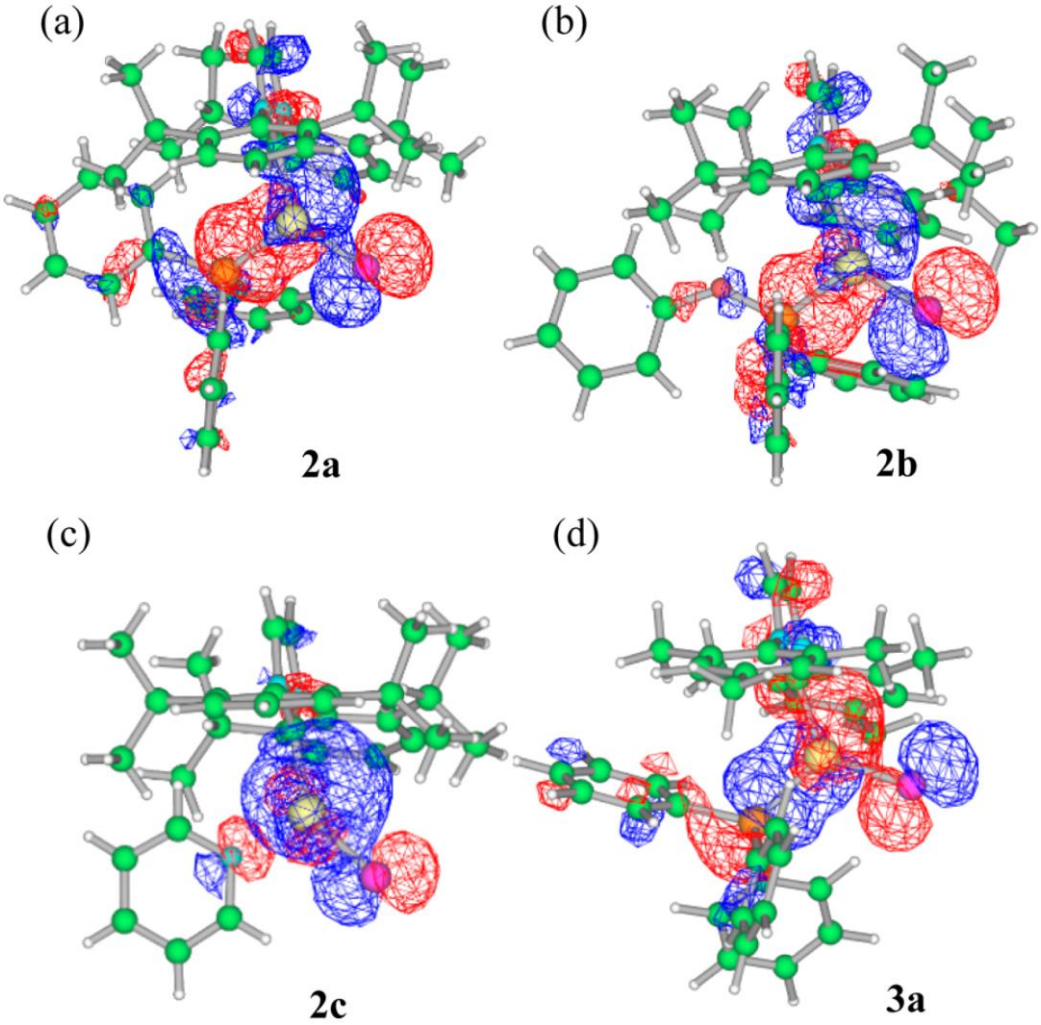

Figure 3-3. SOMOs (red and blue mesh; density isosurface value of 0.02 au) in (a) 2a, (b) 2b, (c) 2c, and (d) 3a obtained from single-point DFT calculations at the B3LYP/6-31G(d,p) level using crystallographic coordinates (nickel, yellow; orange, phosphorus; purple, chlorine; nitrogen, light blue; carbon, green).

Table 3-1. Representative Bond Distances and Angles for 2a, 2b, 2c, 2d, 3a, and 3b

	2a (Y = P)	**2b** (Y = P)	**2c** (Y = N)	**2d** (Y = P)	**3a** (X = Cl)	**3b** (X = Br)
			Bond Lengths (Å)			
Ni(1)−C(1)	1.930(3)	1.928(3)	1.909(4)	1.937(2), 1.939(2)	1.938(4)	1.949(3)
Ni(1)−X(1)	2.1786(9)	2.1545(9)	2.201(1)	2.1973(7), 2.1994(7)	2.188(1)	2.3178(6)
Ni(1)−Y(1)	2.201(1)	2.1170(6)	2.200(3)	2.2042(6), 2.2006(6)	2.205(1)	2.2051(9)
			Bond Angles (deg)			
X(1)−Ni(1)−C(1)	134.2(1)	134.29(6)	142.1(1)	132.29(6), 136.99(6)	132.8(1)	131.03(9)
Y(1)−Ni(1)−C(1)	112.1(1)	109.41(6)	107.2(1)	112.79(6), 111.71(6)	111.6(1)	112.76(9)
X(1)−Ni(1)−Y(1)	113.31(4)	116.30(3)	110.73(9)	114.37(3), 110.72(3)	115.31(5)	115.95(3)
$\sum_{Ni}$	359.5(1)	360.00(6)	360.0(1)	359.45(6), 359.42(6)	359.7(1)	359.74(9)

3-3. Catalysis and Reactivity

3-3-1. Catalytic Applications in Buchwald–Hartwig Amination and Suzuki–Miyaura Cross-Coupling Reactions

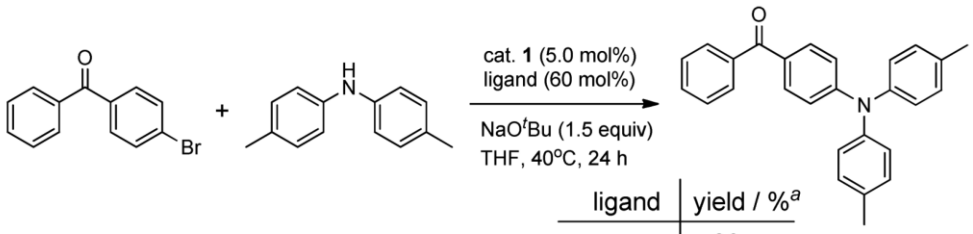

ligand	yield / %[a]
none	80
PPh_3	99
$P(OPh)_3$	39
pyridine	98

[a]The yields were determined after silica gel column chromatography.

Scheme 3-4. Triarylamine Formation via Buchwald−Hartwig Amination

The obtained Ni(I) compounds were used in catalytic cross-coupling reactions. Their catalytic activities were compared by performing Buchwald–Hartwig aminations of bromobenzophenone with diphenylamine, under reaction conditions using **2a** as the catalyst, similar to those previously reported.[8] Scheme 3-4 shows the reaction protocol and yields of the triarylamine products. Excess amounts of the two-electron-donor ligands [PPh_3, $P(OPh)_3$, and pyridine] were added to 5 mol % of **1** to generate the corresponding monomeric Ni(I) complexes **2a**, **2b**, and **2c** in situ. The substrates were then added, and the mixture was stirred at 40 °C for 24 h in THF. The products were isolated after silica gel column chromatography. The ligand strongly affected the product yields, which were 99% for PPh_3, 39% for $P(OPh)_3$, and 98% for pyridine. The smallest ligand, i.e., pyridine, did not inhibit interactions of the substrates with nickel. Pyridine can be easily eliminated from **2c** to generate the active form **1**, whereas little $P(OPh)_3$ is eliminated from **2b**, preventing generation of the active species. Interestingly, PPh_3 adequately controls the concentration of **1** and stabilizes the unstable active species to form the monomeric complex as the resting state.

Table 3-2. Suzuki−Miyaura Cross-Coupling Reactions of Aryl Bromides with Phenylboronic Acid

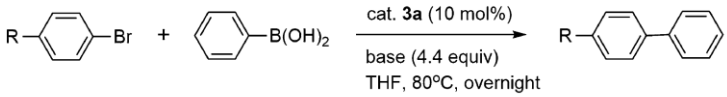

entry	R−	base	solvent	yield/%[a]
1	PhCO−	NaO^{t}Bu	toluene	54
2	PhCO−	KO^{t}Bu	toluene	65
3	PhCO−	K_3PO_4	toluene	66
4	PhCO−	K_2CO_3	toluene	79
5	PhCO−	Cs_2CO_3	toluene	88
6	PhCO−	Cs_2CO_3	THF	68
7	PhCO−	Cs_2CO_3	CPME	72
8	CH_3O−	Cs_2CO_3	toluene	45

a) The yields were determined with GC-MS. Calibration was carried out using a standard sample of 4,4'-dimethoxybiphenyl.

In our preliminary research, a series of IPr complexes of Ni(I) were inactive in the Suzuki cross-coupling reactions of aryl halides. In general, the Suzuki cross-coupling reaction does not require steric hindrance derived from bulky ligands on metal centers,[18] in contrast to Buchwald–Hartwig amination, which does require bulky ligands.[19] In this case, the bulkiness of the ligand is critical in inhibiting the reaction: the IMes complex is catalytically active, but the IPr complex is not. Louie et al. reported Ni(I)-catalyzed Suzuki coupling of aryl halides using a bis(IMes) complex of Ni(I), [NiCl(IMes)$_2$].[4b] Here, we used the analogous complex **3a**, containing PPh_3 instead of IMes.

We used an activated aryl bromide, 4-bromobenzophenone, in cross-coupling with phenylboronic acid in the presence of the Ni(I) chloride complex **3a** (10 mol %) (Table 3-2). Base screening showed that using NaO^{t}Bu and KO^{t}Bu (entries 1 and 2) and potassium phosphonate and carbonate (entries 3 and 4) provided moderate to good yields (54–79%) of the cross-coupling products. Cesium carbonate was the best base and afforded the product in 88% yield (entry 5). Toluene was a better solvent than THF and cyclopentyl methyl ether (CPME) (entries 6 and 7). When the less active bromoanisole

was used as the substrate, the yield after 4 h was moderate (45%; entry 8).[4b]

3-4. Summary

In summary, we have developed synthetic methods for a series of Ni(I) complexes bearing mixed ligands, namely, bulky NHCs and other two-electron-donor ligands. The complex structures were determined using SQUID, ESR, and X-ray crystallography. The chemical structures of the two-electron-donor ligands affected the stabilities, SOMO distributions, and catalytic activities of the corresponding Ni(I) complexes. Pyridine weakly coordinates to Ni(I) and is easily liberated to form the dimeric complex, whereas $P(OPh)_3$ strongly binds to Ni(I) and stabilizes the monomeric form. The monomeric complexes Ni(IPr)Cl(L) were not thermally stable when diphosphines bridged with a three- or two-carbon unit, e.g., dppp or dppe, were introduced, and mixtures of zerovalent and divalent nickel complexes were obtained, probably because of easy electron transfer and subsequent disproportionation. However, a dppb complex of Ni(I) was successfully isolated and characterized, although it was slowly transformed into a mixture of nickel(0) and nickel(II) species. The bulky NHCs IPr and IMes do not affect the electronic structures of the monomeric Ni(I) complexes, but the dimeric IPr complex $[Ni(IPr)]_2(\mu\text{-}Cl)_2$ is much more stable than its IMes analogue. Ni(I) complexes bearing both IPr and IMes ligands are active in cross-coupling reactions of aryl bromides. Buchwald–Hartwig aminations using the monoNi(I) IPr complexes as catalysts proceeded efficiently to yield triarylamines. The IPr complexes did not catalyze the Suzuki cross-coupling reactions of aryl halides, although the active IMes analogues did. These small differences derived from the NHC ligand structures help precisely control catalytic processes. Mechanistic studies of these cross-coupling reactions using Ni(I) complexes and the development of

air-stable Ni(I) catalyst precursors are now in progress.

3-5. References

1. (a) Tasker, S. Z.; Standley, E. A.; Jamison, T. F. Nature 2014, 509, 299−309. (b) Montgomery, J. In Organometallics in Synthesis: Fourth Manual; Lipshutz, B. H., Ed.; John Wiley & Sons: Hoboken, NJ, 2013; Chapter 3, pp 319−428. (c) Modern Organonickel Chemistry; Tamaru, Y., Ed.; Wiley-VCH: Weinheim, 2005. (d) Hassan, J.; Sévignon, M.; Gozzi, C.; Schulz, E.; Lemaire, M. Chem. Rev. 2002, 102, 1359−1469.
2. Ford, L.; Jahn, U. Angew. Chem., Int. Ed. 2009, 48, 6386−6389. (b) Gao, C.-Y.; Cao, X.; Yang, L.-M. Org. Biomol. Chem. 2009, 7, 3922−3925. (c) Breitenfeld, J.; Ruiz, J.; Wodrich, M. D.; Hu, X. J. Am. Chem. Soc. 2013, 135, 12004−12012. (d) Ren, P.; Vechorkin, O.; vonAllmen, K.; Scopelliti, R.; Hu, X. J. Am. Chem. Soc. 2011, 133, 7084−7095. (e) Schley, N. D.; Fu, G. C. J. Am. Chem. Soc. 2014, 136, 16588−16593.
3. (a) Chatani, N.; Tobisu, M. Acc. Chem. Res. 2015, 48, 1717−1726. (b) Weix, D. J. Acc. Chem. es. 2015, 48, 1767−1775. (c) Liu, D.; Li, Y.; Qi, X.; Liu, C.; Lan, Y.; Lei, A. Org. Lett. 2015, 17, 998−1001. (d) Gutierrez, O.; Tellis, J. C.; Primer, D. N.; Molander, G. A.;Kozlowski, M. C. J. Am. Chem. Soc. 2015, 137, 4896−4899. (e) Biswas, S.; Weix, D. J. J. Am. Chem. Soc. 2013, 135, 16192−16197. (f) Anderson, T. J.; Jones, G. D.; Vicic, D. A. J. Am. Chem. Soc. 2004, 126, 8100−8101.
4. (a) Miyazaki, S.; Koga, Y.; Matsumoto, T.; Matsubara, K. Chem. Commun. 2010, 46, 1932−1934. (b) Zhang, K.; Conda-Sheridan, M. Cooke, S. R.; Louie, J. Organometallics 2011, 30, 2546−2552. (c) Page, M. J.; Lu, W. Y.; Poulten, R. C.; Carter, E.; Algarra, A. G.; Kariuki, B. M.; Macgregor, S. A.; Mahon, M. F.; Cavell, K. J.; Murphy, D. M.; Whittlesey, M. K. Chem. - Eur. J. 2013, 19, 2158−2167.
5. (a) Jones, G. D.; Martin, J. L.; McFarland, C.; Allen, O. R.; Hall, R. E.; Haley, A. D.; Brandon, R. J.; Konovalova, T.; Desrochers, P. J.; Pulay, P.; Vicic, D. A. J. Am. Chem. Soc. 2006, 128, 13175−13183. (b) Lin, X.; Phillips, D. L. J. Org. Chem. 2008, 73, 3680−3688.
6. (a) Kitiachvili, K. D.; Mindiola, D. J.; Hillhouse, G. L. J. Am. Chem. Soc. 2004, 126, 10554−10555. (b) Melenkivitz, R.; Mindiola, D. J.; Hillhouse, G. L. J. Am. Chem. Soc. 2002, 124, 3846−3847. (c) Holland, P. L.; Cundari, T. R.; Perez, L. L.; Eckert, N. A.; Lachicotte, R. J. J. Am. Chem. Soc. 2002, 124, 14416−14424. (d) Eckert, N. A.; Dinescu, A.; Cundari, T. R.; Holland, P. L. Inorg. Chem. 2005, 44, 7702−7704. (e) Fujita, K.; Rheingold, A. L.; Riordan, C. G. Dalton Trans. 2003, 2004−2008. (f) Eaborn, C.; Hill, M. S.; Hitchcock, P. B.; Smith, J. D. Chem. Commun. 2000, 691−692. (g) Ito, M.; Matsumoto, T.; Tatsumi, K. Inorg. Chem. 2009, 48, 2215−2223. (h) Marlier, E. E.; Tereniak, S. J.; Ding, K.; Mulliken, J. E.; Lu, C. C. Inorg. Chem. 2011, 50, 9290−9299. (i) Laskowski, C. A.; Bungum, D. J.; Baldwin, S. M.; Ciello, S. A. D.; Iluc, V. M.; Hillhouse, G. L. J. Am. Chem. Soc. 2013, 135, 18272−18275.

7. Dible, R. B.; Arif, M. A.; Sigman, S. M. Inorg. Chem. 2005, 44, 3774−3776.
8. Nagao, S.; Matsumoto, T.; Koga, Y.; Matsubara, K. Chem. Lett. 2011, 40, 1036−1038.
9. Sanford, M. S.; Love, J. A.; Grubbs, R. H. J. Am. Chem. Soc. 2001, 123, 6543−6554.
10. (a) N-Heterocyclic Carbenes; Nolan, S. P., Ed.; Wiley-VCH: Weinheim, 2014. (b) Hopkinson, N. M.; Richter, C.; Schedler, M.; Glorius, F. Nature 2014, 510, 485−496. (c) Nelson, J. D. Eur. J. Inorg. Chem. 2015, 2015, 2012−2027.
11. Davies, C. J. E.; Page, M. J.; Ellul, C. E.; Mahon, M. F.; Whittlesey, M. K. Chem. Commun. 2010, 46, 5151−5153.
12. (a) Matsubara, K.; Ueno, K.; Shibata, Y. Organometallics 2006, 25, 3422−3427. (b) Liu, Z.-H.; Xu, Y.-C.; Xie, L.-Z.; Sun, H.-M.; Shen, Q.; Zhang, Y. Dalton Trans. 2011, 40, 4697−4706.
13. Lejkowski, L. M.; Lindner, R.; Kageyama, T.; Bodizs, E. G.; Plessow, N. P.; Muller, B. I.; Schafer, A.; Rominger, F.; Hofmann, P.; Futter, C.; Schunk, A. S.; Michael, L. Chem. - Eur. J. 2012, 18, 14017−14025.
14. (a) Bricout, H.; Carpentier, J.-F.; Mortreux, A. Tetrahedron Lett. 1997, 38, 1053−1056. (b) Bricout, H.; Carpentier, J.-F.; Mortreux, A. Tetrahedron 1998, 54, 1073−1084. (c) Edwards, J. A.; Retbùll, M.; Wenger, E. Acta Crystallogr., Sect. E: Struct. Rep. Online 2002, 58, 375− 377. (d) Retbøll, M.; Edwards, J. A.; Rae, A. D.; Willis, C. A.; Bennett, A. M.; Wenger, E. J. Am. Chem. Soc. 2002, 124, 8348−8360. (e) Fischer, R.; Langer, J.; Malassa, A.; Walther, D.; Gorls, H.; Vaughan, G. Chem. Commun. 2006, 2510−2512.
15. Serron, S. A.; Aldridge, W. S., III; Fleming, C. N.; Danell, R. M.; Baik, M.-H.; Sykora, M.; Dattelbaum, D. M.; Meyer, T. J. J. Am. Chem. Soc. 2004, 126, 14506−14514.
16. Because identification of each signal in the NMR spectra of the paramagnetic compounds 2 was difficult, the values of the ratios between 1 and 2 were not determined.
17. For example, see: Kogut, E.; Wiencko, H. L.; Zhang, L.; Cordeau, D. E.; Warren, T. H. J. Am. Chem. Soc. 2005, 127, 11248−11249.
18. (a) Han, F.-S. Chem. Soc. Rev. 2013, 42, 5270−5298. (b) Maluenda, I.; Navarro, O. Molecules 2015, 20, 7528−7557.
19. (a) Wolfe, J. P.; Wagaw, S.; Marcoux, J.-F.; Buchwald, S. T. Acc. Chem. Res. 1998, 31, 805−818. (b) Hartwig, J. F. Acc. Chem. Res. 2008, 41, 1534−1544.
20. Jafarpour, L.; Stevens, E. D.; Nolan, S. P. J. Organomet. Chem. 2000, 606, 49−54.
21. Matsubara, K.; Miyazaki, S.; Koga, Y.; Nibu, Y.; Hashimura, T.; Matsumoto, T. Organometallics 2008, 27, 6020−6024.
22. CrystalStructure 4.0: Crystal Structure Analysis Package; Tokyo 196-8666, Japan, 2000−2011.
23. SIR2008: Burla, M. C.; Caliandro, R.; Camalli, M.; Carrozzini, B.; Cascarano, G. L.; De Caro, L.; Giacovazzo, C.; Polidori, G.; Siliqi, D.; Spagna, R. J. Appl. Crystallogr. 2007, 40, 609−613.
24. Sheldrick, G. M. SHELXL97; University of Gottingen: Germany, 1997.

25. Frisch, M. J.; Trucks, G. W.; Schlegel, H. B.; et al. Gaussian 09, Revision D.01; Gaussian, Inc.: Wallingford, CT, 2013.

Chapter 4

4. Monomeric Ni(I)/NHC species bearing bidentate 4e Donor Ligand in catalysis

4-1. Introduction

Nickel-catalysed organic transformations involving active nickel intermediates with odd-valence numbers have been challenging targets in recent chemistry of catalysis.[1] This has become an intriguing unsolved problem, occurring with chemical advances such as the search for catalytically active species and analysis of reaction mechanisms by computational chemistry. Although monovalent nickel complexes are thermally stable and can be easily isolated under an inert-gas atmosphere,[2] direct involvement of Ni(I) in catalytic cycles has not been observed for decades. Recently, however, several reports have proposed catalytic pathways that involve mononuclear Ni(I)-L and dinuclear L-Ni(I)-Ni(I)-L complexes, where L is monodentate or bidentate ligand, such as phosphine and N-heterocyclic carbine (NHC).[3-7] Depending on the structure of the ligands or the type of reactions, mononuclear Ni(I) is generated as an off-cycle product or can act as a key intermediate in the cycle. If it is revealed that Ni(I) complexes can act as a true active intermediate, development of new types of reactions using nickel catalysts could be possible. Furthermore, a Ni(I)-Ni(III) cycle can be considered to be analogous to a Pd(0)-Pd(II) cycle, where various highly efficient catalytic reactions have been developed. That is because a Ni(0) complex is easily oxidised to the corresponding Ni(II) and hardly reduced back to Ni(0), while a 2e-oxidation of Ni(I) into Ni(III) can be relatively difficult but 2e-oxidised intermediate Ni(III) can be easily reduced.[3]

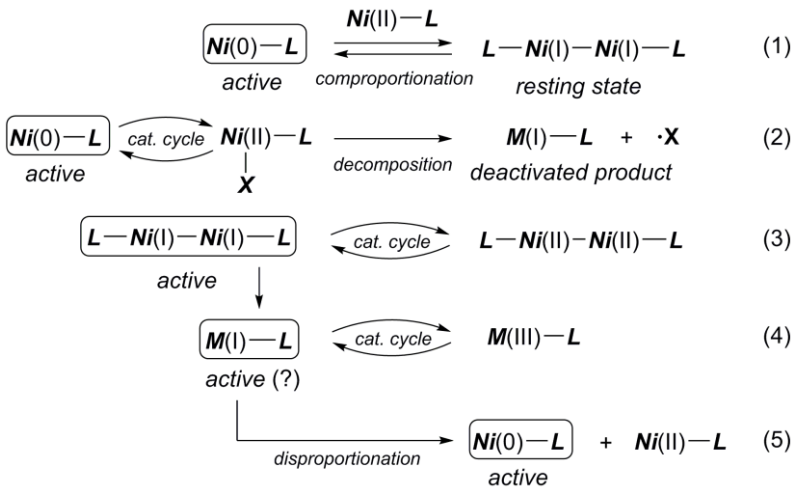

Chart 4-1. Various pathways of the active intermediates in nickel-catalysed systems involving monomeric Ni(0), Ni(I), and Ni(II) complexes and Ni(I) dimer

As shown in Chart 1, one of the possible pathways involving Ni(I) intermediates is (1) an active Ni(0) intermediate couples with Ni(II) into a stable Ni(I) dimer reaching a resting state equilibrium,[4] (2) monomeric Ni(I) forms in situ to become a deactivated complex as an off-cycle product,[5] and (3) unsaturated Ni(I) dimer promotes the catalytic cycle as a key intermediate.[6] Alternatively, (4) an active mononuclear Ni(I) intermediate in a catalytic cycle is also proposed using stable Ni(I) complexes.[7] However, it is quite difficult to experimentally prove that a Ni(I) complex acts as a true active intermediate in a catalytic cycle, because (5) it sometimes disproportionates into Ni(0) and Ni(II), which can be the real active species in catalysis.[8] There are several theories that support the Ni(I)-Ni(III) cycle but no clear experimental evidence to the best of our knowledge.[9]

Dinuclear L-Ni(I)-Ni(I)-L often forms a mononuclear active catalyst in literature.[10-12] Based on theoretical calculations, Chirik et al. proposed the generation of a mononuclear Ni(I) hydride complex in catalytic hydrosilylation which can be formed from a dinickel(I) hydride complex bearing redox-active ligands as a result of a one-electron reduction of the ligand.[10] Hazari et al. showed that a Ni(I) dimer,

$[Ni(NHC)]_2(\mu\text{-}Cl)(\mu\text{-}\eta^3\text{-}Cp)$, and its disproportionation product, monomeric Ni(I) complex CpNi(IPr), where Cp is a η^5-cyclopentadienyl, and IPr is 1,3-bis(2,6-diisopropylphenyl)imidazol-2-ylidne, were catalytically active in the Suzuki-Miyaura cross coupling of 4-chlorotoluene.[11] They concluded that homolytic cleavage of the Ni(I)-Ni(I) bond into the monomer complexes is necessary to activate the dimer for catalysis. Our group also reported that the Sigman's Ni(I) dimer, $[Ni(IPr)]_2(\mu\text{-}Cl)_2$,[12] cleaves its Ni(I)-Ni(I) bond in the presence of phosphines and pyridine to give mononuclear Ni(I) complexes.[13] Both monomer and dimer complexes can catalyse Kumada-Tamao-Corriu coupling and Buchwald-Hartwig amination of aryl halides. However, even in these reactions, it is unclear how the monomeric Ni(I) complexes behave in catalysis, as the real intermediate such as Ni(III) species, have not been detected or isolated experimentally.

Generally, an unpaired electron on the monovalent nickel promotes facile elimination of ligands and/or products, and smooth single electron transfer (SET) enables facile activation of substrates. Therefore, if coordinatively-unsaturated mononuclear Ni(I) complexes can be appropriately used not as a deactivator but as active key catalyst, it will be a very important finding, potentially leading to development of new catalytic transformations.

Recently, based on our and other groups' studies using nickel complexes bearing bulky NHCs, thermally stable nickel(I) complexes have been defined and applied to several catalytic processes.[13,14] Electron-donating NHC ligands may destabilize low-valent metal species such as Ni(0), probably by supressing competing Ni(0)-catalysed systems. However, a recent study showed that IPr-Ni(0) system can also catalyse Ni(0)-Ni(II)

systems in the amination of pyridyl chloride.[15] Therefore, clear evidence is needed to show that Ni(I) complexes can act as key intermediates in such catalytic reactions.

Herein, monomeric IPr-Ni(I) complexes are found to be the active species in the Buchwald-Hartwig amination of aryl bromide. The ligand 2,2'-bipyridyl (Bipy) provided the air-stable mononuclear tetrahedral IPr-Ni(I) complexes at least in the solid state, for more than several minutes. Experimental and theoretical studies also suggested that easy elimination of Bipy forms a linear two-coordinate (13e) IPr-Ni(I) complexes as the active species, one of which was isolated and well determined. Furthermore, the paramagnetic intermediates were successfully detected in a X-band EPR spectrum at low temperature, upon oxidative addition of aryl bromide to the IPr-Ni(I), indicating the existence of the Ni(I)-Ni(III) cycle in the NHC-Ni-catalysed system for the first time experimentally.

4-2. Synthesis and Characterizations

4-2-1. Preparation and Structures of Ni(I) Bipyridyl Complexes.

Addition of Bipy to a pale-yellow solution of di-Ni(I) halides $[Ni(iPr)]_2(\mu\text{-}X)_2$ [**1a** (X = Cl) and **1b** (X = Br)] bearing a bulky N-heterocyclic carbene, IPr, immediately afforded monomeric tetra-coordinate Ni(I) halides Ni(IPr)X(Bipy) [**2a** (X = Cl) and **2b** (X = Br)] (Scheme 1). Compounds **2a** and **2b** were successfully isolated as dark purple crystals upon recrystallization in 95 and 93% yields, respectively.

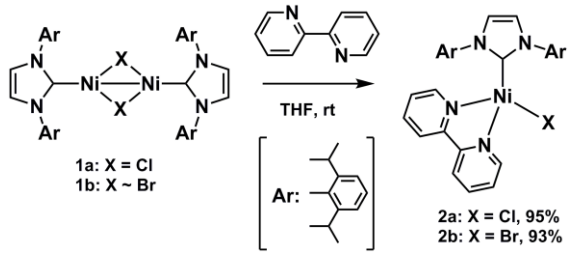

Scheme 4-1. Preparation of monomeric Ni(I) halides with 2,2'-bipyridyl.

Although the previously reported three-coordinated 15e Ni(I) complexes Ni(IPr)Cl(L), where L was pyridine, triphenylphosphine, and triphenylphosphite, were very unstable in the air and rapidly oxidised even in the solid state, the complex **2a** is rather stable, at least in the solid state. The half-lives of the crystals were about 15 minutes at room temperature. The corresponding bromide analogue **2b** was more stable than the chloride analogue **2a**. It should be noted that the ^{1}H NMR spectra for **2a** and **2b** did not show any signals assigned as the starting materials **1a** and **1b**, even though the analogous three-coordinate Ni(I) complexes readily regenerate the dimeric nickel complexes **1a** and **1b** in equilibrium.[13] This result indicated that chelating Bipy ligand in **2a** and **2b** can stabilize the Ni(I) complexes, compared to monodentate pyridine and phosphines in three-coordinate Ni(I) complexes.[13] These complexes were characterised by NMR spectroscopy, ESI-TOF MS, SQUID, and elemental analysis. The ^{1}H NMR spectra of **2a** and **2b** showed characteristic broadened signals due to paramagnetic nature of nickel (See ESI). The spin states of the complexes were studied based on SQUID measurements. The SQUID measurements supported the existence of an unpaired electron on the nickel atom. In our previous reports, the three-coordinate Ni(I) complexes had S = 1/2 (χ_{mol}/T = 0.34 - 0.52 cm^3 K mol^{-1} at 20 K, where χ_{mol} is molar magnetic susceptibility). In complexes 2a and 2b, the values were 0.68 and 0.72 at 20 K, respectively, higher than those of the three-coordinate complexes and the theoretical χ_{mol}/T value, which is 0.375 cm^3 K mol^{-1} when S = 1/2. The large difference of the χ_{mol}/T values in **2a** and **2b** could be attributed to the spin state of the unpaired electron in nickel, probably in the degenerate electron orbitals, composed of the pseudo-tetrahedral nickel orbitals. Additionally, the χ_{mol}/T values did not depend on temperature T even at 10 K, suggesting that other electronic structures, such

as high-spin Ni(II) and a bipyridyl anion radical, can be ruled out according to Curie's law.

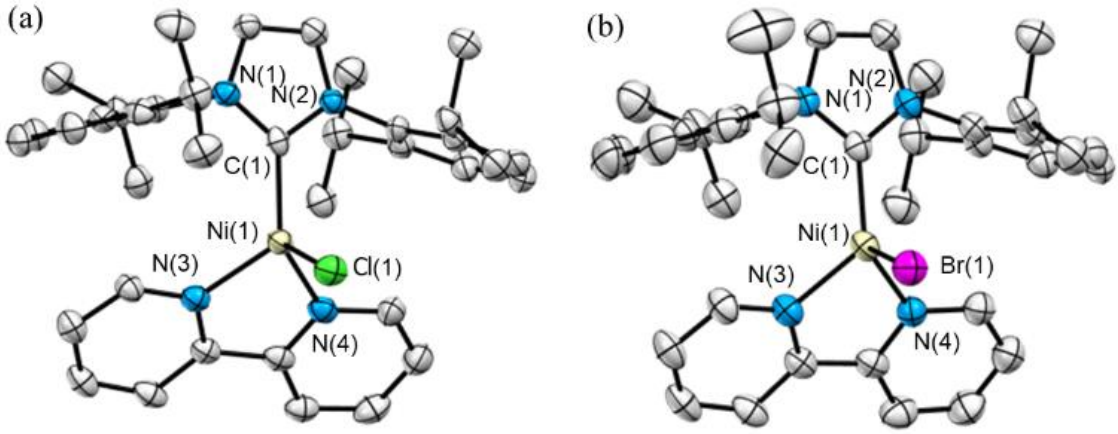

Figure 4-1. ORTEP drawings of complexes (a) 2a and (b) 2b with 50% thermal ellipsoids. Hydrogen atoms and two co-crystallised THF molecules were omitted for clarity.

Suitable crystals suitable for X-ray crystallography were obtained from a THF/hexane solution at −30 ºC, enabling the confirmation of the crystal structures of these complexes (Figure 1). The representative bond distances and angles of **2a** and **2b** are listed in Table 1. These complexes have distorted tetrahedral geometry around the nickel atoms. The distances of nickel-carbene bonds for **2a** and **2b** were 1.982(5) and 1.959(4) Å, respectively, similar to those of the analogous 15e complexes of Ni(IPr)Cl(L).

Table 4-1. Representative bond distances (Å) and angles (°) of **2a** and **2b**.

2a		**2b**	
Bond Distances (Å)			
Ni(1)-C(1)	1.982(5)	Ni(1)-C(1)	1.959(4)
Ni(1)-Cl(1)	2.3399(17)	Ni(1)-Br(1)	2.4450(8)
Ni(1)-N(3)	1.984(4)	Ni(1)-N(3)	1.968(4)
Ni(1)-N(4)	1.995(4)	Ni(1)-N(4)	1.972(4)
Bond Angles (°)			
C(1)-Ni(1)-Cl(1)	112.99(13)	C(1)-Ni(1)-Br(1)	111.46(13)
N(3)-Ni(1)-Cl(1)	102.94(13)	N(3)-Ni(1)-Br(1)	108.07(11)
N(4)-Ni(1)-Cl(1)	112.75(12)	N(4)-Ni(1)-Br(1)	106.81(10)

4-3. Catalysis and Reactivity

4-3-1. Buchwald-Hartwig Amination of 4-Halobenzophenone Using 2a and 2b.

The well-defined complex 2a catalysed the Buchwald-Hartwig amination of 4-chloro- and 4-bromo-benzophenone with diphenylamine even at 40ºC to yield 4-N,N-diphenylamino-benzophenone in 18 and 95% yields, respectively (Scheme 2).

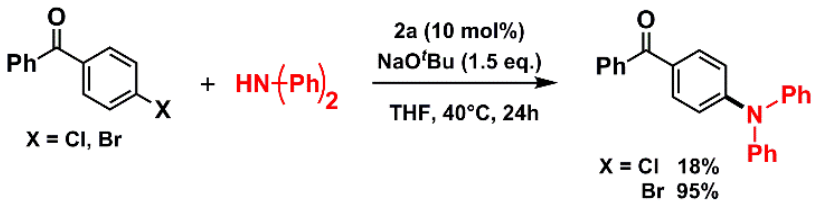

Scheme 4-2. Buchwald-Hartwig amination of 4-chloro- and 4-bromo-benzophenone with diphenylamine.

The results encouraged us to search the scope of amines as listed in Table 2 for the reaction with 4-bromobenzophenone mediated by 2a and also 2b under the similar conditions. Most of the triarylamines were obtained in good to excellent yields, 58–96%. Electron-donating and withdrawing substituents on the diarylamines did not affect the yields of the products. However, sterically demanding groups, such as a naphthyl group deactivated the process. The reaction with carbazole gave several by-products in contrast to the other reactions, reducing the yield of the amination product to 58%. The reaction

with indole, (4-cyanophenyl)phenylamine, and (4-nitrophenyl)phenylamine resulted in recovery of the starting materials. In these unsuccessful reactions, the colour of the solution of the reaction mixture was different from those providing the desired products. For instance, the successful conditions gave dark green solutions of nickel, whereas the addition of the unsuccessful substrates provided yellowish brown or reddish brown solutions, suggesting that the nickel complexes were deactivated in the presence of these substrates. Electron-withdrawing groups on the aryl halides can accept an electron from the electron donor Ni(I) to form an ion pair composed of anionic radical species and cationic Ni(II), which might lead to the deactivated nickel species. Therefore, 2 equiv of nitrobenzene was added to the reaction media using 2a at 40ºC for 24 h. The colour of the solution changed into black, and the reaction was completely inhibited (see S.I.).

Table 4-2. Buchwald-Hartwig amination of 4-bromobenzophenone with diarylamines mediated by **2a** and **2b**.[a]

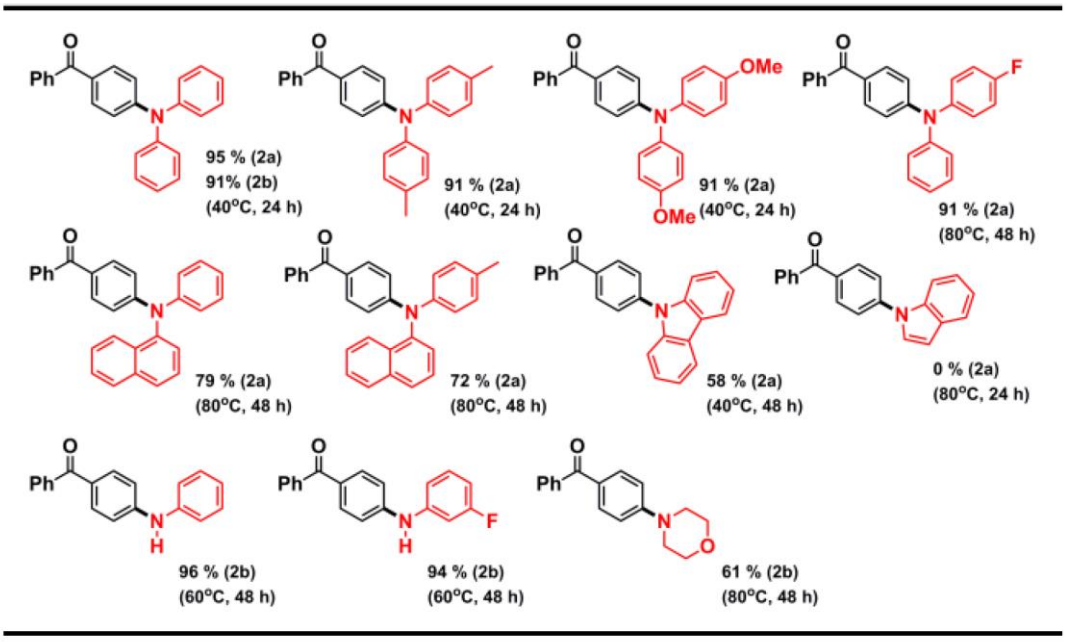

a) All yields were determined after colum chromatography.

4.3-2. Isolation of intermediary compounds.

According to our previous reports studying catalytic amination of 4-bromobenzophenone, the catalytic activity of **2a** is comparable to those of the three-coordinate Ni(I) complexes, NiCl(IPr)L (L = PPh3, pyridine).13 The two-coordinate Ni(I) complex, Ni(IPr)Cl, is proposed as the key intermediate in the catalytic cycle, because the ligands L in the three-coordinate analogues can be removed easily. However, coordination of Bipy to Ni(I) is stronger than the phosphorus ligands or pyridine, as noted above. Therefore, we are interested in how these efficient reactions occur using **2a** as the catalyst.

Addition of diphenylamine to the dark-purple solution of **2a** in the presence of sodium *tert*-butoxide at ambient temperature immediately gave a dark-blue solution, containing Ni(I) amide complex Ni(IPr)(NPh_2)(bipy) (**3a**) (Scheme 3). The complex **3a** was successfully isolated upon recrystallization in 24% yield. Similarly, 4,4'-dimethyldiphenylamine also gave the analogous complex **3b** in 12% yield upon recrystallization (Scheme 3). Interestingly, although indole did not provide its amination product with **2a**, the transmetallation product **3c** was obtained in low yield, 5% and thus was not fully characterised, although the structure was successfully determined by X-ray crystallography.

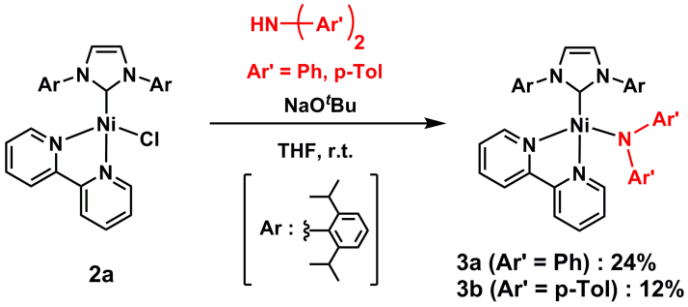

Scheme 4-3. Stoichiometric reaction of **2a** with diarylamines.

One of the most remarkable results in this study is that the two-coordinate Ni(I) amide complex Ni(IPr)(NPh_2) (**4**), which may be one of the true active species in amination, was successfully isolated (83% upon recrystallization) and characterized. Compound **4** was obtained from the rapid reaction of **1a** with diphenylamine in the presence of sodium *tert*-butoxide at room temperature (Scheme 4). Compound **4** was stable under an inert atmosphere in solution. The similar monoamino Ni(I) complexes have also been previously reported.[16]

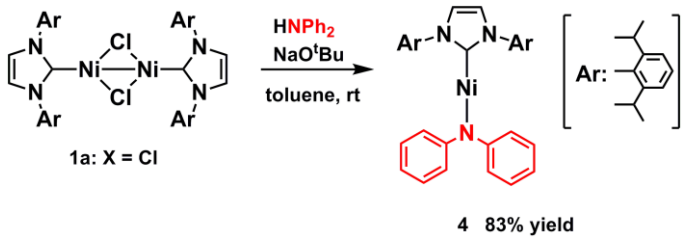

Scheme 4-4. Stoichiometric reaction of **1a** with diphenylamine.

The paramagnetic complexes **3** and **4** were characterised by ^{1}H NMR, UV-Vis, SQUID, and elemental analysis. Finally, the structures were confirmed by X-ray crystallography. SQUID for **3a** and **3b** showed similar magnetic susceptibilities to those of **2a** and **2b**: $\chi_{mol}T$ = 0.70 and 0.73 at 100 K, respectively, corresponding to S = 1/2. The crystal structures of **3a** and **4** were determined by X-ray crystallography (Figure 2). Nickel, nitrogen, and carbene carbon atoms are arranged in a tetrahedral position in **3a**, which is similar to **2a** and **2b**. In compound **4**: the angle of the three atoms was almost linear with an angle of 169.11(11)°, whereas that of bis(trimethylsilyl)amido Ni(I) was 163.2(2)° in previous reports.[16]

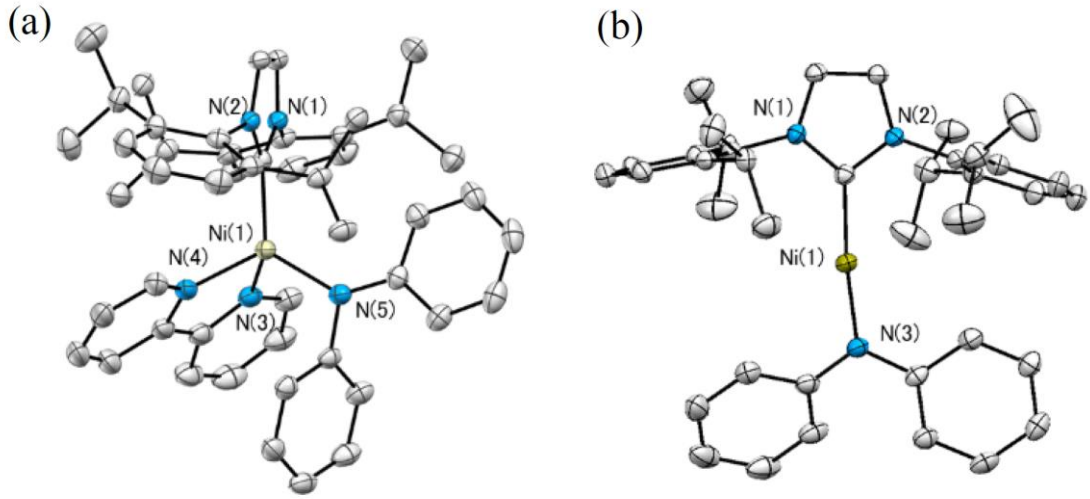

Figure 4-2. ORTEP drawings of complexes (a) 3a and (b) 4 with 50% thermal ellipsoids. Hydrogen atoms and solvent molecules (toluene in the crystals of 4) were omitted for clarity.

4-3-3. Reactions of the intermediates.

Isolation of Ni(I) amido complexes **3a** and **4** prompted us to conduct stoichiometric reactions of them with 4-bromobenzophenone at room temperature. Addition of aryl bromide to a THF solution of **3a** or **4** immediately changed colour and the ^{1}H NMR spectra of the crude mixtures showed the efficient generation of a cross-coupling product, 4-*N*,*N*-diphenylaminobenzophenone (Scheme 5).

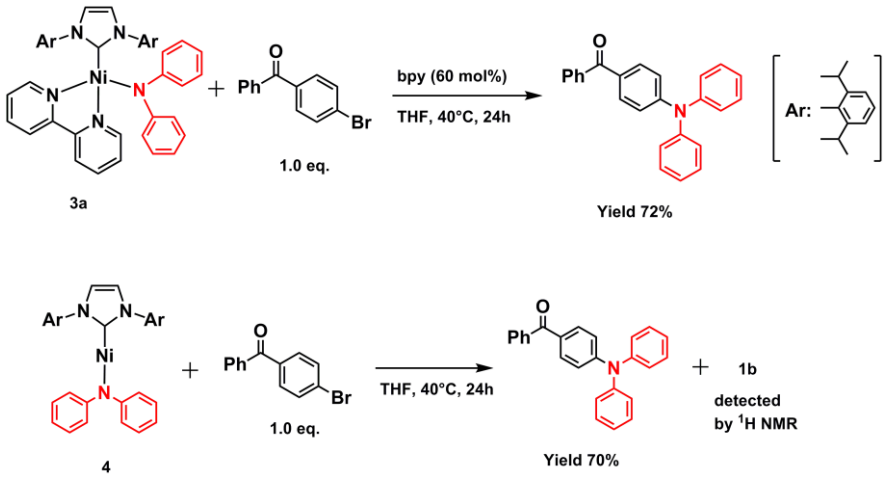

Scheme 5. Stoichiometric reaction of 3a and 4 with 4-bromobenzophenone.

In particular, the diamagnetic complex **1b**, which is one of the starting compounds in this catalysis, was clearly detected in the crude product mixture by ^{1}H NMR spectroscopy (See ESI). The triarylamine product was isolated after silica gel column chromatography in 72 and 70% yields from **3a** and **4**, respectively. Additionally, the complex **3a** was revealed to be active in the catalytic amination of 4-bromobenzophenone to yield the desired product in 47% yield, strongly suggesting that complex **3a** exists in the catalytic cycle (Scheme 6).

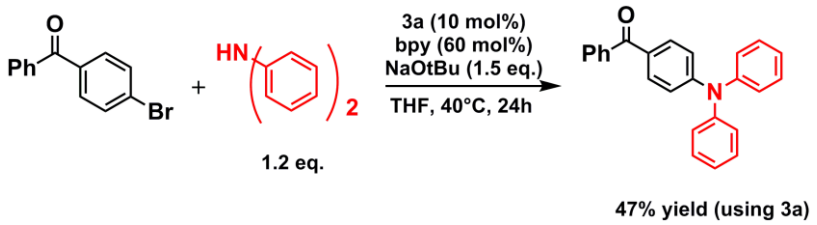

Scheme 4-6. Catalytic reaction of diphenylamine with 4-bromobenzophenone using **3a** as catalyst.

We considered that complex **3a** can exist at the resting state, and elimination of Bipy forms **4** as the active species. That is, the equilibria of elimination and coordination of the Bipy ligand between **3** and **4**, and **2** and **1** occurs in activation and stabilization of these Ni(I) complexes. However, because ligand elimination equilibrium between **2** with Bipy and **1** cannot be observed, as noted above, we have to demonstrate whether elimination of this generally robust chelating ligand occurs from **2a** or **2b** even at room temperature.[17] Interestingly, as a result, it can be rapidly released from **2b** at room temperature in the presence of another ligand. The UV-visible spectrum was monitored during the addition of 2,2'-biquinoline (Biq) to a THF solution of **2b** (Scheme 7). Because Biq can coordinate more strongly than Bipy does, due to its rigid structure derived from expanded π-conjugation, Biq could irreversibly replace Bipy on the Ni(I) complex.

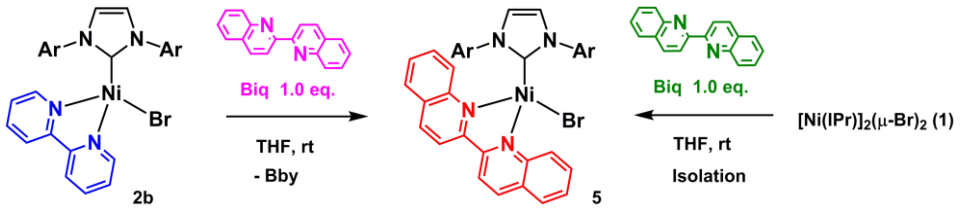

Scheme 4-7. Ligand exchange reactions of 2b with 2,2'-biquinoline (Biq) at room temperature.

Therefore, we added Biq to complex **2b** and observed UV spectral changes in the solution at room temperature. Since UV absorption of the complexes varied greatly by substituting the ligand, the spectral changes were clearly observed. As expected, the substitution of Bipy ligand in **2b** with Biq occurred immediately, resulting in a colour change from dark purple to dark blue. The spectra of the resulting solution containing **2b** and Biq agreed well with the isolated Biq complex **5** (Figure 3).

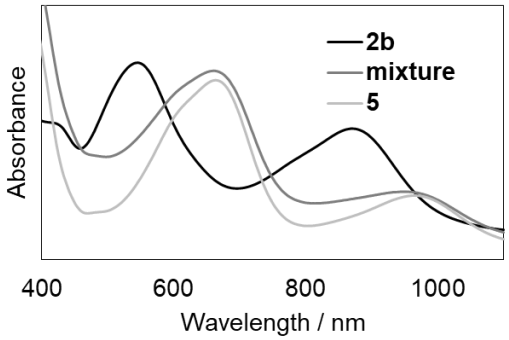

Figure 4-3. UV-vis spectra for compound 2b before (black) and after addition of Biq (gray), and for isolated Biq complex 5 (pale gray)..

Thus, complexes **2** and **3** are considered to have elimination equilibria in solutions, resulting in the formation of a mononuclear Ni(IPr)Cl or Ni(IPr)NR_2 (**4**) with free Bipy in solution. Although such facile elimination of Bipy is believed to be unusual,[17] this low elimination energy barrier is also supported by DFT calculation (See S.I.). In contrast, ligand exchange for the NHC ligand was much slower than for Bipy when free IMes was added to a solution of **2b**. This is supported by a previous study where a slower ligand

exchange occurs for IPr in mononuclear Ni(I) bisIPr complexes than with triphenylphosphine.[6a]

Next, we attempted to detect the intermediate of the reaction of **1b** with amine in the presence or absence of base. However, detection of such intermediate compounds was unsuccessful using NMR and EPR spectroscopy under any conditions. In our previous study, a pyridine molecule coordinated to a IPr-Ni(I) chloride to form a three-coordinate complex, Ni(IPr)(Cl)(pyridine), was thermally stable in the solid state and observed in the ^{1}H NMR spectrum as an equilibrium mixture with **1a** in C_6D_6.[13] Therefore, we suppose that due to the weak coordination ability of diphenylamine onto the Ni(I) centre, the corresponding three-coordinate complex, Ni(IPr)(Br)(diphenylamine), is less stable than the dinuclear Ni(I) bromide.

4-3-4. Detection of oxidative addition intermediate by EPR.

Getting mechanistic insights into the oxidative addition of aryl halide to the Ni(I) centre is a most interesting and challenging target. This is because a Ni(III) intermediate has never been directly observed in previous mechanistic studies of catalytic cycles, although some reports have shown the structures of Ni(III) complexes and their reductive elimination processes.[3] Unfortunately, several attempts to isolate the intermediate complex at −30ºC was unsuccessful, as this compound was thermally unstable at higher temperatures, leading to fast decomposition into a mixture composed of **1b** and triarylamine in a few minutes at around 20ºC. The ^{1}H NMR spectrum of the mixture after heating to room temperature showed only the existence of these expected side products (see S.I.). Therefore, we attempted direct observation of the Ni(III) intermediate using EPR spectroscopy at low temperature. After addition of 1 equiv of

4-bromoanisole to the two-coordinate Ni(I) complex **4** in ether at −40ºC, removal of the solvent under reduced pressure gave a dark green crystalline solid. Then, the residue was dissolved in THF in a sample tube and rapidly immersed into liquid N_2 just before the EPR measurement. As shown in Figure 4, signals due to new compounds appeared in the EPR spectrum of the reaction mixture. In contrast, no obvious signals were detected when the crystalline solid of starting complex **4** was used as the sample. Whittlesey et al. reported that an unquenched orbital angular momentum can be a reason why there are no signals in the X- and Q-band when the EPR spectrum of the two-coordinate bis-NHC Ni(I) complex were measured, even though the *S* value of the complex was 1/2.[18] The observed signals suggested presence of a mixture of Ni(I) and Ni(III) complexes, where the spin quantum number $S = 1/2$, based on computer simulations and DFT calculations (see S.I.). The Ni(III) intermediate is likely formed after oxidative addition of 4-bromoanisole to Ni(I) amide. Additionally, some three-coordinated Ni(I) amide complex was also possible to exist as one of the products detected in the EPR spectrum. The signals due to one of the compounds, which could be a Ni(III) intermediate, were assigned as rhombic distortion with $g_x = 2.125$, $g_y = 2.104$ and $g_z = 2.009$, whereas the others were rhombic with $g_x = 2.555$, $g_y = 2.308$ and $g_z = 2.094$. There are several examples of well-defined Ni(III) complexes having square planar or square pyramidal geometry around the nickel centre in literatures, showing average *g* values of ca. 2.13-2.17,[19] which are close to the value of $g_{av} = 2.08$ for the proposed Ni(III) intermediate. An alternative pathway can also be proposed from the Ni(I) complexes where disproportionation into diamagnetic Ni(0) and Ni(II) complexes occurs as demonstrated in literatures.[8] Cárdenas, et al. recently proposed an alternative radical oxidative addition pathway on the basis of DFT evidence, in which two molecules of Ni(I) react with one alkyl halide to form Ni(II) alkyl

and Ni(II) halide, independently.[20] However, because we cannot find the corresponding Ni(0) and/or Ni(II) IPr complexes in the reaction mixture of 4-bromoanisole with **4a** or **3a**, as noted above, these possibilities are unlikely, at least under these conditions.

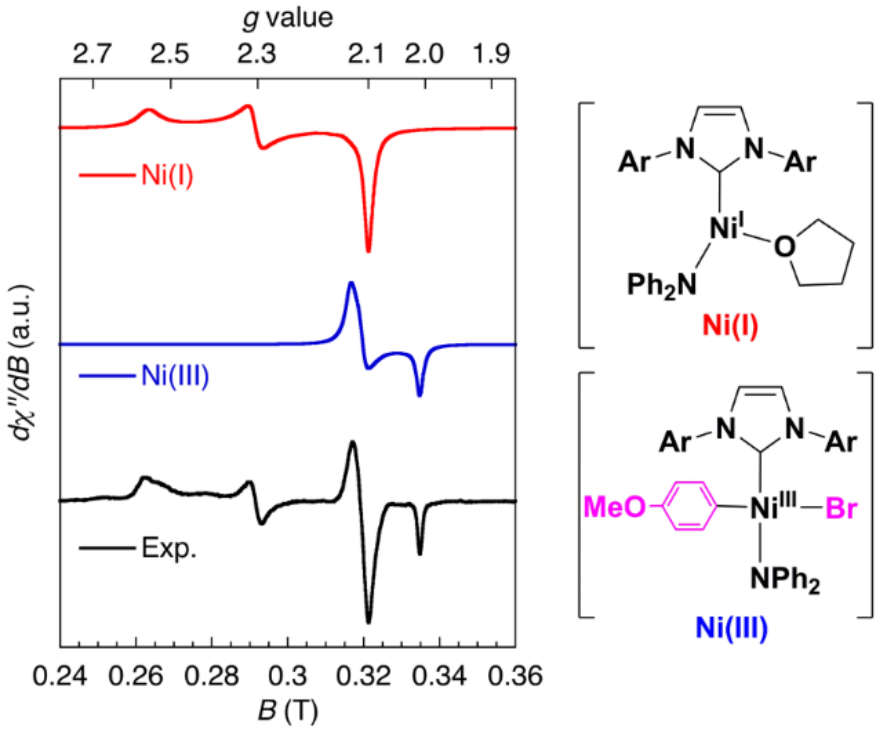

Figure 4-4. X-band EPR spectrum for the reaction mixture of 4 with 1 equiv of 4-bromoanisole (THF glass, at −178ºC) (black), which can be reproduced by computer simulation of the proposed compounds: mononuclear Ni(I) intermediate (red, rhombic: g_x = 2.555, g_y = 2.308 and g_z = 2.094) and Ni(III) product (blue, rhombic: g_x = 2.125, g_y = 2.104 and g_z = 2.009).

4-3-4. Proposed catalytic cycle.

Based on the above aspects, we proposed a possible catalytic cycle for Ni(I)-catalysed Buchwald-Hartwig amination of an aryl halide (Figure 5). From two-coordinate mononuclear Ni(I) chloride, transmetallation occurs with an amine and a base. Proton abstraction from the amine can proceed before and/or after coordination to the Ni centre with the base. Because amide complex **4** has a monomeric structure, active mononickel intermediates are favourable throughout this catalytic cycle. Complex **4** reacts with the aryl halide to form the Ni(III) oxidative addition product,

which can easily eliminate triarylamine, resulting in a reduction to the starting Ni(I) halide. Reversible coordination of Bipy to two-coordinate Ni(IPr)X and Ni(IPr)NAr_2 (**4**) forms stabilised tetrahedral 17e Ni(I) complexes as resting states, and thermal elimination of these complexes can regenerate the active intermediates. The existence of the resting states can decrease the concentration of these highly active intermediates to avoid catalyst deactivation pathways at the late stage of the reaction. Transmetallation of Ni(I) species involved in the catalytic cross-coupling cycle has also been proposed as a mechanism of Ni(I)-catalysed cross-coupling reactions in literature.[9] However, the other possible pathway, via oxidative addition on Ni(I) halide and subsequent transmetallation, may still be possible and should be studied in the future.

There have been strong evidences in the literatures that Ni(0)/Ni(II) cycle is dominant using Ni(I) phosphine complexes. Although we do not have direct evidence, electron-donating ability of NHC ligand may differenciate the catalytic cycles. NHC ligand is generally stronger σ-donor than phosphorus ligand, resulting in stabilization of the higher valence metal centres such as Ni(I) and Ni(III), which can act as catalysts without disproportionation into Ni(0) and Ni(II) species.

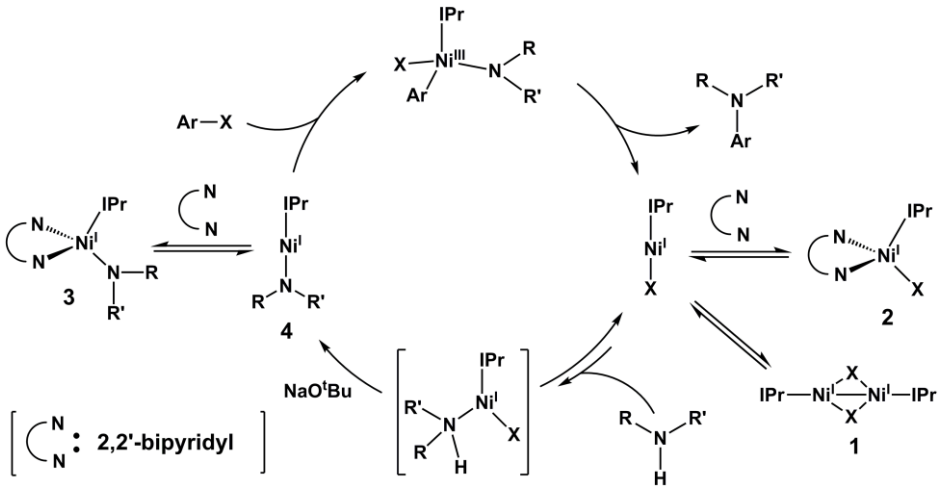

Figure 4-5. Proposed reaction mechanism of Ni(I)-catalysed Buchwald-Hartwig amination of aryl halides.

4-4. Summary

In summary, we have uncovered one of the catalytic cycles involved in the Buchwald-Hartwig amination of aryl bromides mediated by Ni(I) NHC complexes. Although a catalytic system between Ni(I) and Ni(III) has been discussed as a possible pathway in many previous reports, experimental studies determining such intermediate key compounds have been poorly defined. Our findings in this study showed that mononuclear Ni(I) and Ni(III) NHC complexes are experimentally and theoretically possible as intermediates in the catalytic cross-coupling reaction. A bidentate ligand, 2,2'-bipyridyl, can stabilize Ni(I) NHC complexes, which efficiently mediate amination of aryl bromides with several amines attempted. Several stoichiometric chemical reactions revealed the presence of a two-coordinate 13e IPr-Ni(I) intermediate. The Ni(III) intermediate was thermally unstable, but its existence was strongly suggested by EPR measurements, followed by the thermal formation of cross-coupling product and diamagnetic dinuclear Ni(I) halide complex. 2,2'-Bipyridyl was able to behave as a hemi-labile ligand to the Ni(I) centre, leading the highly reactive intermediates to stable resting states. Alternatively, the NHC ligand appears to bind to the nickel centre in a stable manner, conserving the mononuclear Ni(I) intermediates to some extent. We are now in the process of studying further this unusual and highly active catalytic process by conducting thorough experiments and discussions which include kinetic analysis.

4-5. References

1. a) S. Z. Tasker, E. A. Stanley and T. F. Jamison, Nature, 2014, 509, 299-309; b) C.-Y. Lin and P. P. Power, Chem. Soc. Rev., 2017, 46, 5347-5399; c) P. Zimmermann, and C. Limberg, J. Am. Chem. Soc., 2017, 139, 4233−4242; d)J. Gu, X. Wang, W. Xue and H. Gong, Org. Chem. Front., 2015, 2, 1411-1421; e) T. Inatomi, Y. Koga and K. Matsubara, Molecules, 2018, 23, 140-160; f) V. Ritleng, M. Henrion and M. J. Chetcuti, ACS Catal., 2016, 6, 890−906; g) M. Tobisu and N. Chatani, Acc. Chem. Res., 2015, 48, 1717-1726.
2. For examples, a) C. Eaborn, M. S. Hill, P. B. Hitchcock and J. D. Smith, Chem. Commun., 2000, 691-692; b) K. Fujita, A. L. Rheingold and C. G. Riordan, Dalton Trans., 2003, 2004-2008; c) K. D. Kitiachvili, D. J. Mindiola and G. L. Hillhouse, J. Am. Chem. Soc., 2004, 126, 10554-10555; d) N. A. Eckert, A. Dinescu, T. R. Cundari and P. L. Holland, Inorg. Chem., 2005, 44, 7702-7704; e) M. J. Ingleson, B. C. Fullmer, D. T. Buschhorn, H. Fan, M. Pink, J. C. Huffman and K. G. Caulton, Inorg. Chem., 2008, 47, 407-409; f) M. Ito, T. Matsumoto and K. Tatsumi, Inorg. Chem., 2009, 48, 2215-2223; g) E. E. Marlier, S. J. Tereniak, K. Ding, J. E. Mulliken and C. C. Lu, Inorg. Chem., 2011, 50, 9290–9299; h) R. Beck, M. Shoshani, J. Krasinkiewicz, J. A. Hatnean and S. A. Johnson, Dalton Trans., 2013, 42, 1461–1475; i) C. Yoo, S. Oh, J. Kim and Y. Lee, Chem. Sci., 2014, 5, 3853–3858; j) U. Chakraborty, F. Urban, B. Mühldorf, B. de Bruin, N. van Velzen, S. Harder and R. Wolf, Organometallics, 2016, 35, 1624−1631.
3. a) B. Zheng, F. Tang, J. Luo, J. W. Schultz, N. P. Rath and L. M. Mirica, J. Am. Chem. Soc., 2014, 136, 6499−6504; b) P. Pirovano, B. Twamley and A. R. McDonald, Chem. Eur. J., 2018, 24, 5238–5245; c) J. B. Diccianni, C. Hu and T. Diao, Angew. Chem. Int. Ed., 2017, 56, 3635–3639.
4. a) R. J. Somerville, L. V. A. Hale, E. Gómez-Bengoa, J. Burés and R. Martin, J. Am. Chem. Soc., 2018, 140, 8771−8780; b) N. I. Saper and J. F. Hartwig, J. Am. Chem. Soc., 2017, 139, 17667−17676.
5. a) A. Manzoor, P. Wienefeld and M. C. Baird, Organometallics, 2017, 36, 3508−3519; b) S. Bajo, G. Laidlaw, A. R. Kennedy, S. Sproules and D. J. Nelson, Organometallics, 2017, 36, 1662−1672; c) I. E. Soshnikov, N. V. Semikolenova, K. P. Bryliakov, V. A. Zakharov, W.-H. Sun and E. P. Talsi, Organometallics, 2015, 34, 3222−3227; d) G. Yin, I. Kalvet, U. Englert and F. Schoenebeck, J. Am. Chem. Soc., 2015, 137, 4164−4172.
6. a) K. Matsubara, H. Yamamoto, S. Miyazaki, T. Inatomi, K. Nonaka, Y. Koga, Y. Yamada, L. F. Veiros and K. Kirchner, Organometallics, 2017, 36, 255-265; b) C. A. Laskowski and G. L. Hillhouse, Organometallics, 2009, 28, 6114–6120; c) R. Beck and S. A. Johnson, Chem. Commun., 2011, 47, 9233–9235; d) A. B. Dürr, H. C. Fisher, I. Kalvet, K.-N. Truong and F. Schoenebeck, Angew. Chem. Int. Ed., 2017, 56, 13431–13435; Angew. Chem., 2017, 129, 13616-13620; e) C. Uyeda, T. J. Steiman and S. Pal, Synlett, 2016, 27, 814-820; f) S. Pal, Y.-Y. Zhou and C. Uyeda,

J. Am. Chem. Soc., 2017, 139, 11686−11689; g) D. R. Hartline, M. Zeller and C. Uyeda, J. Am. Chem. Soc., 2017, 139, 13672–13675.

7. a) N. D. Schley and G. C. Fu, J. Am. Chem. Soc., 2014, 136, 16588−16593; b) S. Miyazaki, Y. Koga, T. Matsumoto and K. Matsubara, Chem. Commun., 2010, 46, 1932-1934; c) C. J. E. Davies, M. J. Page, C. E. Ellul, M. F. Mahon and M. K. Whittlesey, Chem. Commun., 2010, 46, 5151–5153; d) K. Zhang, M. Conda-Sheridan, S. R. Cooke and J. Louie, Organometallics, 2011, 30, 2546–2552; e) S. Nagao, T. Matsumoto, Y. Koga and K. Matsubara, Chem. Lett., 2011, 40, 1036-1038; f) A. Klein, A. Kaiser, B. Sarkar, M. Wanner and J. Fiedler, Eur. J. Inorg. Chem., 2007, 965–976; g) X. Zhang, X. Xie, Y. Liu, Chem. Sci., 2016, 7, 5815-5820; h) Z.-C. Cao, S.-J. Xie, H. Fang, Z.-J. Shi, J. Am. Chem. Soc., 2018, 140, 13575-13579.
8. a) M. M. Beromi, G. Banerjee, G. W. Brudvig, N. Hazari and B. Q. Mercado, ACS Catal., 2018, 8, 2526−2533; b) D. D. Beattie, G. Lascoumettes, P. Kennepohl, J. A. Love and L. L. Schafer, Organometallics, 2018, 37, 1392−1399.
9. a) I. Kalvet, Q. Guo, G. J. Tizzard and F. Schoenebeck, ACS Catal., 2017, 7, 2126−2132; b) L. Szatkowski and M. B. Hall, Dalton Trans., 2016, 45, 16869–16877; c) L. Iffland, A. Petuker, M. van Gastel and U.-P. Apfel, Inorganics, 2017, 5, 78-91; d) C.-H. Lim, M. Kudisch, B. Liu, and G. M. Miyake, J. Am. Chem. Soc., 2018, 140, 7667−767. e) X. Lin and D. L. Phillips, J. Org. Chem., 2008, 73, 3680–3688; f) V. B. Phapale, M. Guisán-Ceinos, E. Buñuel and D. J. Cárdenas, Chem. Eur. J., 2009, 15, 12681 –12688; g) G. D. Jones, J. L. Martin, C. McFarland, O. R. Allen, R. E. Hall, A. D. Haley, R. J. Brandon, T. Konovalova, P. J. Desrochers, P. Pulay and D. A. Vicic, J. Am. Chem. Soc., 2006, 128, 13175-13183.
10. a) I. Pappas, S. Treacy and P. J. Chirik, ACS Catal., 2016, 6, 4105−4109; b) M. V. Joannou, M. Bezdek, K. Albahily, I. Korobkov and P. J. Chirik, Organometallics, 2018, 37, 3389−3393.
11. J. Wu, A. Nova, D. Balcells, G. W. Brudvig, W. Dai, L. M. Guard, N. Hazari, P.-H. Lin, R. Pokhrel and M. K. Takase, Chem. Eur. J., 2014, 20, 5327–5337.
12. B. R. Dible, M. S. Sigman and A. M. Arif, Inorg. Chem., 2005, 44, 3774−3776.
13. K. Matsubara, Y. Fukahori, T. Inatomi, S. Tazaki, Y. Yamada, Y. Koga, S. Kanegawa and T. Nakamura, Organometallics, 2016, 35, 3281-3287.
14. M. J. Page, W. Y. Lu, R. C. Poulten, E. Carter, A. G. Algarra, B. M. Kariuki, S. A. Macgregor, M. F. Mahon, K. J. Cavell, D. M. Murphy and M. K. Whittlesey, Chem. Eur. J., 2013, 19, 2158–2167.
15. S. G. Rull, I. Funes-Ardoiz, C. Maya, F. Maseras, M. R. Fructos, T. R. Belderrain and M. C. Nicasio, ACS Catal., 2018, 8, 3733−3742.
16. a) C. A. Laskowski and G. L. Hillhouse, J. Am. Chem. Soc., 2008, 130, 13846–13847; b) M. I. Lipschutz and T. D. Tilley, Organometallics, 2014, 33, 5566−5570; c) D. D. Beattie, E. G. Bowes, M. W. Drover, J. A. Love and L. L. Schafer, Angew.Chem. Int. Ed., 2016, 55, 13290–13295.

17. Fore examples, see; a) T. P. Yoon, M. A. Ischay and J. Du, Nature Chem., 2010, 2, 527-532; b) B. Happ, A. Winter, M. D. Hager and U. S. Schubert, Chem. Soc. Rev., 2012, 41, 2222–2255; c) A. Barbieri, B. Ventura and R. Ziessel, Coord. Chem. Rev., 2012, 256, 1732– 1741; C. E. Housecroft and E. C. Constable, Coord. Chem. Rev., 2017, 350, 155-177.
18. a) R. C. Poulten, M. J. Page, A. G. Algarra, J. J. Le Roy, I. López, E. Carter, A. Llobet, S. A. Macgregor, M. F. Mahon, D. M. Murphy, M. Murugesu and M. K. Whittlesey, J. Am. Chem. Soc., 2013, 135, 13640−13643; b) C. A. Laskowski, D. J. Bungum, S. M. Baldwin, S. A. Del Ciello, V. M. Iluc and G. L. Hillhouse, J. Am. Chem. Soc., 2013, 135, 18272−18275; c) C.-Y. Lin, J. C. Fettinger, F. Grandjean, G. J. Long and P. P. Power, Inorg. Chem., 2014, 53, 9400−9406.
19. For examples, see; a) M. Eckshtain-Levi, M. Orio, R. Lavi and L. Benisvy, Dalton Trans., 2013, 42, 13323–13326; b) P. Pirovano, E. R. Farquhar, M. Swart, A. J. Fitzpatrick, G. G. Morgan and A. R. McDonald, Chem. Eur. J., 2015, 21, 3785–3790; c) P. Pirovano, E. R. Farquhar, M. Swart and A. R. McDonald, J. Am. Chem. Soc., 2016, 138, 14362−14370; d) P. Pirovano, B. Twamley and A. R. McDonald, Chem. Eur. J., 2018, 24, 5238–5245; e) P. Pirovano, A. R. Berry, M. Swart and A. R. McDonald, Dalton Trans., 2018, 47, 246–250.
20. R. Soler-Yanes, I. Arribas-Álvarez, M. Guisán-Ceinos, E. Buñuel and D. Cárdenas, Chem. Eur. J., 2017, 23, 1584–1590.
21. a) A. B. Holmes and T. Park, WO patent 2002051958; b) J. S. Kang, J. H. Park, S. W. Jun, Y. J. Shin, Y. M. Chang, N. C. Yang, J. K. Park and S. Lee, WO patent 2015026053; c) S. Heyne, M. Zoellner, S. Dorok and J. Wutke, US patent 20150011795; d) A. J. Arduengo III, R. Krafczyk, R. Schmutzler, H. A. Craig, J. R. Goerlich, W. J. Marshall, M. Unverzagt, Tetrahedron, 1999, 55, 14523-14534.
22. N. F. Chilton, R. P. Anderson, L. D. Turner, A. Soncini and K. S. Murray, J. Comput. Chem., 2013, 34, 1164–1175.
23. M. J. Frisch, G. W. Trucks, H. B. Schlegel, et al. Gaussian 09, Revision D.01, Gaussian, Inc., Wallingford CT, 2013.
24. CrystalStructure ver. 4.2: Crystal Structure Analysis Package, Rigaku Co., Tokyo 196–8666, Japan, 2015.
25. SIR2008: M. C. Burla, R. Caliandro, M. Camalli, B. Carrozzini, G. L. Cascarano, L. De Caro, C. Giacovazzo, G. Polidori, D. Siliqi and R. Spagna, J. Appl. Cryst., 2007, 40, 609-613.
26. SHELXL97: G. M. Sheldrick, University of Gottingen, 1997, Germany.

Chapter 5
Conclusion

In this paper, we conducted research to elucidate the significance of the existence of Ni(I) species, one of the important tasks in the field of organometallic chemistry. In doing this research, I was able to obtain some knowledge about the behavior of Ni (I) species by various approaches based on Ni (I) / NHC species. Summarize the main points for each chapter, and show it below.

In [Chapter 2], it is newly discovered that an aryl bridged dinuclear Ni(I) complexes are formed by reacting a normal aryl halides (i.e. 4-chlorotoluene, 4-chloroanisole) with $Ni(cod)_2$ as a Ni(0) source in the presence of an NHC ligand (i.e. IPr). As well as its structure was clarified by various spectroscopic analysis. The following three experimental results suggested that the Ni (I) / NHC species that retained the binuclear structure may act as an important intermediate in the Kumada-Tamao-Corriu cross-coupling reaction. i) Regeneration of binuclear Ni(I) complex by reaction of the obtained aryl bridged dinuclear nickel complex with aryl halide, ii) formation of bis-aryl bridged dinuclear nickel complex as a result of reaction with Grignard reagent, iii) kinetic experiment using 4-chlorotoluene.

In [Chapter 3], by taking advantage of the existence of an equilibrium reaction between bis-carbene Ni(I) complex and halogen bridged dinuclear Ni(I) complex in solution, a new monomeric Ni(I) complexes bearing ancillary ligands (i.e. PPh_3, $P(OPh)_3$, py) was developed, and discussed its structural features and catalysis. These complexes had three-coordinate Y-shaped geometries in both the solid and solution states. Moreover, By SQUID measurements, these complexes have been found to be d^9 species. In addition, in the Suzuki-Miyaura cross-coupling reaction and Buchwald-Hartwig amination using aryl halide, it showed high catalytic activity and selectively gave the desired corresponding product.

In [Chapter 4], compared to previous complexes, we have newly developed a highly stable monomeric Ni(I) complex with 2,2'-bipyridyl ligand introduced, and revealed its specific magnetic properties. In the Buchwald-Hartwig amination reaction, a result showing catalytic activity equivalent to that of a nickel complex having a phosphine ligand was obtained. In view of this surprising results, we studied the reaction mechanism of catalytic reaction using monomeric Ni(I) complex bearing bpy ligand. As a result, we succeeded in isolating a very rare two-coordinate Ni(I) amide complex and clarifying its structure. Further, from the result of stoichiometric reaction with the Ni(I) amide complex and halogenated aryl, it was found that the Ni(I) species is sufficiently acting in the amination. NMR analysis revealed that halogen bridged dinuclear Ni(I) complex, which is important key intermediate, was regenerated in the reaction system.

From Chapter 2, 3 and 4, it is clarified the role of nickel monovalent species, which is an important intermediate chemical species in several cross coupling reactions, in the Ni / NHC catalyst system, and nickel monovalent species are not less than major We have identified the fact that it is involved in the reaction pathway.

Chapter 6
6. Experimental

Experimental Details

S-1-1. General

All experiments were carried out under an inert gas atmosphere using standard Schlenk techniques and glove box (MBraun UniLab) as otherwise noted. THF, hexane, toluene, benzene-d_6 were distilled from benzophenone ketyl before use. Chloroform-*d* was distilled from CaH and stored under a nitrogen atmosphere. Other reagents were used as received or distilled just before use if possible. The ^{1}H NMR spectra were taken with a VARIAN Mercury Y plus 400 MHz spectrometer at room temperature. Chemical shifts (δ) were recorded in ppm from the solvent signal. IR spectra were recorded in cm^{-1} on a PERKIN ELMER Spectrum One spectrometer equipped with a universal diamond ATR. GC-MS spectra were taken with an Agilent 6890N gas chromatograph, coupled with a JEOL JMS-GC mate II mass spectrometer. A 60-m InertCap 1 column (0.25 mm i.d., 0.25 μm film thickness) was used, and the injection temperature was 270 ºC. The elemental analysis was carried out with YANACO CHN Corder MT-5, AUTO-SAMPLER. Column chromatography of organic products was carried out using silica gel (Kanto Kagaku, silica gel 60 N (spherical, neutral)). The *N*-heterocyclic carbene (IPr) was prepared from the imidazolium salt according to the published methods.[1] The zerovalent biscarbene nickel NHC complex was prepared according to our previous report.[2] The complex **2** was prepared according to the published method.[3]

S-1-2. Synthesis of $[Ni(IPr)]_2(\mu\text{-}Cl)(\mu{:}\eta2\text{-}C_6H_4R)$ (1a: R = 4-CH_3, 1b: R = 4-OCH_3) (Scheme 2-2)

In a typical example for **1a**, $Ni(cod)_2$ (165 mg, 0.600 mmol), IPr (245 mg, 0.630 mmol), 4-chlorotoluene (70 μL, 0.60 mmol), and THF (7 mL) were added to a 20 mL Schlenk tube and the solution was stirred at room temperature for 2 h. After the solvent was removed under reduced pressure, the residual solid was washed with hexane and dried to give a yellow crystalline solid (88 mg, 44%).

1a: ^{1}H NMR (400 MHz, C_6D_6)(Figure S-1-2-1): δ 7.38 (t, *J* = 7.6 Hz, 4H, ArH), 7.26 (d, *J* = 7.6 Hz, 8H, ArH), 6.41 (s, 4H, CH=CH), 6.07 (m, 4H, ArH), 3.00 (sept, *J* = 6.8 Hz, 8H, C*H*(CH_3)), 2.09 (s, 3H, CH_3), 1.41 (d, *J* = 6.4 Hz, 24H, CH_3), 1.02 (d, *J* = 6.8 Hz, 24H, CH_3). ^{13}C NMR (100 MHz, C_6D_6) (Figure S-1-2-2): δ 193.21, 146.65, 139.03, 137.81, 133.33, 129.25, 127.64, 126.72, 123.91, 123.75, 28.77, 25.32, 23.56, 20.64. Anal. Calcd for $C_{61}H_{79}N_4ClNi_2$: C, 71.75; H, 7.80; N, 5.49. Found: C, 71.29; H, 7.97; N, 4.67.

1b: ^{1}H NMR (400 MHz, C_6D_6) (Figure S-1-2-3): δ 7.38 (t, *J* = 8.0 Hz, 4H, ArH), 7.27 (d, *J* = 7.6 Hz, 8H, ArH), 6.72 (m, 2H, ArH), 6.43 (s, 4H, CH=CH), 6.17 (m, 2H, ArH), 3.31 (s, 3H, CH_3), 3.01 (sept, *J* = 6.2 Hz, 8H, C*H*(CH_3)), 1.45 (d, *J* = 6.8 Hz, 24H, CH_3), 1.03 (d, *J* = 6.4 Hz, 24H, CH_3). ^{13}C NMR (100 MHz, C_6D_6) (Figure S-1-2-4): δ 196.15 158.15, 146.71, 138.25, 129.25, 128.63, 126.71, 124.74, 123.84, 114.40, 54.08, 28.86, 25.22, 23.70. Anal. Calcd. for $C_{61}H_{79}ON_4ClNi_2$: C, 70.64; H, 7.68; N, 5.40. Found: C, 70.00; H, 8.11; N, 5.65.

S-1-3. Synthesis of [Ni(IPr)]2(μ:η2-$C_6H_4CH_3$)$_2$ (3a) (Scheme 2-3)

In a 20 mL Schlenk tube, the compound **1a** (102.1 mg, 0.10 mmol) was dissolved in 1,4-dioxane (2.0 mL). Then, the solution was stirred at room temperature, and a 3.0 M solution of (*p*-tolyl)MgCl in THF (198 μL, 0.39 mmol) was slowly dropwise into the reaction media. The solution was stirred for 18 h. After the solvent was removed under reduced pressure, the residual solid was extracted with toluene (15 mL) and the suspension was filtered through celite to yield a dark green crystalline solid of **3a** (15 mg, 11%).

3a: ^{1}H NMR (400 MHz, C_6D_6) (Figure S-1-3-1): δ 7.36 (t, *J* = 7.6 Hz, 4H, ArH), 7.19 (d, *J* = 7.6 Hz, 8H, ArH), 6.35 (s, 4H, CH=CH), 6.23 (d, *J* = 7.2, 4H, ArH), 5.91 (d, *J* = 8.0 Hz, 4H, CH=CH), 3.01 (sept, *J* = 6.8 Hz, 8H, C*H*(CH_3)), 2.15 (s, 6H, CH_3), 1.12 (d, *J* = 7.2 Hz, 24H, CH_3), 0.93 (d, *J* =6.8 Hz, 24H, CH_3). ^{13}C NMR (100 MHz, C_6D_6) (Figure S-1-3-2): δ 196.87, 145.95, 138.51, 135.58, 130.17, 128.78, 126.68, 125.86, 124.05, 122.93, 28.48, 25.09, 22.91, 21.40. Anal. Calcd. for $C_{68}H_{90}N_4Ni_2$: C, 75.56; H, 8.39; N, 5.18. Found: C, 69.76; H, 7.92; N, 4.66.

Because the by-products, **1a** and **2**, being formed in the transmetalation of **1a** with tolylmagnesium chloride, were co-crystallized into the crystals of **3a** upon recrystallization, complete purification of **3a** in this method was impossible. Therefore, the elemental analysis result of **3a** did not agree with the theoretical values, unfortunately, maybe including some amount of **1a** and **2**.

S-1-4. Kumada cross-coupling reaction of aryl halide with phenylmagnesium chloride catalyzed by 4 and 1a (Table 2-2)

In a typical example, to a 20 mL Schlenk tube, the complex **1a** (10.2 mg, 0.010 mmol), aryl halide (1.0 mmol) and THF (1.0 mL) were added and stirred for 5 min. Then, a 2.0 M solution of phenylmagnesium chloride in THF (0.75 mL, 1.50 mmol) was added at room temperature. After stirring for 18 h, water (20 mL) was added to quench the reaction. Organic layer was extracted with CH_2Cl_2 (20 mL × 4), and dried over $MgSO_4$. The products were purified by silica gel column chromatography, eluted with hexane/CH_2Cl_2.

S-1-5. Stoichiometric reaction of 1a with *p*-haloanisole and phenylmagnesium chloride (Scheme 2-8)

In a 20 mL Schlenk tube, the complex **1a** (153 mg, 0.15 mmol) was dissolved in THF (2 mL), and then a mixture of a 2.0 M solution of phenylmagnesium chloride in THF (75 μl, 0.15 mmol), 4-chloroanisole (18 μL, 0.15 mmol) or 4-bromoanisole (24 μL, 0.15 mol), and THF (1.0 mL) was added to the solution. The reaction mixture was stirred at room temperature for 23 h. After the solvent was removed under reduced pressure, a sample was taken to measure the ^{1}H NMR spectra. Water (20 mL) was added to the reaction mixture and the organic layer was extracted with CH_2Cl_2 under an argon

atmosphere. After drying over Na_2SO_4, a pale-yellow solid was afforded. Determination of the contents in the mixture was conducted with GC-MS spectroscopy.

S-1-6. Stoichiometric reaction of 1a with 4-chlorotoluene (Scheme 2-7)

To a 20 mL Schlenk tube the complex **1a** (51.1 mg, 0.050 mmol), 4-chlorotoluene (178 μL, 1.50 mmol), THF (0.50 mL) were added and stirred at room temperature for 24 h. After the solvent was removed under reduced pressure, a sample was taken to measure the ^{1}H NMR spectra. Water (20 mL) was added to the reaction mixture and the organic layer was extracted with CH_2Cl_2 under an argon atmosphere. After drying over Na_2SO_4, a pale-yellow solid was given. Determination of the contents in the mixture was conducted with GC-MS spectroscopy.

S-1-7. Kinetics in the reaction of 1a with 4-chlorotoluene (Scheme 2-9)

To a 20 mL Schlenk tube the complex **1a** (51.1 mg, 0.050 mmol), $Si(SiMe_3)_4$ as an internal standard (3.2 mg, 0.010 mmol), THF (0.50 mL) were added and stirred at room temperature. In another 20 mL Schlenk tube, 4-chlorotoluene (178 μL, 1.50 mmol) was dissolved in THF (0.5 mL). After both the Schlenk tubes were cooled under -98 ºC, the latter solution of 4-chlorotoluene was added to the former solution of **1a**. At that time, a sample was taken, put into a NMR sample tube equipped with a teflon valve, and volatile chemicals including 4-chlorotoluene were removed under reduced pressure immediately. Benzene-d_6 was added to the tube by vac-to-vac and sealed under reduced pressure to measure a ^{1}H NMR spectrum (t = 0 h). The reaction mixture was then warmed to the regulated temperature, -43, -55, -70, or -80 ºC in each experiment. Three or four samples were taken to monitor the reaction in each temperature. Decreasing integrated ratios of an independent signal at δ 6.06 assigned as aromatic proton of the *p*-tolyl group bridging between nickel centers of **1a** was monitored calibrating with that of the signal at δ 0.3 due to the internal standard, $Si(SiMe_3)_4$.

The reaction rate (v) is defined using the rate constant, and the concentration of **1a** and 4-chlorotoluene, k, C**1a** and S, respectively:

$$\upsilon = -\frac{dC_{1a}}{dt} = kC_S C_{1a} \qquad (1)$$

Because excess amount (30 eq.) of 4-chlorotoluene was added, the concentration of 4-chlorotoluene (Cs) can be regarded to be constant. Thefore, the equation (1) is as follows, using k' as an alternative rate constant:

$$\upsilon = -\frac{dC_{1a}}{dt} = \mathrm{k}' C_{1a} \qquad (2)$$

$$\mathrm{k}' = \mathrm{k} C_S^0 \qquad (3)$$

If the initial concentration of **1a** is defined as C**1a 0** (t = 0), the equation (2) can be changed:

$$\ln C_{1a} = -k't + \ln C_{1a}^0 \qquad (4)$$

The plots of time (t, min) and concentration (ln$C$**1a**) according to the equation (4) are as follows

(Figure S-1-7-1):

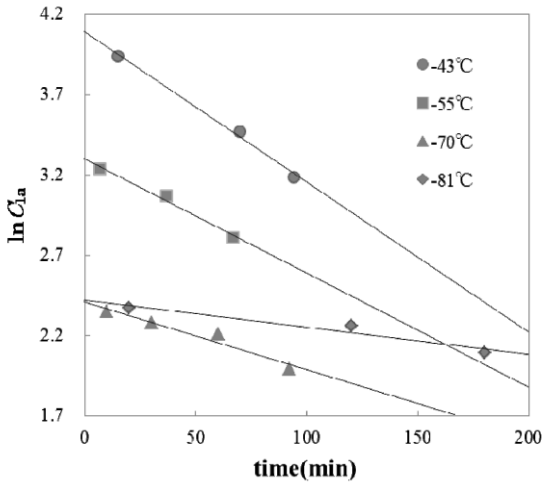

Figure S-1-7-1. Time and ln*C***1a** plots for the reaction-rate constant (*k'*)

As a result, the rate constants *k'* (min-1) were 9.73 × 10^{-3} (230 K), 7.22 × 10^{-3} (218 K), 4.18 × 10^{-3} (203 K), and 2.79 × 10^{-3} (192 K).

S-1-8. Reaction of 3,5-dichloropyridine with 2 (Scheme 2-10)

In a glovebox, $[Ni(IPr)]_2(\mu\text{-}Cl)_2$ (2) (58.0 mg, 0.060 mmol) and 3,5-dichloropyridine (18 mg, 0.120 mmol) was dissolved in THF (0.5 mL). The reaction immediately occurred at room temperature, and the colour of the solution turned from yellow to dark red. To the resulted solution, n-hexane (1.5 mL) was added and cooled to -30 ºC. After several days, dark brown crystals were obtained (40.2 mg, 60%). Anal. Calcd. for $C_{118}H_{150}N_{10}Cl_8Ni_4$: C, 63.64; H, 6.79; N, 6.29. Found: C, 63.17; H, 6.67; N, 6.78. In the reaction of **2** with 3,5-dichloropyridine, only one of the two C-Cl bonds in 3,5- dichloropyridine had been cleaved, and the 3-σ-pyridyl groups were combined with a pair of central nickel atoms in compound **4** (Scheme S-1-8-1). These pyridyl groups were also coordinated to the other terminal nickel atoms forming Ni-N bonds (Figure S-1-8-1). This suggested that the oxidative addition of one of the C-Cl bonds of 3,5-dichloropyridine had proceeded, and that intermediate species X' was stabilized by the N-coordination of the pyridyl group after the disproportionation process, leading to the tetranuclear structure. Given that the formation of compound **4** required about a day, it would not be possible for this compound to be the real intermediate in the Kumada coupling. Of course, this result does not support completely any process requiring the formation of **X** as part of the catalytic cycle, because many other intermediates could also be formed during the course of the oxidative addition process.

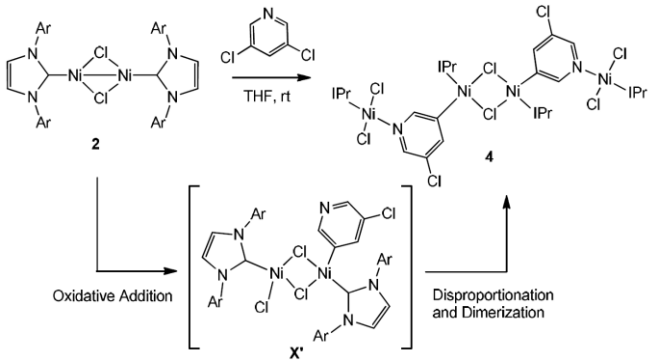

Scheme S-1-8-1. Stoichiometric reaction of 2 with 3,5-dichloropyridine.

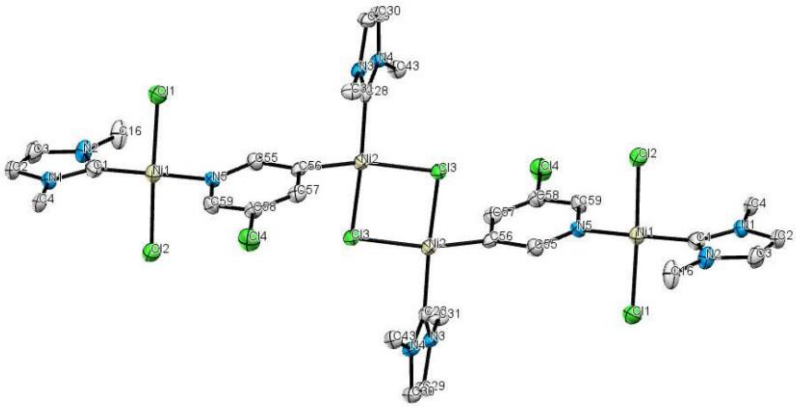

Figure S-1-8-1. ORTEP drawing of the tetranickel complex **4** (50% propability of thermal ellipsoids). Hydrogen atoms and the aromatic groups are omitted for clarity.

S-1-9. X-ray diffraction studies

Single crystals of **1a**, **1b**, **3a**, and **4** for X-ray diffraction studies were grown at -30°C from toluene/hexane or THF/hexane solutions. The data were collected at 110 K on a Rigaku Saturn CCD diffractometer, using graphite monochromated Mo Kα radiation (λ = 0.71070 A). Data reductions of the measured reflections were carried out using the software package, CrystalStructure. The structures were solved by a direct method (SIR-2007)[4] and refined by full-matrix least-squares fitting based on F2 using the program SHELXL 97-2 PC version.[5] All non-hydrogen atoms were refined with anisotropic displacement parameters. All H atoms were located at ideal positions and were included in the refinement, but were restricted to ride on the atom to which they were bonded. Detail data were shown in CIF files of them.

S-1-10. DFT calculations

Calculations were performed using the GAUSSIAN 09 software package,[6] and the PBE0 functional, without symmetry constraints. That functional uses a hybrid generalized gradient approximation (GGA), including 25 % mixture of Hartree-Fock[7] exchange with DFT[8] exchange-correlation, given

by Perdew, Burke and Ernzerhof functional (PBE).[9] The optimized geometries were obtained with the Stuttgart Effective Core Potentials and associated basis set[10] for Ni, and a standard 6-31G(d,p)[11] for the remaining elements. Frequency calculations were performed to confirm the nature of the stationary points, yielding one imaginary frequency for the transition states and none for the minima. Each transition state was further confirmed by following its vibrational mode downhill on both sides and obtaining the minima presented on the energy profile. The free energy values presented along the text (298.15 K and **1a**tm) were obtained from zero point energy and thermal energy corrections based on structural and vibration frequency data.

Additional DFT calculation was conducted by Dr. Y. Yamada at Fukuoka University for the oxidative addition process of $[Ni(IPr)]_2(\mu\text{-}Cl)_2$ (2) with chlorobenzene. The simpler model complex, $[Ni(IMe)]_2(\mu\text{-}Cl)_2$, bearing 1,3-bis(methyl)imidazol-2-ylidene (IMe) was also used for the B3LYP[12] calculation with basis sets of 3-21G for C, H, and N, 6-31G* for Cl, and the relativistic effective core potential (ECP) and basis set of Los Alamos ECP plus DZ (LANL2DZ)[13] for Ni. The reaction similarly proceeds to the intermediary dinickel adduct to the reaction of **1a** with chlorobenzene (see main text). Details are shown in Figure S-1-10-1.

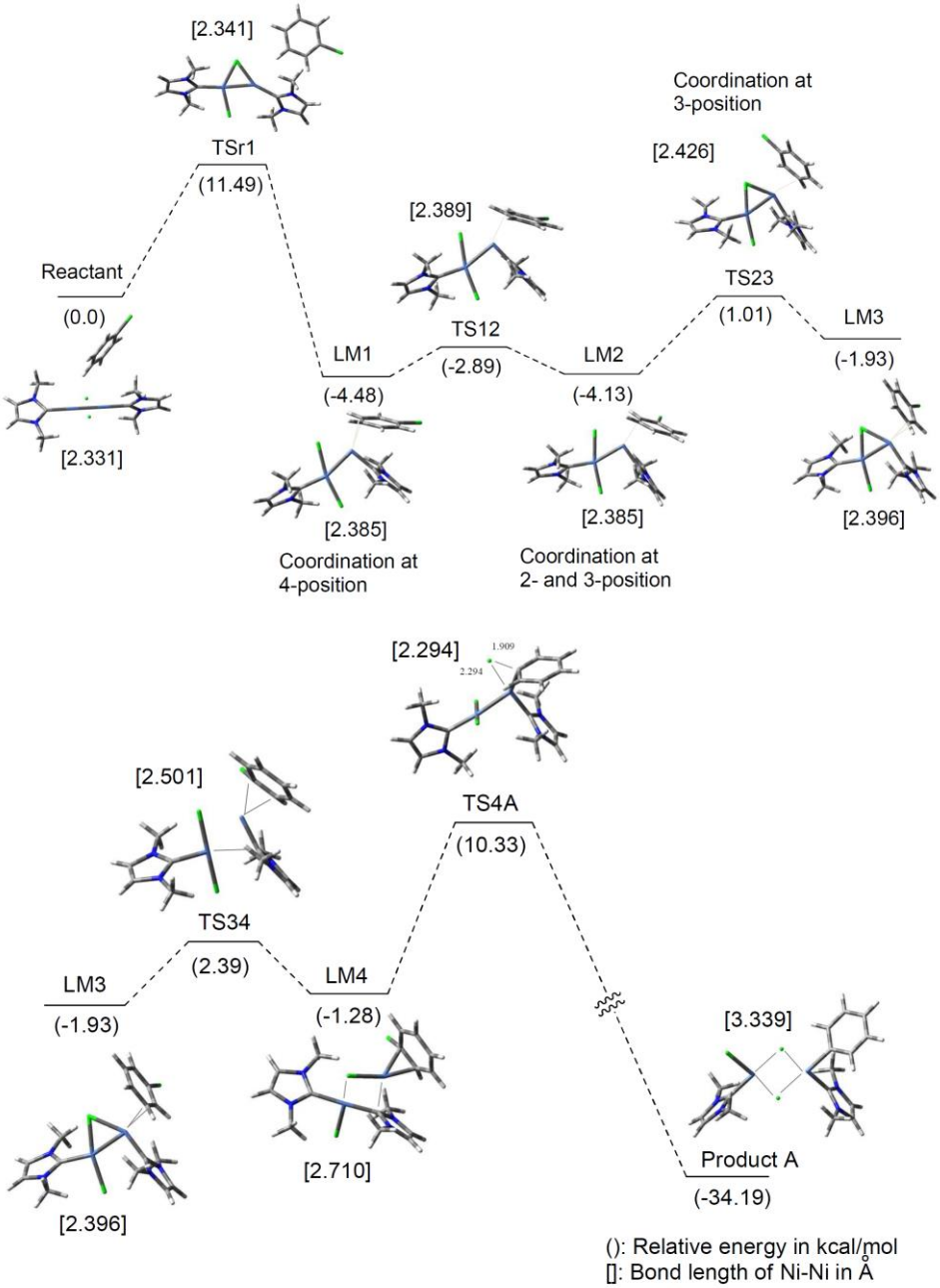

Figure S-1-10-1. Reaction profile of the computed relative Gibbs free energies for the reaction of $[Ni(IMe)]_2(\mu\text{-}Cl)_2$ (Reactant) with chlorobenzene to give Product A by B3LYP calculation with basis sets of 3-21G for C, H, and N, 6-31G* for Cl, and CEP/LanL2DZ for Ni.

S-1-11. NMR spectra

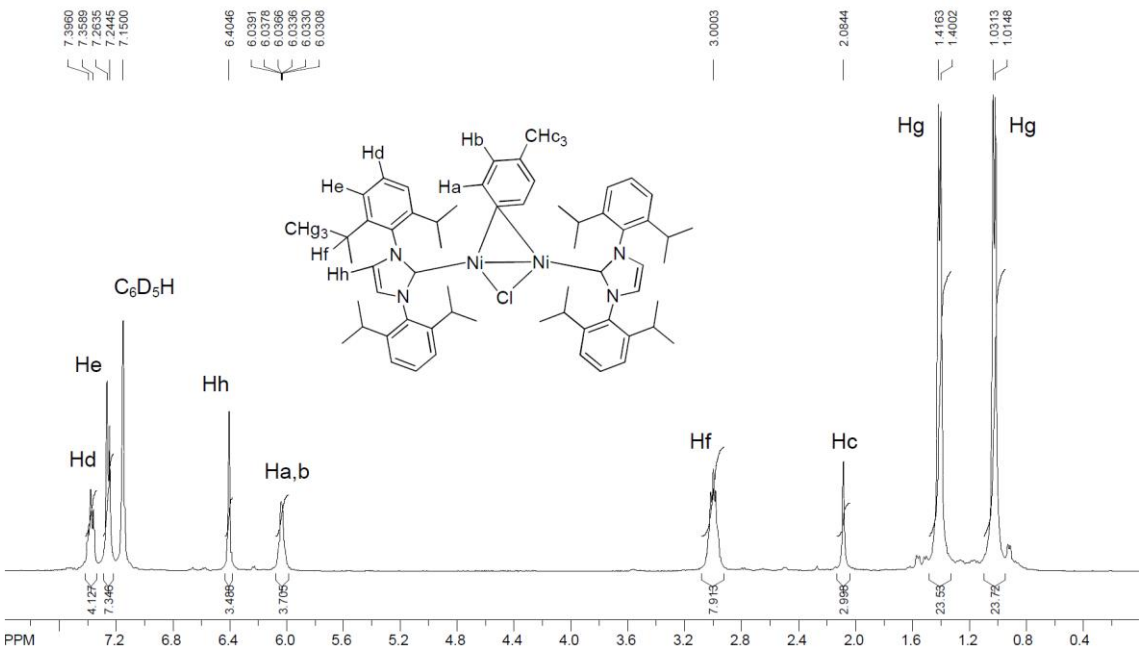

Figure S1-2-1. ^{1}H NMR spectrum for **1a** (400 MHz, C_6D_6).

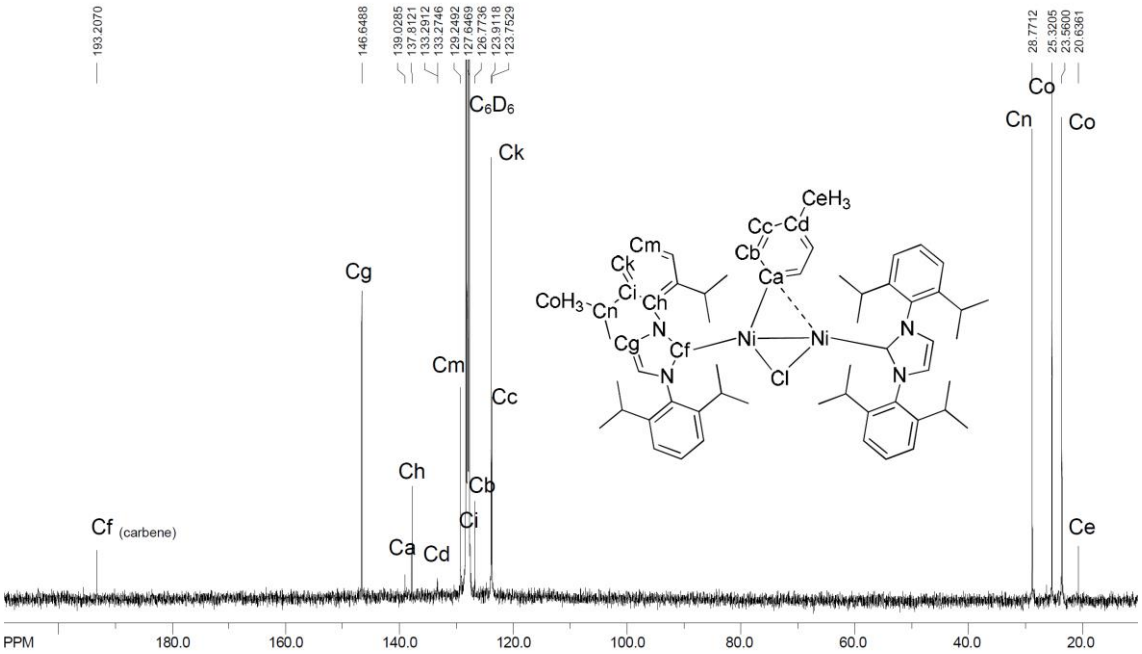

Figure S1-2-2. ^{13}C NMR spectrum for **1a** (100 MHz, C_6D_6).

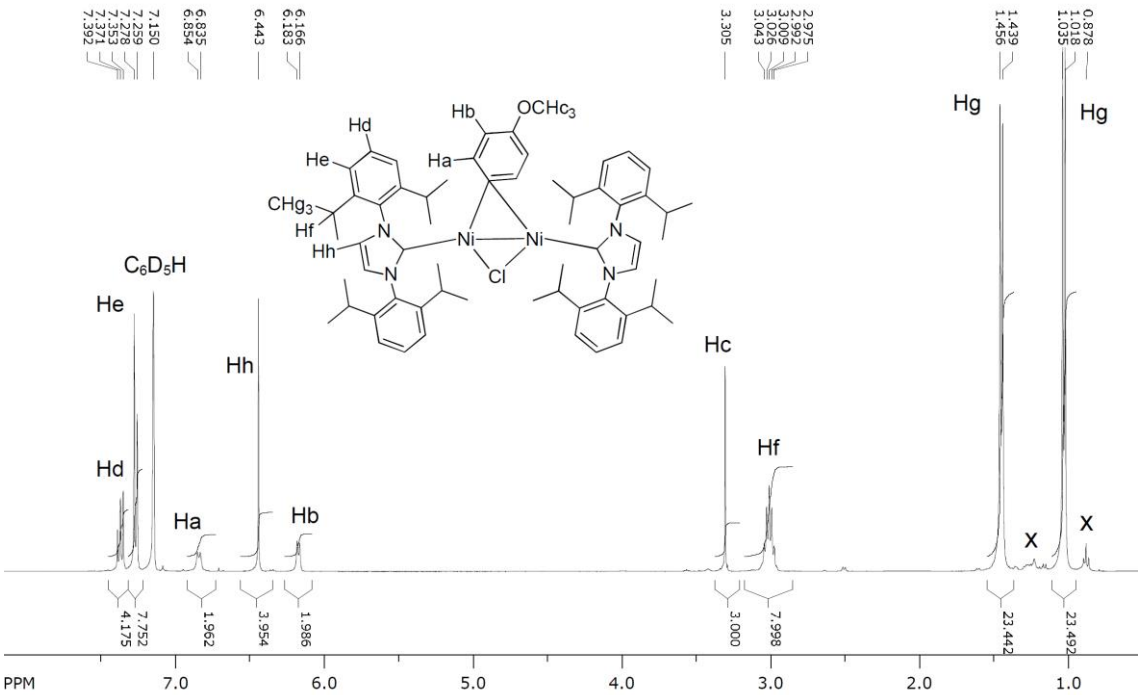

Figure S-1-2-3. ^{1}H NMR spectrum for **1b** (400 MHz, C_6D_6).

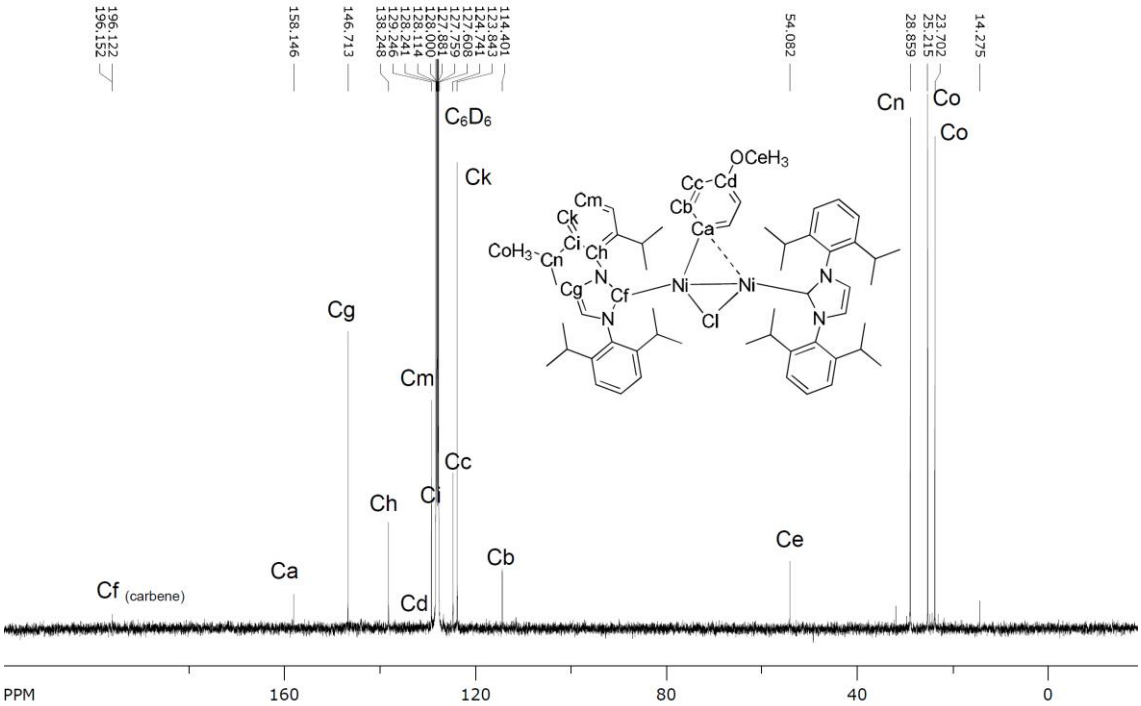

Figure S-1-2-4. ^{13}C NMR spectrum for **1b** (100 MHz, C_6D_6).

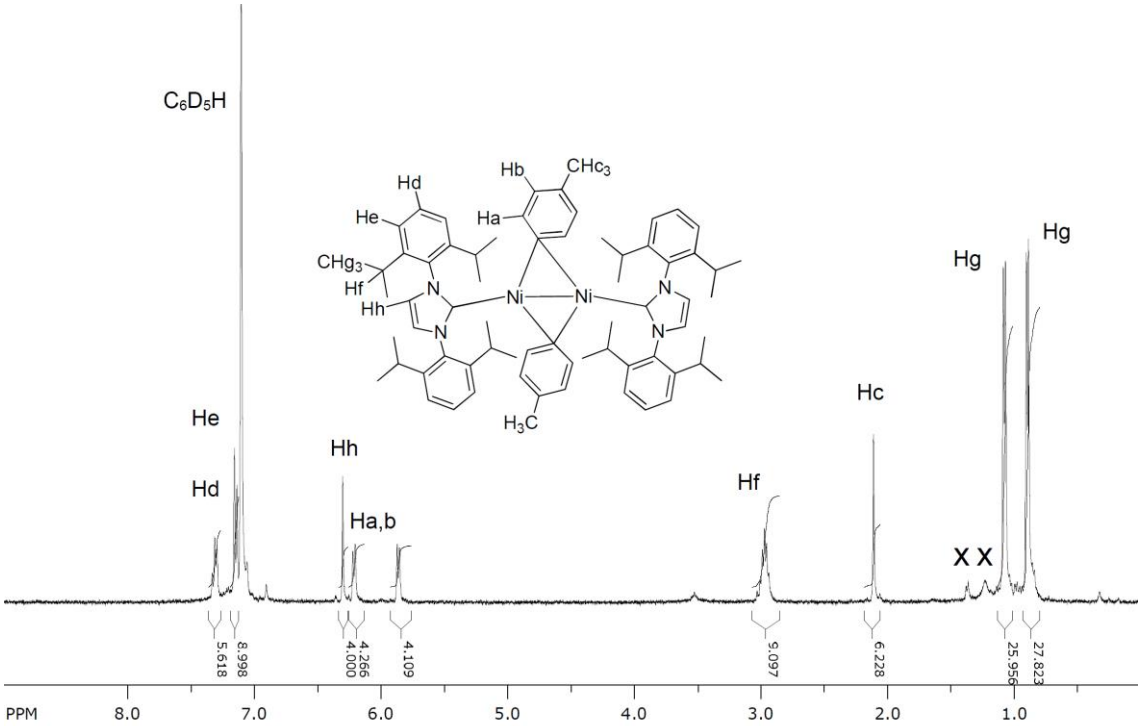

Figure S-1-3-1. 1H NMR spectrum for **3a** (400 MHz, C_6D_6).

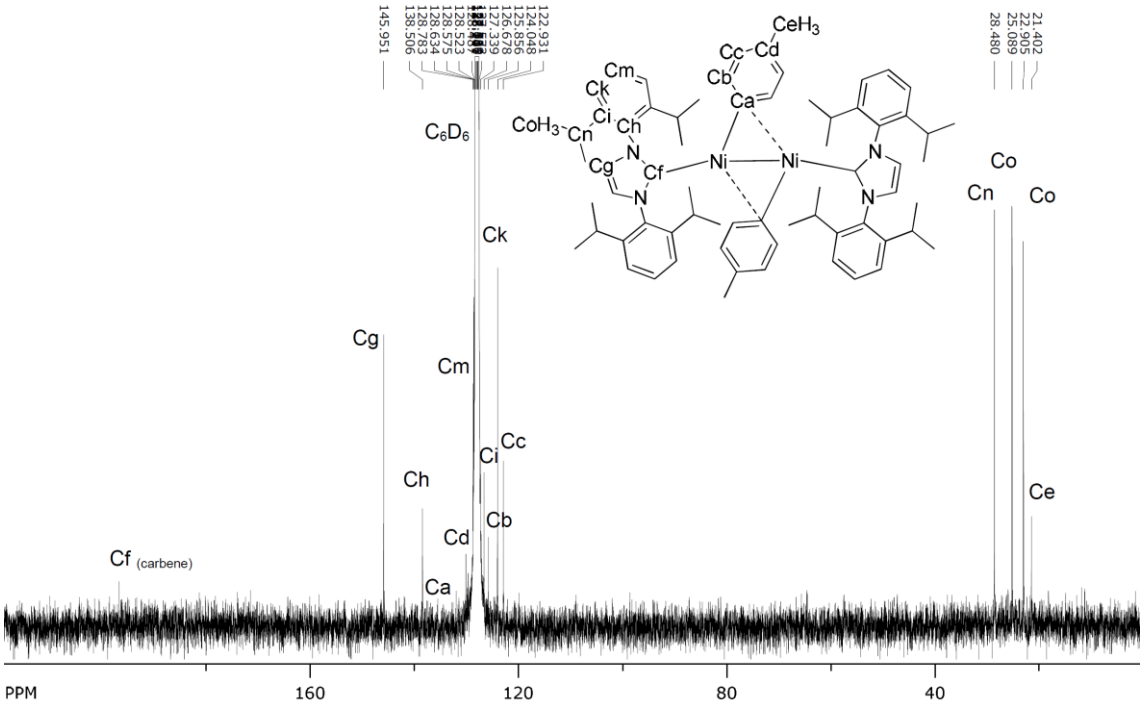

Figure S-1-3-2. 13C NMR spectrum for **3a** (100 MHz, C_6D_6).

S-1-12. X-ray crystal structure of 1b

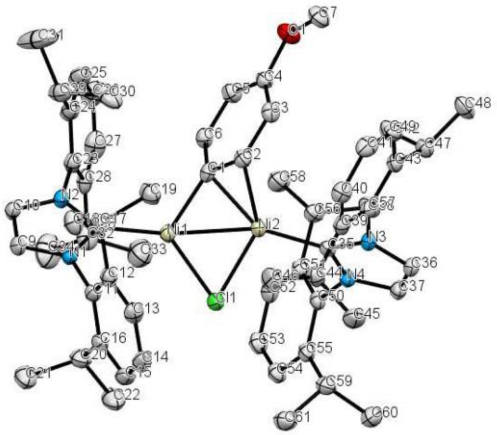

Figure S-2-2-1. ORTEP drawing of **1b** (50% probability of thermal ellipsoids). Hydrogen

S-1-13. References

1. Jafarpour, L.; Stevens, E. D.; Nolan, S. P. *J. Organomet. Chem.* **2000**, *606*, 49–54.
2. Matsubara, K.; Miyazaki, S.; Koga, Y.; Nibu, Y.; Hashimura, T.; Matsumoto, T. *Organometallics* **2008**, *27*, 6020-6024.
3. Dible, B. R.; Sigman, M. S.; Arif, A. M. *Inorg. Chem.* **2005**, *44*, 3774–3776.
4. Caliandro, R.; Carrozzini, B.; Cascarano, G. L.; de Caro, L.; Giacovazzo, C.; Siliqi, D. *J. Appl. Crystallogr.* **2007**, *40*, 883-890.
5. SHELXL97-2: Sheldrick, G. M. **1997**. University of Gottingen, Germany.
6. Gaussian 09, Revision A.02, Frisch, M. J.; Trucks, G. W.; Schlegel, H. B.; Scuseria, G. E.; Robb, M. A.; Cheeseman, J. R.; Scalmani, G.; Barone, V.; Mennucci, B.; Petersson, G. A.; Nakatsuji, H.; Caricato, M.; Li, X.; Hratchian, H. P.; Izmaylov, A. F.; Bloino, J.; Zheng, G.; Sonnenberg, J. L.; Hada, M.; Ehara, M.; Toyota, K.; Fukuda, R.; Hasegawa, J.; Ishida, M.; Nakajima, T.; Honda, Y.; Kitao, O.; Nakai, H.; Vreven, T.; Montgomery, Jr., J. A.; Peralta, J. E.; Ogliaro, F.; Bearpark, M.; Heyd, J. J.; Brothers, E.; Kudin, K. N.; Staroverov, V. N.; Kobayashi, R.; Normand, J.; Raghavachari, K.; Rendell, A.; Burant, J. C.; Iyengar, S. S.; Tomasi, J.; Cossi, M.; Rega, N.; Millam, J. M.; Klene, M.; Knox, J. E.; Cross, J. B.; Bakken, V.; Adamo, C.; Jaramillo, J.; Gomperts, R.; Stratmann, R. E.; Yazyev, O.; Austin, A. J.; Cammi, R.; Pomelli, C.; Ochterski, J. W.; Martin, R. L.; Morokuma, K.; Zakrzewski, V. G.; Voth, G. A.; Salvador, P.; Dannenberg, J. J.; Dapprich, S.; Daniels, A. D.; Farkas, O.; Foresman, J. B.; Ortiz, J. V.; Cioslowski, J.; Fox, D. J. Gaussian, Inc., Wallingford CT, USA, 2009.
7. Hehre, W. J.; Radom, L.; Schleyer, P. von R.; Pople, J. A. *Ab Initio Molecular Orbital Theory*, John Wiley & Sons, NY, 1986.
8. (a) Perdew, J. P.; Burke, K.; Ernzerhof, M. *Phys. Rev. Lett.* **1997**, *78*, 1396-1396. (b) Perdew, J.

P. *Phys. Rev. B* **1986**, *33*, 8822-8824.

9. (a) Perdew, J. P.; Burke, K.; Ernzerhof, M. *Phys. Rev. Lett.*, **1996**, 77, 3865-3868. (b) Perdew, J. P.; Burke, K.; Ernzerhof, M. *Phys. Rev. Lett.*, **1997**, 78, 1396-1396.
10. (a) Haeusermann, U.; Dolg, M.; Stoll, H.; Preuss, H. *Mol. Phys.* **1993**, *78*, 1211-1224. (b) Kuechle, W.; Dolg, M.; Stoll, H.; Preuss, H. *J. Chem. Phys.* **1994**, *100*, 7535-7542. (c) Leininger, T.; Nicklass, A.; Stoll, H.; Dolg, M.; Schwerdtfeger, P. *J. Chem. Phys.* **1996**, *105*, 1052-1059.
11. Ditchfield, R.; Hehre W. J.; Pople, J. A. *J. Chem. Phys.* **1971**, *54*, 724-728. (b) Hehre, W. J.; Ditchfield R.; Pople, J. A. *J. Chem. Phys.* **1972**, *56*, 2257-2261. (c) Hariharan, P. C.; Pople, J. A. *Mol. Phys.* **1974**, *27*, 209-214. (d) Gordon, M. S. *Chem. Phys. Lett.* **1980**, *76*, 163-168. (e) Hariharan, P. C.; Pople, J. A. *Theor. Chim. Acta* **1973**, *28*, 213-222.
12. Miehlich, B.; Savin, A.; Stoll, H.; Preuss, H. *Chem. Phys. Lett.* **1989**, 157, 200-206.
13. Hay, P. J.; Wadt, W. R. *J. Chem. Phys.* **1985**, 82, 270-283.

S-2-1. General

All experiments were performed in an inert gas atmosphere using standard Schlenk techniques and a glovebox (MBraun UNIlab), unless otherwise stated. THF, hexane, toluene, and benzene-d_6 were distilled from benzophenone ketyl and stored in a nitrogen atmosphere with 4A molecular sieves. Chloroform-*d* was distilled from CaH_2 and stored in a nitrogen atmosphere. Other reagents were used as received or distilled just before use if possible. ^{1}H NMR spectra were obtained at room temperature using a Varian Mercury Y Plus 400 MHz spectrometer. Chemical shifts (δ) were recorded in parts per million from the solvent signal. GC-MS was performed using an Agilent 6890N gas chromatograph coupled with a JEOL JMS-GC mate II mass spectrometer. A 60 m InertCap 1 column (0.25 mm i.d., 0.25 μm film thickness) was used, and the injection temperature was 270 °C. Elemental analysis was performed using a Yanaco CHN Corder MT-5 autosampler. CW X-band ESR spectra were measured by a Bruker E500 ESR spectrometer. The measurement temperature was controlled by an Oxford ESR900 cryostat and an ITC503 temperature controller in the temperature range from 4 to 296 K. The g value was calibrated using a NMR teslameter. The magnetic properties of the materials were investigated using a Quantum Design MPMS-5S SQUID magnetometer. Column chromatography of organic products was performed using silica gel (Kanto Kagaku, silica gel 60 N, spherical, neutral). The NHC was prepared from the imidazolium salts using the published method.[1] The monovalent dinuclear nickel IPr complex 1 was prepared as described in the literature.[2]

S-2-2. Preparation of Monomeric Nickel NHC Complexes [NiCl(L)(IPr)] (2b-d) (Scheme 3-1)

[NiCl(P(OPh)$_3$)(IPr)] (2b)

The Ni(I) complex was prepared according to the similar method with literature.[1] In a glove box, [(μ-Cl)(IPr)Ni]$_2$ (**1**) (0.03 mmol, 30 mg), P(OPh)$_3$ (0.06 mmol, 15 μL), and THF (0.5 mL) were added to a 5 mL screw-capped tube. After the compounds were dissolved, hexane (1.5 mL) was slowly added to the solution and cooled to -30°C. Colorless crystals of **2b** were obtained, after removal of the liquid and washing with small amount of hexane (85 mg, 88% yield). ^{1}H NMR (400 MHz, C_6D_6)(Figure S-2-2-1): δ 1.62 (bs), 4.13 (bs), 6.94 (bs), 7.68 (bs), 8.09~8.31 (bs), 10.44 (bs). Elemental

analysis calcd (%) for $C_{45}H_{51}N_2O_3PClNi$: C, 68.16; H, 6.48; N, 3.53. Found: C, 68.63; H, 6.59; N, 3.57.

[NiCl(Py)(IPr)] (2c)

In a glove box, $[(\mu\text{-Cl})(IPr)Ni]_2$ (**1**) (0.03 mmol, 30 mg), Pyridine (0.12 mmol, 9.6 μL), and THF (0.5 mL) were added to a 5 mL screw-capped tube. After the compounds were dissolved, hexane (1.5 mL) was slowly added to the solution and cooled to -30°C. Vermillion crystals of **2c** were obtained, after removal of the liquid and washing with small amount of hexane (24 mg, 69% yield). ^{1}H NMR (400 MHz, C_6D_6) (Figure S-2-2-2): δ 1.18 (bs), 1.75 (bs), 2.48 (bs), 3.08 (bs) , 6.37 (bs) , 6.95 (bs) , 10.7 (bs). Elemental analysis calcd (%) for $C_{32}H_{41}N_3ClNi$: C, 68.41; H, 7.36; N, 7.48. Found: C, 68.33; H, 7.32; N, 7.38.

[NiCl(IPr)]$_2$(dppb) (2d)

In a glove box, $[(\mu\text{-Cl})(IPr)Ni]_2$ (**1**) (0.05 mmol, 48 mg), dppb (0.05 mmol, 21 mg), and THF (0.5 mL) were added to a 5 mL screw-capped tube. After the compounds were dissolved, hexane (1.5 mL) was slowly added to the solution and cooled to -30°C. Yellow crystals of **2d** were obtained, after removal of the liquid and washing with small amount of hexane (63 mg, 91% yield). ^{1}H NMR (400 MHz, C_6D_6) (Figure S-2-2-3): δ 1.75 (bs), 4.55 (bs), 8.52 (bs), 10.78 (bs). Elemental analysis calcd (%) for $C_{45}H_{51}N_2O_3PClNi$: C, 70.76; H, 7.24; N, 4.03. Found: C, 70.06; H, 7.33; N, 3.77.

S-2-3. Solution Behavior in the Reaction Media with Bidentate Phosphines

Reaction of 1 with dppe and dppp

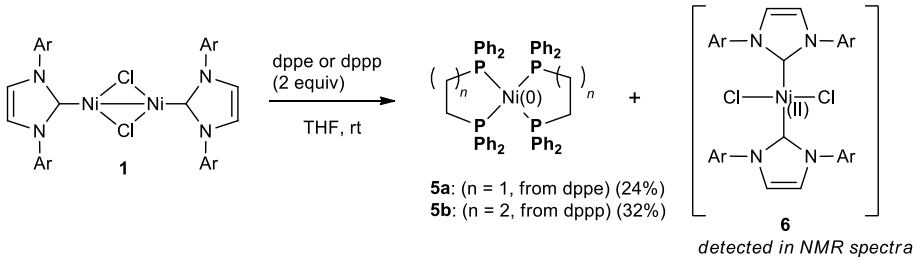

Scheme S-2-3-1. Reactions of 1 with diphosphines, dppe and dppp

The reaction of complex **1** with 2 equiv. of dppe (1,2-bis(diphenylphosphino)ethane) or dppp (1,2-bis(diphenylphosphino)propane) in THF at room temperature occurred to give a mixture of zerovalent Ni(0) complex, $Ni(dppe)_2$ (**5a**) or $Ni(dppp)_2$ and divalent nickel chloride, $NiCl_2(IPr)_2$, which was clearly detected in NMR spectra (Figures S-2-3-1, S-2-3-5). Although the formation of the nickel(II) chloride was confirmed by the ^{1}H NMR spectra of the mixtures, the nickel(0) phosphine complexes were successfully isolated as yellow and red-orange crystals and determined by NMR spectroscopy (Figures S-2-3-2, S-2-3-3, S-2-3-4, S-2-3-6, S-2-3-7, S-2-3-8). The yields of **5a** and **5b** were 24 and 32%, respectively, after crystallization.

Reaction of 1 with dppe

In a glove box, $[Ni(IPr)]_2(\mu\text{-}Cl)_2$ (**1**) (0.03 mmol, 30 mg), DPPE (0.06 mmol, 24 mg), and THF (0.5 mL) were added to a 5 mL screw-capped tube. After the compounds were dissolved, hexane (1.5 mL) was slowly added to the solution and cooled to -30°C. Yellow crystals of **5a** were obtained, after removal of the liquid and washing with small amount of hexane (12 mg, 24% yield). ^{1}H NMR (400 MHz, C_6D_6) (Figure S-2-3-2): δ = 2.10 (t, 4H), 6.93 (m, 12H), 7.47 (br, 8H). ^{13}C NMR (100MHz, C_6D_6) (Figure S-2-3-3): δ = 30.05, 31.32, 32.63, 131.85, 133.43, 14.56. ^{31}P NMR (162MHz, C_6D_6) (Figure S-2-3-4)): δ = 44.08 (s).

Reaction of 1 with dppp

The reaction was similarly conducted to that with dppe. The yield of **5b** waS-22% after crystallization. ^{1}H NMR (400 MHz, C_6D_6) (Figure S-2-3-6): δ = 2.23 (br, 4H), 3.58 (br, 2H), 6.97 (m, 12H), 7.50 (br, 8H). ^{13}C NMR (100MHz, C_6D_6) (Figure S-2-3-7): δ = 18.10, 19.39, 20.71, 30.32, 31.51, 32.71, 126.86, 132.23, 133.80, 142.39. ^{31}P NMR (162MHz, C_6D_6) (Figure S-2-3-8): δ = 13.4 (s).

S-2-4. Monitoring of the Disproportionation of 2d in Benzene-d_6

The isolated crystals of **2d** was dissolved in benzene-d_6 and added to an NMR tube. The ^{1}H and ^{31}P NMR spectra were recorded, and monitored the sample using the NMR spectroscopy. After 18 h, formation of **5c** was confirmed in the ^{31}P NMR spectra (Figure S-2-4-1), showing appearance of the signal at δ 26.97, which was consistent

with that in the literature.[2] Additionally, the characteristic broad signals from **2d** have disappeared and concomitant generation of **6** was detected by the ^{1}H NMR spectra (Figure (Figure S-2-4-2). Some decomposition reactions proceeded concomitantly in the absence of excess amount of DPPB, showing several undefined signals in the ^{31}P and ^{1}H NMR spectra.

S-2-5. Preparation of the Monomeric IMes Complexes (Scheme 3-3)

[NiCl(PPh$_3$)(IMes)] (3a)

The Ni(I) complex was prepared according to the similar method with literature.[3] A solution of 1,3-bis(2,4,6-trimethylphenyl)imidazolium chloride [IMes/HCl] (428 mg, 1.26 mmol) with KN(SiMe$_3$)$_2$ (253 mg, 1.26 mmol) in THF (20 mL) for 3 h was added to a mixture of [Ni (cod)$_2$] (158 mg, 0.57 mmol) and [Ni(PPh$_3$)Cl$_2$] (374 mg, 0.57 mmol). The mixture was stirred at room temperature for overnight to afford a dark yellow solution. The yellow solution was filtered through Celite and the solvent removed under vacuum. The yellow solids were then recrystallized from toluene/hexane. Yield: 634 mg (84%). ^{1}H NMR (400 MHz, C$_6$D$_6$) (Figure S-2-5-1): δ 1.44 (bs), 3.24 (bs), 4.46 (bs), 8.26 (bs), 10.99 (bs). Elemental analysis calcd (%) for C$_{39}$H$_{39}$ClN$_2$NiP: C 70.88, H 5.95, N 4.24; found C 70.52, H 5.97, N 4.31.

[NiBr(PPh$_3$)(IMes)] (3b)

The Ni(I) complex was prepared according to the similar method with literature.[4] A solution of 1,3-bis(2,4,6-trimethylphenyl)imidazolium chloride [IMes/HCl] (427 mg, 1.26 mmol) with KN(SiMe$_3$)$_2$ (256 mg, 1.26 mmol) in THF (20 mL) for 4.5 h was added to a mixture of [Ni (cod)$_2$] (174 mg, 0.63 mmol) and [Ni(PPh$_3$)$_2$Br$_2$] (461 mg, 0.63 mmol). The mixture was stirred at room temperature for overnight to afford a dark yellow solution. The yellow solution was filtered through Celite and the solvent removed under vacuum. The yellow solids were then recrystallized from THF/hexane. Yield: 440 mg (49%). ^{1}H NMR (400 MHz, C$_6$D$_6$) (Figure S-2-5-2): δ 1.51 (bs), 3.20 (bs), 4.35 (bs), 8.23 (d, J = 8.6 Hz, 4H), 10.94 (d, J = 8.3 Hz, 4H). Elemental analysis calcd (%) for C$_{47}$H$_{56}$BrN$_2$NiO$_2$P: C 66.37, H 6.64, N 3.29; found C 66.53, H 6.41, N 3.30.

S-2-6. SQUID Measurement of the Ni(I) Complexes

(a)

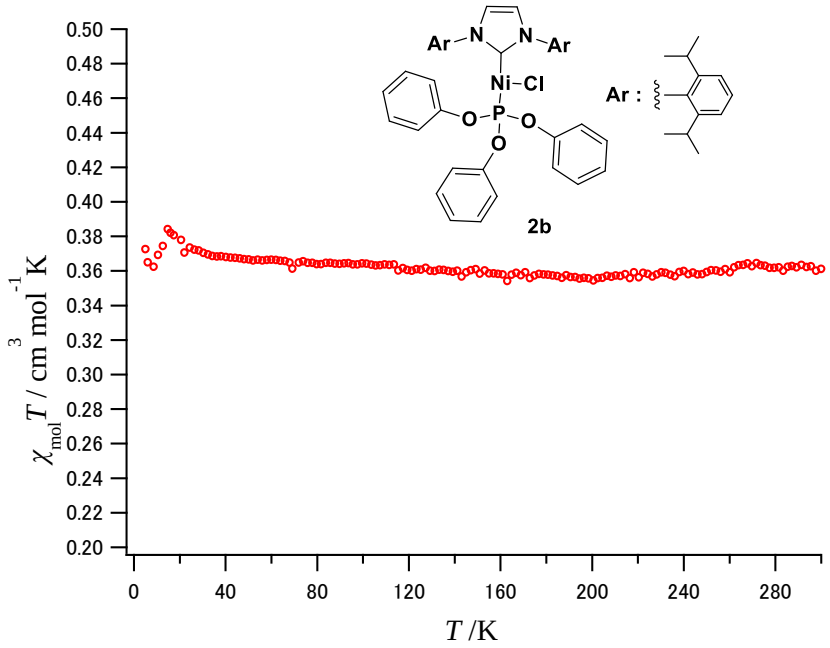

(b)

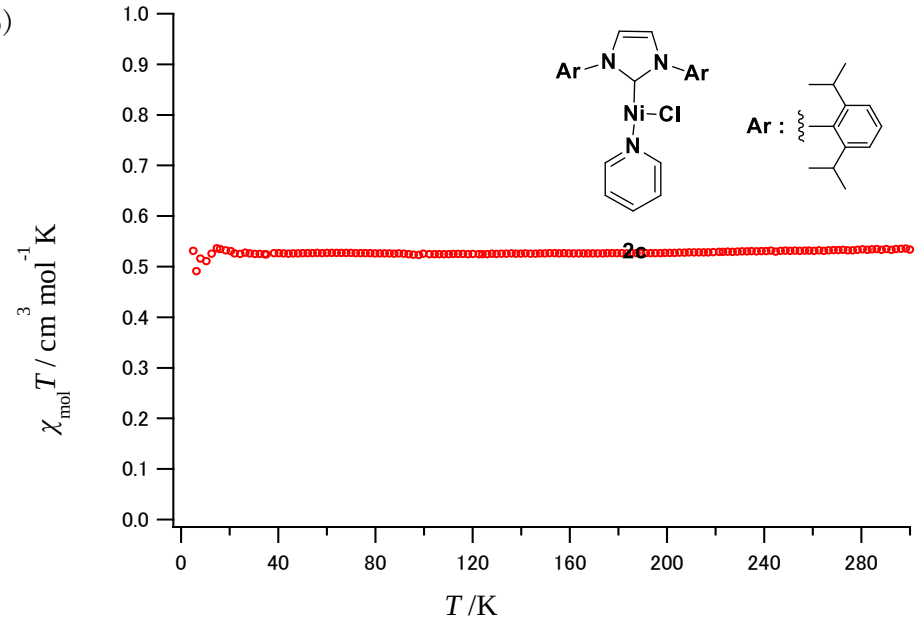

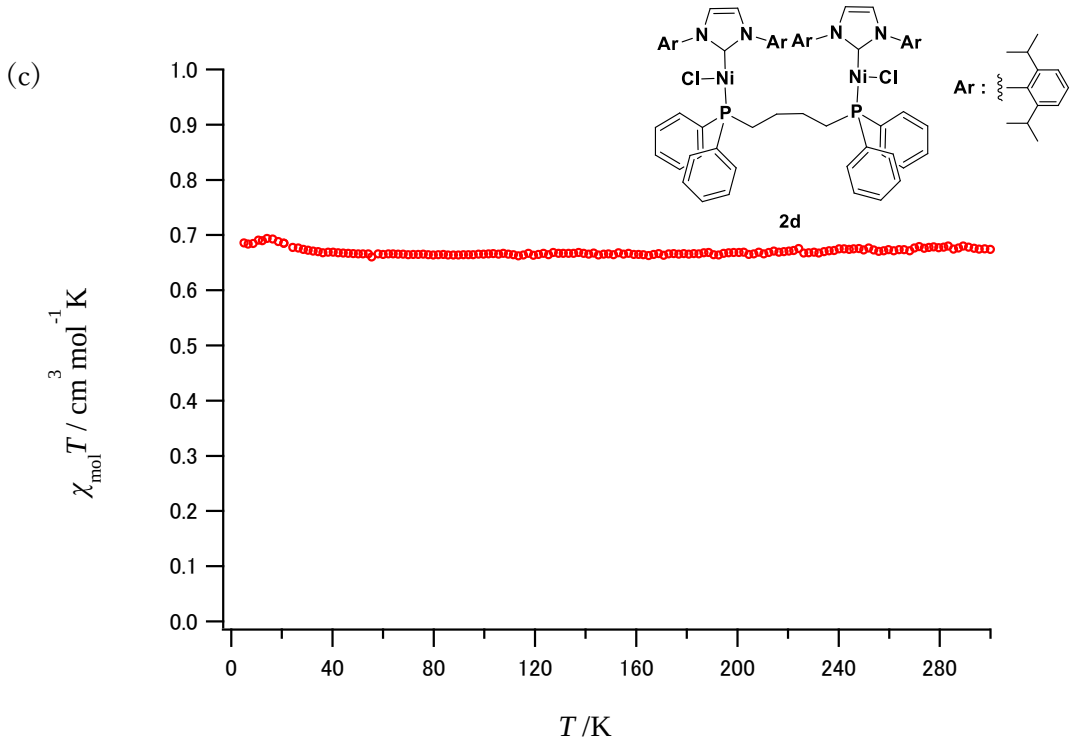

Figure S-2-6-1. Temperature versus $\chi_{mol}T$ plots of complexes (a) **2b**, (b) **2c** and (c) **2d** recorded by means of SQUID.

S-2-7. Buchwald-Hartwig Amination to Yield Triarylamines (Scheme 3-4)

In a typical example, **1** (24.1 mg, 25 μmol) and ligand (300 μmol), Di-*p*-(tolyl)amine (118.4 mg, 0.6 mmol), NaO^{t}Bu (71.1 mg, 0.74 mmol), and 4-bromobenzophenone (130.6 mg, 0.5 mmol), THF(0.2 mL) were added and stirred at 40°C for 24 h. After addition of water, the organic layer was extracted with CH_2Cl_2 at three times. The combined organic layer was washed with saturated NaCl aq. and dried by Na_2SO_4, filtered and concentrated in vacuo. The residue was purified by flash column chromatography eluted with AcOEt/hexane (1/10) to obtain [4-[bis(4-methylphenyl)amino]phenyl]phenylmethanone as a yellow oil. Each of the yields was PPh_3(186.9 mg, 99%), Pyridine(184.9 mg, 98%), $P(OPh)_3$(73.6 mg, 39%).

Product details:

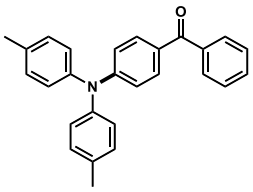

4-(Di-p-tolylamino)benzophenone: (CAS No. 245442-58-4) ^{1}H NMR (400 MHz, $CDCl_3$): δ 2.34 (s, 6H), 6.95 (d, *J* = 8.9 Hz, 2H), 7.08 (d, *J* = 8.6 Hz, 4H), 7.14 (d, *J* = 8.3 Hz, 4H), 7.46 (t, *J* = 7.3 Hz, 2 H), 7.55 (t, *J* = 7.4 Hz, 1 H), 7.68 (d, *J* = 8.9 Hz, 2 H), 7.76 (d, *J* = 7.4 Hz, 2 H)**.**

S-2-8. Suzuki-Miyaura Cross-Coupling Reaction of Aryl Bromide with Phenylboronic Acid (Table 3-2)

In a typical example, Aryl bromides (0.15 mmol), Phenylboronic acid (20 mg, 0.16 mmol, 1.1 equiv.), Base (0.66 mmol, 4.4 equiv.), and 3a (11 mg, 15 μmol, 10 mol%) were dissolved in solvents (1 mL). After stirring for overnight at 80°C, water was added to quench the reaction. The organic layer was extracted with AcOEt. The combined organic layer was dried by Na_2SO_4, filtered and concentrated in vacuo to obtain white solids. Identification of product was NMR spectroscopy and GC-MS analysis.

Product details.

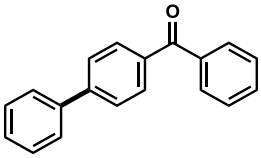

4-phenylbenzophenone: (CAS # 2128-93-0) ^{1}H NMR (400 MHz, $CDCl_3$) δ 7.39-7.43(m, 1H), 7.46-7.53 (m, 4H), 7.58-7.63 (m, 1H), 7.64-7.66 (m, 2H), 7.69-7.72 (d, 2H, J = 8.4 Hz), 7.83-7.85 (d, 2H, J = 8.4 Hz), 7.88-7.91 (d,2H, J = 8.4 Hz). GC-MS calcd for $C_{19}H_{14}$: 258, found: 258.

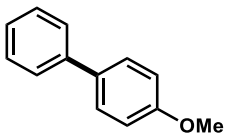

4-methoxybiphenyl: (CAS # 613-37-6) GC-MS calcd for $C_{13}H_{12}$: 184, found 184.

S-2-9. DFT Calculations

All the DFT calculations were performed utilizing the GAUSSIAN 09 package.[4] The B3LYP functional was employed with a standard split valence-type basis set, 6-31G(d,p). The single-point calculations to obtain SOMOs of **2a**. **2b**, **2c**, and **2d** were carried out using crystallographic coordinates without geometry optimization, and done with a tight self-consistent field (SCF) convergence criterion. As to the energy calculation of equilibrium between monomeric and dimeric form of nickel(I) phosphine complexes, geometry optimization and subsequent vibrational frequency analysis at each local minimum were performed at the same criteria without symmetry restriction. The estimation of relative energies (ΔE) was corrected by zero-point energies obtained from vibrational frequency analysis, and furthermore the Gibbs free energies (ΔG) were calculated in the condition of 298.15 K and 1 atm. All the computation was carried out using the computer facilities at Research Institute for Information Technology, Kyushu University.

The stable structures of monomeric, two-coordinate 13e intermediate, and dimeric nickel(I) complexes were obtained by geometry optimization using DFT calculation with B3LYP/6-31G(d,p) level (Figure S-2-9-1). Though the geometry optimizations for two-coordinate intermediates, **A-IPr** and **A-IMes**, were starting from the same structure to monomeric complexes except triphenylphosphine ligand, they relaxed toward linear structures during optimizations.

As to ligand elimination processes, the calculated energies of dimeric complexes (**A-IPr** and **A-IMes**) relative to monomeric ones (**2a** and **3a**) were distinctly different, +15.7 and +20.8 kcal/mol, respectively. This difference may be ascribed to the difference in monomeric complex stability. Comparing the calculated structures between **2a** and **3a,** one should notes that the Ni–P bond length in **2a** is longer by about 0.02 Å and that a particular benzene ring in triphenylphosphine ligand in **2a** is orientated nearly parallel to the N-C bond. These two facts indicated that the triphenylphosphine ligand in **2a** is likely to avoid the electrical repulsion from an isopropyl group, leading to less stable **2a** than **3a**, while dimeric ones showed no distortion derived from steric repulsion of isopropyl groups, meaning similar stability of **1-IPr** and **1-IMes**.

(a) IPr

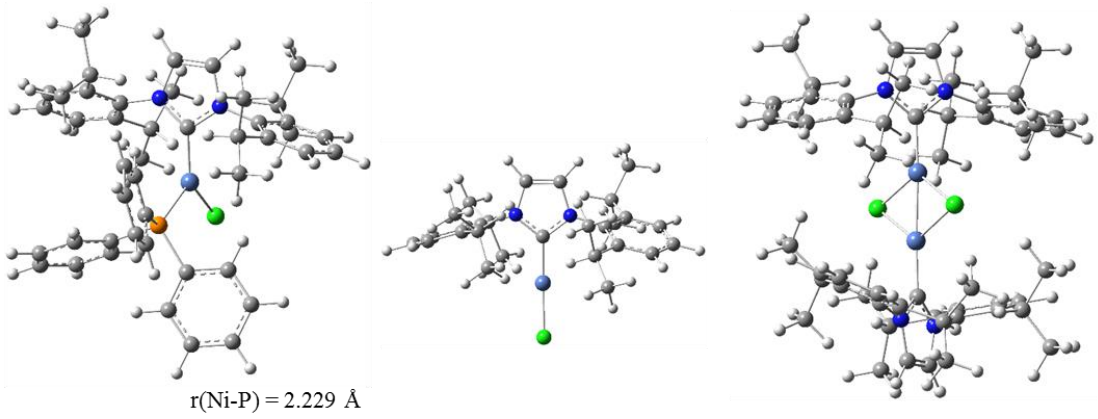

2a A-IPr 1-IPr

(b) IMes

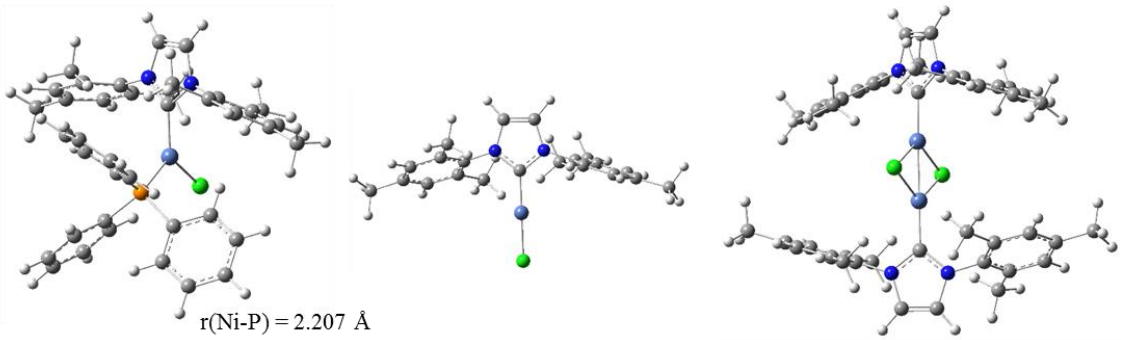

3a A-IMes 1-IMes

Figure S-2-9-1. Stable structures of monomeric, two-coordinate 13e intermediate, dimeric nickel(I) complexes calculated with B3LYP/6-31G(d,p) level.

S-2-10. References

1. Nagao, S.; Matsumoto, T.; Koga, Y. and Matsubara, K. *Chem. Lett*. **2011**, *40*, 1036-1038
2. Fischer, R.; Langer, J.; Malassa, A.; Walther, D.; Görls, H.; Vaughan, G. *Chem. Commun.* **2006**, 2510-2512.
3. Page, J. M.; Lu, Y. W.; Poulten, C. R.; Carter, E.; Algarra, G. A.; Kariuki, M. B.; Macgregor, A. S.; Mahon, F. M.; Cavell, J. K.; Murphy, M. D. and Whittlesey, K. M. *Chem. Eur. J.* **2013**, *19*, 2158 – 2167.

4. Frisch, M. J.; Trucks, G. W.; Schlegel, H. B.; et al. *Gaussian 09*, Revision D.01; Gaussian, Inc.: Wallingford CT, 2013.

S-2-11. NMR spectra

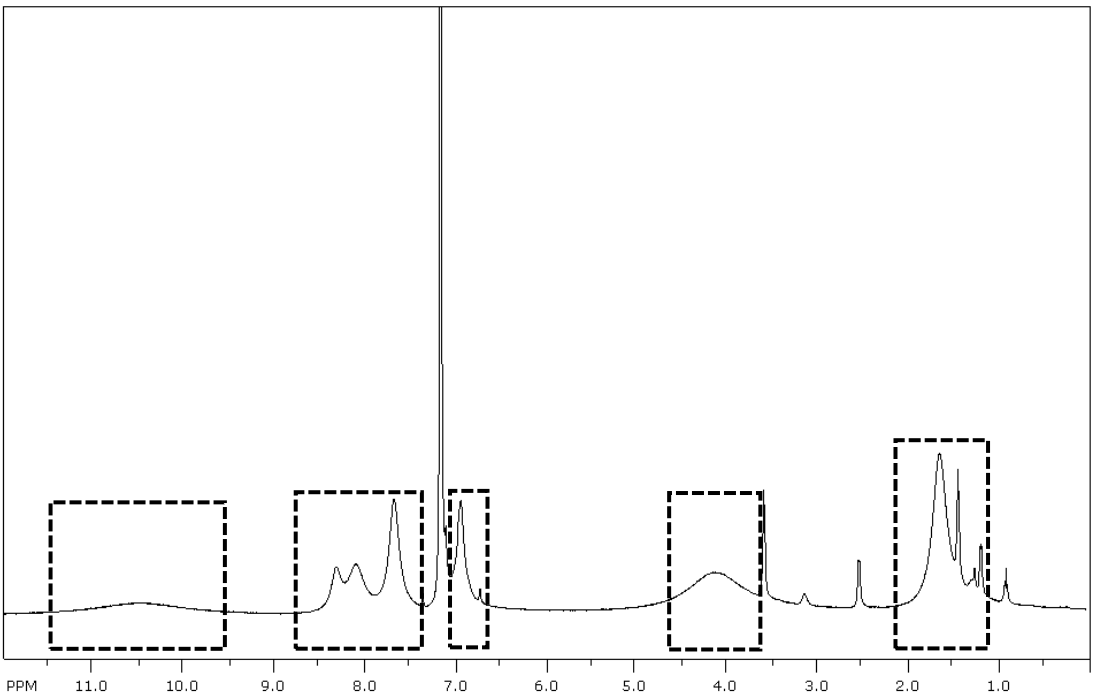

Figure S-2-2-1. ^{1}H NMR spectra for **2b** (400 MHz, benzene-d_6)

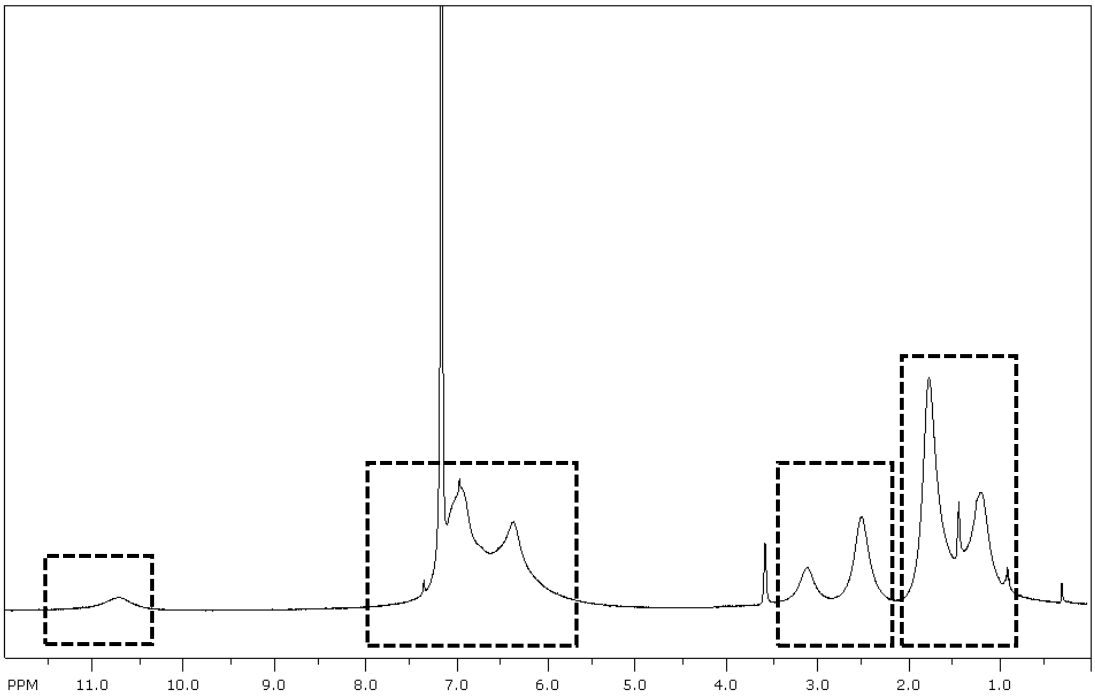

Figure S-2-2-2. ^{1}H NMR spectra for **2c** (400 MHz, benzene-d_6)

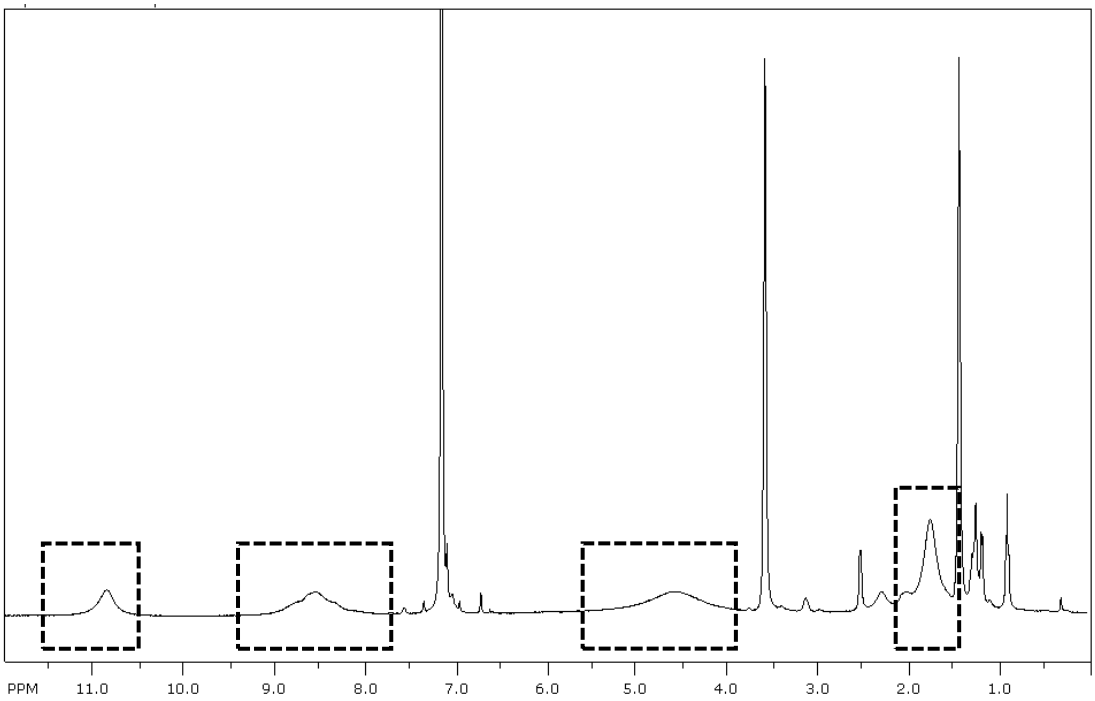

Figure S-2-2-3. ^{1}H NMR spectra for **2d** (400 MHz, benzene-d_6)

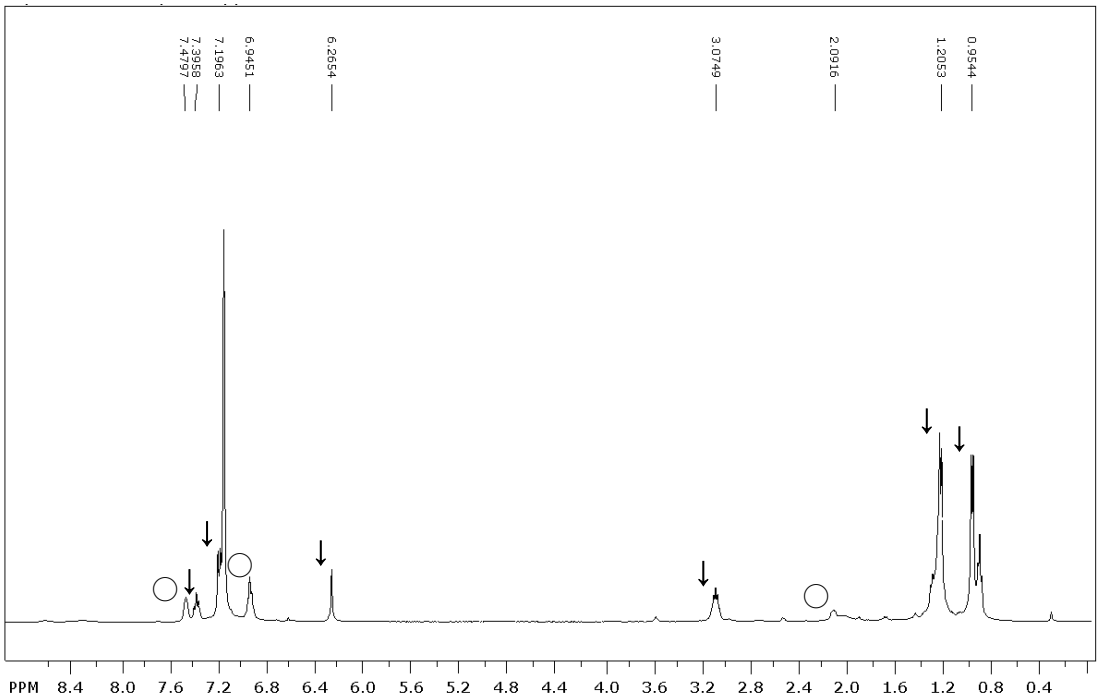

Figure S-2-3-1. ^{1}H NMR spectra (400 MHz, benzene-d_6) of the reaction mixture containing **5a** (○) and **6** (↓)

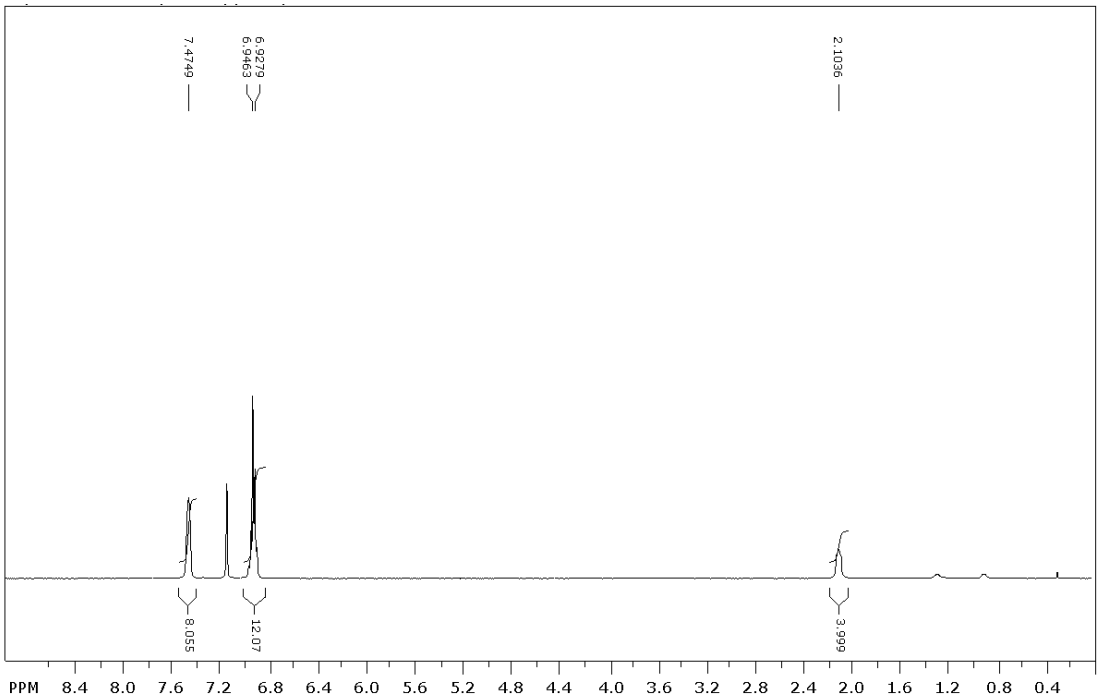

Figure S-2-3-2. ^{1}H NMR spectrum (400 MHz, benzene-d_6) of Ni(dppe)$_2$ (**5a**) after isolation

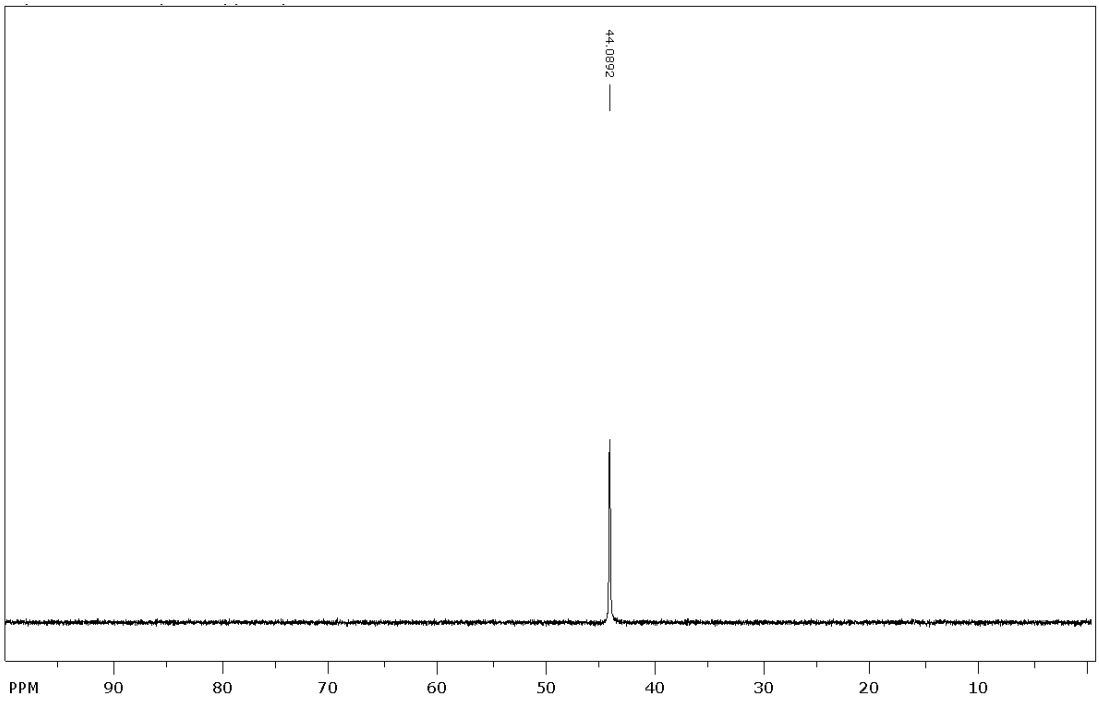

Figure S-2-3-3. ^{31}P NMR spectrum (162MHz, benzene-d_6) of Ni(dppe)$_2$ (**5a**) after isolation

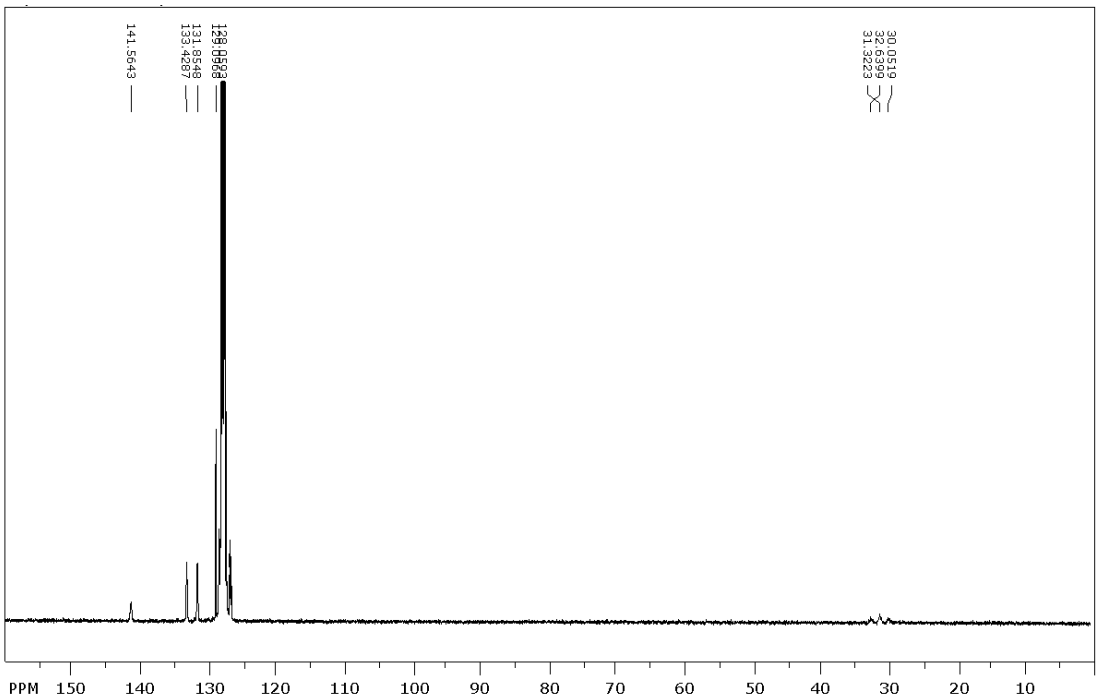

Figure S-2-3-4. ^{13}C NMR spectrum (100 MHz, benzene-d_6) of Ni(dppe)$_2$ (**5a**) after isolation

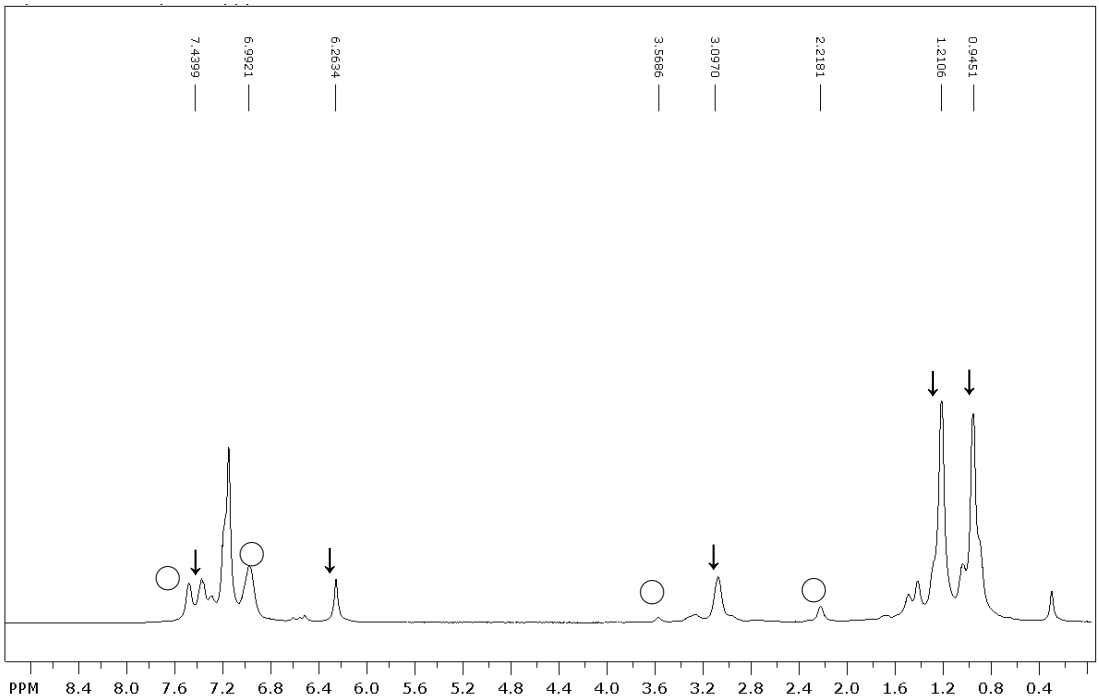

Figure S-2-3-5. ^{1}H NMR spectrum (400 MHz, benzene-d_6) of the reaction mixture containing **5b** (○) and **6** (↓).

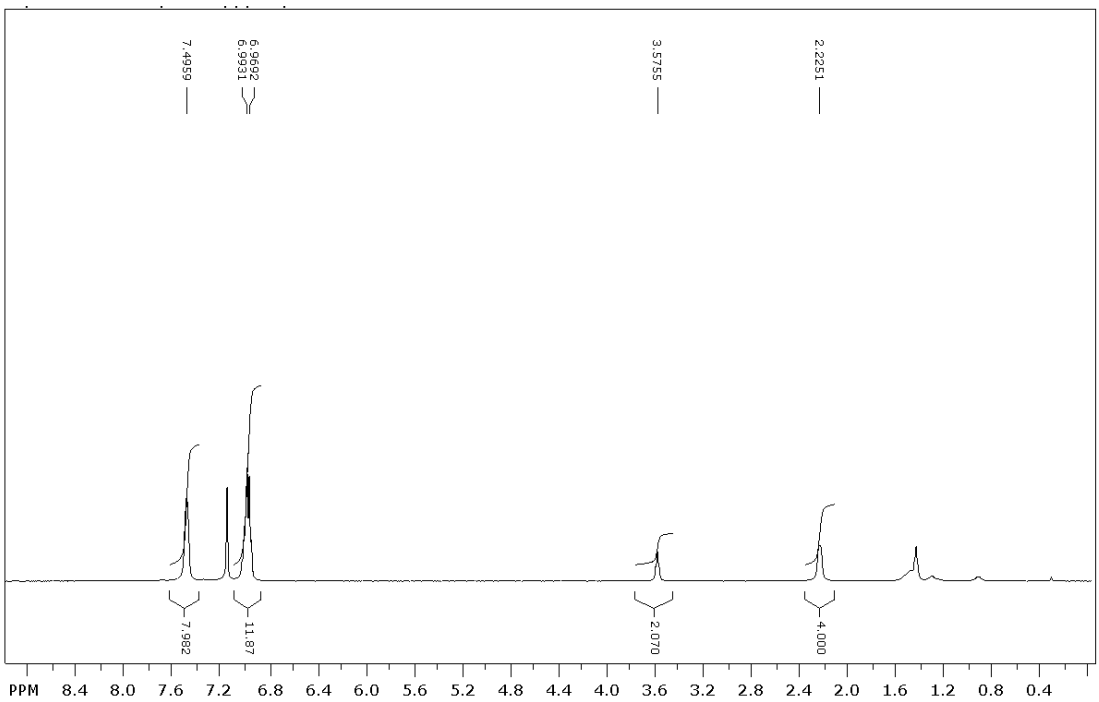

Figure S-2-3-6. ^{1}H NMR spectrum (400 MHz, benzene-d_6) of Ni(dppp)$_2$ (**5b**) after isolation

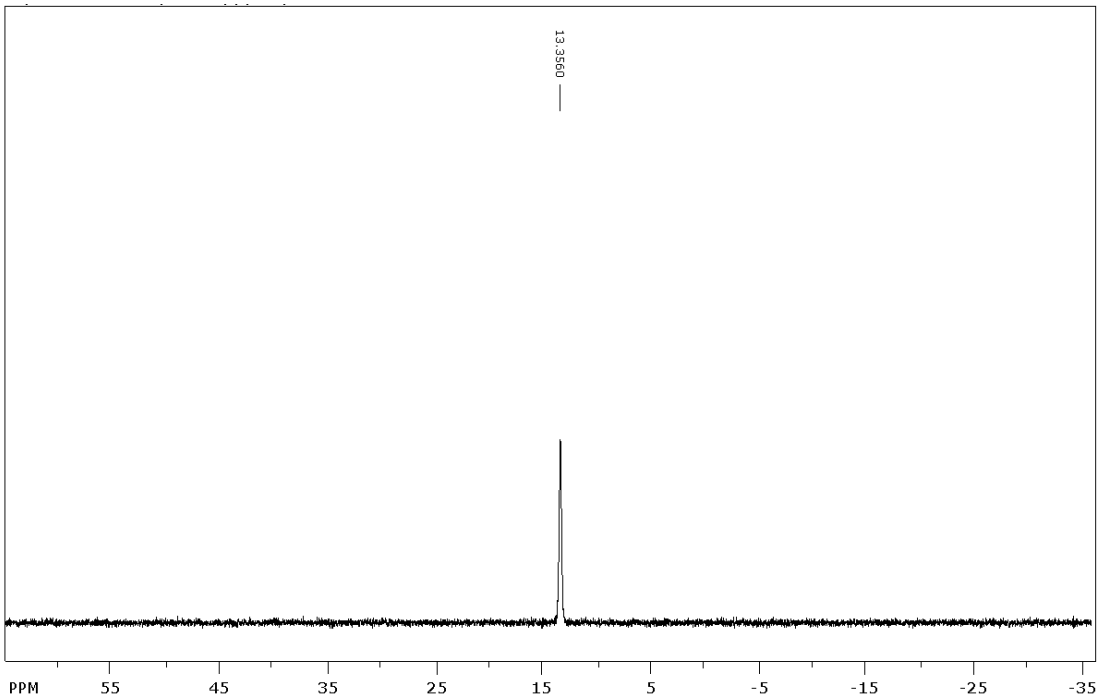

Figure S-2-3-7. ^{31}P NMR spectrum (162MHz, benzene-d_6) of Ni(dppp)$_2$ (**5b**) after isolation

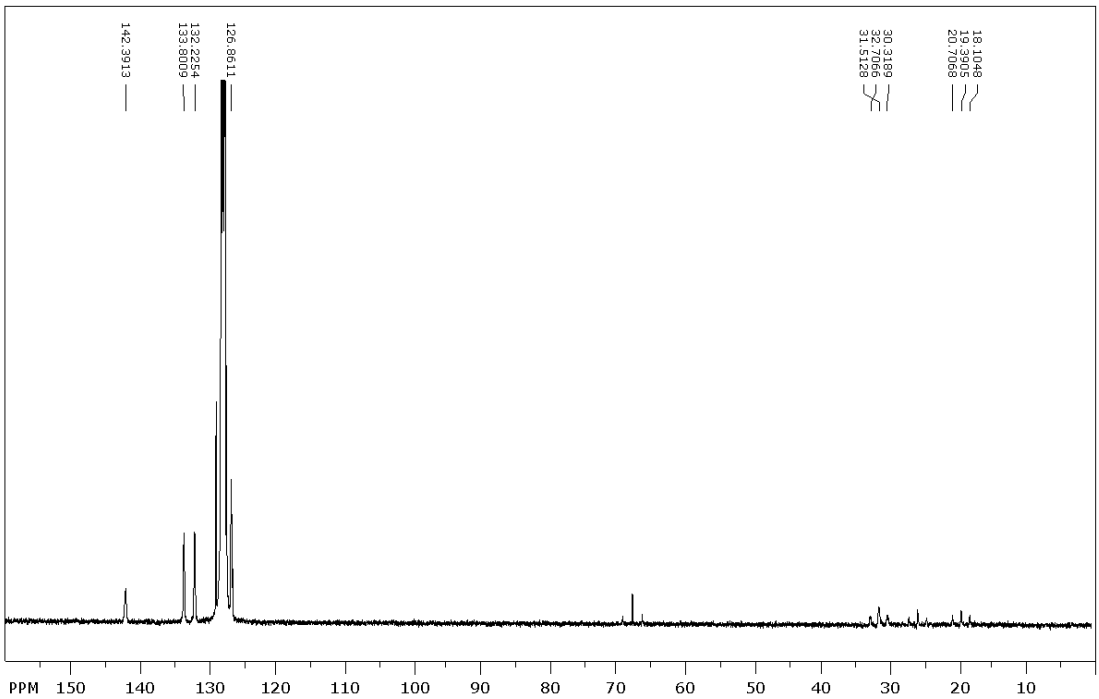

Figure S-2-3-8. ^{13}C NMR spectrum (100 MHz, benzene-d_6) of Ni(dppp)$_2$ (**5b**) after isolation

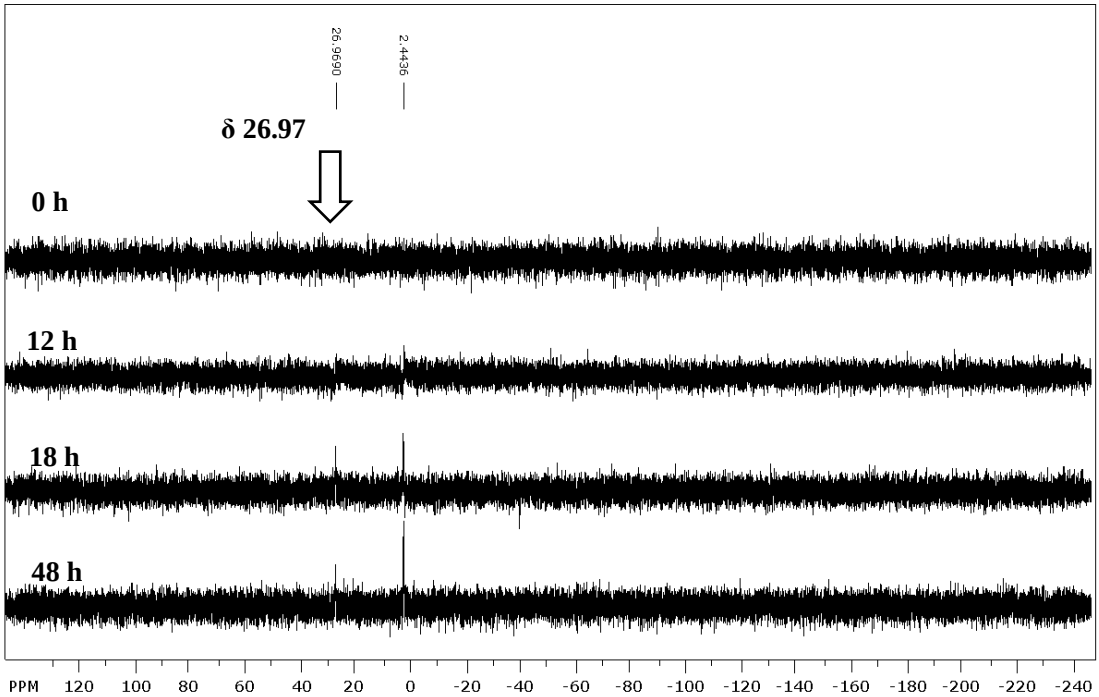

Figure S-2-4-1. Monitoring of the ^{31}P NMR spectroscopy (162 MHz, benzene-d_6) of $[NiCl(IPr)]_2$(dppb) (**2d**) to generate **5c** (δ 26.97) at room temperature for 48 h.

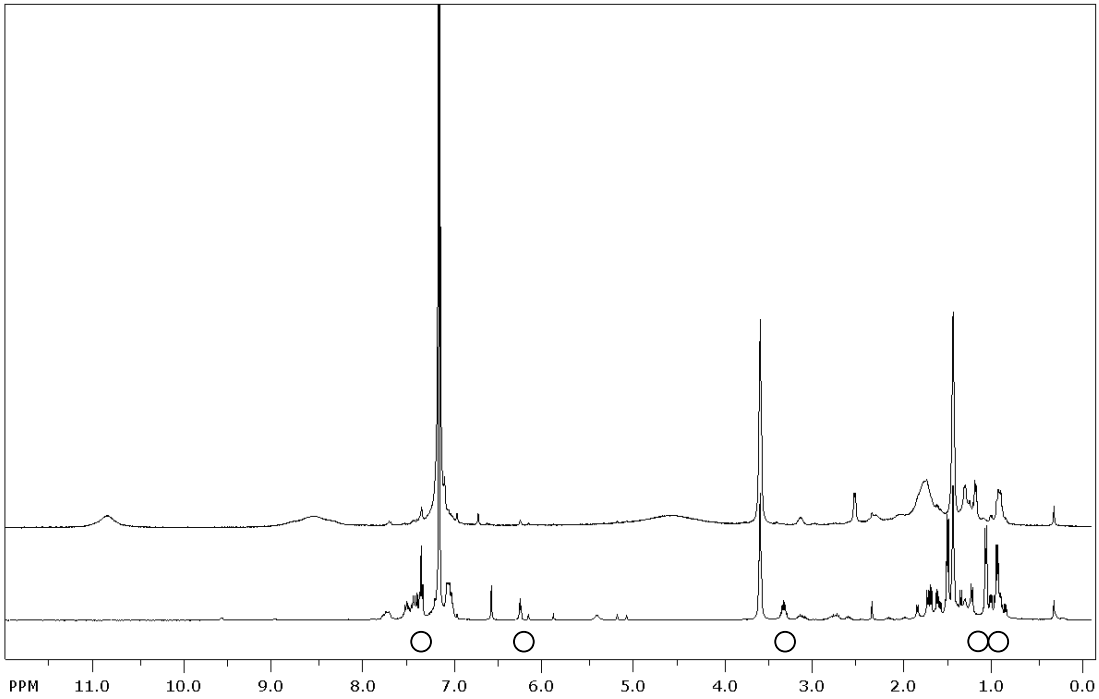

Figure S-2-4-2. ^{1}H NMR spectra (400 MHz, benzene-d_6) of the starting compound $[NiCl(IPr)]_2$(dppb) (**2d**) and that after 18 h to generate **6** (○)

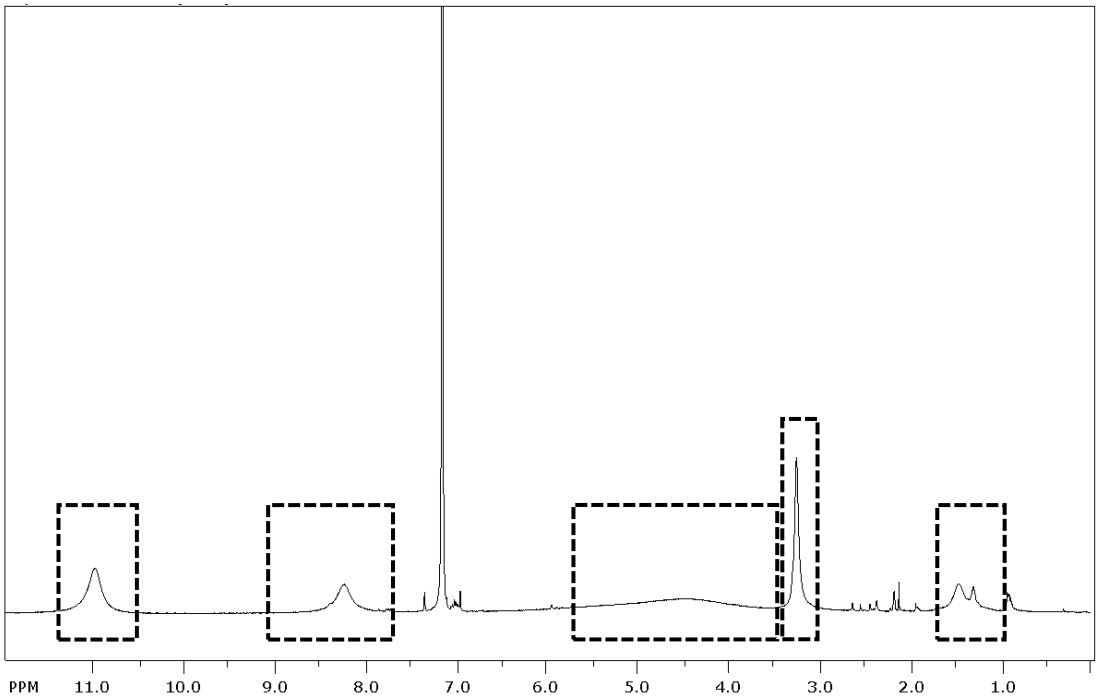

Figure S-2-5-1. ^{1}H NMR spectra for **3a** (400 MHz, benzene-d_6)

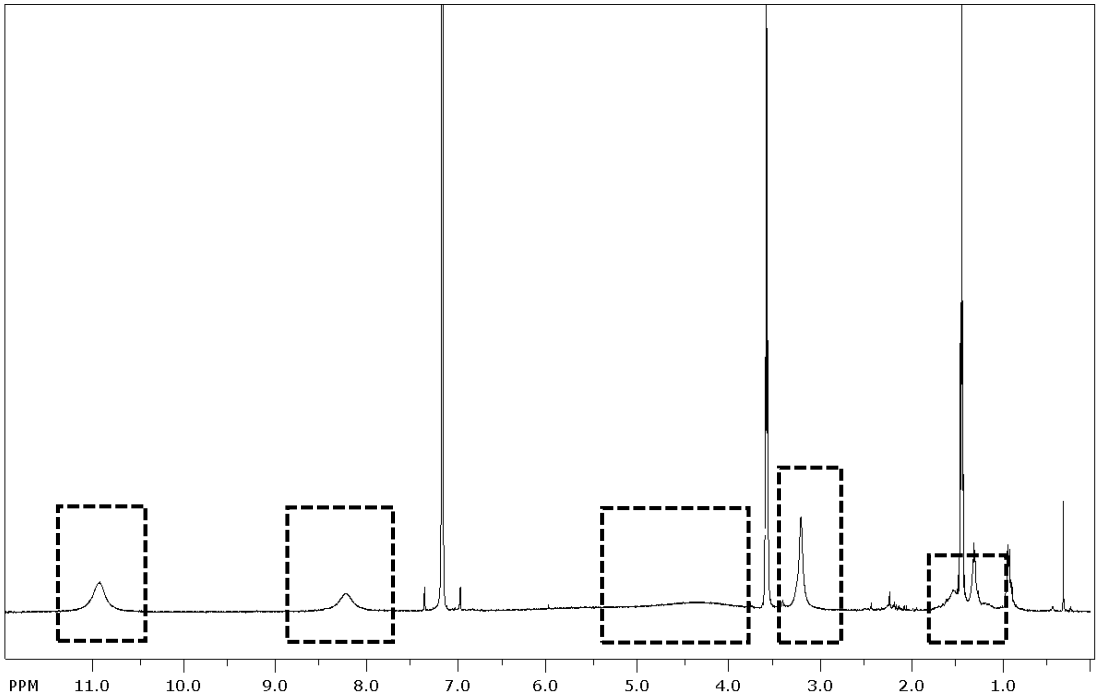

Figure S-2-5-2. ^{1}H NMR spectra for **3b** (400 MHz, benzene-d_6)

S-3-1. General

All experiments were carried out under an inert gas atmosphere using standard Schlenk techniques and glovebox (MBraun UniLab) as otherwise noted. THF, toluene, hexane, benzene-d_6 were distilled from benzophenone ketyl and stored under a nitrogen atmosphere. Volatile organic reagents used for coupling reactions were distilled just before use. Other reagents were used as received. Bis(4-methoxyphenyl)amine,[1a] N-(p-tolyl)-[1,1'-biphenyl]-4-amine,[1b] 4-fluoro-N-phenylaniline,[1a] N-(p-tolyl)naphthalen-1-amine,[1d] and 1,**3b**is(2,6-diisopropylphenyl)imidazol-2-ylidene (IPr)[2] were prepared according to the literature methods. Nickel dimers : $[Ni(IPr)(\mu\text{-}X)]_2$ (X = Cl, Br) (1a, 1b) were prepared according to the literature methods.[3]olumn chromatography of organic products was carried out using slica gel (Kanto Kagaku, silica gel 60N (spherical, neutral)). The ^{1}H NMR spectra were taken with a Bruker Avance-III400 Y pluS-300 MHz spectrometer at room temperature. Chemical shifts (δ) were recorded in ppm from the solvent signal. The magnetic properties of the materials were investigated using a Quantum Design MPMS-5S superconducting quantum interference device (SQUID) magnetometer. The elemental analysis was carried out with YANACO CHN Corder JM-11, AUTO-SAMPLER, using aluminum pan, where the samples were held in a glovebox. The UV-Vis measurements were taken with a PerkinElmer Lambda 35 UV/Vis Spectrometer using either a 10 mm quartz cell. The X-band EPR spectra were collected with a Bruker EMX Plus spectrometer equipped with a continuous flow N_2 cryostat. EPR simulation was conducted using a PHI program.[4]

S-3-2. Preparation of Monomeric Nickel(I) halides Complexes [NiX(bpy)(IPr)] (2a, b)(X = Cl, Br)

***Synthesis of [NiCl(bpy)(IPr)]* (2a)**

The Ni(I) complex **2a** was prepared according to the similar method with a literature.[5] In a glove box, $[(\mu\text{-Cl})(IPr)Ni]_2$ (**1-Cl)** (30 mg, 0.030 mmol), 2,2'-bipyridyl (9.5 mg, 0.061 mmol), and THF (1.0 mL) were added to a 5 mL screw-capped tube. After the compounds were dissolved, hexane (1.5 mL) was slowly added to the solution and cooled to -30ºC. Dark purple crystals of **2a** were obtained, after removal of the liquid and washing with small amount of cold hexane (60 mg, 0.094 mmol, 95% yield). ^{1}H NMR (400 MHz, C_6D_6) (Figurer S-3-2-1): δ 0.81~1.59 (bs), 6.17 (bs), 6.77 (bs). Elemental

analysis calcd (%) for $C_{37}H_{44}ClN_4Ni$: C, 69.55; H, 6.94; N, 8.77. Found: C, 69.18; H, 6.97; N, 8.44.

Synthesis of [NiBr(bpy)(IPr)] **(2b)**

The Ni(I) complex **2b** was prepared according to the similar method with literature.[5] In a glove box, $[(\mu\text{-Br})(IPr)Ni]_2$ (**1-Br**) (110 mg, 0.104 mmol), 2,2'-bipyridyl (40.7 mg, 0.261 mmol), and THF (15 mL) were added to a 25 mL screw-capped tube. After the compounds were dissolved, hexane (23 mL) was slowly added to the solution and cooled to -30ºC. Dark purple crystals of **2b** were obtained, after removal of the liquid and washing with cold hexane (132 mg, 0.193 mmol, 93% yield). ^{1}H NMR (400 MHz, C_6D_6) (Figurer S-3-2-2): δ 1.39 (bs), 6.32 (bs), 6.77 (bs). Elemental analysis calcd (%) for $C_{37}H_{44}BrN_4Ni$: C, 65.03; H, 6.49; N, 8.20. Found: C, 69.18; H, 6.97; N, 8.44.

S-3-3. Buchwald-Hartwig Amination to Yield Triarylamines

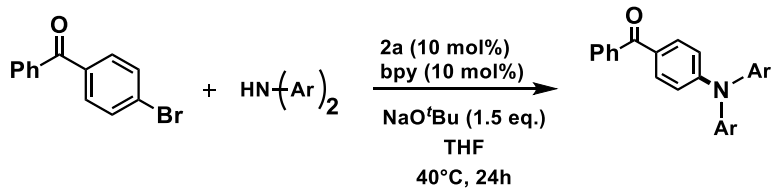

General Procedure for Amination Reaction of 4-Bromobenzophenone with Aromatic Amines.

In a glovebox, a Schlenk tube was charged with **2a** (31.9 mg, 0.05 mmol), 2,2'bipyridyl (15.6 mg, 0.10 mmol), aromatic amine (0.60 mmol), NaO^{t}Bu (71.1 mg, 0.75 mmol), 4-bromobenzophenone (130.6 mg, 0.50 mmol), and THF (0.2 mL). The reaction mixture was stirred at 40~80ºC for 24~48 h. After addition of water, the organic layer was extracted with CH_2Cl_2 for three times. The combined organic layer was washed with brine, dried over Na_2SO_4, and concentrated under reduced pressure. The residue was purified by column chromatography using silica gel eluted with CH_2Cl_2/hexane (1/3) to obtain corresponding triarylamine.

Product details

(4-(diphenylamino)phenyl)(phenyl)methanone)(**5a**)

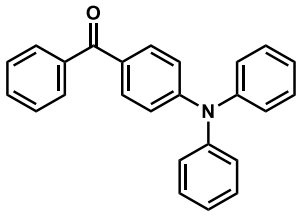

This reaction was conducted with diphenylamine and the reaction condition was 40ºC/24 h. The title compound was isolated as a yellow oil in 95% yield. (CAS No. 16911-33-4) ^{1}H NMR (400 MHz, $CDCl_3$): δ 7.77 (m, 3H), 7.69 (t, *J* = 8.6 Hz, 3H), 7.64-7.44 (m, 5H), 7.33 (t, *J* = 7.9 Hz, 4H), 7.18 (d, *J* = 7.4 Hz, 3H), 7.14 (t, *J* = 7.3 Hz, 2H), 7.01 (d, *J* = 8.9 Hz, 2H).

(4-(di-p-tolylamino)phenyl)(phenyl)methanone)(**5b**)

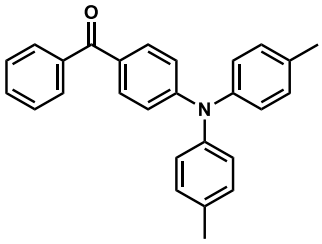

This reaction was conducted with di-*p*-tolylamine and the reaction condition was 40ºC/24 h. The title compound was isolated as a yellow oil in 91% yield. (4-(di-*p*-tolylamino)phenyl)(phenyl)methanone): (CAS No. 245442-58-4) ^{1}H NMR ($CDCl_3$): δ7.76 (d, *J* = 7.4 Hz, 2 H, *Benzoyl*), 7.68 (d, *J* = 8.9 Hz, 2 H, *Benzoyl*), 7.55 (t, *J* = 7.4 Hz, 1 H, *Benzoyl*), 7.46 (t, *J* = 7.3 Hz, 2 H, *Benzoyl*), 7.14 (d, *J* = 8.3 Hz, 4H, *tolyl*), 7.08 (d, *J* = 8.6 Hz, 4H, *tolyl*), 6.95 (d, *J* = 8.9 Hz, 2H, *Benzoyl*), 2.34 (s, 6H, -CH_3). ^{13}C NMR ($CDCl_3$): δ 195.2 (*C*=O), 152.3 (*Benzoyl*), 143.9 (*Tolyl*), 138.7 (*Benzoyl*), 134.6 (*Tolyl*), 132.0 (*Benzoyl*), 131.5 (*Benzoyl*), 130.3 (*Tolyl*), 129.6 (*Benzoyl*), 128.7 (*Benzoyl*), 128.1 (*Tolyl*), 126.2 (*Tolyl*), 118.3 (*Benzoyl*), 20.9 (-CH_3).

(4-(bis(4-methoxyphenyl)amino)phenyl)(phenyl)methanone(**5c**)

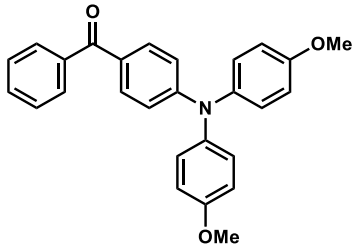

This reaction was conducted with bis(4-methoxyphenyl)amine and the reaction condition was 40°C/24 h. The title compound was isolated as a yellow oil in 91% yield. ^{1}H NMR ($CDCl_3$): δ 7.74 (d, *J* = 6.4 Hz, 2H, *Benzoyl*), 7.67 (d, *J* = 9.0 Hz, 2H, *Benzoyl*), 7.53 (t, *J* = 6.4 Hz, 1H, *Benzoyl*), 7.44 (t, *J* = 7.2 Hz, 2H, *Benzoyl*), 7.14 (d, *J* = 9.0 Hz, 4H, *Anisyl*), 6.88-6.84 (m, 6H), 3.81 (s, 6H, -*OMe*). ^{13}C NMR ($CDCl_3$): δ 195.1 (*C*=O), 157.1 (*Anisyl*), 152.8 (*Benzoyl*), 139.3 (*Anisyl*), 138.8 (*Benzoyl*), 132.1 (*Benzoyl*), 131.5 (*Benzoyl*), 129.6 (*Benzoyl*), 128.1 (*Benzoyl*), 127.9 (*Anisyl*), 116.7 (*Benzoyl*), 115.0 (*Anisyl*), 55.5 (-O*Me*). Elemental analysis calcd (%) for $C_{27}H_{23}NO_3$: C, 79.20; H, 5.66; N, 3.42; found: C, 78.96; H, 5.82; N, 3.26.

(4-((4-fluorophenyl)(phenyl)amino)phenyl)(phenyl)methanone(**5d**)

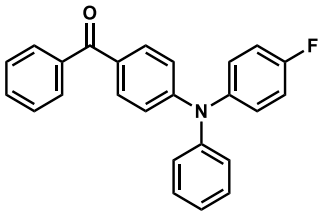

This reaction was conducted with 4-fluoro-N-phenylaniline and the reaction condition was 80ºC/48 h. The title compound was isolated as a yellow oil in 91% yield. ^{1}H NMR ($CDCl_3$): δ 7.77 (d, *J* = 7.0 Hz, 2H, *Benzoyl*), 7.72 (d, *J* = 8.8 Hz, 2H, *Benzoyl*), 7.55 (t, *J* = 7.4 Hz, 1H, *Benzoyl*), 7.46 (t, *J* = 6.8 Hz, 2H, *Ph*), 7.33 (t, *J* = 7.9 Hz, 2H, *Ph*), 7.19-7.12 (m, 5H), 7.04 (t, *J* = 8.6 Hz, 2H, *Ph*), 6.98 (d, *J* = 8.8 Hz , 2H, *Benzoyl*). ^{19}F NMR ($CDCl_3$): δ -116.93. ^{13}C NMR ($CDCl_3$): δ 195.1 (*C*=O), 161.1 (*Ph*, $^{1}J_{C\text{-}F}$ = 243.6 Hz), 151.9 (*Benzoyl*), 146.4 (*Ph*), 142.5 (*Ph*, $^{4}J_{C\text{-}F}$ = 3.1 Hz), 138.4 (*Benzoyl*), 132.0 (*Benzoyl*), 131.7 (*Benzoyl*), 129.7 (*Benzoyl*), 129.6 (*Ph*), 129.5 (*Benzoyl*), 128.1 (*Benzoyl*), 128.0 (*Ph,* $^{3}J_{C\text{-}F}$ = 8.2 Hz), 125.6 (*Benzoyl*), 124.7 (*Ph*), 119.0 (*Ph*), 116.7

(*Ph*, $^2J_{C\text{-}F}$ = 22.5 Hz). Elemental analysis calcd (%) for $C_{25}H_{18}FNO$: C, 81.72; H, 4.94; N, 3.81; found: C, 81.70; H, 5.01; N, 3.78.

(4-(naphthalen-1-yl(phenyl)amino)phenyl)(phenyl)methanone(**5e**)

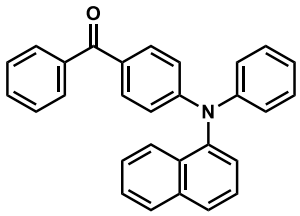

This reaction was conducted with N-phenylnaphthalen-1-amine and the reaction condition was 80ºC/48 h. The title compound was isolated as a yellow oil in 79% yield. ^{1}H NMR ($CDCl_3$): δ 7.90 (t, *J* = 8.0 Hz, 2H, *Benzoyl*), 7.81 (d, *J* = 8.4 Hz, 1H, *Napthyl*), 7.73 (d, *J* = 7.2 Hz, 2H, *Benzoyl*), 7.67 (d, *J* = 8.7 Hz, 2H, *Benzoyl*), 7.50-7.36 (m, 7H), 7.28-7.21 (m, 4H), 7.06 (t, *J* = 7.0 Hz, 1H, *Benzoyl*), 6.88 (d, *J* = 9.0 Hz , 2H, *Benzoyl*). ^{13}C NMR ($CDCl_3$): δ 195.1 (*C*=O), 152.3 (*Benzoyl*), 146.6 (*Ph*), 142.1 (*Naphthyl*), 138.5 (*Benzoyl*), 135.2 (*Naphthyl*), 132.1 (*Benzoyl*), 131.9 (*Benzoyl*), 131.5 (*Benzoyl*), 130.9 (*Benzoyl*), 129.5 (*Ph*), 129.4 (*Naphthyl*), 128.8 (*Naphthyl*), 128.5(*Ph*), 128.0 (*Naphthyl*), 127.5(*Ph*), 127.4 (*Naphthyl*), 126.8 (*Naphthyl*), 126.4 (*Naphthyl*), 126.3(*Ph*), 124.3 (*Benzoyl*), 124.1 (*Naphthyl*), 123.7 (*Naphthyl*), 117.7 (*Benzoyl*). Elemental analysis calcd (%) for $C_{29}H_{21}NO{\cdot}0.5H_2O$: C, 85.27; H, 5.43; N, 3.43; found: C, 85.20; H, 5.35; N, 3.14.

(4-(naphthalen-1-yl(p-tolyl)amino)phenyl)(phenyl)methanone(**5f**)

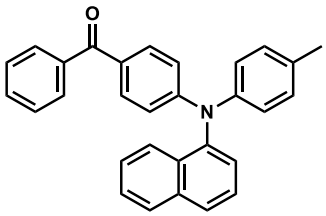

This reaction was conducted with N-(p-tolyl)naphthalen-1-amine and the reaction condition was 80ºC/48 h. The title compound was isolated as a yellow oil in 72% yield. ^{1}H NMR ($CDCl_3$): δ 7.91 (t, *J* = 7.3 Hz, 2H, *Benzoyl*), 7.82 (d, *J* = 7.7 Hz, 1H, *Naphthyl*), 7.73 (d, *J* = 8.2 Hz, 2H, *tolyl*), 7.65 (d, *J* = 9.5 Hz, 2H, *Benzoyl*), 7.53-7.47 (m, 3H), 7.44-7.37 (m, 4H), 7.15 (d, *J* = 8.6 Hz, 2H, *tolyl*), 7.10 (d, *J* = 8.2 Hz , 2H, *tolyl*), 6.81 (d, *J* = 8.6 Hz, 2H, *Benzoyl*), 2.31 (s, 3H, *tolyl*). ^{13}C NMR ($CDCl_3$): δ 195.4 (*C*=O), 152.7

(*Benzoyl*), 143.9 (*tolyl*), 142.3 (*Naphthyl*), 138.7 (*Benzoyl*), 135.3 (*tolyl*), 134.3 (*Naphthyl*), 132.2 (*Benzoyl*), 131.5 (*Benzoyl*), 131.0 (*Benzoyl*), 130.2 (*Benzoyl*), 129.6 (*tolyl*), 128.6 (*Naphthyl*), 128.4 (*Naphthyl*), 128.1 (*tolyl*), 127.4 (*Naphthyl*), 127.3 (*Naphthyl*), 126.8 (*Naphthyl*), 126.4 (*Naphthyl*), 124.8 (*Benzoyl*), 123.9 (*tolyl*), 117.1 (*Benzoyl*), 20.9 (-*C*H_3). Elemental analysis calcd (%) for $C_{30}H_{23}NO \cdot 0.3H_2O$: C, 85.89; H, 5.69; N, 3.34; found: C, 86.00; H, 5.55; N, 3.32.

Phenyl(4-(phenylamino)phenyl)methanone(**5g**)

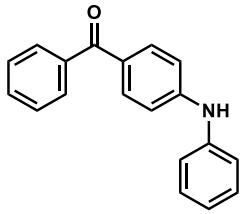

This reaction was conducted with aniline and the reaction condition was 60ºC/48 h. The title compound was isolated as a pale yellow solid in 96% yield. (CAS No. 4058-17-7) ^{1}H NMR ($CDCl_3$): δ 7.77 (dd, *J* = 6.7 Hz, 4H, *Benzoyl*), 7.55 (t, *J* = 7.5 Hz, 1H, *Benzoyl*), 7.47 (t, *J* = 7.4 Hz, 2H, *Benzoyl*), 7.35 (t, *J* = 7.9 Hz, 2H, *Ph*), 7.20 (d, *J* = 7.7 Hz, 2H, *Ph*), 7.09 (t, *J* = 7.4 Hz, 1H, *Ph*), 7.02 (d, *J* = 9.1 Hz, 2H, *Benzoyl*), 6.11 (brs, 1H, -N*H*). ^{13}C NMR ($CDCl_3$): δ 195.2 (*C*=O), 148.2 (*Benzoyl*), 140.6 (*Ph*), 138.7 (*Benzoyl*), 132.7 (*Benzoyl*), 131.6 (*Benzoyl*), 129.6 (*Benzoyl*), 129.5 (*Benzoyl*), 128.8 (*Benzoyl*), 128.1 (*Benzoyl*), 123.4 (*Ph*), 120.7 (*Ph*), 114.4 (*Benzoyl*).

(4-((3-fluorophenyl)amino)phenyl)(phenyl)methanone(**5h**)

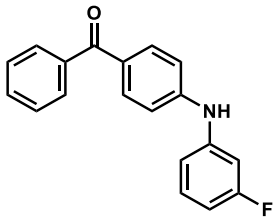

This reaction was conducted with aniline and the reaction condition was 60ºC/48 h. The title compound was isolated as a pale yellow solid in 94% yield. ^{1}H NMR ($CDCl_3$): δ 7.78 (m, 4H), 7.56 (t, *J* = 7.5 Hz, 1H, *Benzoyl*), 7.48 (t, *J* = 7.4 Hz, 2H *Benzoyl*), 7.27 (m, 1H), 7.07 (d, *J* = 7.7 Hz, 2H, *Benzoyl*), 6.93 (m, 2H), 6.74 (m, 1H) 6.22 (brs, 1H, -N*H*). ^{19}F NMR ($CDCl_3$): δ -111.54. ^{13}C NMR ($CDCl_3$): δ 195.2 (*C*=O), 164.8 (*Ph*, $^1J_{C-}$

$_F$ = 243.7 Hz), 147.0 (*Benzoyl*), 142.8 (*Ph*, $^3J_{C\text{-}F}$ = 10.7 Hz), 138.5 (*Benzoyl*), 132.6 (*Benzoyl*), 131.8 (*Benzoyl*), 130.7 (*Ph*, $^3J_{C\text{-}F}$ = 9.7 Hz), 129.6 (*Benzoyl*), 128.2 (*Benzoyl*), 115.3 (*Benzoyl*), 115.2 (*Ph*, $^4J_{C\text{-}F}$ = 2.8 Hz), 109.6 (*Ph*, $^2J_{C\text{-}F}$ = 24.4 Hz), 106.8 (*Ph*, $^2J_{C\text{-}F}$ = 21.1 Hz). Elemental analysis calcd (%) for $C_{19}H_{14}FNO$: C, 78.33; H, 4.84; N, 4.81; found: C, 78.08; H, 4.81; N, 4.75.

(4-morpholinophenyl)(phenyl)methanone(**5i**)

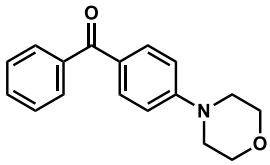

This reaction was conducted with aniline and the reaction condition was 80ºC/48 h. The title compound was isolated as a pale yellow solid in 61% yield. (CAS No. 24758-49-4) ^{1}H NMR ($CDCl_3$): δ 7.80 (d, *J* = 9.0 Hz, 2H, *Benzoyl*), 7.74 (d, *J* = 7.7 Hz, 2H, *Benzoyl*), 7.54 (t, *J* = 7.4 Hz, 1H, *Benzoyl*), 7.46 (t, *J* = 7.4 Hz, 2H, *Benzoyl*), 6.89 (d, *J* = 8.9 Hz, 2H, *Benzoyl*), 3.86 (t, *J* = 4.9 Hz, 4H, *Morpholyl*), 3.32 (t, *J* = 5.0 Hz, 4H, *Morpholyl*). ^{13}C NMR ($CDCl_3$): δ 195.2 (*C*=O), 154.0 (*Benzoyl*), 138.7 (*Benzoyl*), 132.4 (*Benzoyl*), 131.6 (*Benzoyl*), 129.6 (*Benzoyl*), 128.1 (*Benzoyl*), 127.8 (*Benzoyl*), 113.2 (*Benzoyl*), 66.6 (*Morpholyl*), 47.6 (*Morpholyl*).

S-3-4. Ni(I)/NHC catalyzed amination in the presence of nitrobenzene

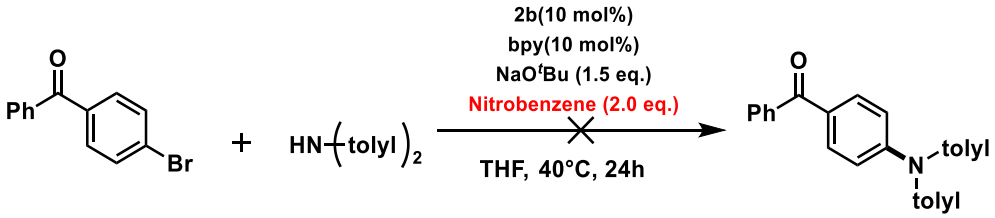

In a glovebox, a 20 mL Schlenk tube was charged with **2b** (34.0 mg, 0.05 mmol), 2,2'-bipyridyl (8.0 mg, 0.05 mmol), di(*p*-tolyl)amine (0.60 mmol), NaO^{t}Bu (71.1 mg, 0.75 mmol), 4-bromobenzophenone (130.6 mg, 0.50 mmol), nitrobenzene (51.2 μL, 1.0 mmol), and THF (0.2 mL). The reaction mixture was stirred at 40°C for 24 h. In ^{1}H NMR spectra of the crude mixture, the corresponding product, 4-N,N-di(p-tolyl)aminobenzophenone were not detected at all as shown in Figure S-3-4-1.

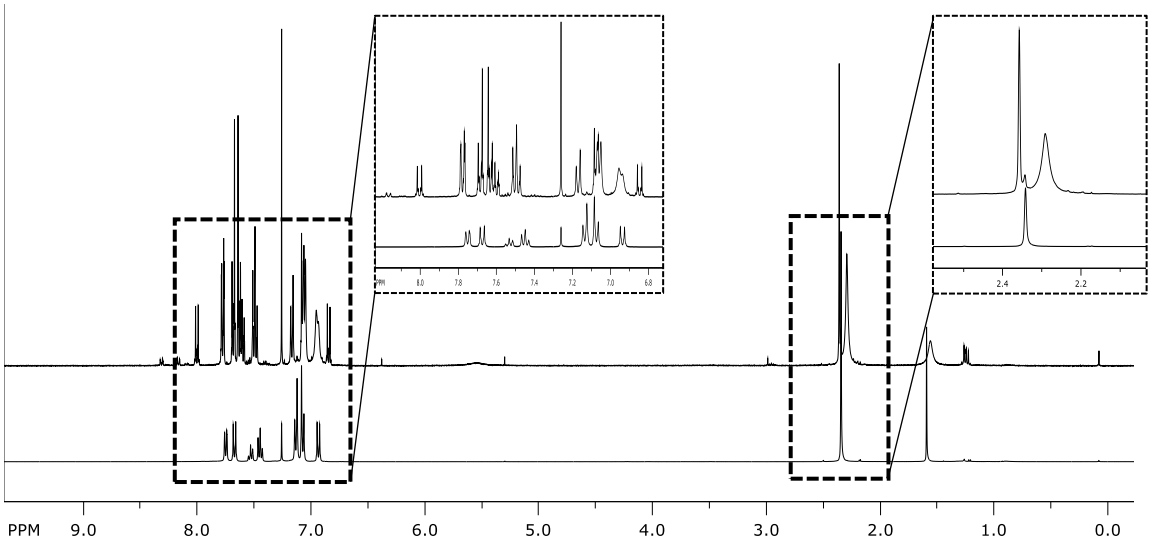

Figure S-3-4-1. ^{1}H NMR spectra of the crude mixture (top) and an authentic sample of 4-N,N-di(p-tolyl)aminobenzophenone (bottom).

S-3-5. [Ni(styrene)$_2$(IPr)] catalyzed amination with 4-bromobenzophenone

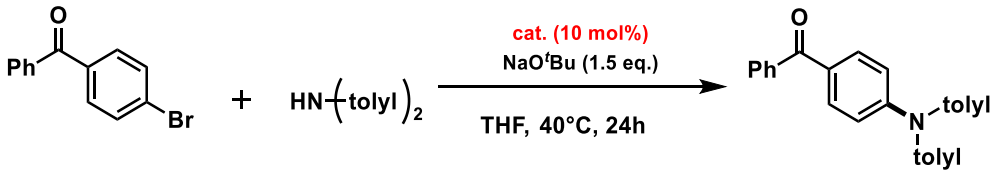

Catalyst: 2b 91%
: Ni(styrene)$_2$(IPr) 88%

In a glovebox, a 20 mL Schlenk tube was charged with **2b** (34.0 mg, 0.05 mmol) or Ni(0)(styrene)$_2$(IPr) (32.8 mg, 0.05 mmol), 2,2'-bipyridyl (8.0 mg, 0.05 mmol), di(*p*-tolyl)amine (0.60 mmol), NaO^{t}Bu (71.1 mg, 0.75 mmol), 4-bromobenzophenone (130.6 mg, 0.50 mmol), and THF (0.2 mL). The reaction mixture was stirred at 40°C for 24 h. After addition of water, the organic layer was extracted with AcOEt for three times. The combined organic layer was washed with brine and dried over Na_2SO_4, filtered and concentrated in vacuo. The residue was purified with silica-gel column chromatography eluted with dichloromethane/hexane (1/3) to obtain the corresponding product, 4-N,N-di(p-tolyl)aminobenzophenone as a yellow oil in 91% (by **2b**) or 88% yield (by Ni(0)).

The result suggested that the active key compound seems to be the same under these conditions with Ni(I) and Ni(0). However, the ^{1}H NMR spectra of both the crude mixtures

after the catalytic reaction in the presence of Ni(0) and Ni(I) complexes were completely different from each other (Figure S-3-5-1).

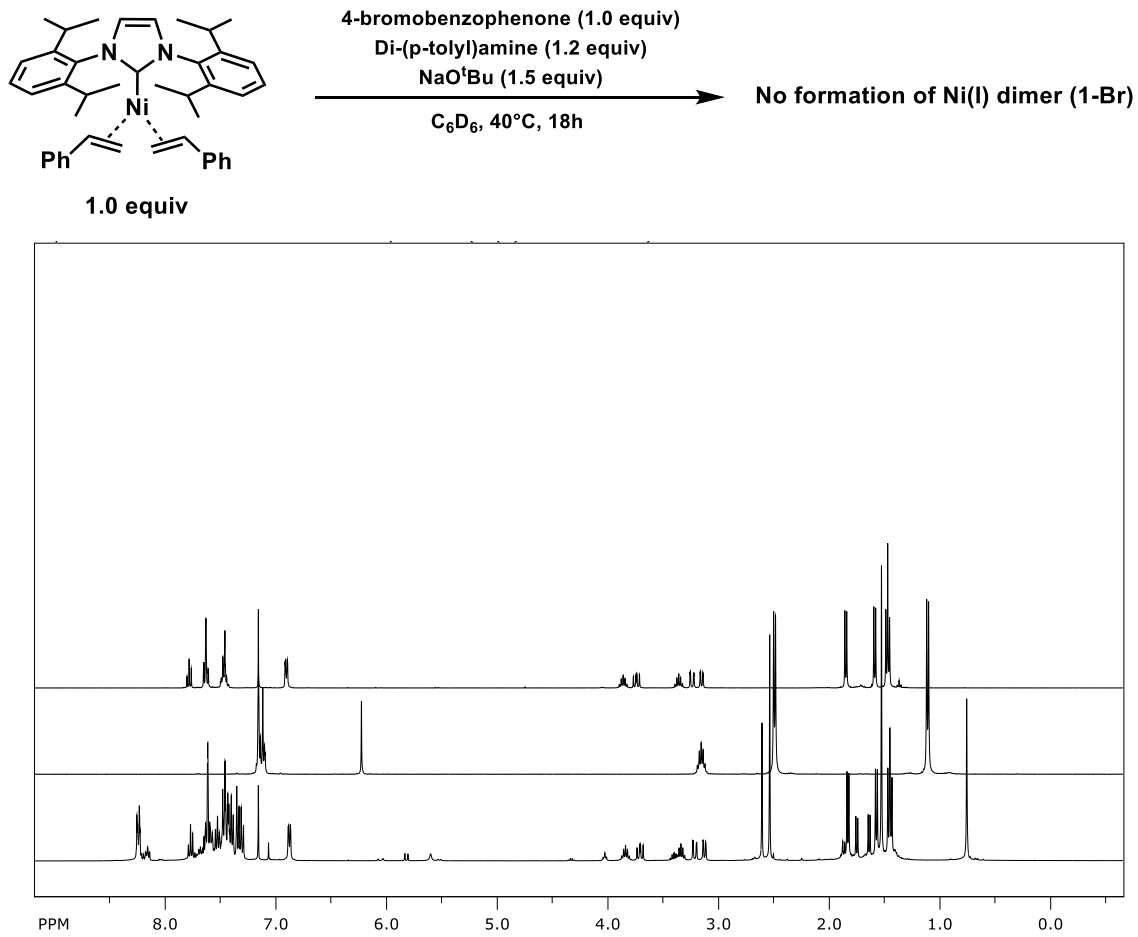

Figure S-3-5-1. Stacked ^{1}H NMR spectra of [Ni(styrene)$_2$(IPr)] (top), [Ni(μ-Br)(IPr)]$_2$ (midle), and reaction mixture (bottom)

S-3-6. Stoichiometric Reaction of Ni(I) complex 2a with diarylamines

In a glovebox, complex **2a** (100 mg, 0.16 mmol), diarylamine (0.16 mmol) and NaO^{t}Bu (34.0 mg, 0.35 mmol) were placed in a 20 mL Schlenk tube in THF (2 mL). The suspension was stirred for 1 hour at room temperature to give a dark purple solution. The volatiles were removed under reduced pressure, the residue was extracted into THF, filtered through celite and evaporated to dryness. The residue was washed with hexane to give **3a-c** as a black solid.

*Complex **3a***

The title compound was isolated as a black solid in 24% yield. Elemental analysis calcd (%) for $C_{49}H_{54}N_5Ni$: C, 76.27; H, 7.05; N, 9.08. Found: C, 69.18; H, 6.97; N, 8.44.

*Complex **3b***

The title compound was isolated as a black solid in 12% yield. Elemental analysis calcd (%) for $C_{51}H_{58}N_5Ni{\cdot}0.3THF$: C, 76.30; H, 7.42; N, 8.50. Found: C, 76.30; H, 7.44; N, 7.78.

*Complex **3c***

The title compound was isolated as a black solid in 5% yield. Elemental analysis calcd (%) for $C_{45}H_{50}N_5Ni$: C, 75.11; H, 7.00; N, 9.73. Found: C, 69.18; H, 6.97; N, 8.44.

S-3-7. Stoichiometric Reaction of Ni(I) complex 2a with diarylamines

In a glovebox, dimer **1-Cl** (50.0 mg, 0.052 mmol), diphenylamine (35.1 mg, 0.207 mmol), and NaO^{t}Bu (24.0 mg, 0.249 mmol) were placed in a 20 mL Schlenk tube in toluene (2 mL). The suspension was stirred for 10 minutes at room temperature to give a dark blue solution. The volatiles were removed under reduced pressure, the residue extracted into toluene and evaporated to dryness. The residue was washed with hexane to give 4 as a purple solid (53.2 mg, 83 % yield).Elemental analysis calcd. (%) for $C_{39}H_{46}N_3Ni{\cdot}Et_2O$: C, 74.89; H, 8.19; N, 6.09. Found: C, 74.63; H, 8.24; N, 6.54.

S-3-8. Stoichiometric Reaction of Ni(I) amide complexes (3a, 4) with 4-bromobenzophene

*Using complex **3a** as a substrate*

In a glovebox, a Schlenk tube was charged with **3a** (50 mg, 0.065 mmol), 2,2'-bipyridyl (51 mg, 0.33 mmol), 4-bromobenzophenone (17 mg, 0.065 mmol), and THF (1.0 mL). The reaction mixture was stirred at 40ºC for 24 h. After addition of water, the organic layer was extracted with CH_2Cl_2 for three times. The combined organic layer was washed with brine and dried over Na_2SO_4, and concentrated under reduced pressure. The residue was purified by column chromatography using silica gel eluted with CH_2Cl_2/hexane (1/3) to obtain corresponding triarylamine (16.3 mg, 0.047 mmol, 72 % yield).

*Using complex **4** as a substrate*

The complex **4** (30 mg, 0.049 mmol), 4-bromobenzophenone (13 mg, 0.049 mmol), and THF (0.2 mL) were treated, being similar to the above method to obtain the corresponding triarylamine (12.0 mg, 0.034 mmol, 70 % yield). By ^{1}H NMR analysis(Figure 3-8-1), we detected that dimer complex(**1-Br**) was regenerated.

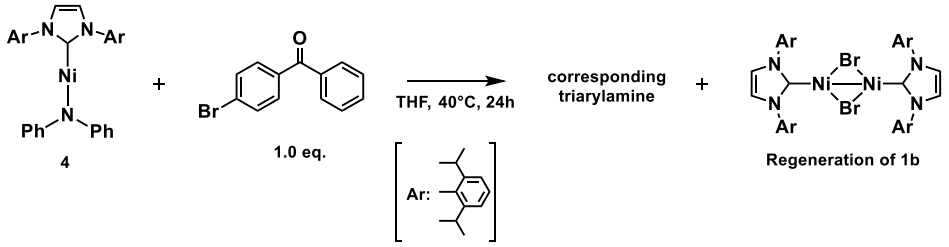

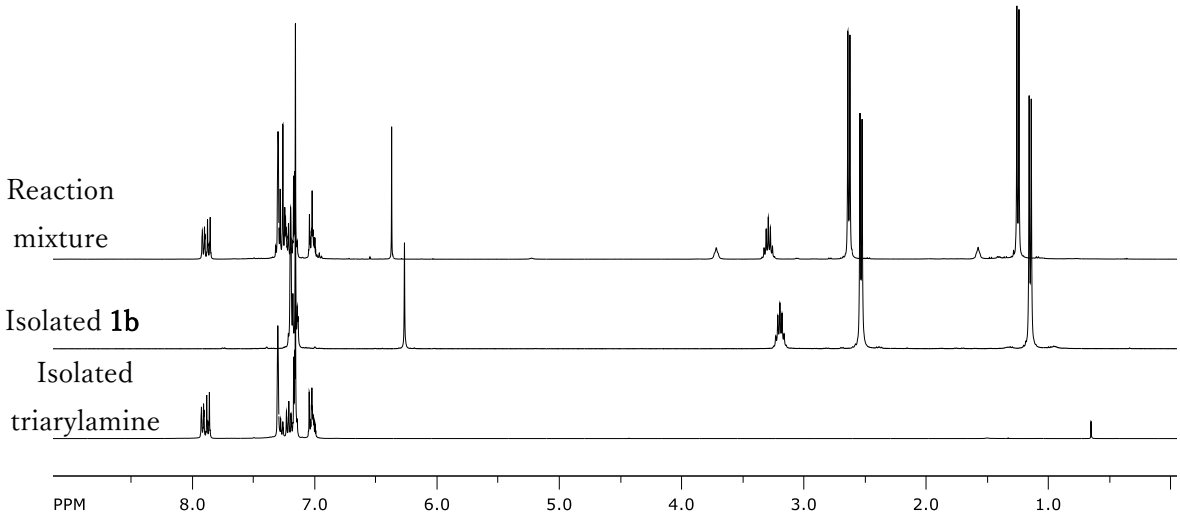

Figure S-3-8-1. Stacked ^{1}H NMR spectra (top: reaction mixture, middle: **1b**, bottom, Isolated triarylamine)

S-3-9. Catalytic Reaction of Diphenylamine with 4-Bromobenzophenone using 3a as catalysts.

*Using complex **3a** as a catalyst*

In a glovebox, a Schlenk tube was charged with **3a** (38.6 mg, 0.050 mmol), 4-bromobenzophenone (130.6 mg, 0.50 mmol), diphenylamine (101.5 mg, 0.60 mmol), 2,2'-bipyridyl (46.9 mg, 0.30 mmol), NaO^{t}Bu (71.1 mg, 0.74 mmol), and THF (0.2 mL). The reaction mixture was stirred at 40ºC for 24 h. After addition of water, the organic layer was extracted with CH_2Cl_2 for three times. The combined organic layer was washed with brine, dried over Na_2SO_4, and concentrated under reduced pressure. The residue was

purified by column chromatography using silica gel eluted with CH_2Cl_2/hexane (1/3) to obtain corresponding triarylamine (82.8 mg, 0.237 mmol, 47 % yield).

S-3-10. Ligand exchange reactions of 2a or 3a with 2,2'-biquinoline at room temperature.

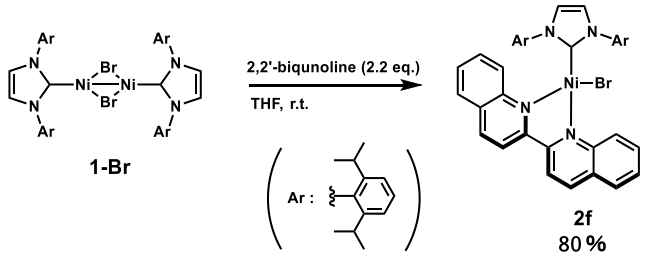

The Ni(I) complex **5** was prepared according to the similar method with a literature.[3] In a glove box, [(μ-Br)(IPr)Ni]$_2$ (**1-Br**) (80 mg, 0.076 mmol), 2,2'-biquinoline (42.8 mg, 0.167 mmol, 2.2 eq.), and THF (1.0 mL) were added to a Schlenk tube. After the compounds were dissolved, hexane (2.0 mL) was slowly added to the solution and cooled to -30ºC. The obtained dark-blue crystals of **2f** were washed with small amount of cold hexane and dried (95.1 mg, 80% yield). ^{1}H NMR (400 MHz, C_6D_6) (Figurer S-3-8-1): δ 14.34 (bs), 11.54 (bs), 6.55 (bs), 5.99 (bs), 1.72 (bs), -0.25 (bs). Elemental analysis calcd (%) for $C_{45}H_{48}BrN_4Ni$: C, 68.98; H, 6.18; N, 7.15. Found: C, 68.24; H, 6.32; N, 6.95.

Because the complex **2f** was pooly characterized, we observed EPR spectrum of **2f** in THF glass at 90 K, which was compared with that of **2b** (Figure S-3-10-1). Because these complexes have similar bidentate ligands, bipyridine and biquinoline, the spectra were also similar, as expeced.

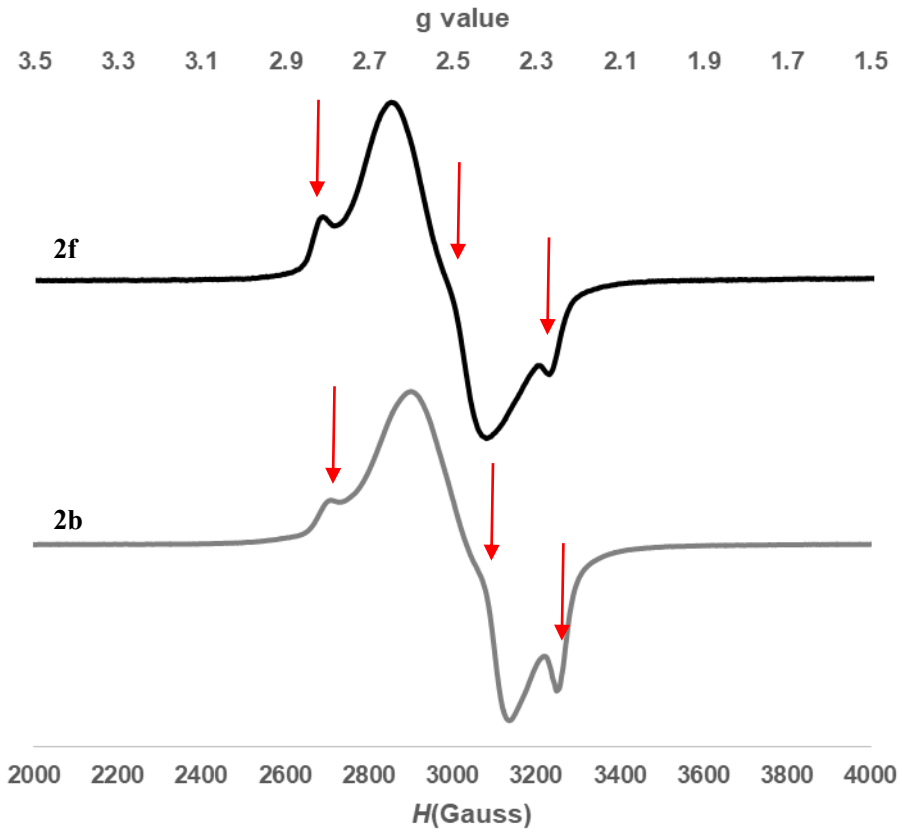

Figure S-3-10-1. EPR spectra of **2f** (top: $g_x = 2.505$, $g_y = 2.27$, $g_x = 2.085$) and **2b** (bottom: $g_x = 2.484$, $g_y = 2.229$, $g_x = 2.07$) in THF glass at 90 K (-183 °C).

Analysis via UV-Vis spectroscopy of the reaction of complex 2d with 2,2'-biquinoline to complex 5.

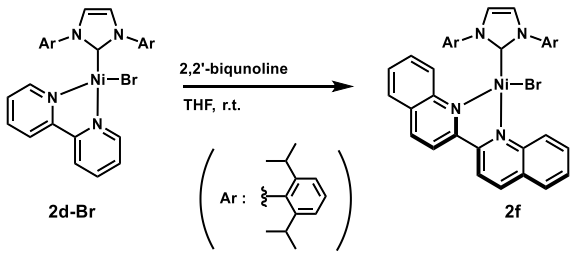

In a glove box, a quartz cell was charged with a solution of complex **2b** in THF (200 μM; 1.0 mL, 2.0 μM) and a solution of 2,2'-biquinoline in THF (200 μM; 1.0 mL, 2.0 μM).

S-3-11. Continuous wave X-band electron paramagnetic resonance (CW X-band EPR) spectroscopy.

CW X-band EPR spectrum was recorded on a Bruker EMX Plus spectrometer equipped with a continuous flow N_2 cryostat. The EPR spectrum was recorded under nonsaturating conditions using the microwave frequency of 9.414 GHz, field modulation of 100 kHz, modulation amplitude of 4 G, microwave power of 0.11 mW, respectively. The EPR spectrum was simulated with the PHI program[6], which is based on the following spin Hamiltonian of $S = 1/2$ system:

$$\hat{H}_{\text{spin}} = g\mu_{\text{B}}\vec{S}\vec{H}$$

where g is the g tensor, μ_{B} is the Bohr magneton, S is the electronic spin and H is the magnetic field.

The best simulation was reproduced by the superimposition of Ni(I) and Ni(III) species. The spin Hamiltonian parameters were determined to be as follows; $g_{x,y} = 2.098$ and $g_z = 2.530$, $W_{x,y} = 0.11$ and $W_z = 0.22$ GHz for Ni(I) species and $g_x = 2.560$, $g_y = 2.309$ and $g_z = 2.009$, $W_x = 0.25$, $W_y = 0.14$ and $W_z = 0.05$ GHz for Ni(III) species, where W is the linewidth.(Figure S-3-11-1) The integral ratios of these simulated spectra have also been determined as shown in Figure S-3-11-2.

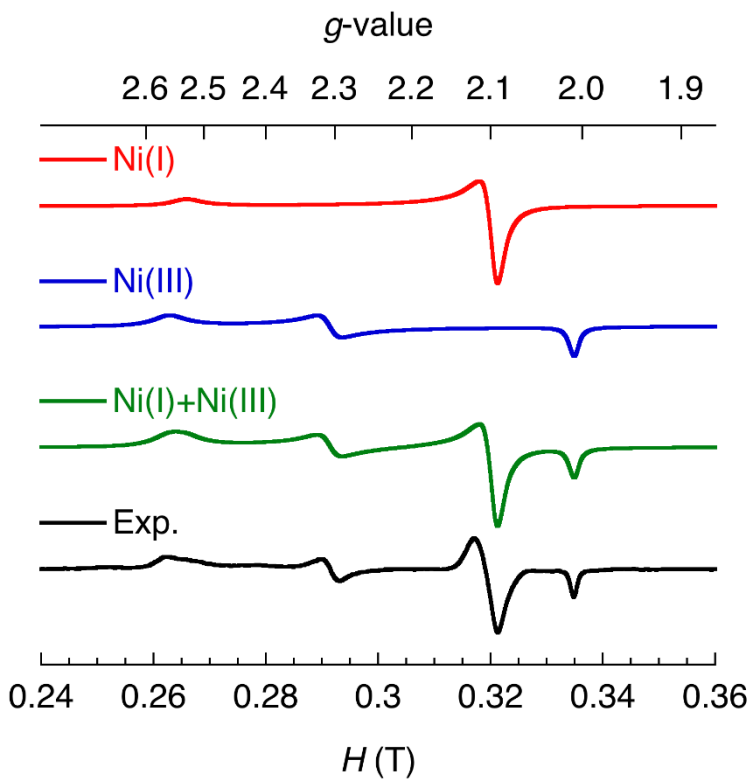

Figure S-3-11-1. X-band EPR spectrum for the reaction mixture of **4** with 1 equiv of 4-bromoanisole (THF glass, at –178ºC) (black), which can be reproduced by those indicated with computer simulation of proposed compounds, mononuclear Ni(I) intermediate (red, axial: $g_{x,y}$ = 2.098 and g_z = 2.530, $W_{x,y}$ = 0.11 and W_z = 0.22 GHz) and Ni(III) product (blue, rhombic: g_x = 2.560, g_y = 2.309 and g_z = 2.009, W_x = 0.25, W_y = 0.14 and W_z = 0.05 GHz) The green represents a data simulated to the two components simultaneously.

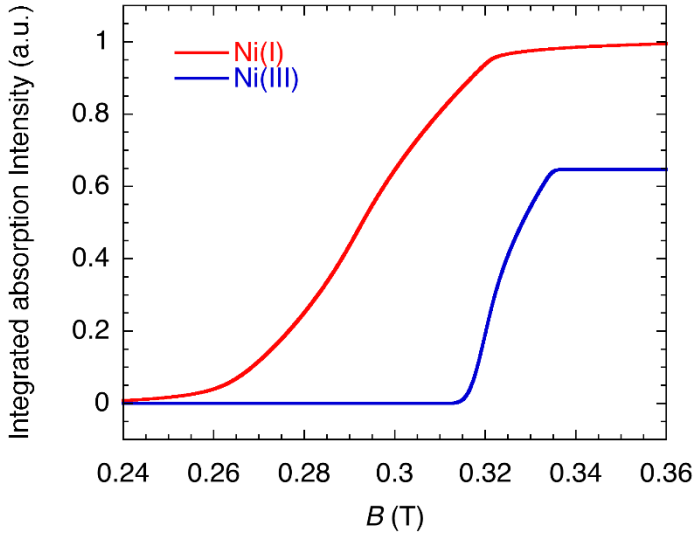

Figure S-3-11-2. Integrated absporption intensity vs. B(T), calculated using the simulated spectra of Ni(I) and Ni(III). It shows the ratio of the two compounds to some extent. Because the intensity of EPR varies to some extent according to the transition probability (Boltzmann distribution) at a certain temperature inherent in these Ni (I) and Ni (III) complexes, the integral ratio of the EPR signal is not necessarily the ratio of the amounts of these compounds.

S-3-12. Computational details.

All the calculations were performed using the GAUSSIAN 09 package.[7] The geometry optimization was performed using the density functional theory (DFT) without symmetry restriction. The subsequent harmonic vibrational analyses were carried out to confirm the nature of the stationary points, yielding no imaginary frequency for the minima.

The dissociation energy of **3a** to **4** with bpy was obtained using the dispersion-corrected B3LYP functional[9] with Becke–Johnson damping [8] (B3LYP-D3BJ) and applying the standard basis set of 6-31G(d,p) to all atoms (Figure S-3-12-1). We also corrected the basis set superposition error (BSSE) by a counterpoise method [9] for more accurate estimation.

For the EPR parameter calculation, more expensive basis sets were utilized because of sensitive dependence on basis set. The B3LYP functional and 6-31G(d) basis set for all atoms were applied in the full geometry optimization, and the single-point

calculation for *g* values at the obtained structure was performed with def2-TZVPP, which was reported to show the relatively good agreement with experimental data of Ni(I) complex.[8] In order to confirm the functional dependency, another famous functional, BP86, was also applied to the geometry optimization and sequential EPR parameter calculation with the basis set of 6-31G(d) and showed similar tendency with B3LYP one (Table S-3-12-1). Furthermore, complex stability of the possible candidates for reaction intermediate, i.e. Ni(III) complexes having square planar (SP) or pyramidal (Th) coordination was examined by estimation of Gibbs free energies at the condition of 298.15 K and 1 atm. In order to confirm the complex stability more accurately, the relative Gibbs free energies were calculated at B3LYP-D3BJ/6-31G(d,p) (Figure S-3-12-2).

All the computation was carried out using the computer facilities at Research Institute for Information Technology, Kyushu University.

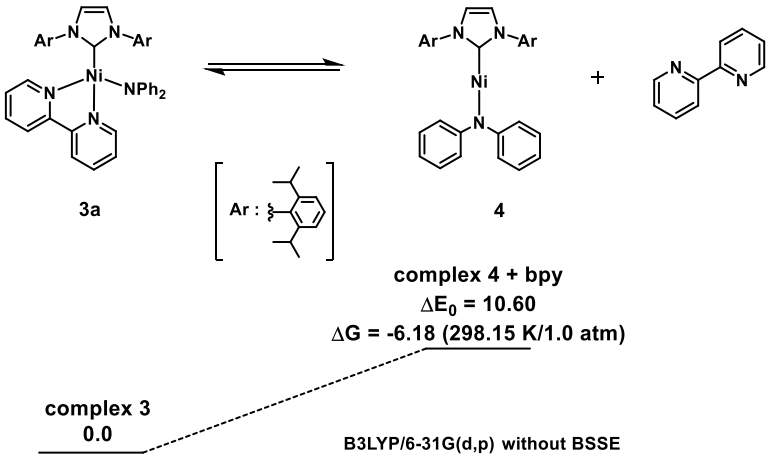

Figure S-3-12-1. Dissociative energy including ZPE correction (ΔE_0) and Gibbs energy (ΔG) in kcal/mol from **3a** to **4** with bpy calculated with B3LYP-D3BJ/6-31G(d,p) level, including BSSE correction.

Table S-3-12-1. Calculated g values ($g_1 > g_2 > g_3$) of complex **4** and its complexes coordinated by 4-bromoanisole reactant and THF solvent, and possible candidates for reaction intermediate, which are Ni(III) complexes having square planar (SP) or pyramidal (Th) coordination.

	B3LYP/def2-TZVPP[a]			BP86/6-31G		
	g_1	g_2	g_3	g_1	g_2	g_3
4	2.696	2.547	2.245	2.684	2.264	2.093
4-BrAn	2.614	2.517	2.191	2.224	2.199	2.089
4-THF	2.515	2.324	2.134	2.399	2.281	2.026
Ni(III)_SP (S = 1/2)	2.032	2.018	2.009	2.215	2.060	2.033
Ni(III)_Th (S = 1/2)	2.376	2.326	2.159	2.210	2.144	2.024
Ni(III)_SP (S = 3/2)	3.465	3.325	3.115	2.986	2.763	2.645

[a] Single point calculation at the structure optimized with B3LYP/6-31G.

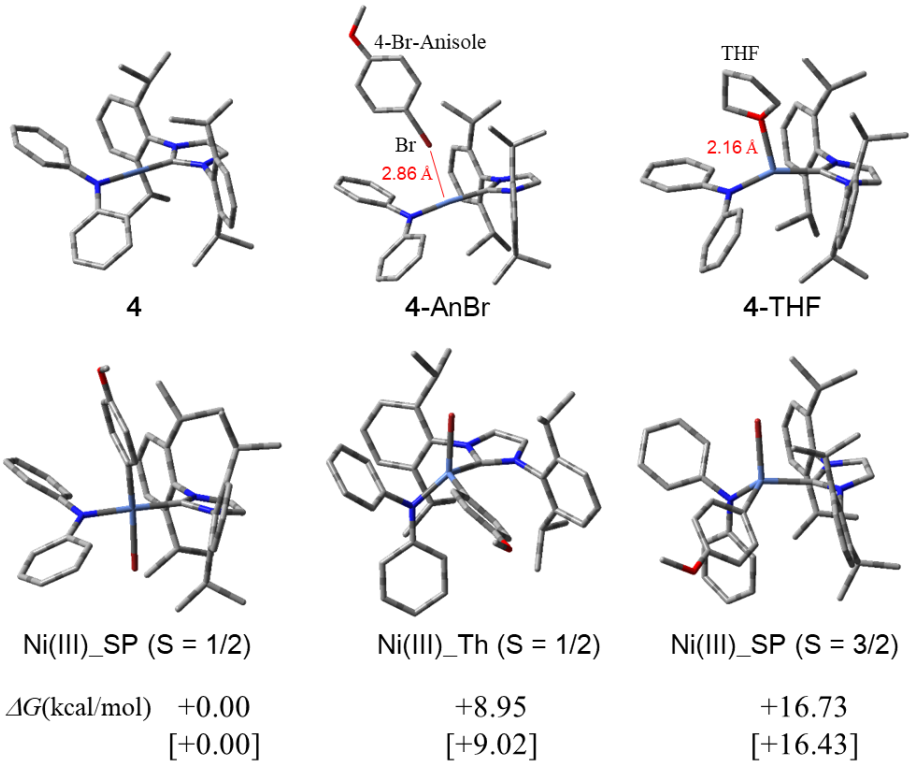

Figure S-3-12-2. Optimized structures of complex **4** and its complexes coordinated by 4-bromoanisole reactant and THF solvent, and possible candidates of Ni(III) for reaction intermediate calculated at B3LYP/6-31G(d) level. Relative Gibbs free energies (ΔG) were also estimated at the condition of 298.15 K and 1 atm. The values in brackets indicates the relative Gibbs free energies calculated at the B3LYP-D3BJ/6-31G(d) level.

S-3-11. References

1. (a) A. B. Holmes, T. Park *WO patent* 2002051958, (b) J. S. Kang, J. H. Park, S. W. Jun, Y. J. Shin, Y. M. Chang, N. C. Yang, J. K. Park, S. Lee *WO patent* 2015026053, (c) S. Heyne, M. Zoellner, S. Dorok, J. Wutke *US patent* 20150011795
2. A. J. Arduengo, III, R. Krafczyk, R Schmutzler *Tetrahedron* 55 1999, 14523.
3. a) B. R. Dible, M. S. Sigman, A. M. Arif, *Inorg. Chem*. 2005, *44*, 3774. b) C. A. Laskowski, D. J. Bungum, S. M. Baldwin, S. A. Del Ciello, V. M. Iluc, G. L. Hillhouse, *J. Am. Chem. Soc*. 2013, 135, 18272.
4. N. F. Chilton, R. P. Anderson, L. D. Turner, A. Soncini, K. S. Murray, *J. Comput. Chem*. 2013, *34*, 1164–1175.
5. K. Matsubara, Y. Fukahori, T. Inatomi, S. Tazaki, Y. Yamada, Y. Koga, S. Kanegawa, T. Nakamura, *Organometallics* 2016*, 35,* 3281.
6. M. J. Frisch, G. W. Trucks, H. B. Schlegel, et al. Gaussian 09, Revision D.01; Gaussian, Inc.: Wallingford CT, 2013.
7. S. Grimme, J. Antony, S. Ehrlich and H. Krieg, *J. Chem. Phys.* **2010**, *132*, 154104.
8. S. Grimme, S. Ehrlich and L. Goerigk, *J. Comp. Chem.* **2011**, *32*, 1456-65.
9. S. Simon, M. Duran, and J. J. Dannenberg, *J. Chem. Phys.* **1996**, *105*, 11024-31.

S-3-12. NMR Spectra

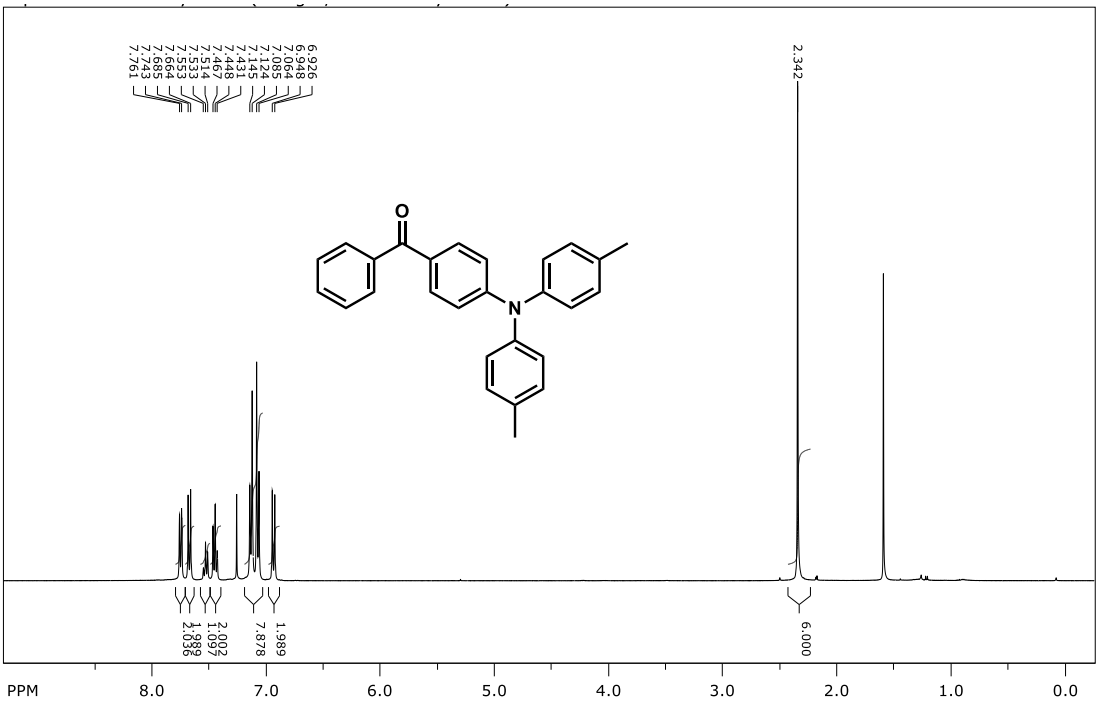

Figure S-3-3-1. ^{1}H NMR spectra for **5b** (400 MHz, $CDCl_3$)

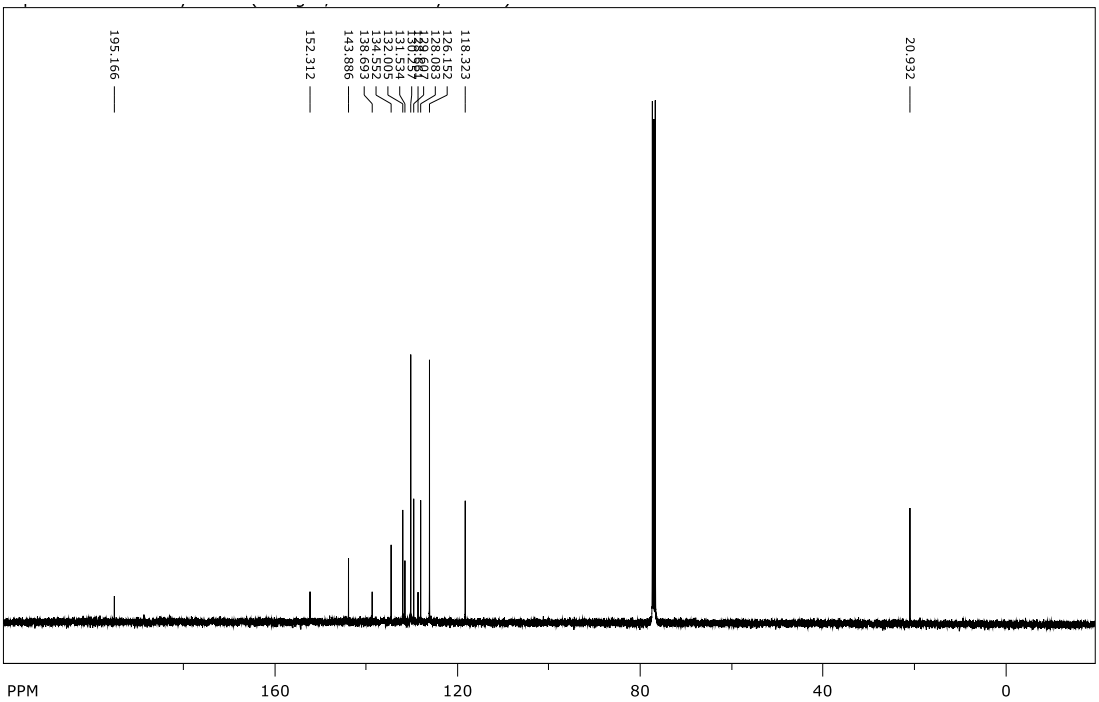

Figure S-3-3-2. ^{1}H NMR spectra for **5b** (400 MHz, $CDCl_3$)

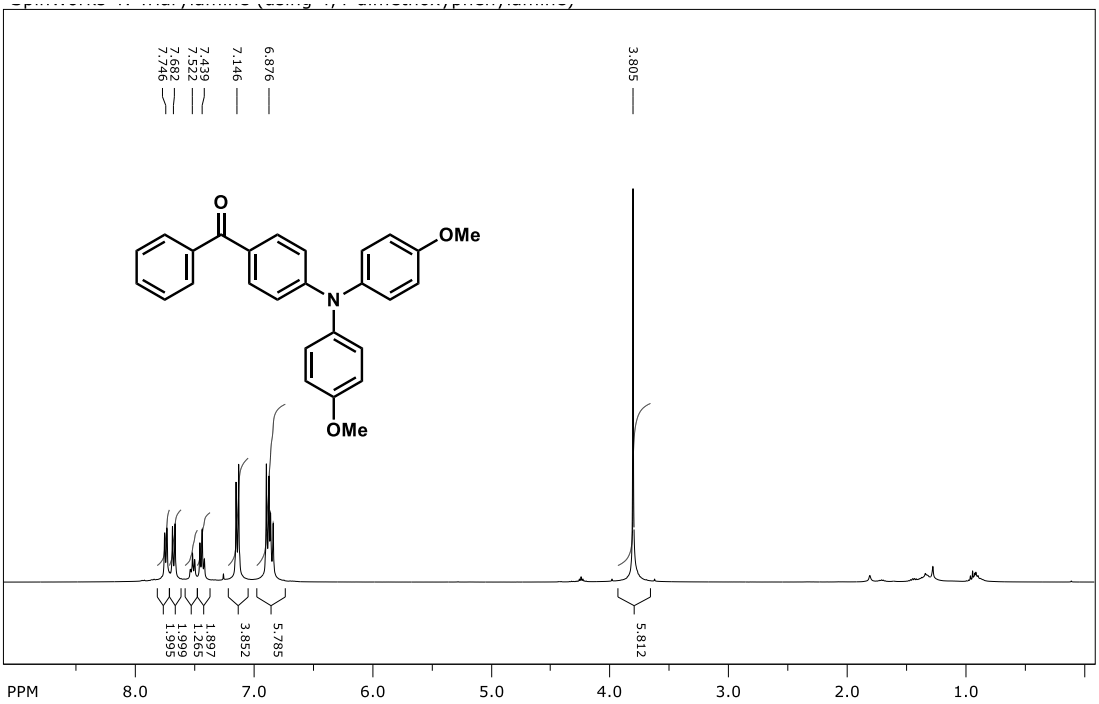

Figure S-3-3-3. ^{1}H NMR spectra for **5c** (400 MHz, $CDCl_3$)

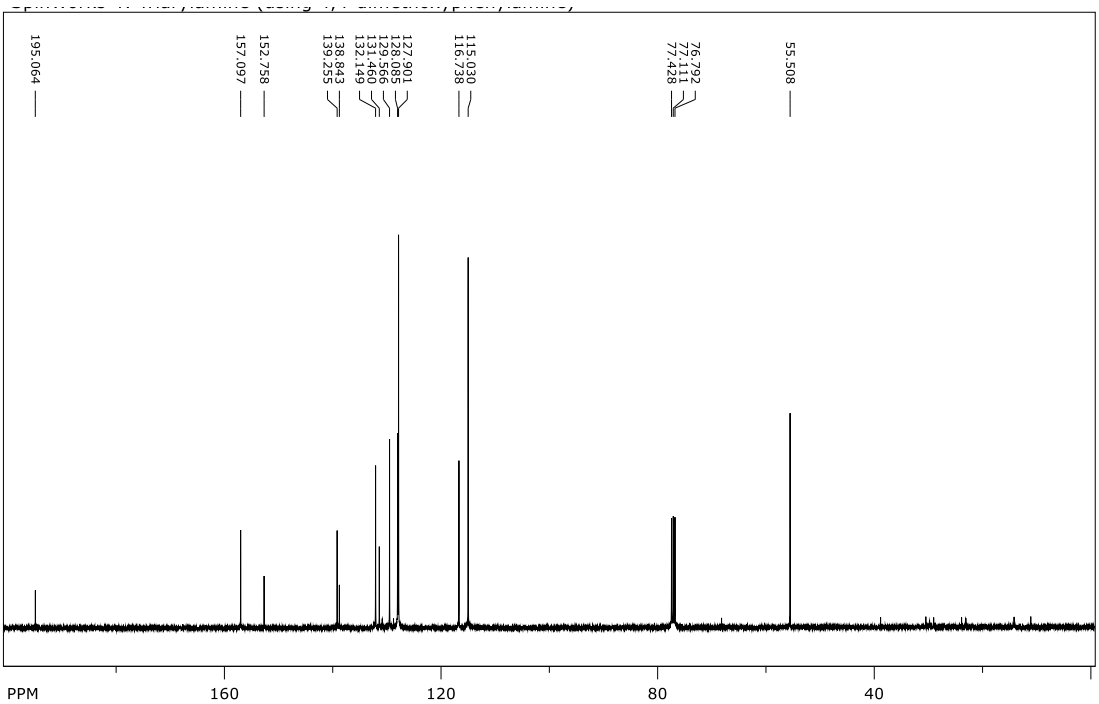

Figure S-3-3-4. ^{1}H NMR spectra for **5c** (400 MHz, $CDCl_3$)

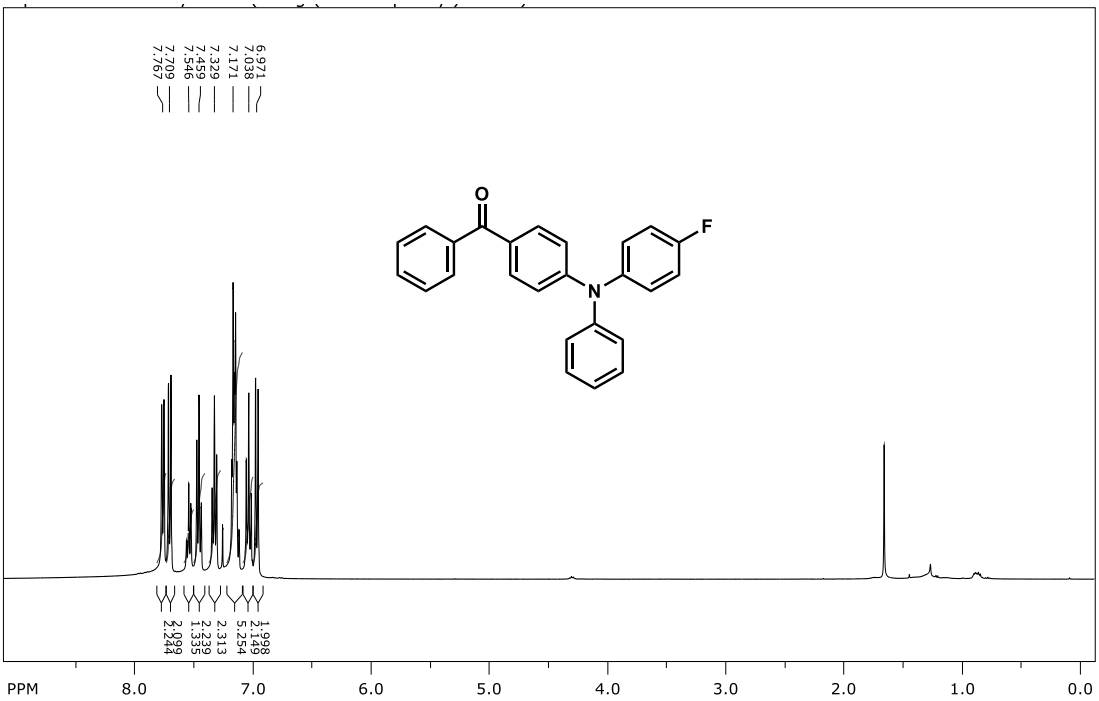

Figure S-3-3-5. ^{1}H NMR spectra for **5d** (400 MHz, $CDCl_3$)

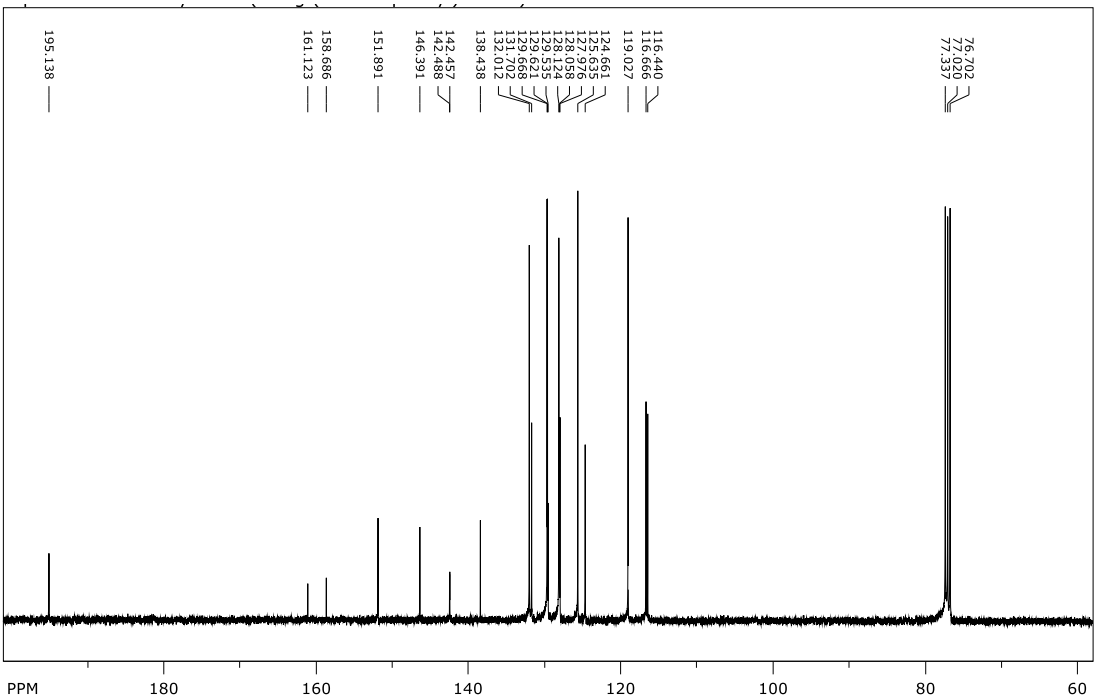

Figure S-3-3-6. ^{1}H NMR spectra for **5d** (400 MHz, $CDCl_3$)

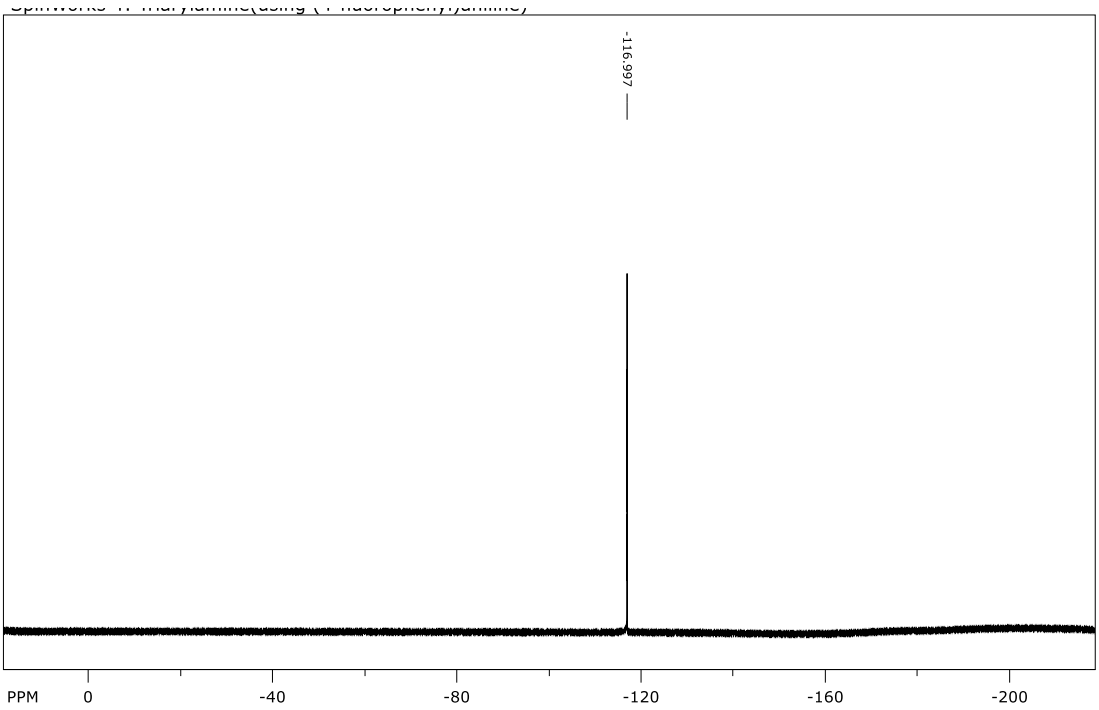

Figure S-3-3-7. ^{1}H NMR spectra for **5d** (400 MHz, $CDCl_3$)

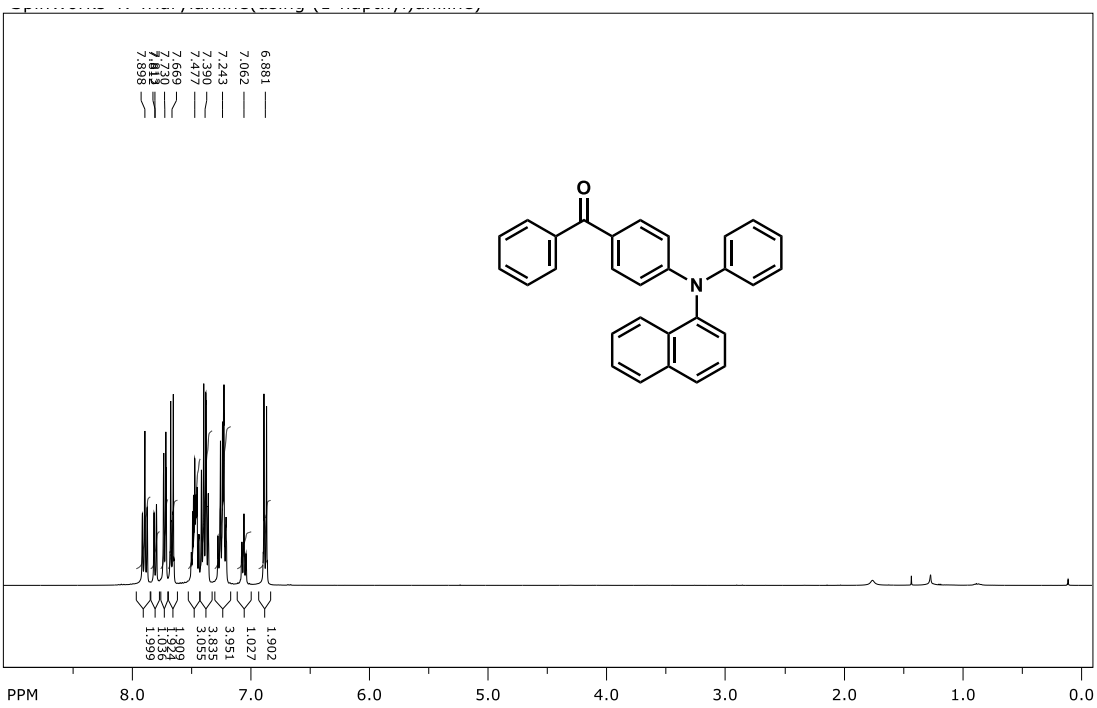

Figure S-3-3-8. ^{1}H NMR spectra for **5e** (400 MHz, $CDCl_3$)

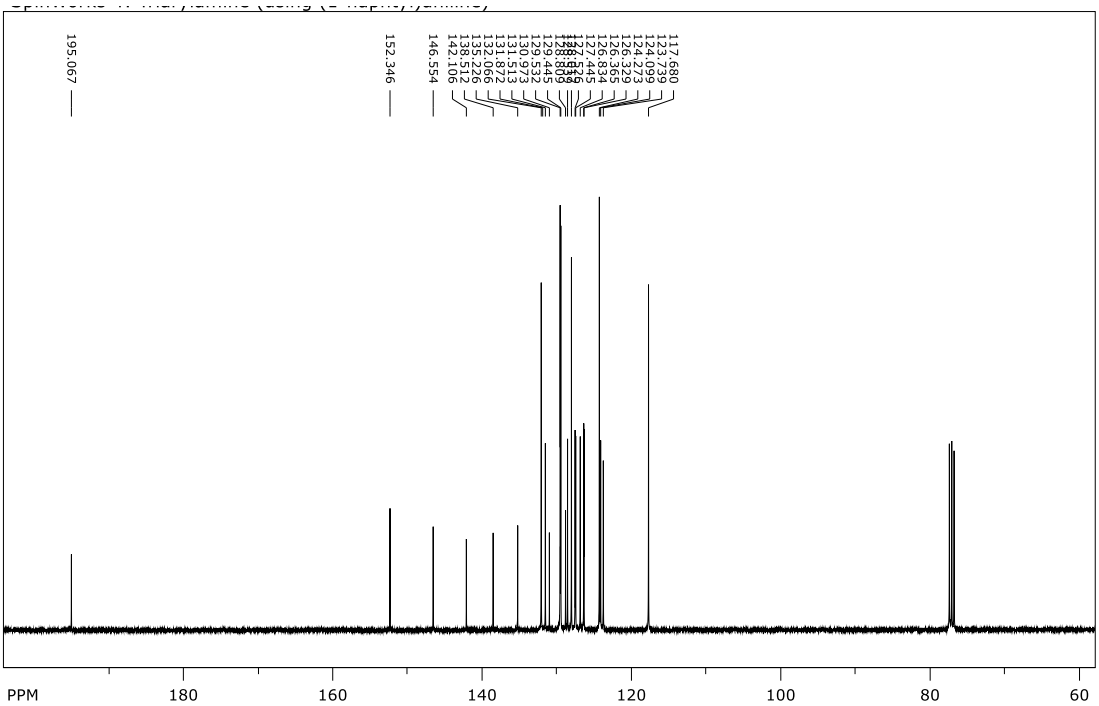

Figure S-3-3-9. ^{1}H NMR spectra for **5e** (400 MHz, $CDCl_3$)

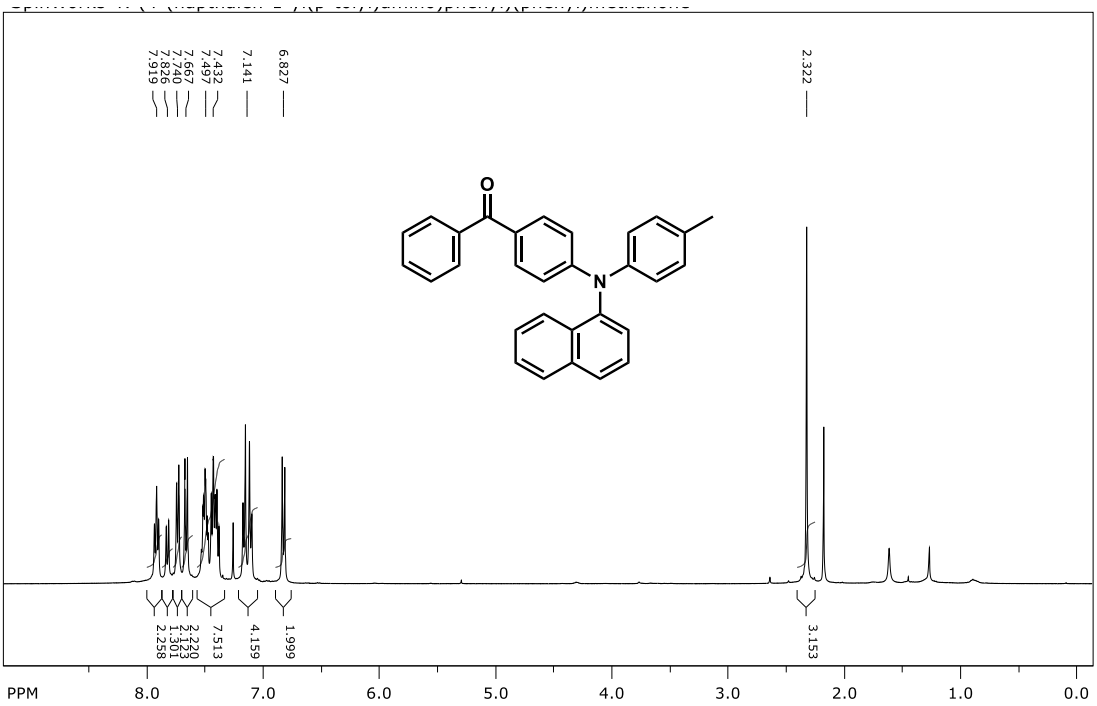

Figure S-3-3-10. ^{1}H NMR spectra for **5f** (400 MHz, $CDCl_3$)

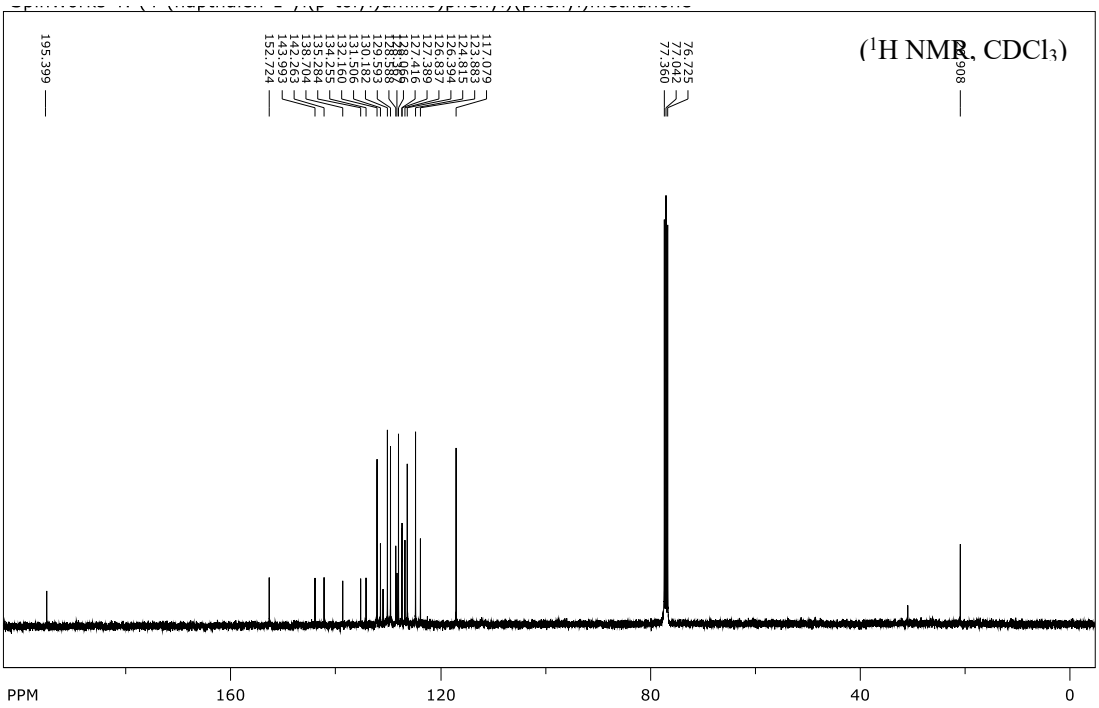

Figure S-3-3-11. ^{1}H NMR spectra for **5f** (400 MHz, $CDCl_3$)

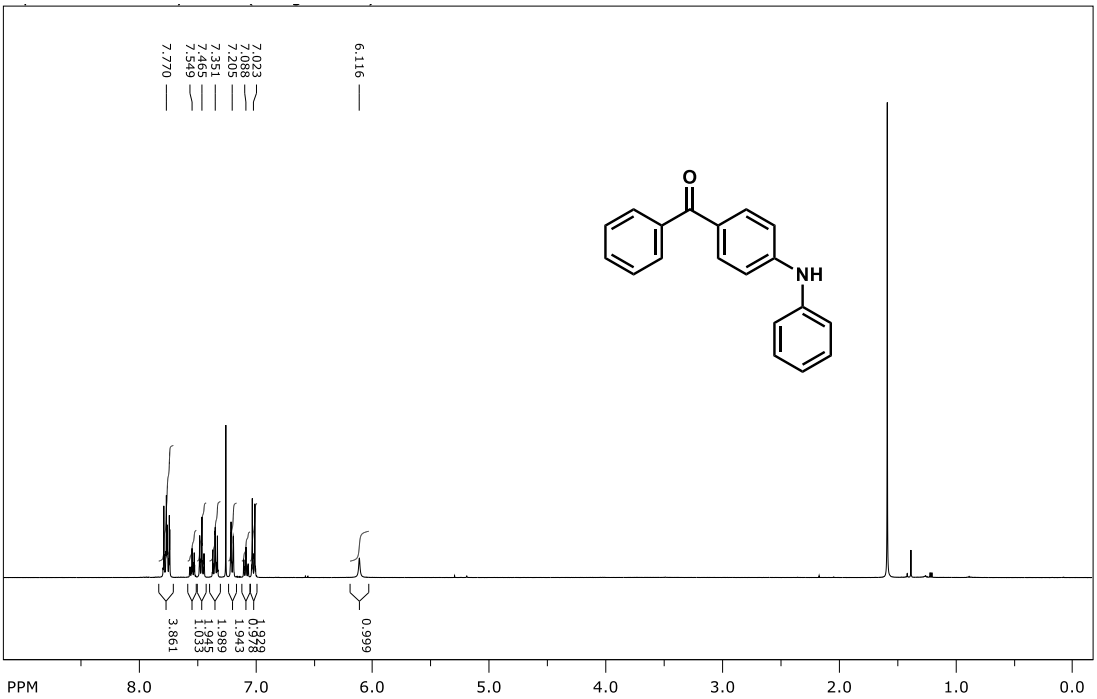

Figure S-3-3-12. ^{1}H NMR spectra for **5g** (400 MHz, $CDCl_3$)

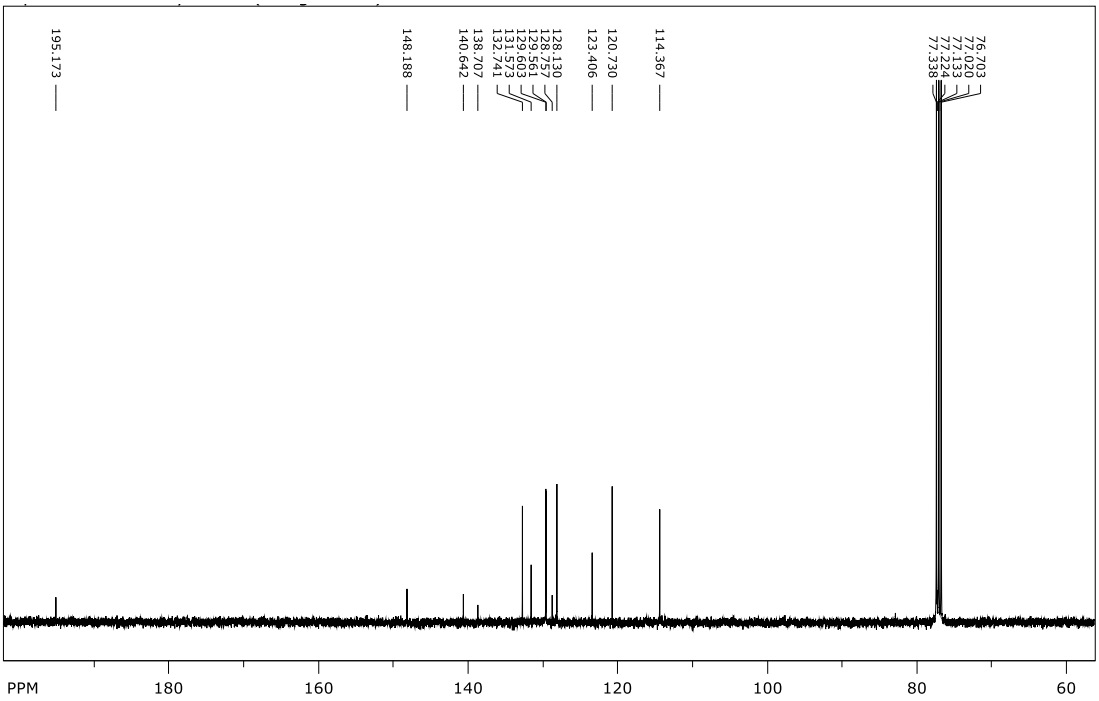

Figure S-3-3-13. ^{1}H NMR spectra for **5g** (400 MHz, $CDCl_3$)

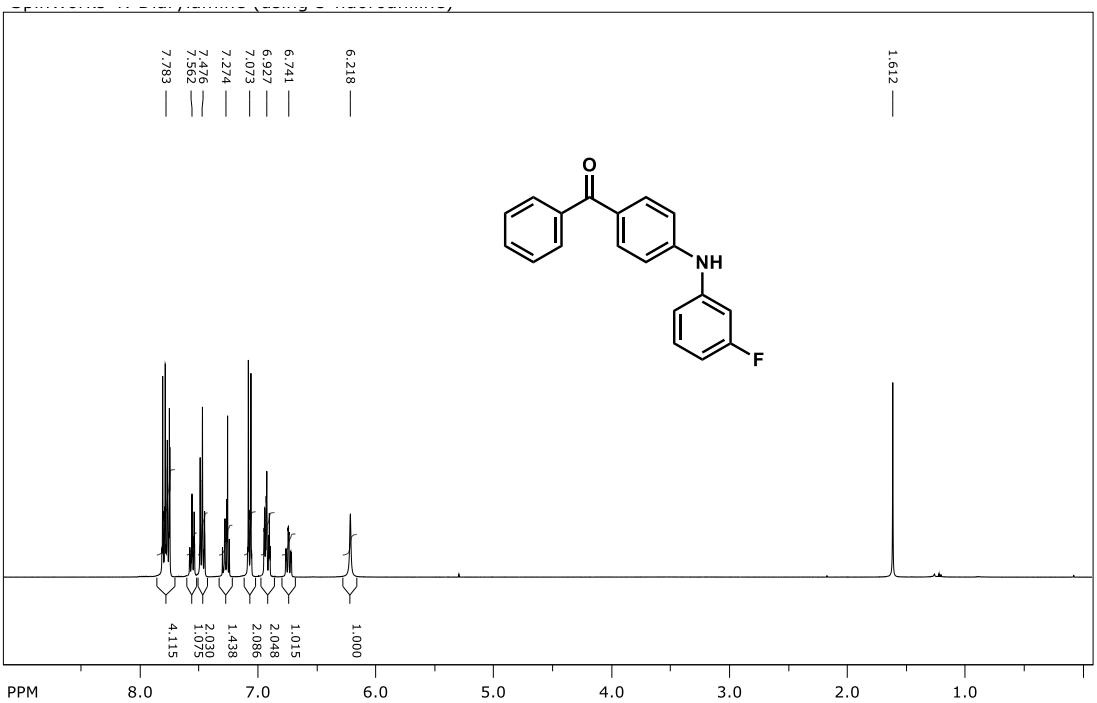

Figure S-3-3-14. ^{1}H NMR spectra for **5h** (400 MHz, $CDCl_3$)

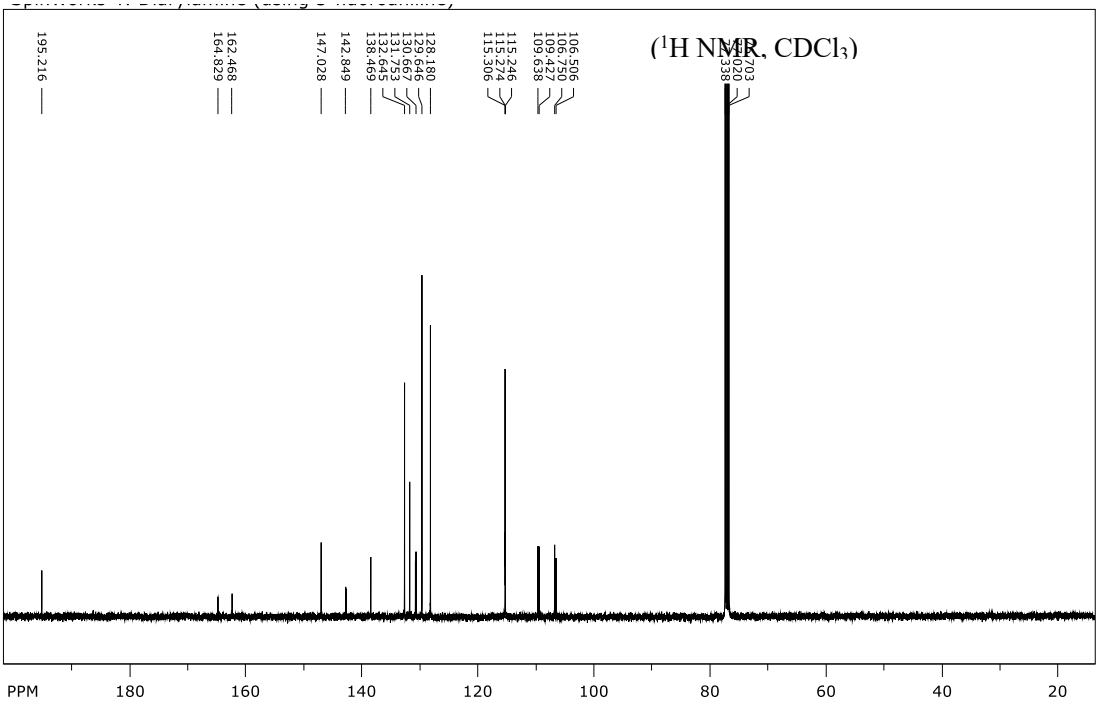

Figure S-3-3-15. ^{1}H NMR spectra for **5h** (400 MHz, $CDCl_3$)

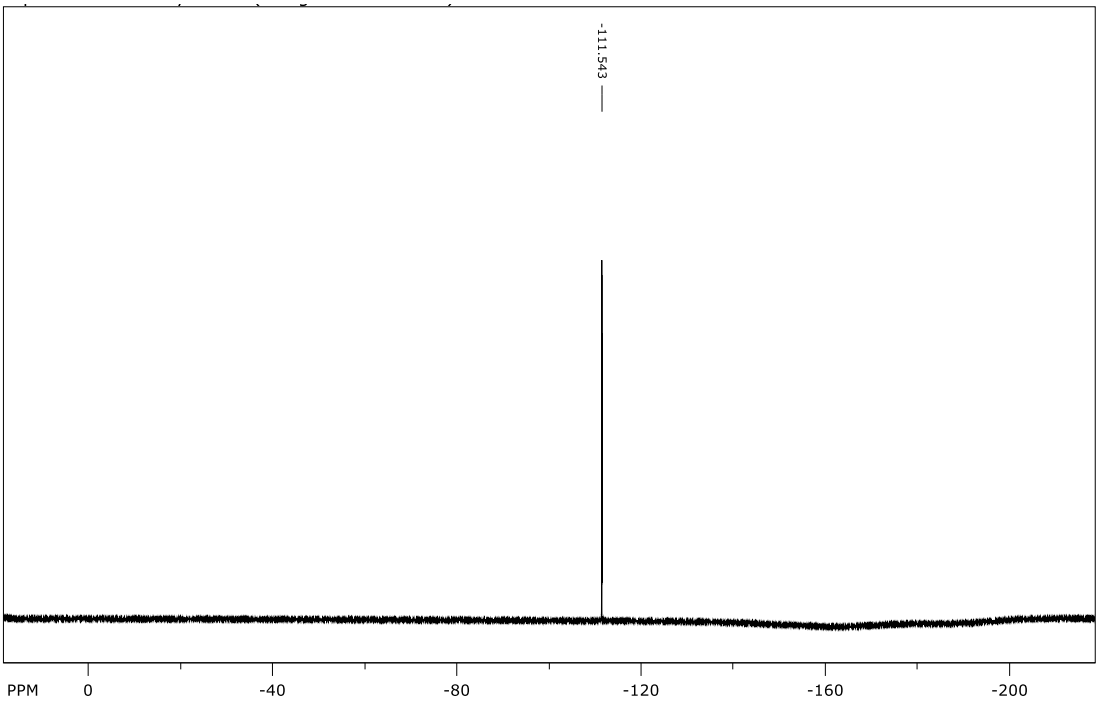

Figure S-3-3-16. ^{1}H NMR spectra for **5h** (400 MHz, $CDCl_3$)

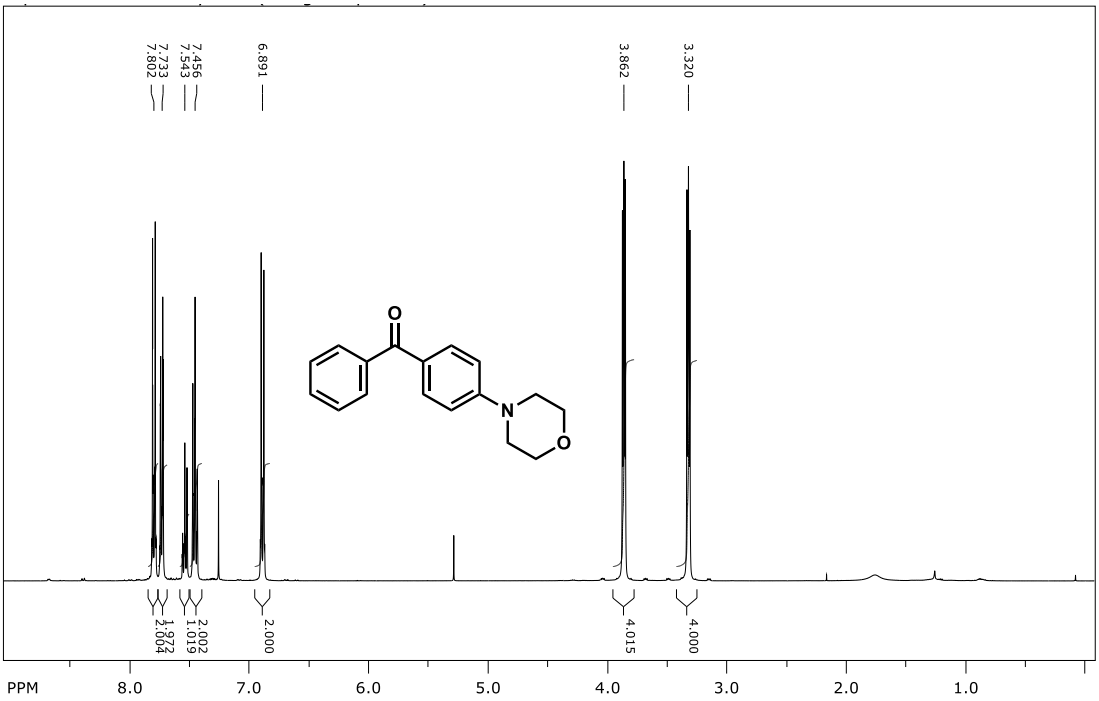

Figure S-3-3-17. ^{1}H NMR spectra for **5i** (400 MHz, $CDCl_3$)

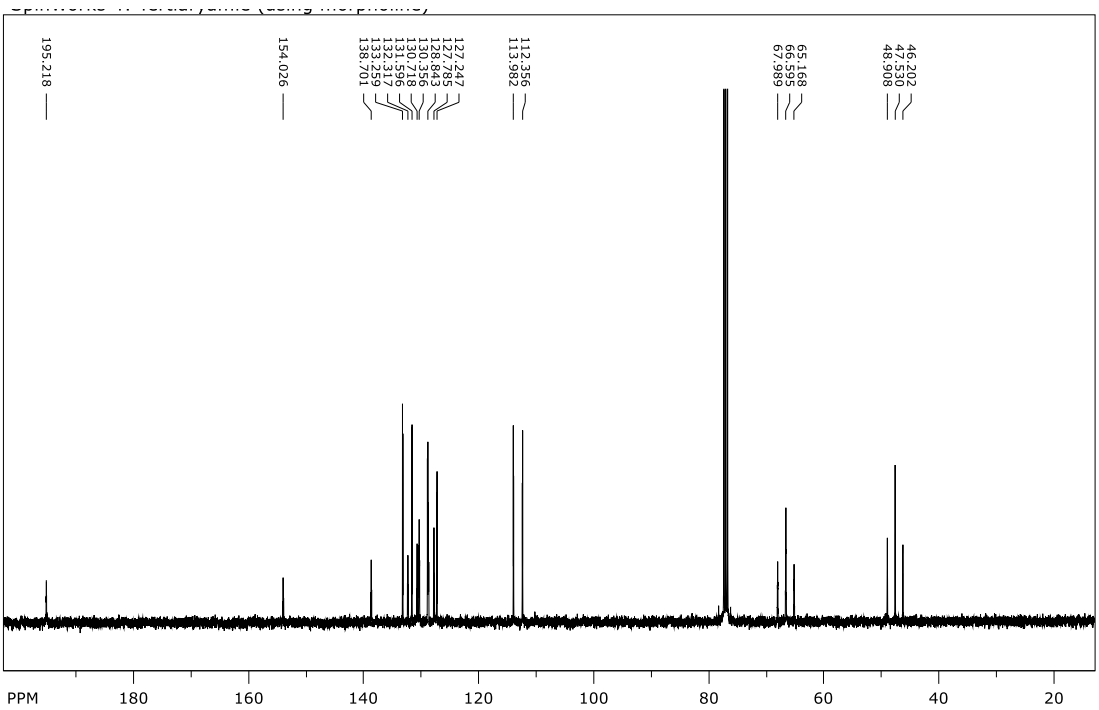

Figure S-3-3-18. ^{1}H NMR spectra for **5i** (400 MHz, $CDCl_3$)

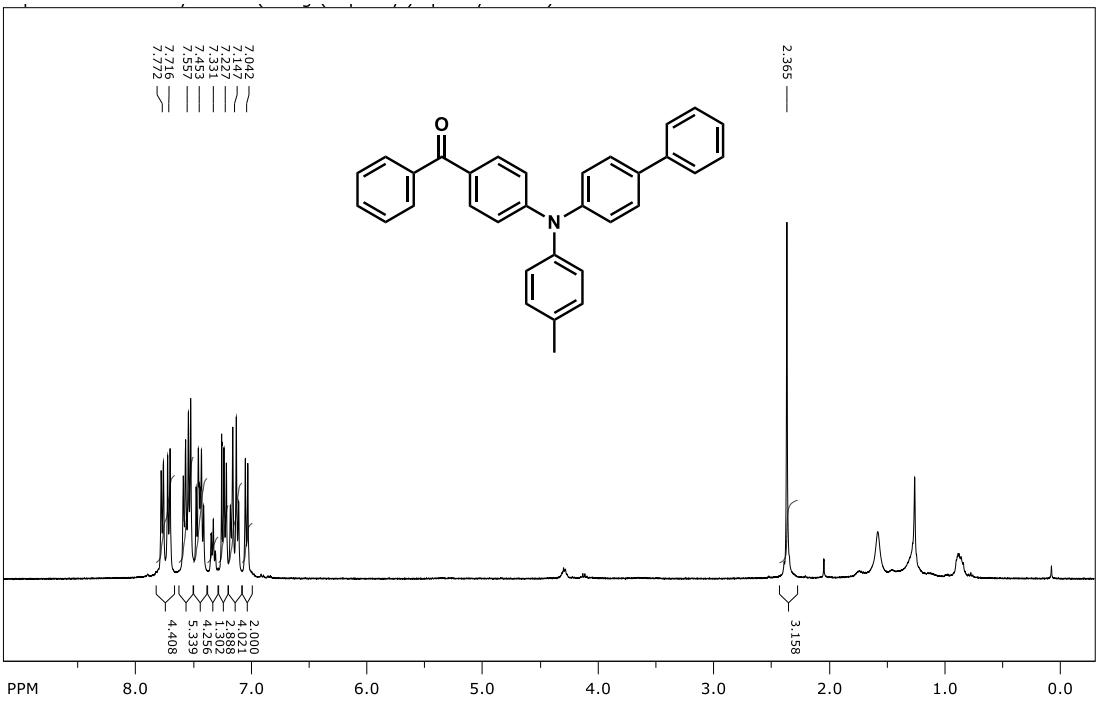

Figure S-3-3-19. ^{1}H NMR spectra for 5a (400 MHz, $CDCl_3$)

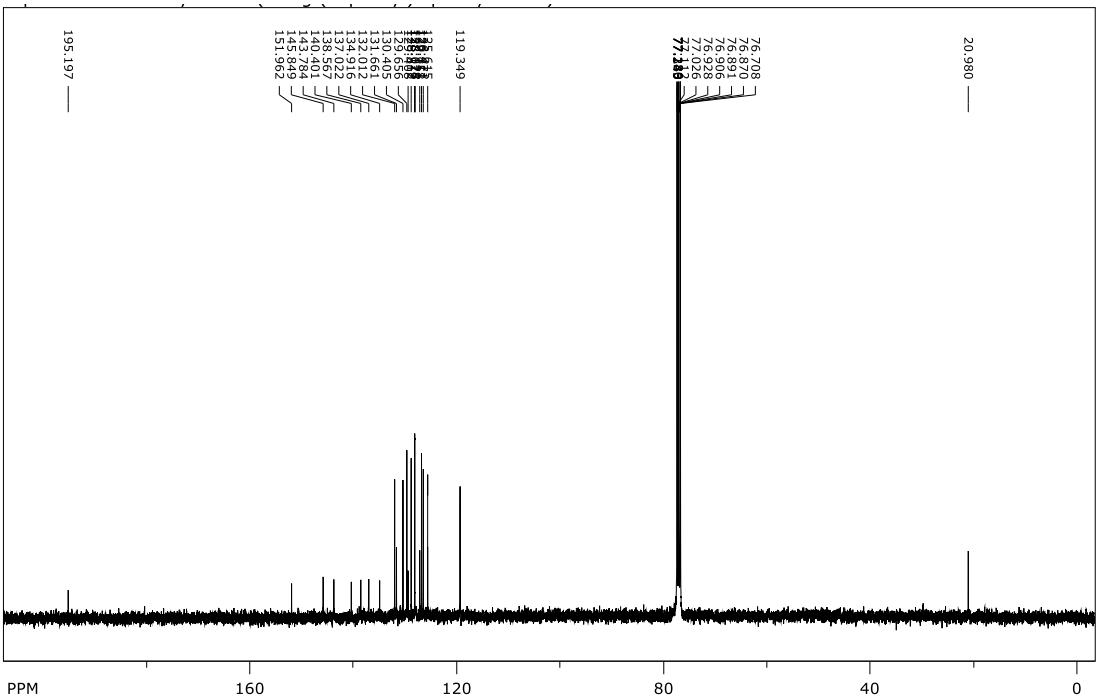

Figure S-3-3-20. ^{1}H NMR spectra for 5a (400 MHz, $CDCl_3$)

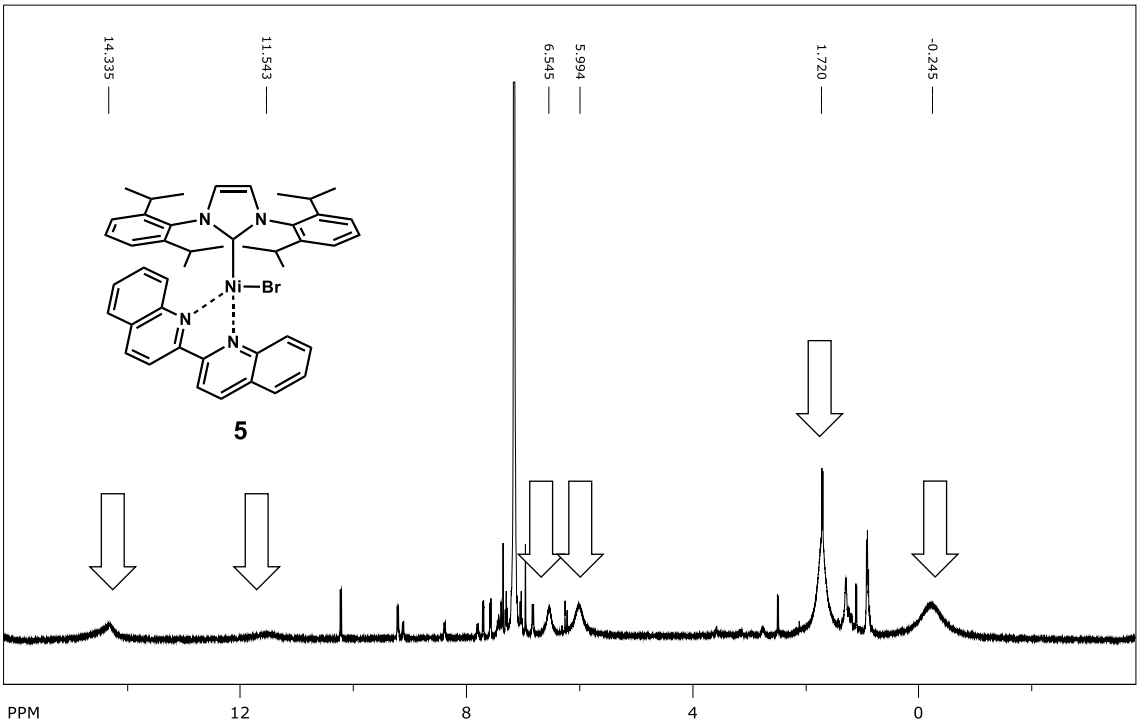

Figure S-3-8-1. ^{1}H NMR spectra for **2f** (400 MHz, C_6D_6)

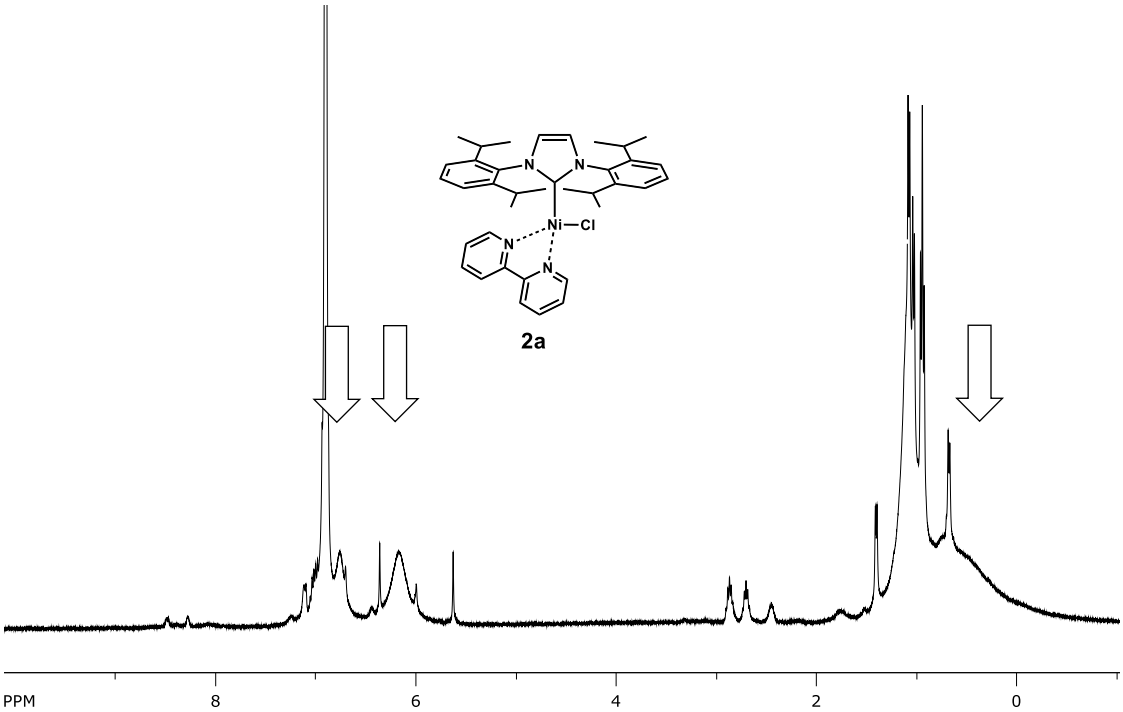

Figure S-3-2-1. ^{1}H NMR spectra for **2a** (400 MHz, C_6D_6)

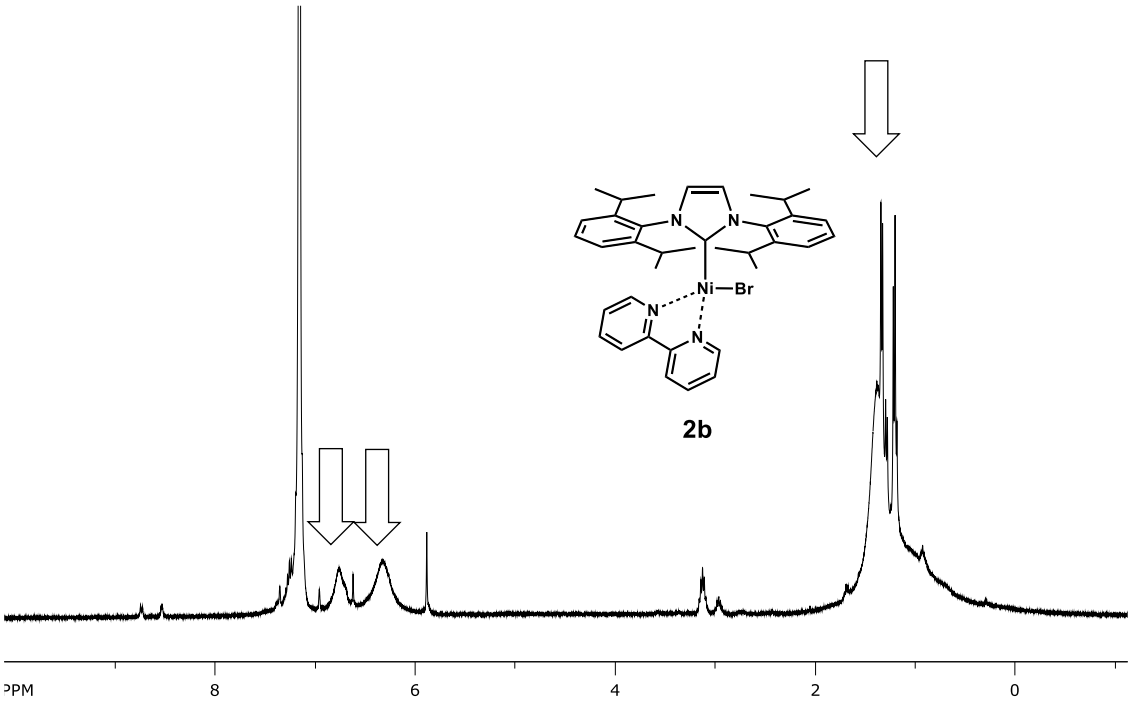

Figure S-3-2-2. ^{1}H NMR spectra for **2b** (400 MHz, C_6D_6)

Chapter 7
Acknowledgments

I would like to thank Prof. Kouki Matsubara for guidance and Prof. Osamu Hayasida, Assistant Prof. Yuji Koga, Assistant Prof. Shuhei Kusano(Current Position; RIKEN Center for Sustainable Resource Science), Assistant Prof. Setsuko Ando for valuable discussions. I appreciate the help received from Assistant Prof. Shinji Kanegawa(Institute for Advanced Materials Chemistry and Engineering, Kyushu University) with SQUID measurement, Assistant Prof. Ryuta Ishikawa with EPR measurement and Assistant Prof. Yuji Yamada with several DFT calculations. I also express thanks to Prof. Kentaro Okuma, Prof. Satoshi Kawata, Assistant Prof. Noriyoshi Nagahora for their continuous interest and encouragement. I am indebted to Yuki P laboratory member. Especially, I gratefully acknowledge the work of past and present members of our laboratory. (Especially, Ms. Hitomi Yamamoto, Ms. Yukino Fukahori, Ms. Haruka Iwasaki, Mr Keita Nonaka, Ms. Saeko Tazaki, Mr. Takahiro Fujii, Mr. Rion Hosokawa) Finally, I appreciate the many supports from my family.